Doctoral   Science

2011-11

The Role of Colour Duplex Ultrasound in the Surveillance of Patients Undergoing Endovascular Aneurysm Repair

Cleona Gray
Technological University Dublin

Recommended Citation

The Role of Colour Duplex Ultrasound in the Surveillance of Patients Undergoing Endovascular Aneurysm Repair

Submitted for the Award of Doctor of Philosophy to the Dublin Institute of Technology

School of Physics

Cleona Gray MSc, AVT

November 2011

Supervisors
Professor Patrick Goodman
Mr Ciaran McDonnell
Mr Martin O'Donohoe

Table of Contents

Chapter 5

Declaration

I certify that this thesis which I now submit for examination for the award of postgraduate doctorate, is entirely my own work and has not been taken from the work of others, save to the extent that such work has been cited and acknowledged within the text of my work.

This thesis was prepared according to the regulations for postgraduate study by research of the Dublin Institute of Technology and has not been submitted in whole or in part for another award in any institute.

The work reported on in this thesis conforms to the principles and requirements of the institutes guidelines for ethics in research.

The institute has permission to keep, lend or copy this thesis in whole or in part, on condition that any such use of the material of the thesis be duly acknowledged.

Signature_____   Date_____

Acknowledgements

This thesis has been a great academic and personal learning curve for which there are many people that I would like to acknowledge and thank for their support along the way. To all of you I extend my deepest appreciation.

First and foremost I offer my sincere gratitude to Mr. Ciaran McDonnell who has supported me throughout this research with his patience and knowledge whilst allowing me the room to work in my own way. His endless support, guidance and encouragement as well as his pain-staking effort in proof reading the drafts are greatly appreciated.

My profound thanks to Professor Patrick Goodman, for the encouragement guidance and support that he has given me throughout this research project.

I attribute the level of this thesis to the encouragement and effort of both of you. Without both your support and encouragement this thesis would never have come together.

With a level of awe and admiration I would like to thank Dr. Patricia Fitzgerald who instilled a love of Vascular Technology through her teaching and encouragement in the early days of my career.

I would like to express my sincere appreciation to Mr. Martin O' Donohoe and Mr Kevin O Malley, Department of Surgery, Mater Misericordiae University Hospital. For their continued guidance, insight and support since my appointment at the hospital, but above all for affording me the opportunity to carry out this research.

To Katrina, Grainne, Edel and Mark, the fabulous staff of the Vascular Laboratory in the Mater Hospital, for your endless motivation, support and for putting up with me!

I would like to acknowledge the tremendous sacrifices that my parents have made to ensure that I had an excellent education. For their never-ending support, encouragement and love in everything that I do. For this and for much more I am forever in their depth.

Finally I would like to thank my husband Michael, for his endless patience and encouragement during this journey. Without whom I would have struggled to find the inspiration and motivation needed to complete this thesis, and it is to you I dedicate this work.

Abbreviations

AAA-Abdominal Aortic Aneurysm
ABI – Ankle Brachial Indices
ACAS- Asymptomatic Carotid Atherosclerosis Study
ACST- Asymptomatic Carotid Surgery Trial
ADAM- Aneurysm Detection and Management
A-MODE – Amplitude Mode
ATA – Anterior Tibial Artery
BA – Brachial Artery
B-MODE - Brightness Mode
CAD – Carotid Artery Disease
CCA – Common Carotid Artery
CDU – Colour Duplex Ultrasound
CEA – Carotid Endertrectomy
CFA – Common Femoral Artery
CIA – Common Iliac Artery
CT – Computed Tomography
CVD – Cerebro Vascular Disease
DPA – Dorsalis Pedal Artery
DREAM – Dutch Randomised Endovascular Aneurysm Repair Trial
DSA – Digital Subtraction Angiography
ECA – External Carotid Artery
EIA – External Iliac Artery
EVAR – Endovascular Aneurysm Repair
EQT - Equation
ICA – Internal Carotid Artery
ICSS- International Carotid Stenting Study
IIA –Internal Iliac Artery
LDL- Low Density Lipoprotein
MASS – Multicentre Aneurysm Screening Study
MMUH – Mater Misericordiae University Hospital
MRI – Magnetic Resonance Imaging
NACSET – North American Symptomatic Carotid Endertrectomy Trial
PA – Popliteal Artery
PAD –Peripheral Artery Disease
PER- Peroneal Artery
PFA- Profunda Femoral Artery
PPG- Photoplethysmography
PTA- Posterior Tibial Artery
pt - Patient
SFA- Superficial Femoral Artery
SVT- Society of Vascular Technology
SPACE- Stent Supported Percutaneous Angioplasty of the Carotid Artery versus Endarterectomy Study
TBI – Toe Brachial Indices

TIA- Transient Ischaemic Attack
TPT – Tibio Peroneal Trunk
UKSAT – United Kingdom Small Aneurysm Trial

List of Figures

List of Tables

List of Equations

Chapter 1

Introduction

Abdominal Aortic Aneurysms (AAA's) are the end result of a mutifactorial disease process affecting a high proportion of our elderly population. Ruptured AAA's are the tenth leading causes of death in elderly males and about half of all patients with an AAA can expect to die of rupture if their aneurysm is not surgically treated (Siegel and Cohan. 1994 and Schei et al., 2003). If left untreated, aneurysms undergo progressive, merciless enlargement until rupture occurs. They are often described as "silent killers" with rupture quite often being the first presenting symptom. The natural history of an AAA is characterised by progressive expansion and rupture. AAA's are thought to be present in 4.7% of men and 1.2% of women aged between 65-74 years. Most aortic aneurysms are localised to the infra renal portion of the vessel (Ouriel, Greenberg and Clair, 2002).

The aorta is the largest artery in the body consisting of the ascending aorta, the aortic arch the descending thoracic aorta, and the abdominal aorta (Chapter 2.0, figure 2.1). Rupture of an AAA is a catastrophic event, many die without even reaching the operating table, and only approximately 50% of those undergoing emergency open surgical repair survive beyond 30 days (The United Kingdom small aneurysm trial participants). Hence, screening programmes are essential to detect AAA's and appropriate follow up programmes for such patients enabling vascular surgeons to offer patients the opportunity to have their aneurysms repaired electively when they are younger, fitter and asymptomatic, with an associated improved survival rate.

Traditionally the procedure of choice was open surgical repair as described by Dubost in the 1950's. However, since Parodi reported the first successful case

of endovascular repair of an AAA in 1991 the surgical management of aneurysms has altered dramatically. Endovascular surgery is a less invasive, lower risk option for repairing AAA's. It has also made it possible for older and higher risk patients, previously deemed unfit for open surgery to be considered for repair.

Cardiovascular disease is widely accepted as a leading cause of death in the western world and is the most common cause of death in Ireland; in 2001 the Irish Heart Foundation reported that cardiovascular disease accounted for over 40% of all deaths and 37% of deaths under 65 years in Ireland. In 2009 the Irish heart foundation stated that despite a fall in cardiovascular deaths, it still remained the number one killer in Ireland with just under 10,000 people dying each year.

Non invasive imaging techniques have become increasing popular and have played an important role in the detection, diagnosis and management of such conditions. Imaging modalities such as colour duplex ultrasound (CDU), have become widely accepted and are a cost effective method of accurately diagnosing cardiovascular disease when performed by a skilled operator.

The aim of this thesis is to investigate the role that CDU plays in the detection, diagnosis and management of patients with AAA's, with particular relevance to those undergoing endovascular aneurysm repair (EVAR).

Objectives of this thesis

i Chapter one through five provides an overview of the normal arterial anatomy and disease processes that affect the circulatory system, the physics that underlies ultrasound and its use with particular reference to the methodology pertaining to each of the individual studies that are outlined below.

ii Chapter six examines the incidence of carotid artery disease (CAD) and peripheral arterial disease (PAD) in the 389 patients currently on the aneurysm surveillance programme using ultrasound based imaging techniques. The aim of this part of the study is to determine if patients with AAA's are a reasonable focus group to screen for atherosclerotic conditions in other vascular territories.

iii Chapter 7 compares the two imaging modalities of CDU and computed tomography (CT) in assessment of the maximum aneurysm diameter in 126 patients under surveillance for AAA. It is an attempt to demonstrate that CDU is a reliable surveillance tool prior to intervention

iv Chapter 8 compares CDU with CT in the post operative surveillance of 145 patients who have undergone EVAR. The aim of this study is to evaluate the role of CDU in the postoperative surveillance of such patients and determine whether CDU could supplant CT as the first line screening tool following EVAR.

v Chapter 9 evaluates the alterations in aneurysm sac size in 106 patients following EVAR using CDU based imaging techniques. The aim of this study is to determine the rate of residual aneurysm sac regression and determine if there is a relationship between sac regression, pre existing risk factors and the presence of a type 2 endoleak.

vi Chapter 10 attempts to determine the effect of AAA repair on arterial stiffness using CDU as the sole method of investigation. This study examines the affect of implanting an endovascular aortic graft on a patients pulse wave velocity compared to patients who underwent the traditional open surgical repair.

Chapter 2

Arterial Anatomy

2.1 Introduction

The anatomy of the normal abdominal aorta, peripheral arterial circulation and the carotid and vertebral arteries are outlined in this chapter.

2.2 Structure of an Arterial Wall

Arteries have a similar structure throughout the body. An arterial wall is composed of three layers.

Tunica Adventitia

Tunica Media

Tunica Intima
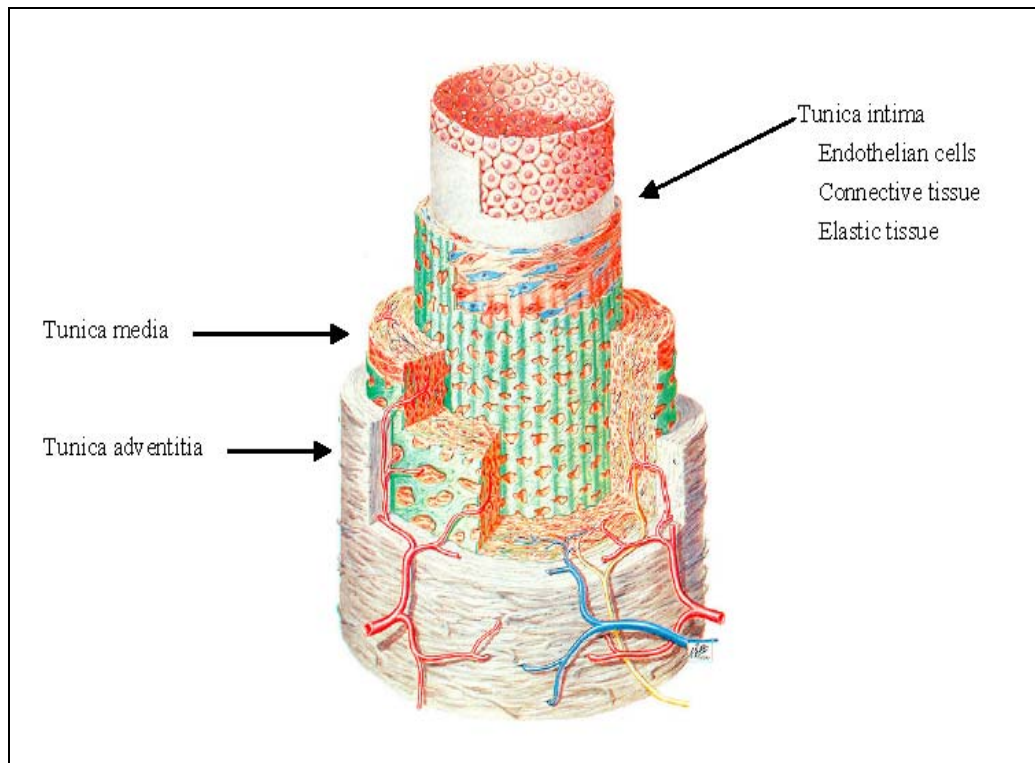
Figure 2.0: The structure of an arterial wall

The tunica adventitia is the outermost layer consisting mainly of elastic lamina enclosed by fibrous tissue. It is primarily fibro-cellular and provides the major portion of the tensile strength of the vessel. The adventitia contains both the vasa vasorum and the nerves which supply the vessel. The vasa vasorum is a network of smaller blood vessels within the larger vessels whose function is to nourish the walls of the larger vessels as well as acting as a conduit for eliminating waste products.

The tunica media is the middle layer of the blood vessel. It is made up of smooth muscle cells and elastic tissue; it is distinguished from the other two layers by its colour and the transverse arrangement of its fibres. It contains bundles of elastic fibres and collagen. The smooth muscle component is responsible for variations in the tone of the vessel wall. The external elastic lamina separates the tunica

34

adventitia from the tunica media and its function is to determine the elasticity of the artery.

The tunica intima is the inner layer of the blood vessel which is extremely thin. It consists of a single layer of endothelial cells separated from the internal elastic lamina by a thin layer of mixed cells. These endothelial cells are in direct contact with blood flow and have multiple functions such as preventing platelet aggregation and thrombosis. They regulate the smooth muscle tone and they also control the entry of lipoproteins into the vessel wall.

2.3 The Abdominal Aorta

2.3.1 General Overview

The aorta is the largest artery in the body. It becomes the abdominal aorta on passing through the aortic hiatus of the diaphragm, in front of the lower border of the body of the twelfth thoracic vertebra, descending in front of the vertebral column and ending at the level of the fourth lumbar vertebra.
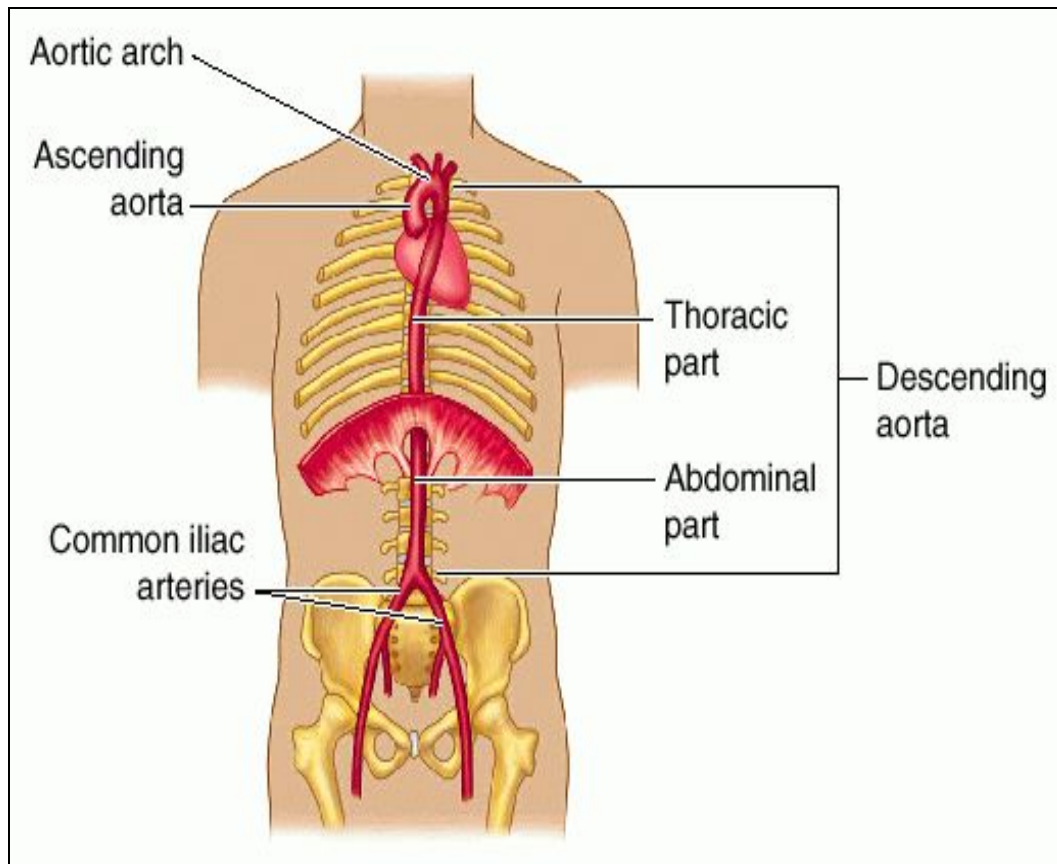
Figure 2.1: The abdominal aorta

The aorta runs anterior to the spinal column and slightly to the left of the midline. It bifurcates into the two common iliac arteries which in turn divide into the internal and external iliac arteries. These vessels supply oxygenated blood to the lower abdomen, pelvis and the legs.

As it lies upon the bodies of the vertebra, the curve which the aorta describes is convex forward, the summit of the convexity corresponding to the third lumbar vertebrae.

The abdominal aorta and its major arterial branches are highly elastic. During systole, they expand rapidly to accommodate increased blood flow. The vessels

recoil during diastole and elastic fibres ensure that this contraction also serves to drive blood through the arterial vessels.

2.3.2 Branches of the Abdominal Aorta

These can be divided into visceral, parietal and terminal branches (table 2.1 and figure 2.2). The visceral branches supply the organs in the abdomen, as well as the kidneys and gonads. The parietal branches supply the diaphragm and the posterior walls of the abdomen. The terminal branches supply the organs of the pelvis, the pelvic wall and the paired common iliac arteries.

Visceral Branches	Parietal Branches	Terminal Branches
coeliac artery	inferior phrenic arteries	right common Iliac artery
superior mesenteric artery	lumbar arteries	left common Iliac artery
inferior mesenteric artery	median sacral artery	
middle suprarenal arteries		
right and left renal arteries		
gonadal arteries		

Table 2.1: Classification of aortic branches
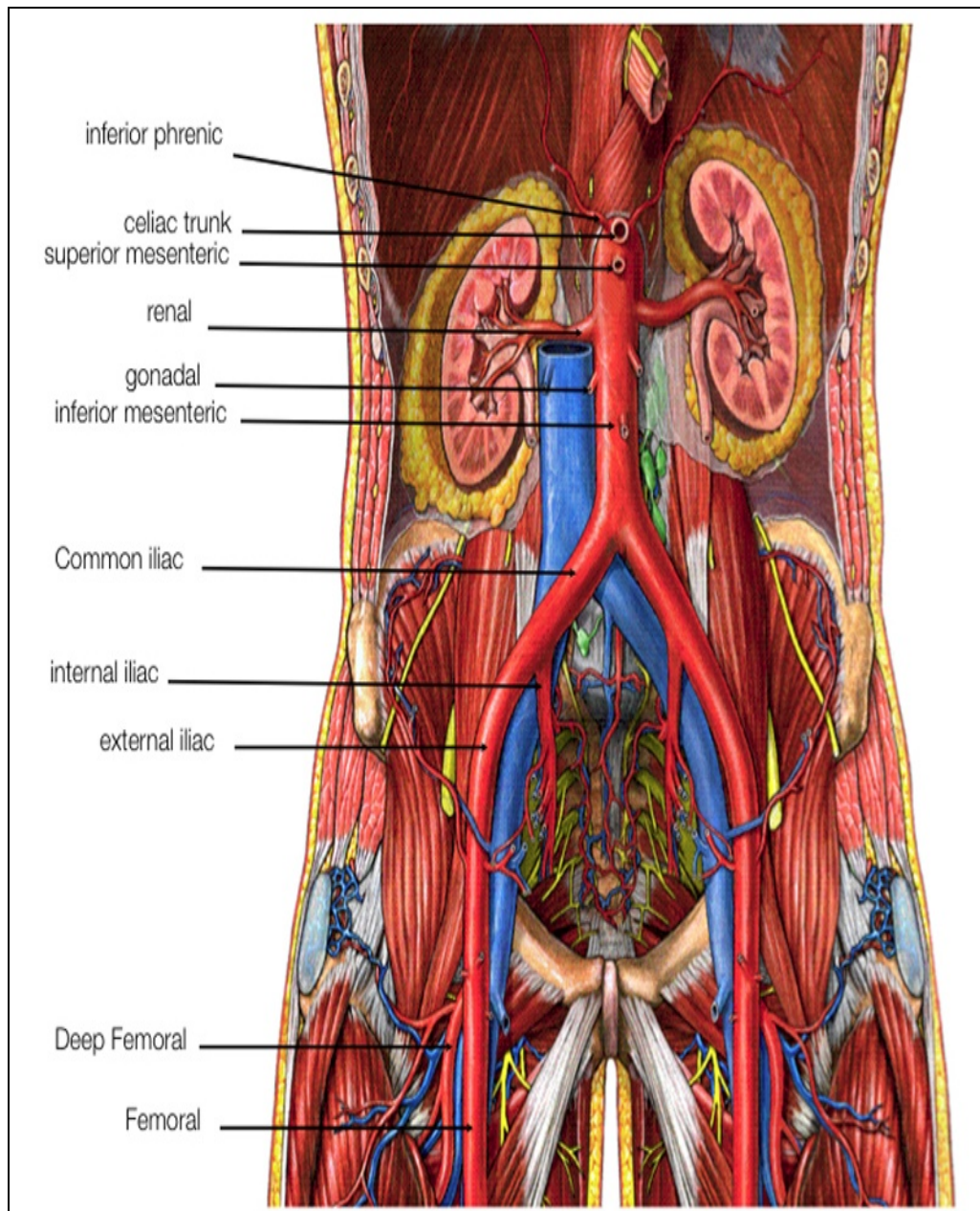
Figure 2.2: The abdominal aorta and its branches

Of the visceral arteries the coeliac artery, the superior and the inferior mesenteric arteries are unpaired. The suprarenal, renal, gonadal, inferior phrenic, lumbar and all the terminal arteries are paired.

The coeliac artery arises from the anterior aspect of the aorta below the aortic hiatus of the diaphragm. It divides into three branches the left gastric artery, the hepatic artery and the splenic artery. The left gastric artery distributes branches to the oesophagus and the cardiac orifice of the stomach. The hepatic artery divides into the right and left hepatic arteries which supply the corresponding lobes of the liver. The splenic artery supplies blood to the spleen and follows a course superior to the pancreas.

The superior mesenteric artery also arises from the anterior aspect of the aorta and supplies the whole length of the small intestine with the exception of the proximal duodenum. It also supplies the caecum, the ascending colon and the proximal two thirds of the transverse colon.

The inferior mesenteric artery supplies blood to the transverse colon, the descending sigmoid colon and the majority of the rectum. It arises from the infrarenal aorta roughly 3-4cm above the iliac bifurcation.

The middle supra renal arteries arise from either side of the aorta and supply the anteromedial portion of the suprarenal glands.

The renal arteries arise from either side of the aorta below the level of the superior mesenteric artery. The right renal artery is longer than the left. Before reaching the kidney each renal artery often divides into several branches which lie between the renal vein and the urethra. It is possible for one or two accessory renal arteries to exist, especially on the left side as they usually arise from the aorta and may come off above or below the main artery. Instead of entering the kidney at the hilum, they usually pierce the upper or the lower part of the organ.

The gonadal arteries arise from the anterior aspect of the aorta approximately at the level of the renal arteries. They pass obliquely over the urethra and the lower part of the external iliac artery to reach the internal inguinal ring. Once they pass through here they accompany the other constituents of the spermatic cord along the inguinal canal to the scrotum in the male or in the female they pass inwards between the two layers of the ovariopelvic ligament and the broad ligament of the uterus to the ovary.

The lumbar arteries arise from the posterior wall of the aorta commonly existing as four pairs of vessels. Muscular branches are supplied from each lumbar artery. The middle sacral artery arises from the posterior aspect of the aorta just before it bifurcates into the right and left common iliac arteries. It descends near the midline in front of the fourth and the fifth lumbar vertebrae, the sacrum and the coccyx to the glomus coccygeum. Branches pass to the posterior surface of the rectum, at the last lumbar vertebrae it anastomoses with the lumbar branch of the iliolumbar artery, in front of the sacrum it anastomoses with the lateral sacral arteries and sends offsets into the anterior sacral foramina.

The aorta divides into the right and the left common iliac arteries at approximately the level of the fourth lumbar vertebra (figure 2.2).

2.4 The Lower Limb Arterial System

2.4.1 General Overview

The common iliac arteries (CIA) arise from the bifurcation of the aorta and in turn divided into two branches at the brim of the pelvis. The external and internal iliac arteries (IIA) as in figure 2.2. The IIA supplies the pelvic viscera and the musculature via their visceral and parietal branches.

The external iliac artery (EIA) gives rise to the inferior epigastric artery and the deep circumflex iliac artery, then passing inferolaterally along the medial border of the psoas major muscle from the common iliac bifurcation to the inguinal ligament, midway between the anterior superior spine of the ilum and the symphysis pubis where it enters the thigh to become the common femoral artery (CFA) as described in figure 2.2.

The CFA branches in to 2 major arteries (figure 2.2) the profunda femoris artery (PFA) also known as the deep femoral artery and the superficial femoral artery (SFA).

The PFA runs posterolaterally and supplies the musculature of the thigh. It does not leave the thigh, communicating with the popliteal artery (PA) at the level of the adductor canal through collateral vessels.

The SFA (figure 2.2) supplies the greater part of the lower extremity. It runs as a single trunk from the upper thigh to the lower border of the popliteus muscle (figure 2.3). It passes down the front and medial side of the thigh and ends at the junction of the lower one third of the thigh where it passes through an opening in the adductor magnus muscle to become the PA (figure 2.4). The PA lies within the adductor canal coursing posteriorly into the popliteal fossa behind the knee.
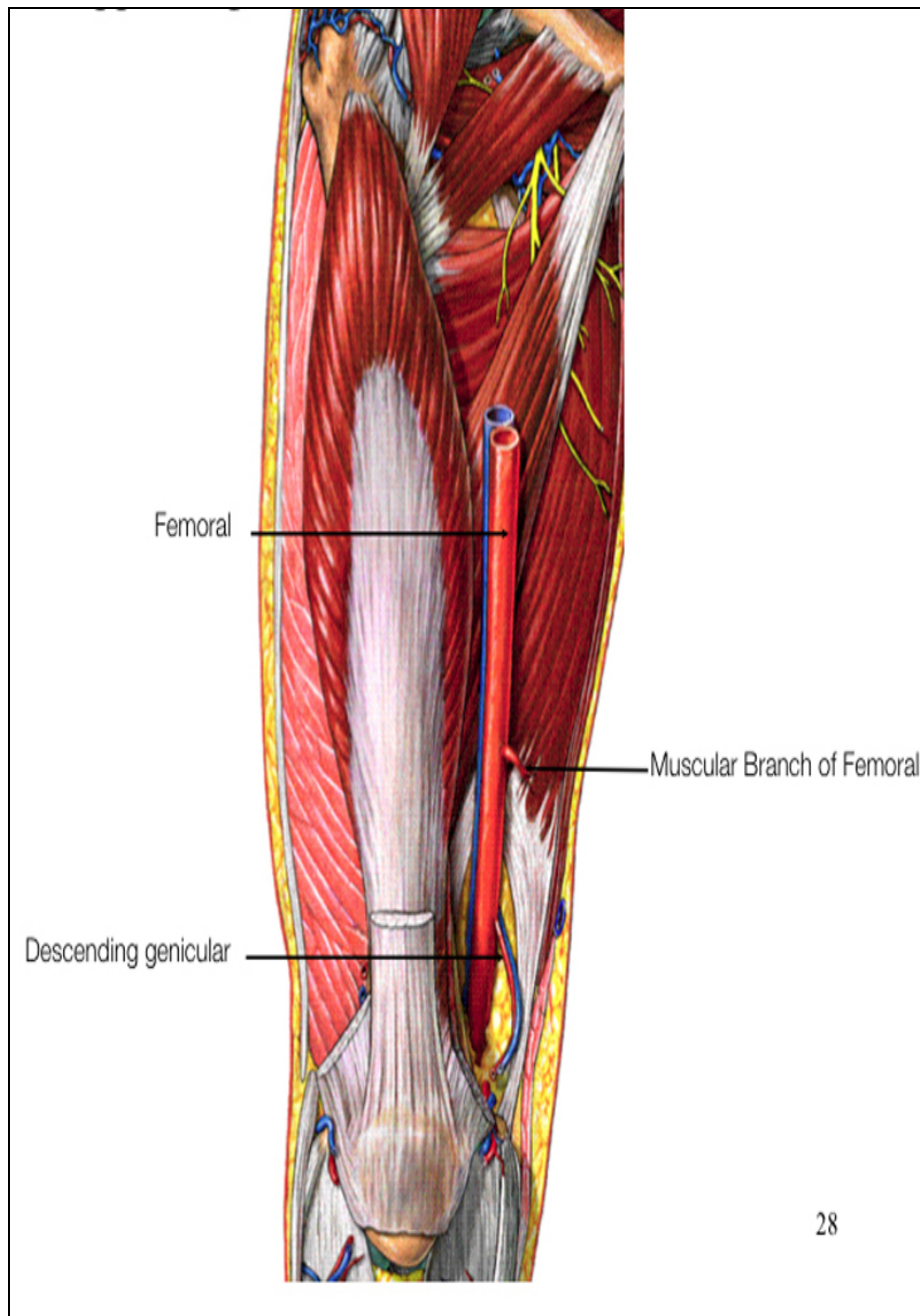
Figure 2.3: The arteries in the thigh
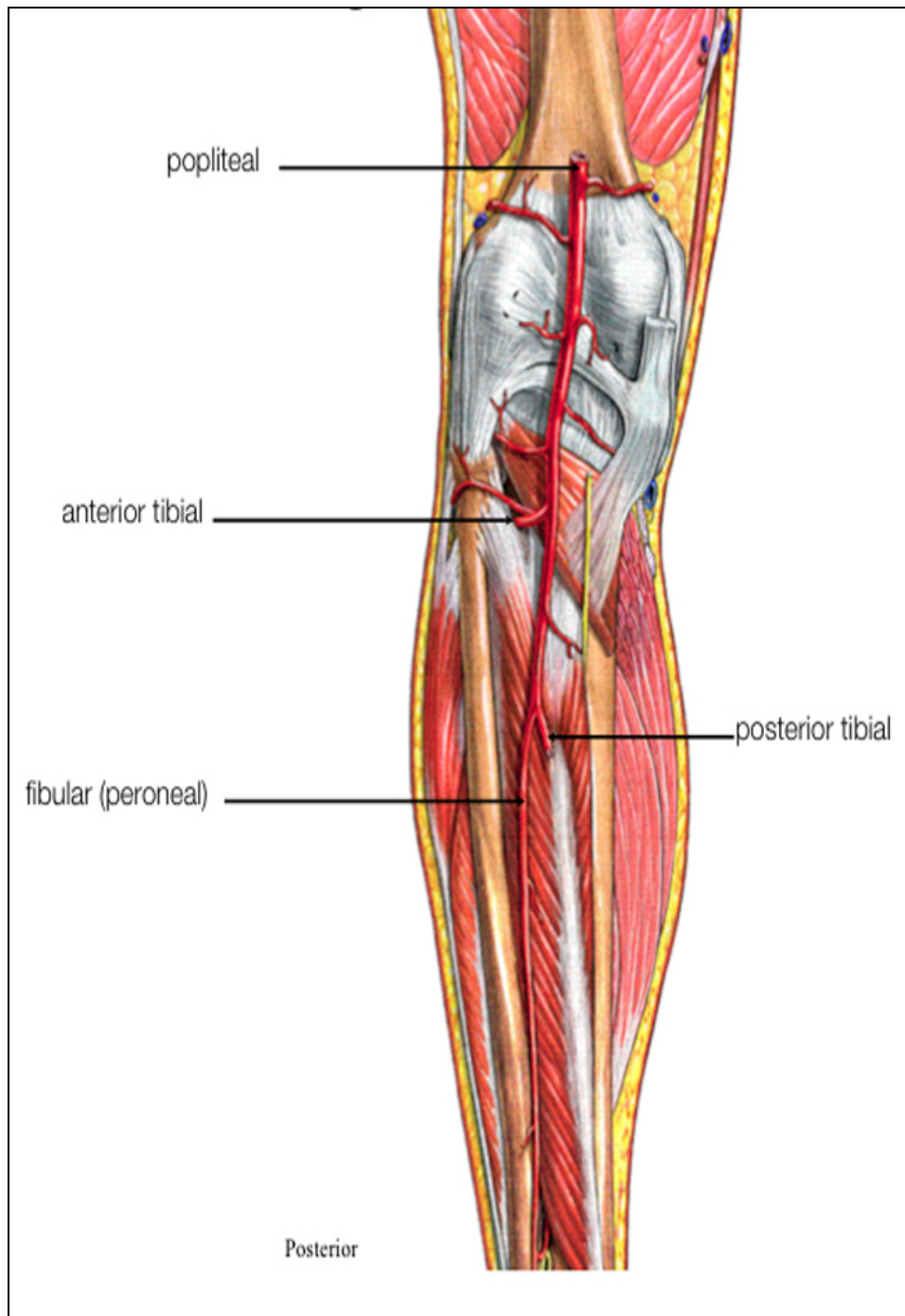
Figure 2.4: The arteries below the knee

The PA supplies blood to the knee joint and muscles of the calf through numerous smaller branches. It branches into the anterior tibial artery (ATA) and the tibio peroneal trunk (TPT) below the knee joint (figure 2.4).

The ATA arches over the upper edge of the tibio fibular interosseous membrane to enter the anterior compartment of the lower leg (figure 2.4). It is positioned anterolateraly in the calf between the tibia and the fibula, supplying the extensor muscles of the foot. It crosses the ankle on the anterior aspect of the foot to become the dorsalis pedis artery (DPA).

The tibio peroneal trunk (TPT) is a continuation of the popliteal artery after it gives rise to the ATA. It bifurcates into the posterior tibial artery (PTA) and the peroneal artery (PER) within a few centimetres of the origin of the ATA (figure 2.4).

The PTA (figure 2.4) supplies the flexor muscles on the medial aspect of the calf. It lies behind the medial malleolus and has multiple small branches. The PTA carries blood to the posterior compartment of the leg and the plantar surface of the foot were it gives rise to the medial and lateral plantar artery. The PER artery runs deeper than and more lateral than the PTA (figure 2.5). It lies in the deep posterior compartment just medial to the fibula. The PER divides on the lateral aspect of the foot to form the external maleolar artery, the lateral tarsal artery, and the external plantar artery.

Collectively the ATA, PTA and PER artery are all known as the crural arteries or the tibial vessels.
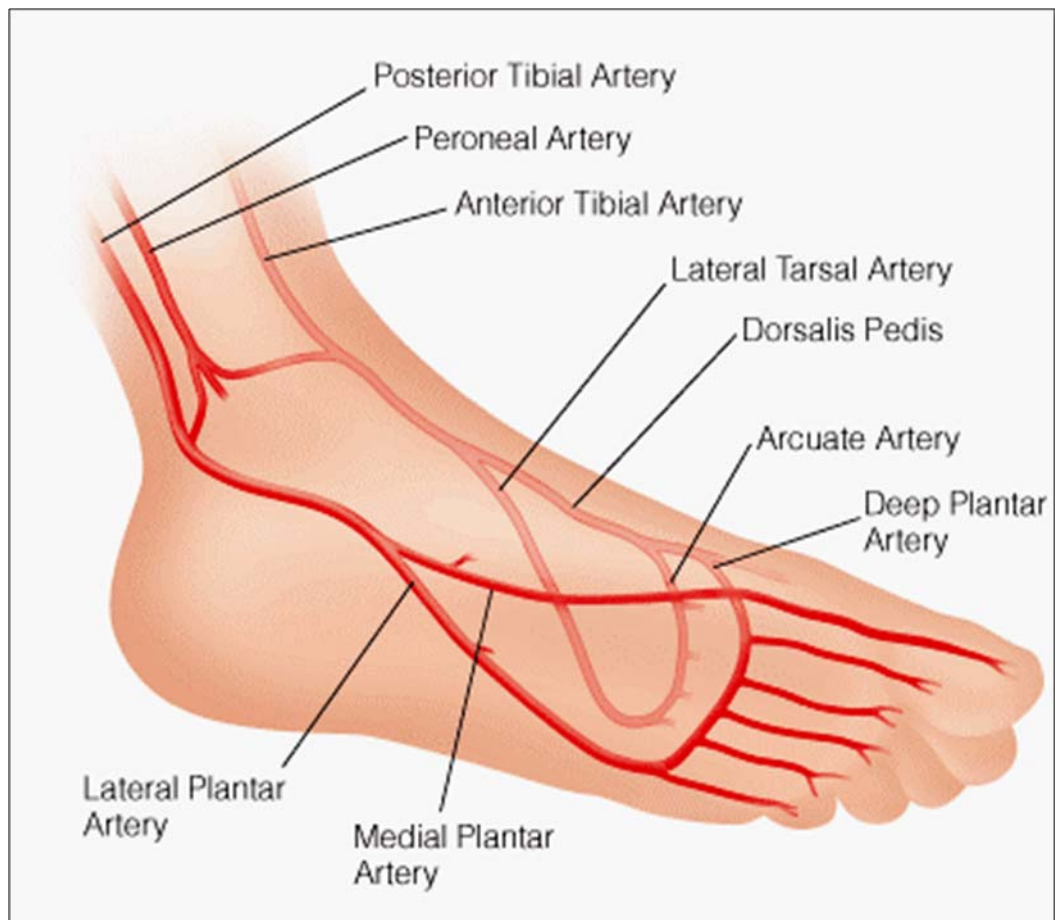
Figure 2.5: The arteries in the foot

2.5 The Extracranial Carotid Arteries

2.5.1 General Overview

The blood supply to the brain is via the two internal carotid arteries (ICA) and the two vertebral arteries. The aortic arch gives rise to the brachiocephalic artery which travels superiorly and bifurcates into the right common carotid artery (CCA) and the right subclavian artery at the right sternoclavicular junction. The left CCA arises directly from the aortic arch. The CCA's divide into the ICA and external carotid arteries (ECA) at the level of the upper border of the thyroid cartilage.
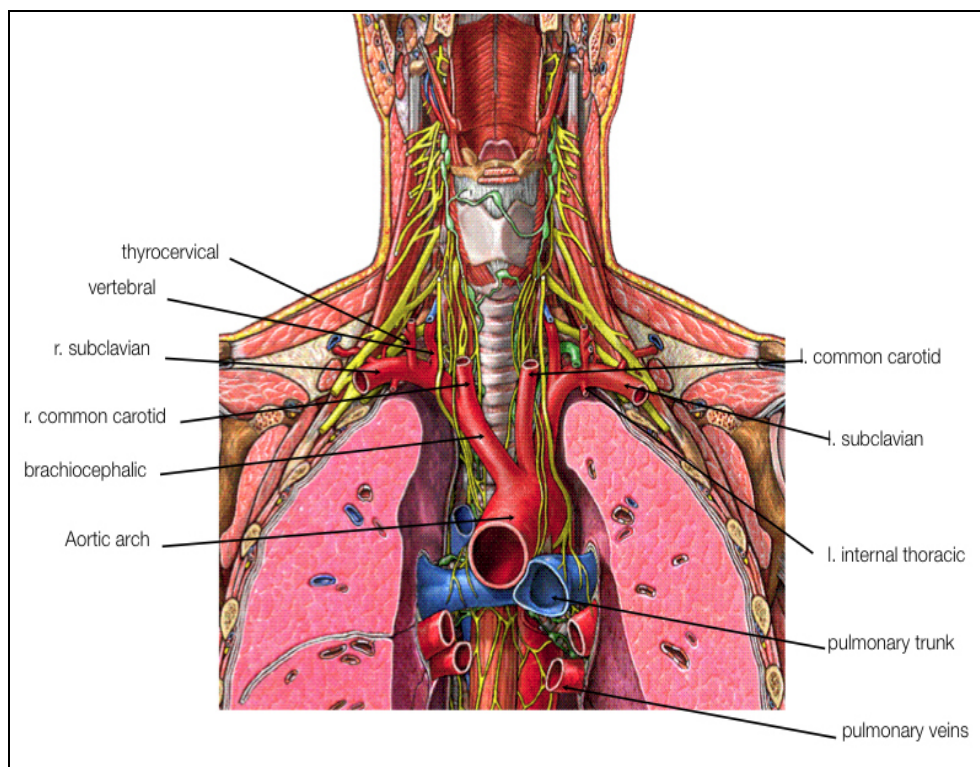
Figure 2.6: The extracranial carotid arteries

2.5.2 The Internal Carotid Artery

The majority of the anterior circulation to the brain and the eyes is supplied by the right and left ICA's (figure 2.7). The ICA has no extracranial branches and is usually larger in calibre than the ECA. As the ICA passes intracranially it ascends in a series of curves; this section is referred to as the carotid siphon. It is at this point that the ICA gives off one of its most important branches, the ophthalmic artery which supplies blood to the eye. Branches of the ophthalmic artery supply all the structures in the orbit as well as some structures in the nose, face and meninges.

The ICA ascends and finally divides into the middle cerebral artery and the anterior cerebral artery (figure 2.8). The right and the left anterior cerebral arteries are connected by a small vessel called the anterior communicating artery.

Figure 2.7: The internal carotid artery

Figure 2.8: The intracranial carotid circulation

2.5.3 The External Carotid Artery

The right and the left ECA's supply the exterior of the head, the face and the greater part of the neck (figure 2.9). It usually lies anterolateraly and is more often than not of smaller calibre than the ICA. The ECA has numerous branches; however it is usually only the first branch, the superior thyroid artery that is visualised during a colour duplex ultrasound (CDU) scan.

Its multiple branches become important collateral pathways when an ICA or vertebral artery occlusion occurs. The ECA branches that are of most importance in the formation of collateral pathways are those that communicate with the ophthalmic artery and those that interconnect between the muscular branches of the occipital and vertebral arteries.
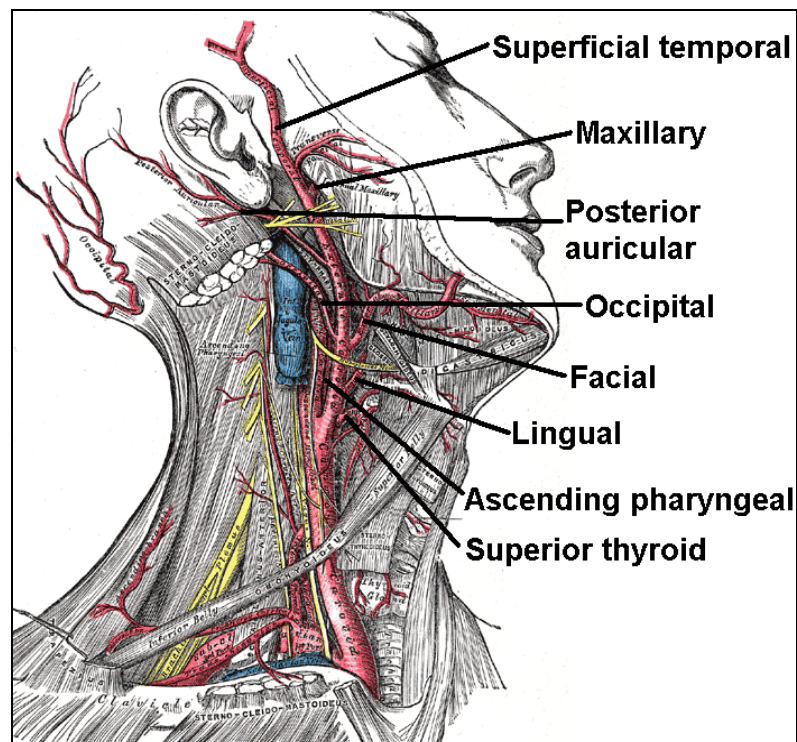
Figure 2.9: External carotid artery and its branches

2.5.4 The Vertebral Arteries

The posterior circulation to the brain is via the right and the left vertebral arteries (figure 2.10). These vessels originate from the subclavian artery and course within the foramina transversarium of the upper cervical vertebrae entering the subarachnoid pace at the side of the medulla oblongata at the level of the atlanto-occipital interspace. They continue cephalad and anteriorly until they reach the pontomedullary level were they join to form the single basilar artery (figure 2.11).

The basilar artery ascends towards the brain and divides into the posterior cerebral artery and the posterior communicating artery (figure 2.8). The right and left communicating arteries, the right and the left middle cerebral arteries, the right and the left anterior cerebral arteries and the anterior communicating artery all constitute a structure called the circle of Willis (figure 2.11), which may or may not constitute a complete circle.
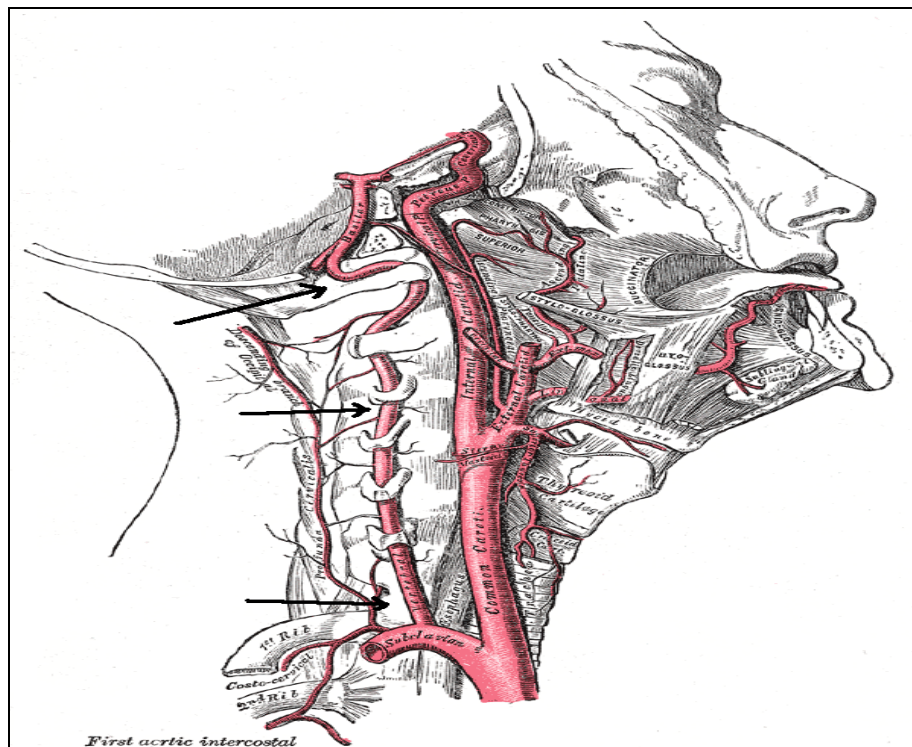
Figure 2.10: The vertebral arteries
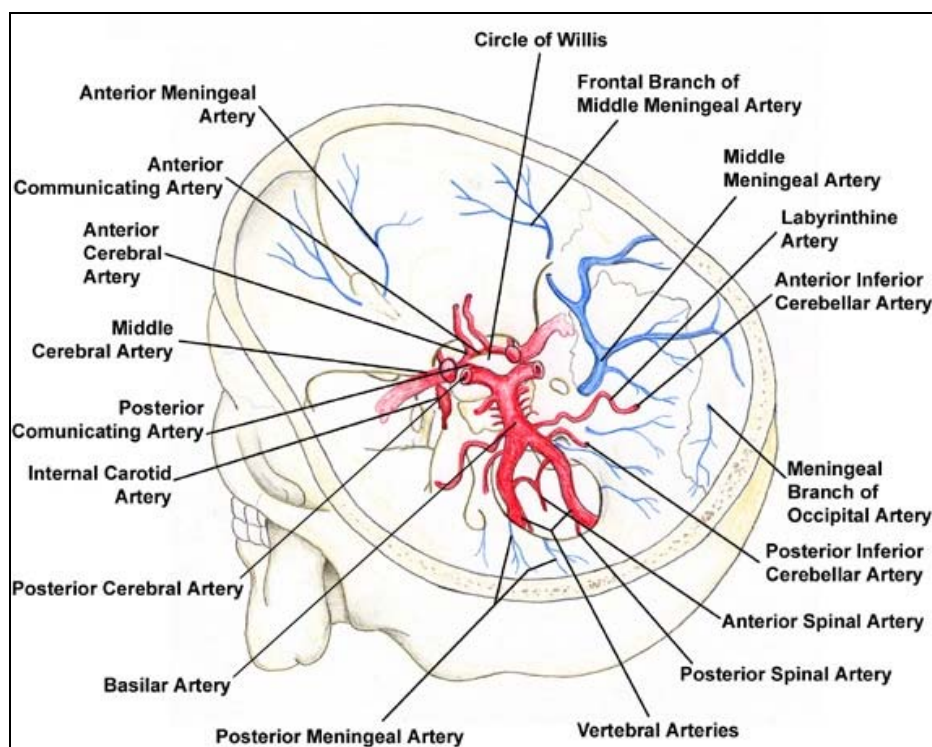
Figure 2.11: The circle of willis

Chapter 3

Pathology and Physiology of Vascular Disease

3.1 Atherosclerosis

Atherosclerosis is a systemic disease affecting the entire arterial tree, it is characterised by endothelial dysfunction, vascular inflammation and the build up of lipids such a cholesterol, calcium and cellular debris within the intima of the vessel wall (figure 3.0). This complex series of events results in the formation of atherosclerotic plaque which may significantly reduced the patent lumen of any vessel, thus creating abnormalities in blood flow through the vessel and a decreased oxygen supply to the tissues supplied by that vessel.
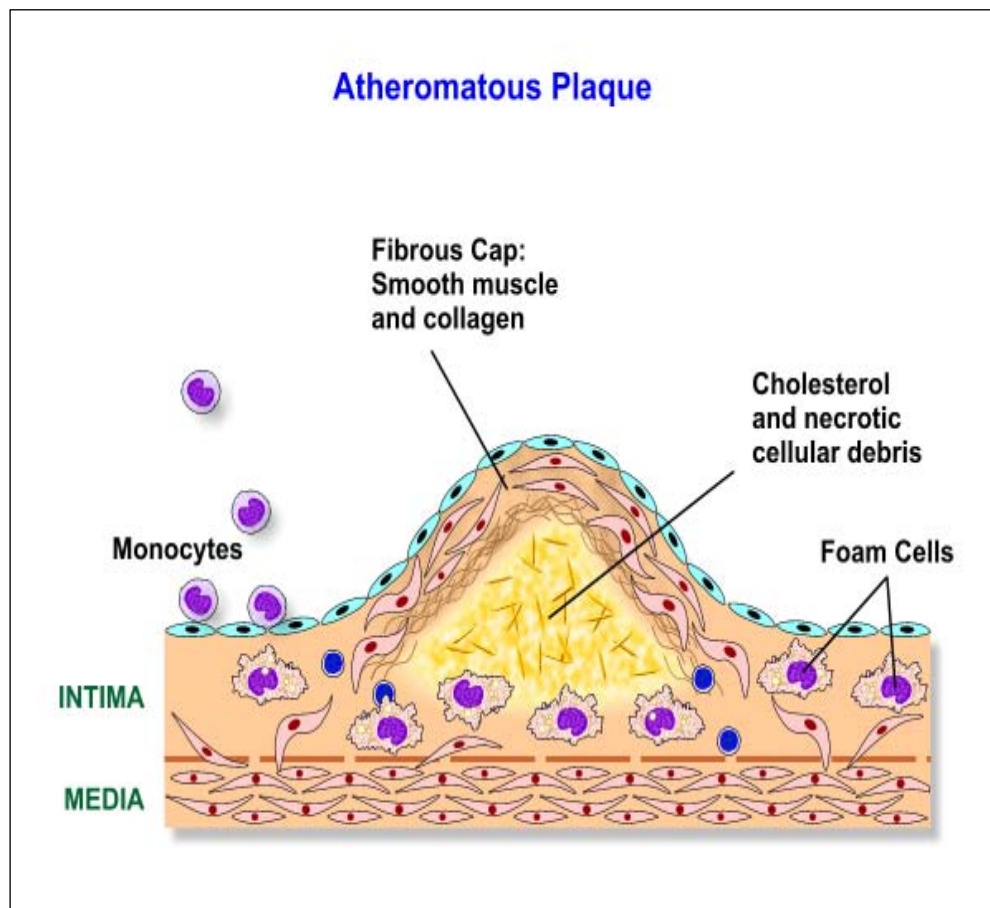
Figure 3.0: Atherosclerosis of an arterial Wall

Diminished blood flow to a particular tissue or organ manifests as a reduction in its normal function. Thus a decrease in blood flow and oxygen to the heart may result in a heart attack, if the blood flow to the brain is affected the patient may suffer a stroke and a decrease in blood flow to the lower limbs may lead to claudication or ultimately limb loss. Symptoms usually occur when the lesions become advanced and complicated by haemorrhage into plaque, emboli or thrombosis.

There are a number of risk factors that predispose to the pathogenesis of atherosclerosis, although the general consensus appears to be that atherosclerosis is governed by the interaction of genetic and environmental factors, which have an effect on the arterial tree.

Atherosclerosis initially affects the intima of the artery where there is a build up of fatty deposits in the intima as "foam cells". These are monocytes, (white blood cells) which absorb cholesterol. Early build up of plaque is often referred to as fatty streaks (figure 3.1). The disease is contained within the wall and the endothelium covering the plaque remains intact. As the plaque develops and increases in thickness it maintains a homogenous appearance. The plaque gradually develops into a complex structure (figure 3.2). This leads to a breakdown in the endothelium covering the plaque, exposing the underlying tissue of the vessel wall, leading to platelet aggregation and the formation of thrombus.

Atherosclerotic lesions tend to be localised and occur at common sites along the arterial tree such as bifurcations of the common carotid artery (CCA) and the common femoral artery (CFA) due to the turbulent flow that can occur at these sites.
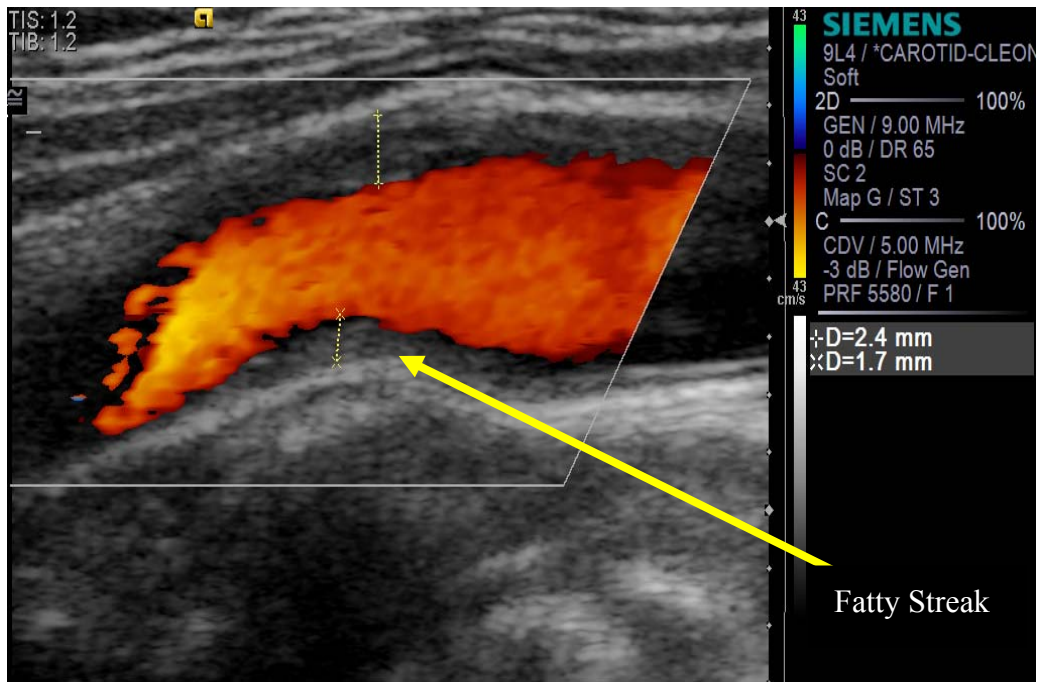
Figure 3.1: Initial stages of atheroma
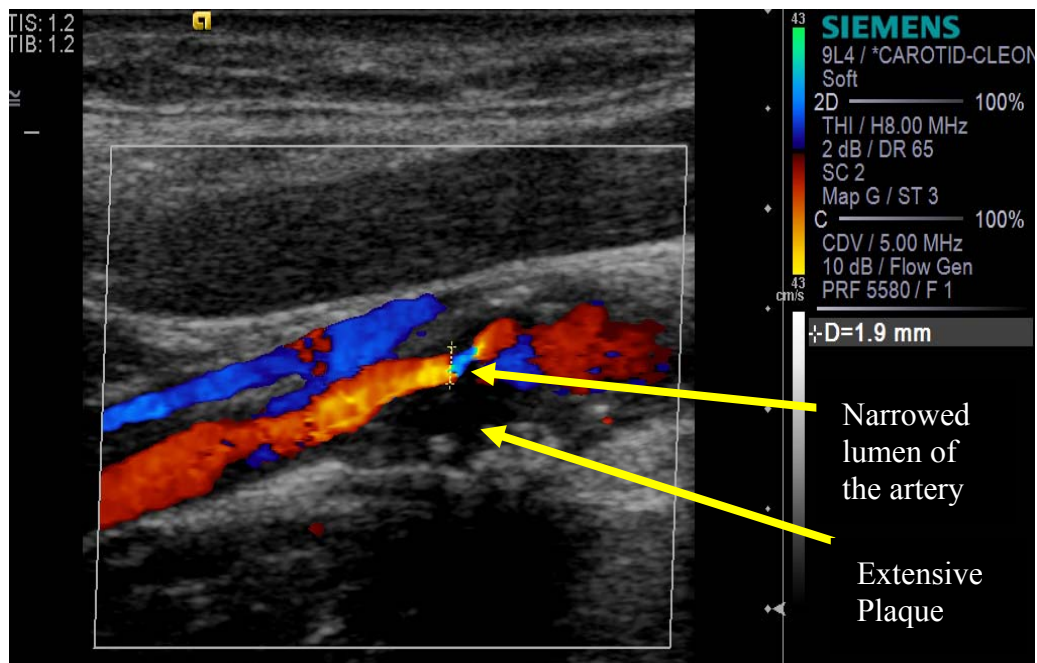
Figure 3.2: Extensive plaque

Figure 3.1 demonstrates the initial stages of atherosclerosis along an arterial wall. This build up of atheroma does not limit the flow through the vessel. This atheroma eventually develops into extensive plaque (figure 3.2) greatly reducing the lumen of the vessel, inevitable resulting in decreased flow and increased pressure through the vessel and may become a source of emboli.

3.1.1 The Causes and Effects of Atherosclerosis

Atherosclerosis is thought to be caused by damage to the endothelium of the vessel wall, although the underlying mechanism may vary, it is the resulting endothelial injury that is the common initiating factor in the development of the disease. Risk factors such as cigarette smoking, hypertension and hypercholesterolemia have been implicated in its cause. When the vessel lumen is reduced by 50% or greater (figure 3.2) the flow through the vessel may become compromised.

3.1.2 Risk Factors for Atherosclerosis

The most commonly recognised risk factors associated with the development of atherosclerosis are tobacco smoking, diabetes, hypertension, hypercholesterolemia, low density lipoprotein, high homocysteine levels, family history, obesity and gender. The majority of these risk factors are modifiable and essential to reverse the effects of atherosclerosis or at least control the effects.

3.2 Peripheral Arterial Disease

3.2.1 Introduction

The peripheral vascular system refers to the blood vessels in the body which are located outside of the heart and the brain. Peripheral arterial disease (PAD) refers to the restriction of blood flow to the legs and in rare cases the arms due to a build up of plaque along the arteries of these limbs. PAD is often asymptomatic, under recognised and undertreated when compared with other cardiovascular diseases (Lovell et al., 2009). There are several possible causes of lower extremity arterial disease such as atherosclerosis (by far the most common), thromboangiitis obliterans (Buerger's disease) vasculitis, arterial trauma, popliteal arterial entrapment and cystic adventitial disease.

Patients presenting with PAD may suffer with a wide range of symptoms depending on the severity of the disease. As with any condition the baseline assessment for PAD is by history taking and physical examination. Ankle brachial pressures (ABI's) are then carried out to quantify the extent of disease present prior to further investigation with colour Duplex ultrasound (CDU), magnetic resonance imaging (MRI) or conventional angiography to further define the extent and localisation of the disease.

PAD can take many forms; mild PAD may be initially asymptomatic progressing to pain exacerbated by exercise, severe PAD manifests as rest pain, ischemic ulcers and gangrene.

Treatment of PAD usually varies depending on its severity and extent. Mild PAD may be treated with risk factor modification, exercise and pharmacological

treatment. However, severe PAD may require surgical or radiological intervention to relieve symptoms and prevent amputation.

Mortality rates for PAD may be as high as coronary artery disease and cerebrovascular disease (CVD) and it is common for all three conditions to co-exist together. The presence of symptomatic PAD confers a threefold risk of cardiovascular death relative to the general population (McDermott. 2006).

3.2.2 Aetiology

The prevalence of PAD increases markedly with older age and in persons with diabetes or a history of smoking; prevalence also is elevated in persons with hyperlipidaemia, hypertension or chronic renal disease (McDermott. 2006).

3.2.3 Signs and Symptoms

In most cases the first sign of PAD is lower limb claudication, also referred to as "intermittent claudication". This is described as pain or discomfort in the leg, exacerbated by exercise and relieved by rest. Pain develops when the exercising muscle is unable to meet the requirements of increased metabolic activity due to inadequate blood supply. The location of the pain usually predicts the location of the arterial disease. Aorta iliac disease will usually cause pain in the buttock or thigh region with femoral popliteal disease usually causing pain in the calf region. As the disease progresses the distance that the patient can walk before they experience pain (the claudication distance) becomes progressively shorter.

A large number of trophic changes may occur in the appearance of a patient's limb with severe arterial insuffiency. The skin becomes pale and shiny with loss of hair and nails become brittle. The limb will be cold and capillary refill time prolonged.

In advanced disease ulcers will occur in areas of pressure such as the heel malleolus or the toes. Gangrene may also occur (figure 3.3). As tissue dies because of an insufficient blood supply, gangrene classically begins in the tissue bed furthest away from the heart, i.e. at the tips of the toes and over pressures points.

Figure 3.3: A patient's foot with gangrene

Critical limb ischemia is the term given to the presence of ischemic rest pain and tissue loss, i.e. non healing ulcers and gangrene. Critical ischemia will progress to major limb loss unless reversed. Rest pain, usually described by the patient as foot pain in bed which is present at night, relieved by placing the foot in a dependent position usually over the side of the bed. An ankle systolic pressure of less than 50mmHg or, a toe systolic pressure of less than 30mmHg or both will often be

present. Critical limb ischemia may be acute but in the majority of cases its chronic as a result of progressive disease. The development of critical limb ischemia usually involves multiple sites of arterial obstruction or occlusion. Acute lower limb ischemia may be caused by embolisation of thrombus from a more proximal vessel. Thrombus (figure 3.4) may arise from any part of the arterial tree commencing in the left atrium. This thrombus travels distally and occludes one or more vessel in the lower limb. Presentation is always acute with the patient presenting with a pale, cold, painful limb which may become paralysed as the ischemia progresses.
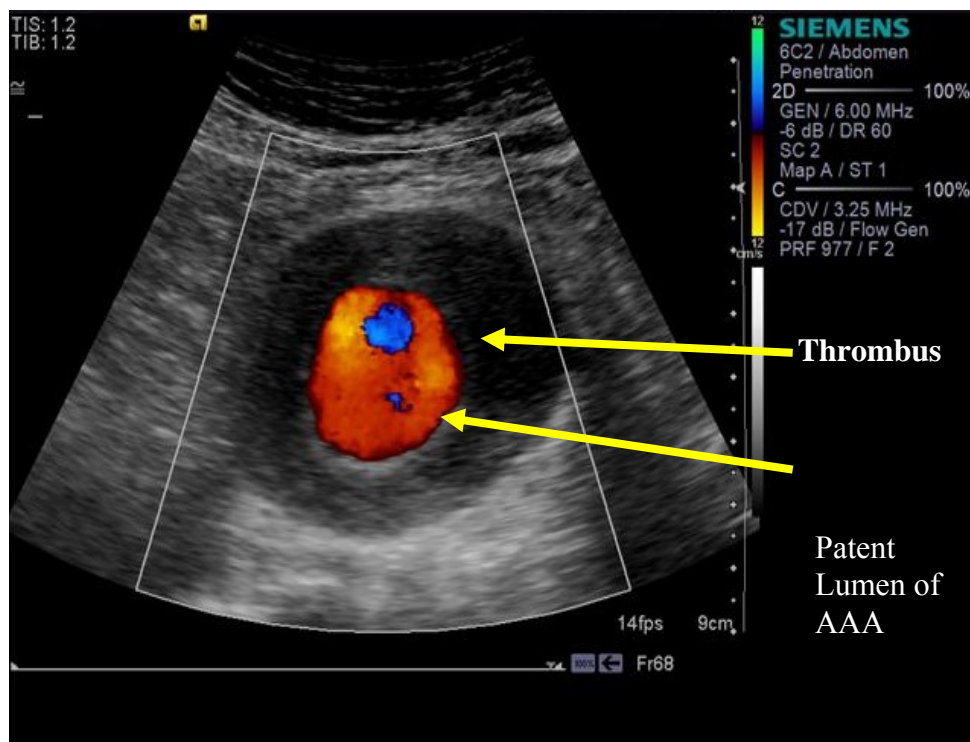
Figure 3.4: A large core of thrombus within an AAA

3.2.4 Diagnosis

The baseline investigation for patients suffering from PAD is the ankle brachial pressure index (ABI). This technique is non invasive and reproducible, providing a rapid and quantitative assessment of the arterial disease of the entire limb above the ankle. Exercise tests can stress the patient's resting ABI to further quantifying the disease.

Toe brachial indices (TBI's) are a useful investigation, particularly in diabetics whose pedal vessels are often spared the calcification that can affect the tibial arteries causing them to be incompressible, thus rendering the standard ABI reading to be falsely elevated. The clinical measurement protocol for the performance of ABI and TBI's is detailed in Chapter 5.0 section 5.1.4 and 5.1.7.

3.2.5 Treatment

The majority of patients with PAD can be treated conservatively with lifestyle changes and medication. A systematic review of patient's risk factors is necessary for the appropriate management to be instigated. Treatment of PAD can ultimately be divided into three categories depending on the severity and the extent of the disease and its affect on each patient. These categories are risk factor modification and lifestyle change, pharmacological intervention and invasive strategies.

i   ***Risk factor Modification and Lifestyle Change***

The development of PAD is associated with similar risk factors to other atherosclerotic diseases such as coronary artery disease and carotid artery disease (CAD).

Diabetic control: The risk of atherosclerotic disease is markedly increased in patients with diabetes; the increased risk is independent of, and additive to other cardiovascular risk factors (Marso and Hiatt. 2006). Atherosclerosis is responsible for most of the death and disability in patients with diabetes, particularly type 2 diabetes (Marso and Hiatt. 2006). Diabetic atherosclerosis is more diffuse, more severe and manifests itself at an earlier age. Atherosclerosis is more aggressive in diabetic patients and often involves the tibial and micro vessels making it more difficult to treat. The risk of amputation in diabetic patients is 15 to 46 times higher than in non diabetics (Yesil et al., 2009). Aggressive glycaemic control is a mandatory part of managing diabetics with PAD.

Smoking cessation: Cigarette smoking has been shown in the Framingham study to increase the risk of PAD in both males and females, with heavy smokers showing a fourfold risk of developing PAD. Smoking cessation is associated with a rapid decline in the incidence of PAD. The risk for ex smokers 1 year after quitting is approximately the same as that for non smokers (Groechenig. 2003).

Hypertension: Elevated blood pressure is a well established risk factor for mortality, cardiovascular and cerebrovascular events. Approx half of the patients with PAD have elevated blood pressure. Prolonged increased blood pressure is associated with increased risk of heart attack and stroke (Henry et al., 2002)

Cholesterol Lowering: Many randomised control trials have assessed the impact of cholesterol lowering on cardiovascular events in people with PAD. In the LEADER study, 1568 men with PAD were randomised to either bezafibrate 400mg daily or a placebo. Treatment with bezafibrate had a positive outcome on the incidence of non fatal coronary events but did not reduce the incidence of total fatal and non fatal cardiovascular events. The authors concluded that all PAD patients with a total cholesterol level of greater than 3.5mmol/l should be treated with a statin (Meade et al., 2002).

Weight reduction: Obesity, defined as a body mass index of greater than 30Kg/m2 has been associated with an increase risk of cardiovascular mortality.

Aggressive modification of the aforementioned risk factors will lower the need for intervention and lower the risk of limb loss. It is well documented that smoking cessation alone significantly reduces the likely hood of amputation and may increase the patients walking distance and ankle brachial pressure measurement (Dieter et al., 2002).

Lifestyle changes

Exercise: Any form of physical activity will maintain health, lower blood pressure aid in weight reduction and promote a general sense of well being. For individuals with diabetes and PAD, physical activity in the form of walking is recommended because success in treatment of PAD may be measured in distance walked without pain. Clinical trials have shown that supervised exercise programmes in patients with symptomatic claudication, are effective in increasing walking time when compared to standard care (Leng, Fowler and Ernst. 2000). Higher levels or longer

duration of physical activity is related to longer survival and lower risk of death from cardiovascular disease among PAD patients (Garg et al., 2007).

ii. *Pharmacological Intervention*

Medical therapy for patients suffering with PAD is mandatory to reduce blood pressure, cholesterol and plasma glucose as these cannot be achieved with lifestyle changes alone. Antiplatelet therapy such as aspirin should be instigated to reduce the risk of stroke, or vascular death. Statin therapy may be indicated in patients with elevated low density lipoprotein (LDL) cholesterol. Antihypertensive therapy should be prescribed in patients with elevated blood pressure to achieve a goal of less than 140/90mmHg for individuals without diabetes and, 130/80 mmHg for patients with diabetes and renal disease to minimise the risk of stroke, heart attack and cardiovascular death.

iii. *Invasive Strategies*

In a minority of patients lifestyle changes and medication alone are not sufficient. In these cases intervention is inevitable for limb salvage. Such intervention may include angioplasty, stenting or surgical bypass of the diseased vessel.

Angioplasty is an endovascular procedure that may be used to dilate a stenosed or occluded blood vessel. A catheter with a deflated balloon on its tip is passed over a guide wire into the stenosed arterial segment (figure 3.5, step A). The balloon is then inflated to open up the narrowed segment and the catheter is withdrawn as demonstrated in figure 3.5 steps B and C.
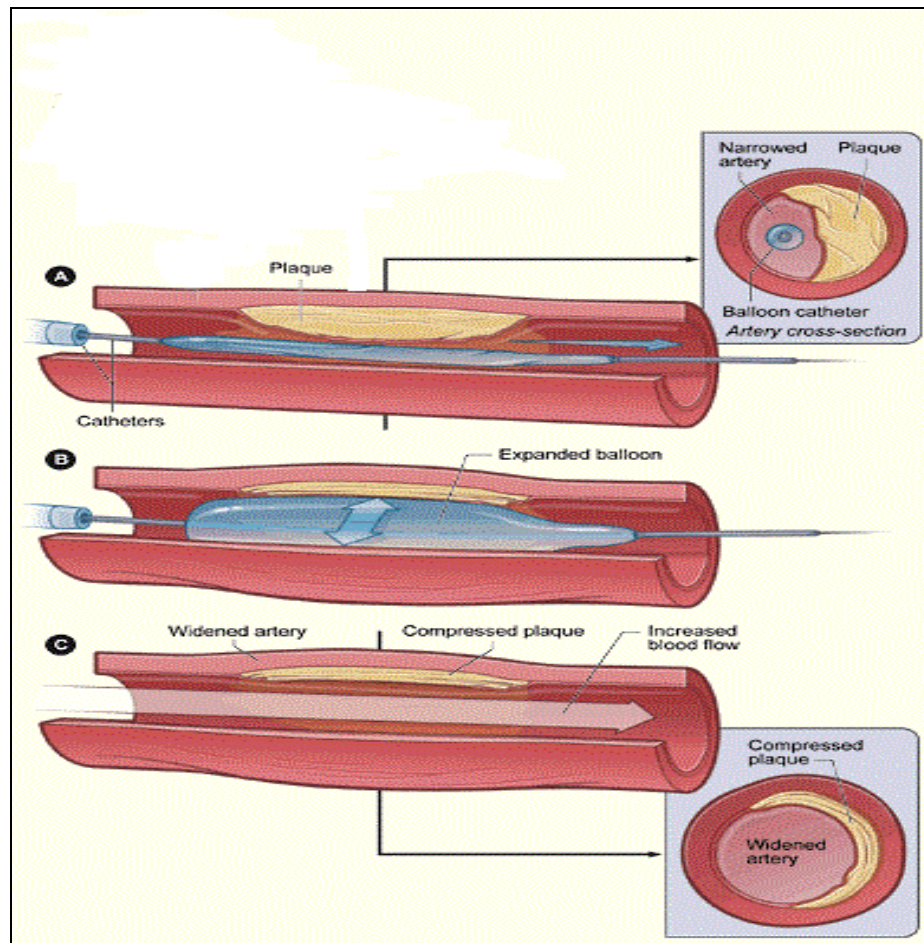
Figure 3.5: Balloon angioplasty of a narrowed artery

A stent may also be deployed at this stage to prevent restenosis of the treated vessel. A stent may be described as a cylindrical wire mesh tube (figure 3.6, A). The stent is deployed in the segment of the vessel that has undergone angioplasty (figure 3.6, B); it will remain in this position maintaining the patency of the vessel (figure 3.6, C). Figure 3.7 demonstrates how a patent stent appears within an artery.
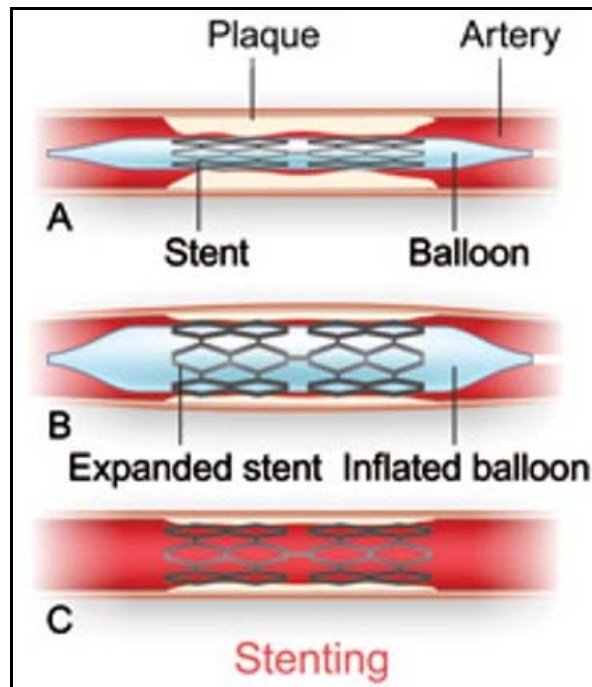
Figure 3.6: Arterial stenting technique

Stent within
and artery
CDU image
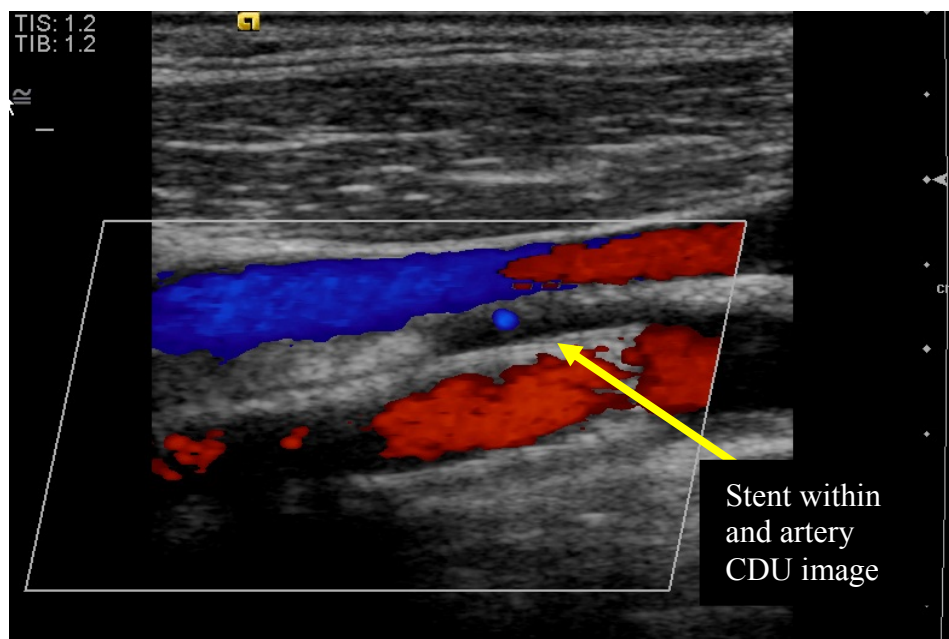
Figure 3.7: A CDU image of a stent deployed in an artery

Lower limb reconstruction is achieved by surgically bypassing the diseased portion of the artery with a segment of vein or a synthetic graft. Bypass surgery is usually indicated when the stenosed or occluded artery is not amenable to angioplasty or stenting. The graft is anastomosed proximal to the diseased segment of artery (figure 3.8). Thus, it provides an alternative route for the blood to flow around the blocked or narrowed segment of artery and supply blood to the lower limb. Surgical intervention requires regular surveillance with ABI's and CDU in order to ensure patency of the graft.
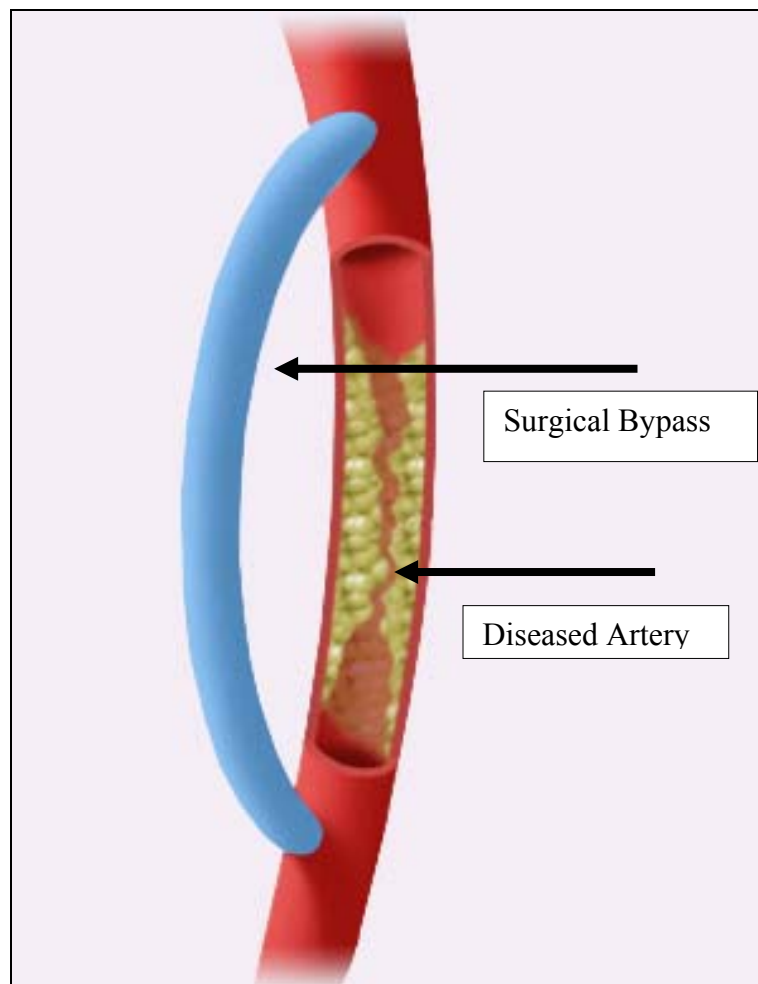
Figure 3.8: Surgical bypass of a diseased artery

3.2.6 Lower Limb Amputation

In very rare cases limb loss occurs despite attempts at revascularisation. The risk of a person with claudication progressing to critical ischemia resulting in amputation is as low as 1% per year (Transatlantic inter society consensus document). In these cases intervention usually occurs as a result of multiple diseased arteries in the lower limbs (Leiner et al., 2003). Patients that present with critical limb ischemia have a one year amputation rate of 30% and a mortality rate of 25% (Feiring et al., 2010).The need for amputation is 5-10 times higher in diabetic patients than those without diabetes (Norgren at al., 2007). However, a large portion of patients that are diagnosed with PAD never need to undergo any form of intervention.

The main aims of amputation of a major limb are removal of diseased tissue, obtaining adequate pain relief and achieving healing of the amputation at the chosen level to facilitate construction of a stump which will allow the amputee to mobilise on a prosthetic limb.

The majority of lower limb amputations are performed for vascular and infectious complications of diabetes mellitus, 15-35% of these patients will lose a second leg within 5 years (High et al., 1984).

Amputations are performed at the level at which healing is most likely to occur and permit the most effective use of the limb after surgery. However, despite successful amputation of a limb complications can occur late in the recovery phase inhibiting the patient's ability to use their prosthesis.

3.3 Carotid Artery Disease

3.3.1 Introduction

Stroke is the third leading cause of death in the world. The world health organisation in 2007 documented that 15 million people suffer a stroke worldwide each year, 5 million die and another 5 million are left permanently disabled. It is the most common life threatening neurological disease and the leading cause of adult disability in Europe (Higashida and Meyers. 2006).

Europe averages approximately 650,000 strokes per year. In developed countries, the incidence of stroke is declining which the world health organisation feels is largely due to efforts to lower blood pressure and increase smoking cessation. However, the overall rate of stroke remains high due to the ageing population.

Transient Ischemic attack or TIA's as they are more commonly known have a prevalence of 5 per 1000 of the population. Between 10-12% of this group of patients will go on to develop a stroke within the first week of their TIA (Gulli, Khan and Markus. 2009). A TIA is defined as the complete resolution of focal cerebral ischemia symptoms within 24 hours (Zweibel, Fifth edition, 2005, page 107). After a TIA, the risk of stroke is 12-13% during the first year and increases to 30-37% within 5 years (Henry et al., 2000). Patients who have suffered a TIA have a 13 fold risk of stroke during the first year and a 7 fold risk over the first 7 years compared with people without TIA's (Dennis et al., 1990).

The national institute of neurological disorders and stroke suggests that one third of patients who suffer a TIA will go on to have an acute stroke in the future.

3.3.2 Aetiology

A stroke may be due to cerebral ischemia or cerebral haemorrhage. Ischemia occurs due to an arterial occlusion or stenosis and haemorrhage due to rupture of an artery. Differentiation cannot be made on clinical exam alone cerebral imaging such as computed tomography (CT) or magnetic resonance imaging (MRI) is necessary in order to definitely establish a diagnosis. The current recognised ischemic stroke mechanisms are embolism, decreased perfusion and thrombosis. Embolism to the brain may be cardiac or arterial in origin.

Plaques present in the aortic arch can act as a source of atheroembolic embolism. A transoesophageal echo will allow detection of these plaques, the presence of which is an established risk factor for ischemic stroke being associated with a 2.5 to 9 fold increase in the stroke risk in case controlled studies (Tullio et al., 2009). Treatments with oral anticoagulants, antiplatelet agents or surgery to remove the plaque are all options. The presence of severe stenosis in the carotid arteries and basilar artery may lead to stroke due to perfusion failure. Carotid artery stenosis is generally thought to induce stroke by either compromising cerebral perfusion or by embolic phenomena. Intracranial atherosclerosis accounts for 29% of all ischemic events (Higashida and Meyers. 2006). Ninety percent of all extracranial carotid lesions are due to atherosclerosis (Singh, O'Donnell and Gillespie. 2010).

3.3.3 Signs and Symptoms

The main presenting signs and symptoms are focal and non focal symptoms which may be transient or permanent, carotid bruits and anatomical abnormalities

i   Focal and Non focal symptoms

Focal symptoms only relate to one side of the body and are usually called lateralising. They may be attributed to problems in only one of the hemispheres relevant to the anterior circulation. Focal brain ischemia occurs when a blood clot has occluded a cerebral vessel, thus reducing the blood flow to that particular portion of the brain and increasing the chances of cell death in that area. Focal symptoms include transient blindness in one eye (amaurosis fugax), speech disturbances and loss of power to one arm or leg or even loss of power to one complete side of the body.

Non focal symptoms are difficult to assign to one particular side of the brain. They may be associated with the posterior circulation or the brain stem resulting from vertobasilar disease. Non focal symptoms may be dizziness, ataxia, syncope, confusion and bilateral vision loss.

ii   Carotid Bruit

A carotid bruit is a systolic sound heard over the carotid arteries during physical examination of the patient, it occurs as a consequence of the turbulent flow within the artery which can be due to either a stenosis or a tortuous carotid artery system. It is very unreliable clinical sign.

iii Altered Anatomy

Visible or palpable pulsitile swellings at various sites may indicate the presence of an aneurysm or pseudo aneurysm which may give rise to cerebrovascular symptoms if left untreated. The carotid bifurcation is a common site of carotid artery aneurysms and carotid body tumours (figure 3.9) may occur typically within the bifurcation splaying the vessels apart as it enlarges.
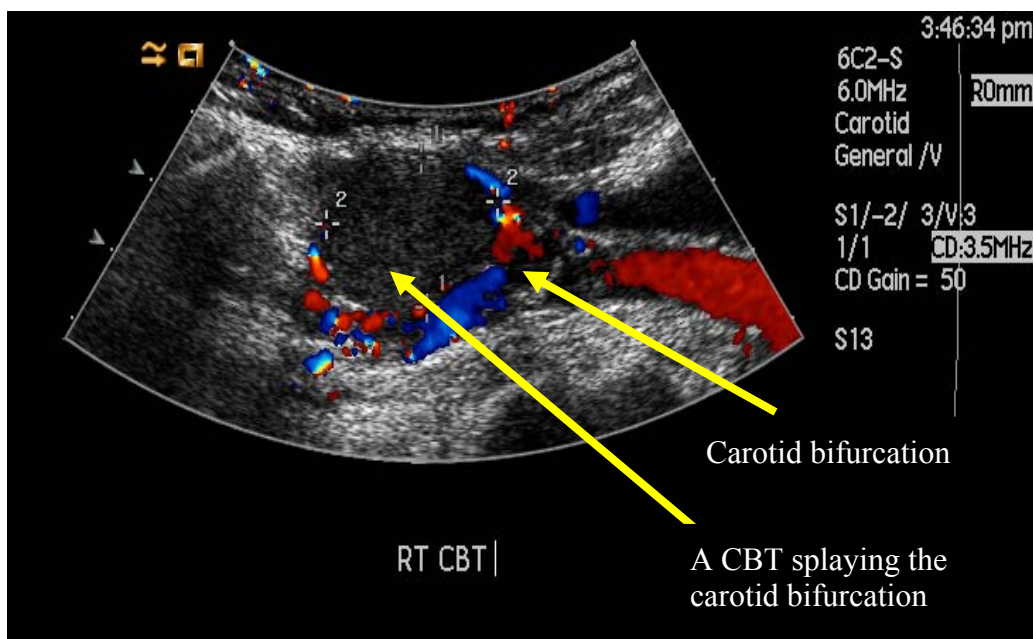
Figure 3.9: A carotid body tumour

Figure 3.9 illustrates a typical carotid body tumour that is lying between the internal carotid artery (ICA) and the external carotid artery (ECA) at the carotid bifurcation and splaying the vessels around the tumour.

3.3.4 Clinical Assessment

An acute onset focal neurological deficit must be regarded as a stroke or TIA until proven otherwise. A rapidly performed brain CT will exclude haemorrhage. It is thought that ~50% of all ischemic, carotid territory TIA's or stroke occurs as a consequence of thrombo embolism or atheroembolic debris from extracranial carotid lesions (Silvennoinen et al., 2007). Transient monocular blindness sometimes referred to as amaurosis fugax is typically described by patients as a transient shadow or curtain obscuring all or part of the visual field in one eye (Cole, Norris and Walker. 2001). This may last only a few seconds or may persist for several hours; it may be caused by an embolism into the ophthalmic artery which is the first major branch of the intracranial portion of the ICA.

Embolisation from the ICA commonly leads to a temporary or permanent focal neurological deficit in the middle cerebral artery territory. Emboli from the ICA may enter the middle cerebral artery and less commonly enters the anterior communicating artery. Patients that present with typical carotid artery territory symptoms may benefit from intervention.

3.3.5 Treatment of Carotid Artery Disease

i   Carotid Endarterectomy

The aim of carotid artery intervention is to prevent cerebrovascular events in the ICA territory. Approximately 15-20% of stroke patients report a previous TIA, the time window for prevention of a stroke is small with over 40% of TIA's occurring during the week preceding the stroke (Rothwell. 2008).

Multiple studies have shown that symptomatic patients with a >70% ICA stenosis will benefit from a carotid endarterectomy (CEA) and thus reduce the risk of a subsequent ipsilateral stroke.

The North American Symptomatic Carotid Endertrectomy Trial (NASCET) which included data from 50 clinical centres around the United States and Canada demonstrates the benefits of surgery in patients with an ICA stenosis of between 70-99% who have suffered a recent TIA or stroke. It randomised 2226 patients with a symptomatic ICA stenosis to medical care or CEA. Patients had their TIA or stroke within 4 months of enrolment and were categorised into the 30-69% group and the 70-99% group. For patients in the greater than 70% stenosis group, CEA reduced the risk of any ipsilateral stroke from 26% to 9% at 2 years (North American Symptomatic Carotid Endertrectomy Trialists' Collaborative Group. 1991).

The Asymptomatic Carotid Atherosclerosis Study (ACAS) demonstrated the benefits of surgery for a stenosis greater than or equal to 60% with low rates or preioperative complications. This trial randomised 1662 asymptomatic patients

with a 60% or greater ICA stenosis to CEA and medical therapy or medical therapy alone (Moore et al., 1998).

CEA reduced the estimated risk of ipsilateral stroke or death from 11% to 5.1%. These findings led to a major increase in the number of CEA's performed in asymptomatic patients in the United States, in contrast the ACAS results had little effect on the number of CEA's performed in other countries such as the United Kingdom, where it was felt that the benefit did not justify the cost. It was estimated that 40 operations were needed to prevent 1 disabling or fatal stroke after 5 years. (Rothwell and Goldstein. 2004).

The Asymptomatic Carotid Surgery Trial (ACST) published in 2004 was an international multicentre randomised trial set up to compare the efficacy of CEA performed in conjunction with medical therapy with that of medical therapy alone in prolonging stroke free survival time in patients with asymptomatic ICA stenosis. Patients were included in the study if they had either a unilateral or bilateral ICA stenosis considered for surgery, who had experienced no symptoms of TIA or stoke within the past 6 months, had no history of disabling stroke and had no contraindication for CEA. The authors concluded that at 5 years the risk of stroke or death in the CEA group was 6.4% when compared to 11.8% in the best medical management group. They also demonstrated that asymptomatic patients were less likely to have a fatal or disabling stroke, 3.5% in the CEA group when compared to 6.1% in the best medical therapy group (Hallinday and Mansfield. 1994)

The ACST study confirmed the findings of the ACAS trial. ACST confirms the overall benefit from surgery in patients with asymptomatic ICA narrowing of 60-99% with the most benefit noted in patients under the age of 75 years.

Digital subtraction angiography (DSA) has long been considered the gold standard method of assessing carotid artery stenosis. CDU, MRI and CT are now all widely accepted methods of assessing the extracranial carotid arteries with a lower risk to the patient. Due to the risk of morbidity and mortality associated with the invasive procedure of cerebral angiogram most centres have employed the use of the non-invasive method of CDU in the detection and grading of carotid artery stenosis. CDU has a sensitivity of 98% and a specificity of 88% when compared with angiography (Jahromi et al., 2004).When CDU is inconclusive an MRA or CT angiogram maybe performed and DSA is now only used when there is discordance between two imaging modalities.
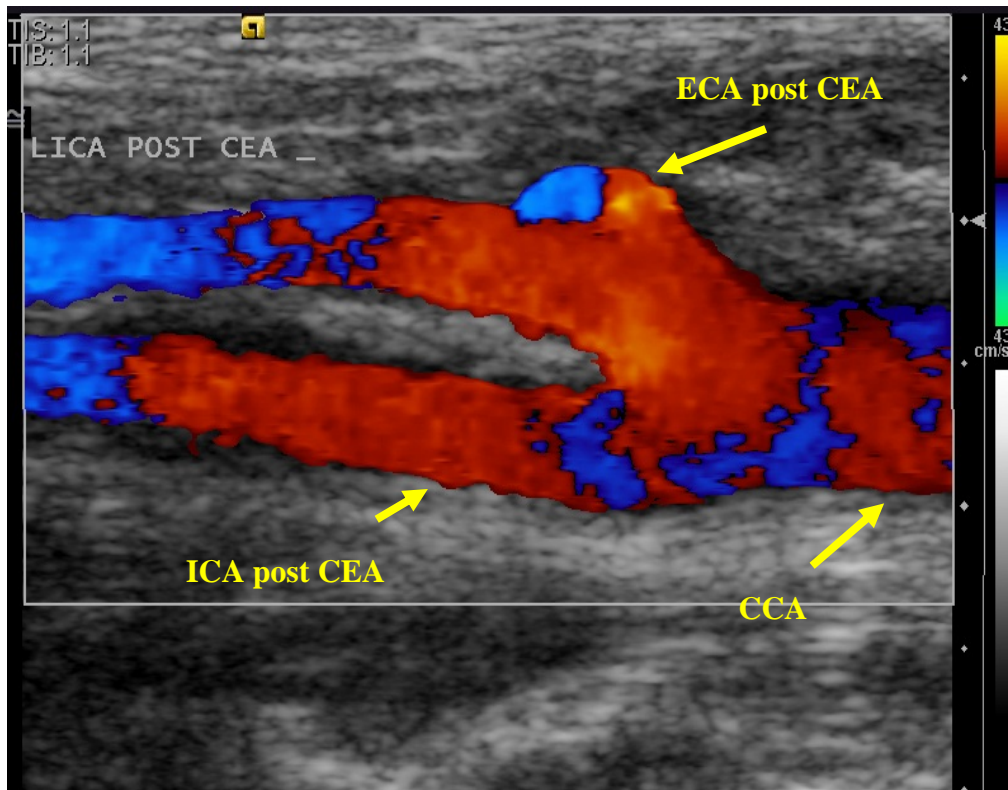
Figure 3.10: The carotid bifurcation after CEA

ii. *Carotid artery stenting*

With advantages such as being less invasive, no neck incision, no risk of cranial nerve injury and a shorter hospital stay, carotid artery stenting was thought to play a huge role in carotid artery surgery. However, a consensus has not yet been established. A Cochrane review carried out in 2007 showed that there was no significant difference in late stroke risk and they subsequently concluded that there was no current data to support a move away from the traditional method of surgery CEA.

In 2006, results of a randomised control trial for carotid stenting versus CEA in symptomatic patients, the Stent-Supported Percutaneous Angioplasty of the Carotid Artery versus Endarterectomy (SPACE) trial failed to demonstrate the advantages of carotid artery stenting over CEA. This study of over 1200 patients showed a higher rate of ipsilateral ischemic stroke and death at 30 days in patients undergoing carotid artery stenting. The trial concluded that there was no evidence to justify the widespread use of carotid artery stenting for the treatment of CAD.

The international carotid stenting study (ICSS) also compared carotid artery stenting to CEA in symptomatic patients. The authors demonstrated that a higher incidence of stroke and death with stenting when compared to CEA. These results were consistent with those found in the SPACE trial. However they also documented that carotid artery stenting was more costly than CEA, and concluded that it should perhaps be reserved for a select group of patients for whom CEA cannot be offered (Paraskevas. 2010).

3.4 Abdominal Aortic Aneurysms

3.4.1 Introduction

Abdominal Aortic Aneurysms (AAA's) are the end result of a mutifactorial disease process affecting a high proportion of our elderly population. Ruptured AAA's are among the tenth leading causes of death in elderly males and about half of all patients with an AAA can expect to die of rupture if their aneurysm is not surgically treated (Siegel and Cohen. 1994). It is thought that between 4-11% of the elderly population over the age of 60 has an AAA, they are rarely present in persons under the age of 65 (Posacioglu et al., 2002). The general consensus from the multiple screening studies that have been carried out is that AAA's occur in 2-13% of males and 6% of females over 65 years of age and approximately 90% of aneurysms discovered on screening programmes are less than 3.5cm. Only 30-40% of aneurysms are noted on physical examination with detection dependent on aneurysm size and limited by factors such as obesity. An AAA may be present in 85% of patients with femoral aneurysms and 62% of those with popliteal artery aneurysms. However, only 14% of patients with an AAA will have a femoral or a popliteal artery aneurysm (Chaikof et al., 2009).

The prevalence of AAA is increasing probably due to increased life expectancy. AAA's are often co-incidentally discovered on other examinations such as ultrasound or CT being performed for other disease processes. They are clinically silent and therefore rupture is often the first presentation. The mortality rate for ruptured AAA's is substantial, as many as 2 of 3 patients with ruptured AAA's die before reaching the hospital. Of the patients that reach hospital, as many as one

fifth die before undergoing surgery and the overall in hospital mortality rate still averages approximately 49% (Tan. 2010).

The discovery of an aneurysm at an early stage means that a patient can then be entered into a surveillance programme and monitored closely for growth of the AAA allowing consideration for repair of the aneurysm at the correct stage.

The term aneurysm is derived from the Greek word "aneurysma" meaning "a widening". With much variation in the literature as to the correct definition of an aneurysm the following is perhaps the most widely accepted "An artery is considered aneurysmal when its diameter equals or exceeds 1.5 times the normal diameter of the artery in question". The normal diameter of the aorta in the majority of adults does not exceed 2cm and so it is considered aneurymsal at 3cm" (Zweibel. 2005). Normal arterial diameter is dependent on factors such as age, gender and body size so, by practical convention an aneurysm is defined as a localised dilation of an artery at least 50% larger than the normal adjacent portion of the same artery. (Rutherford, Fifth edition, page 1241). Diffuse enlargement of several arterial sections along the arterial tree is referred to as "arteriomegaly".

The majority of AAA (approximately 90%) occur below the origin of the renal arteries and extend to the iliac bifurcation (Dobrin. 1989). Approximately 10% of all aneurysms involve the renal arteries (Siegel and Cohen. 1994).

Surveillance of an AAA depends on its maximum transverse diameter or anterior to posterior wall diameter and follow up periods may vary from centre to centre. Recommended guidelines for surveillance of an infra renal AAA are summarised in the following table.

Maximum diameter of AAA	Follow up period
2.6cm-2.9cm	5 yearly intervals
3.0cm-3.5cm	3 yearly intervals
3.5cm-4.4cm	1 yearly interval
4.5cm-5.4cm	6 monthly intervals

Table 3.1: Recommended surveillance for abdominal aortic aneurysms

(Chaikof et al., 2009)

Maximum AAA diameter remains the most widespread criterion to assess AAA rupture risk, but a variety of alternative parameters have been proposed as more sensitive predictors of rupture risk including AAA expansion rate, increased intraluminal thrombus thickening, wall stiffness, wall tension and peak AAA wall stress. In the majority of cases surgery is usually considered when an aneurysm reaches 5.5cm in males and 5cm in females. Table 3.2 summarises the risk of rupture of an AAA.

Size of AAA	Risk of rupture
<4.0cm	Minimal
4.0cm-5cm	0.5-5%
5.0cm-6cm	3-15%
6.0cm –7cm	10-20%
7.0cm- 8cm	20-40%
>8.0cm	30-50%

Table 3.2: Risk of rupture of abdominal aortic aneurysms

(Brewster et al., 2003)

Larger aneurysm enlarge rapidly were as smaller ones tend to expand very little. The majority of smaller aneurysms grow at a rate of 0.3cm – 0.5cm per year (Lederle. 2003). Rapid enlargement of the AAA between consecutive 6 monthly visits is also an indication for urgent repair of an AAA.

CDU has become the method of choice for AAA screening and surveillance. The methodology of AAA measurement is a constant source of debate with some advocating outer wall to outer wall, inner wall to inner wall or outer wall to inner wall.

Outer wall to outer wall is what surgeons see when operating, so perhaps this is the correct method. The most important factor is that all measurements are consistent and reproducible from visit to visit. Measurements are always taken and compared from visit to visit in a transverse plane. Measurements taken in an axial plane are thought to be overestimated and therefore should be avoided. This is due to the fact that lateral borders are sometimes not clearly seen and the presence of mural thrombus often makes it difficult to pick out the walls of the aorta accurately.

As AAA's are predominantly silent and asymptomatic, screening of a high risk population of elderly patients for detection of an AAA is necessary for effective treatment. The U.S Preventative Task Force recommends one time screening for males 65-75 years of age who have ever smoked at least 100 cigarettes in their life time. The Multi Centre Aneurysm Screen Study (MASS) suggested that there was a 32% reduction in AAA related deaths in a screened population of men. The Aneurysm detection and Management Veteran Affairs Cooperative study group (ADAM) compared the long term follow up of patients. Those followed with

surveillance and surgical intervention when the aneurysm reached 5.5cm versus the immediate surgical repair of an AAA <5.5cm. No significant difference was discovered between the two groups in terms of long term follow up and mortality and thus the study concluded that there was no long term benefit to repairing asymptomatic aneurysms less than 5.5cm. The United Kingdom Small Aneurysm Trial (UKSAT) followed its 10,000 participants for a period of 10 years and also documented no long term benefit to electively repairing asymptomatic AAA's greater than 5.5cm. Chaikof et al in 2009 recommended that one time ultrasound screening for an AAA for all men at or older than 65 years, or as early as 55 years in males with a family history of AAA. They also recommended that AAA screening should be carried out in females greater than 65 years who smoked and had a family history of AAA.

3.4.2 Etiology

i   Risk Factors

Risk factors such as advanced age, greater height; coronary artery disease, atherosclerosis, hypercholesterolemia, hypertension, smoking and gender are associated with a greater risk of developing an AAA (ADAM).

Smoking has been found to be the most significant factor associated with increase in aneurysm size, more commonly the number of years the person has smoked compared to the number of cigarettes smoked per day. A smoker has a sevenfold increased risk of developing an AAA than a non smoker. Family members are also at a greater risk of developing an AAA with a 12% to 19% of those undergoing aneurysm repair having a first degree relative with an AAA (Chaikof et al., 2009).

AAA's rarely affect people younger than 40 years of age, with a six fold greater incidence in males than females (Chaikof et al., 2009). Other less common causes of AAA's can be infection, arthritis, cystic medial necrosis, trauma, inherited connective tissue disorders.

ii   Signs, Symptoms and Diagnosis

The majority are asymptomatic and are largely discovered coincidently on other examinations such as a routine clinical exam, x-ray, ultrasounds and CT's performed for other disease processes.

AAA's rarely produce any definite signs, if the patient is thin a pulsation or a swelling in their mid abdomen may be palpated, this would not be evident in larger patients. Detection of an aneurysm during a physical exam depends on factors such as body habitus with only 76% of aneurysm being noted on physical exam being greater than 5cm, 3cm-3.9cm aneurysms are only palpated in 29% of patients (Chaikof et al., 2009).

The major complications are due to rupture, thrombosis or embolism of some thrombus from the aneurysm to the lower limbs causing ischemia. Patients presenting with severe abdominal or back pain, hypotension and a pulsatile abdomen would be of high suspicion for a ruptured AAA.

3.4.3 Treatment of Abdominal Aortic Aneurysms

Aneurysms of the abdominal aorta can take many shapes and forms however, can generally be classified according to their location, size, shape and etiology. The shape of an aneurysm may be described as fusiform or saccular. However the size, shape and extent of the aneurysm may vary quite significantly from patient to patient.
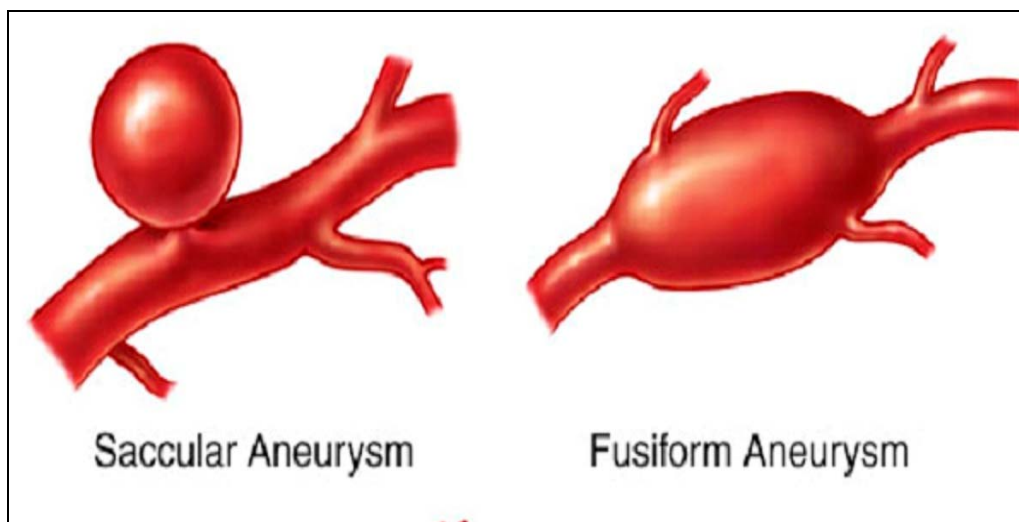
Figure 3.11: A saccular and a fusiform aneurysm of the abdominal aorta

The aetiology is the most important consideration. Although the causes of most aneurysms are known some are non specific. The majority of abdominal aneurysms are atherosclerotic however congenital aneurysms associated with arteritis and connective tissue abnormalities can occur.

These factors are taken into account along with the patient's physical condition and age when deciding which treatment is best for that patient. It is widely documented amongst the literature that patients should be considered for AAA

repair when their aneurysm reaches 5.5cm or when there has been a rapid increase in the size of the AAA (>0.5cm) between consecutive 6 monthly visits with very little evidence to support the treatment of aneurysms less than 5.5cm (UKSAT).

Two methods of AAA repair are widely practiced - open surgical repair and endovascular aneurysm repair (EVAR).

3.5 Open Surgical Repair

3.5.1 Introduction

Surgical aneurysm repair or "open" aneurysm repair is the traditional method of choice for repair for AAA's. The first described treatment of an aneurysm was reported by Antyllus in the 2nd century who recommended ligating the artery above and below the aneurysm and incising the sac and its contents. This method remained the basis of direct arterial operations for the next 1500 years (Rutherford. 2000).

The current technique of open AAA repair, replacing the aneurysmal aorta with a portion of another artery or vein was devised in the early 20th century by the 1912 Nobel Laureat Alexis Carrell who only ever performed this procedure on an animal (Dente and Feliciano. 2005).

In 1951 Charles DuBost reported the first replacement of an infra renal AAA. The use of these homografts was ceased due to the risk of rupture and degeneration that was associated with them. In 1954 Blakemore and Voorhees published their results in 16 patients who had an AAA repair with a Vinyon N graft with a 56% survival rate. In 1958 Michael DeBakey reported the use of a knitted Dacron Graft to repair infra renal AAA in a number of patients.

The principle behind any procedure to treat an AAA is to prevent rupture of the aneurysm by its exclusion from systemic circulation. Open repair achieves this with an interposition synthetic graft. To date open repair has been reported to be the most durable method of AAA repair. Elective surgical repair has been reported to have a mortality rate of less than 5% compared to the 90% mortality rate of ruptured AAA's (Johansen et al., 1991).

3.5.2 Technique

Prior to open surgical repair of an AAA a patient usually undergoes a CT scan to determine the shape of the aneurysm and its relationship to the renal and iliac arteries. If the aneurysm involves the iliac arteries or if the iliac arteries have occlusive disease present then a bifurcated graft may be used with the distal anastomosis onto either the iliac or the femoral vessels.

The aneurysm is usually approached via a midline transperitoneal approach (Figure 3.12 & figure 3.13), although a transverse incision or a left retroperitoneal approach have also been described. The small bowel is then displaced to the right side of the abdomen to expose the base of the mesentery. The posterior peritoneum is then incised from the ligament of treitz to the aorta bifurcation. This excision can be extended further if the aneurysm involves some of or all of the iliac arteries. Clamps are then placed on the distal vessels and the proximal aorta to arrest blood flow through the aneurysm and ensure that the risk of distal embolisation is minimal (figure 3.12). The aneurysm sac is opened longitudinally and any thrombus that is present is evacuated.

The graft is then sewn into place (figure 3.12). The aneurysm sac is closed over the graft to prevent contact of the graft and the intestines reducing the risk of subsequent aorto-enteric fistula.
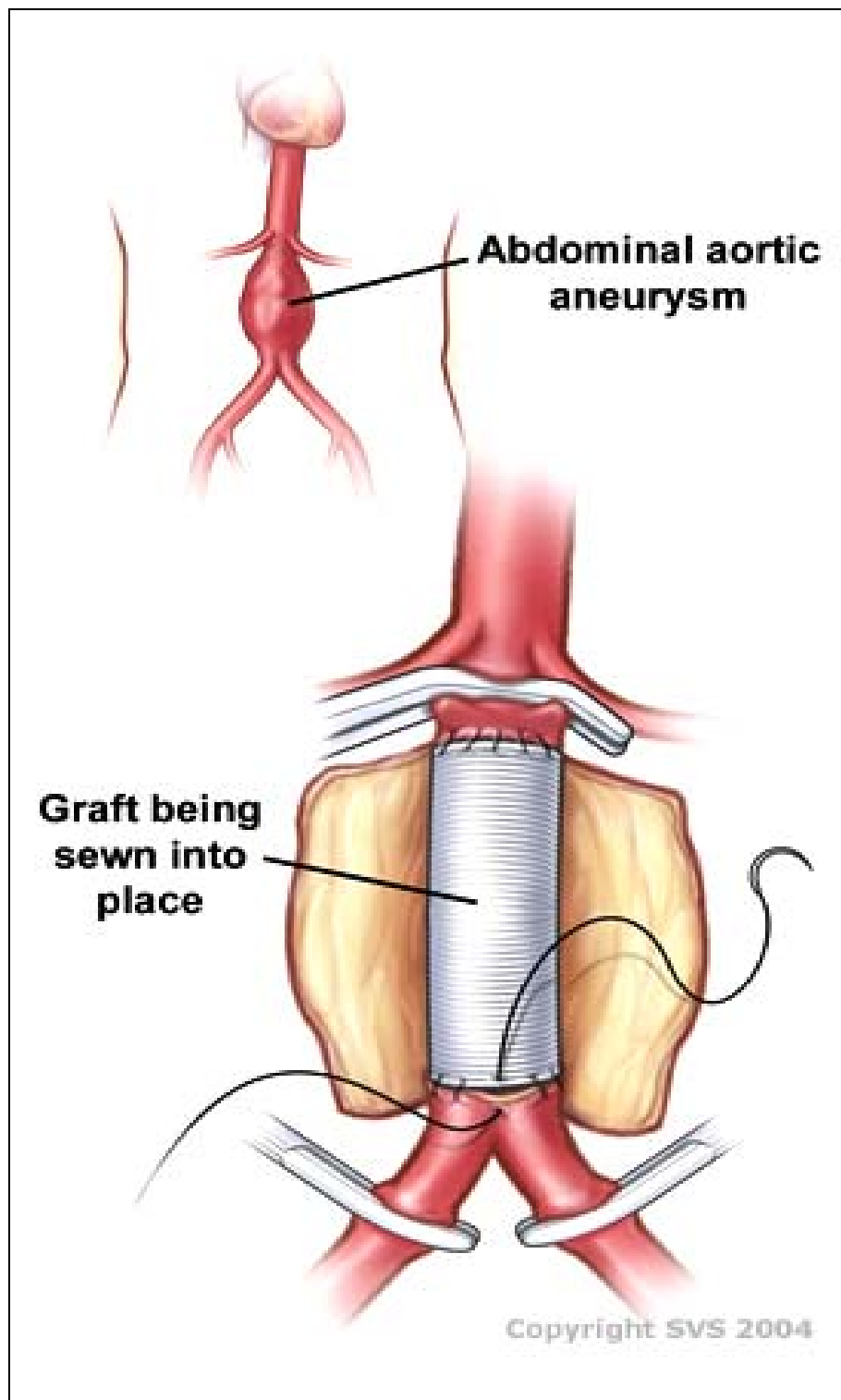
Figure 3.12: Diagrammatic representation of open surgical repair

Figure 3.13: An AAA exposed prior to open surgical repair

3.6 Endovascular Aneurysm Repair

3.6.1 Introduction

EVAR involves the transluminal placement of a graft within the aneurysm that completely excludes the aneurysm from the systemic circulation (figure 3.14). The graft is held in place by a self expandable metal frame which supports the graft and provides a seal proximal and distal to the aortic aneurysm. Once the graft is fixed within the AAA it permits flow to only go through the graft and therefore excludes the aneurysm from systemic circulation however, in contrast to open surgical repair the native aneurysm remains in place.

The first reported series of endografts used in high risk patients was in 1991 by Parodi and colleagues. Since then the use of endovascular grafts to repair AAA's has increased dramatically such that is no longer a novel technique to vascular surgeons.

In the majority of cases the stent is deployed just below the renal arteries and as close to the iliac bifurcation as possible, previously this precluded the repair of aneurysms that commenced at or above the level of the renal arteries by endovascular means. There are now commercially available devices which can repair AAA's that involve the renal arteries.

As deployment of an endovascular stent avoids the need for a laparotomy, cross clamping of the aorta, ischemia reperfusion injury and the obvious reduced blood loss associated with opening an aneurysm, EVAR rapidly became the method of choice for AAA repair for the vast majority of vascular surgeons. It has also been proven by large multicentre trials such as the Dutch Randomised Endovascular

Aneurysm Management trail (DREAM) and the Endovascular Aneurysm Repair 1 and 2 trials (EVAR 1 and 2 trials) that EVAR has a lower 30 day post operative mortality when compared to the open surgical method.
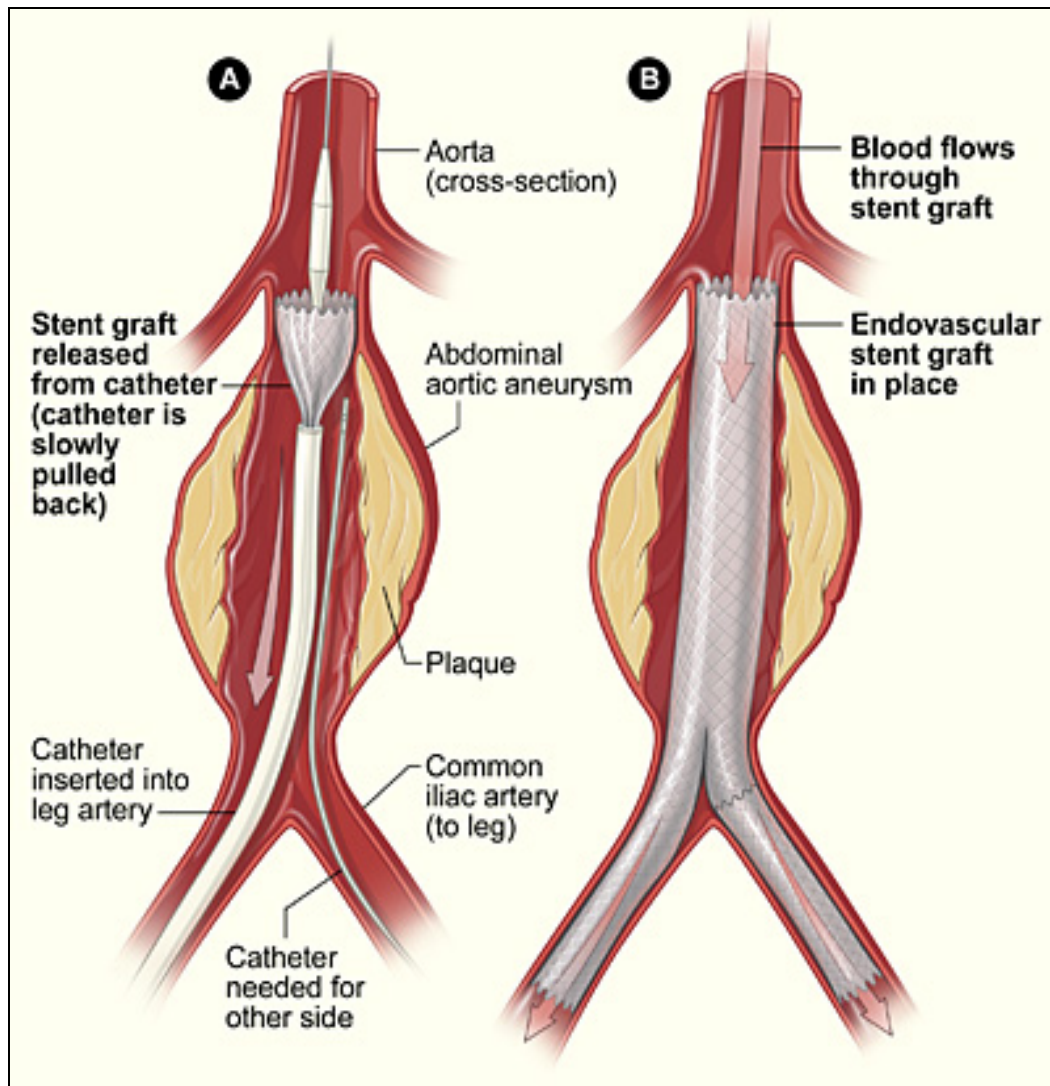
Figure 3.14: Deployment of an endovascular stent

It is also possible to carry out other procedure at the same time of EVAR such a
femoral to femoral crossover grafts for bypassing iliac artery occlusions (figure
3.15).
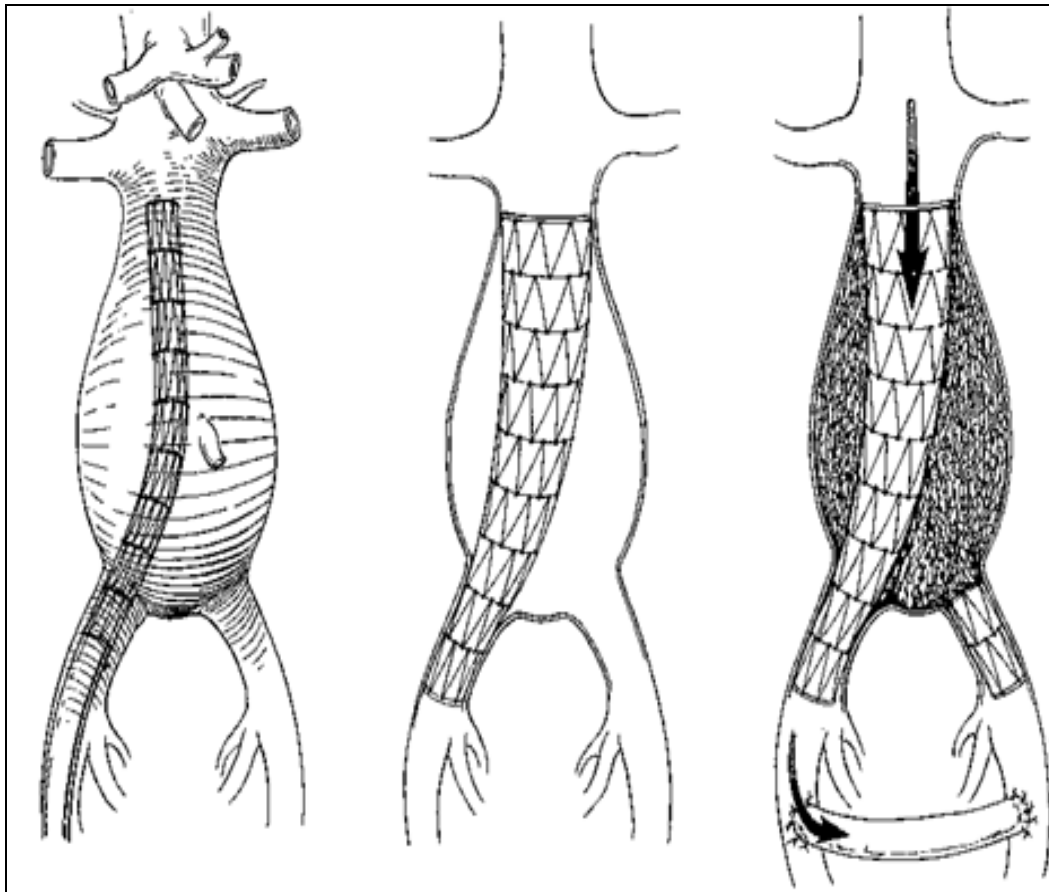
Figure 3.15: Deployment of an aorta uni-iliac graft and femoral to femoral

crossover graft
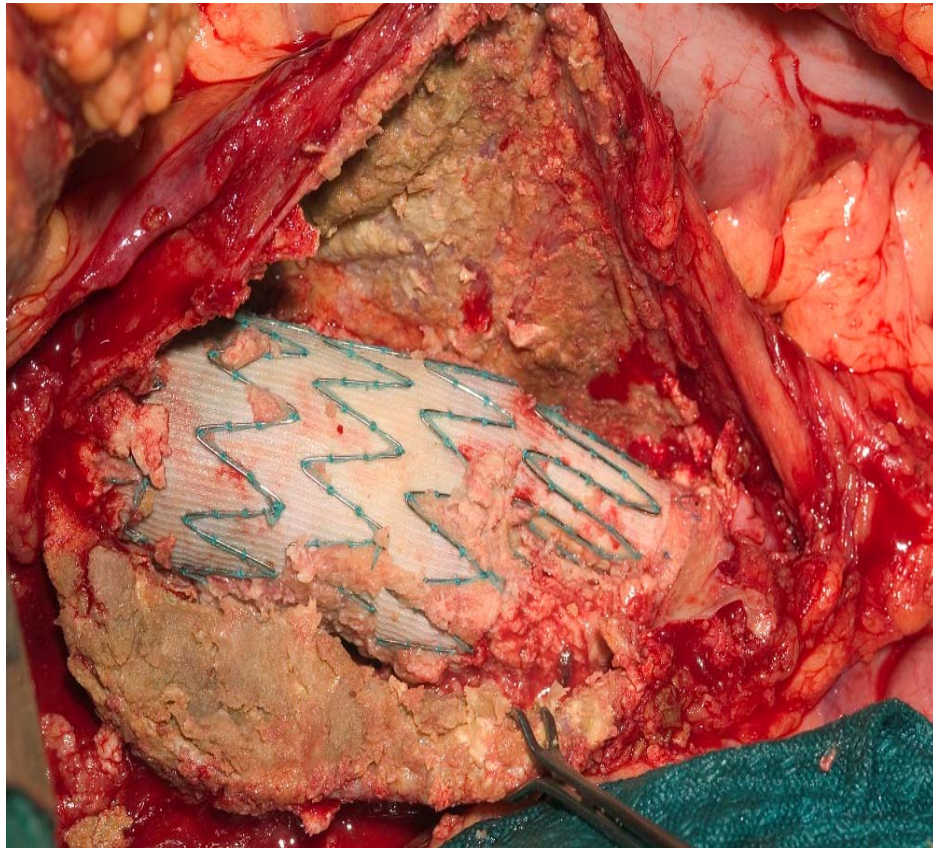
Figure 3.16: An endovascular stent deployed within an AAA

Figure 3.16 demonstrates an endovascular graft within an AAA. This patient initially underwent EVAR repair of their aneurysm however, was later converted to open repair due to complication referred to as endotension which is discussed later in this chapter.

There are a number of advantages to EVAR, other than the reduced 30 day mortality making it the primary method of choice for AAA repair. The most documented being the use of a small incision in both groins instead of the large abdominal incision needed for open surgical repair, no need for a laparotomy or prolonged clamping of the aorta, a reduced hospital stay and a quicker overall recovery time (Visser et al., 2006).

However, as with all surgeries there are also a number of disadvantages to this new technique and EVAR has its own unique set of complications. The commonest of these complications being termed "endoleaks".

The term endoleak was first described by White and colleagues in 1996. Endoleaks are defined as the persistence of flow outside the lumen of the endoluminal graft but within an aneurysm sac or adjacent vascular segment being treated by the graft (Rutherford. 2000). Thus, the aneurysm is not completely excluded from systemic circulation and is still at a risk of rupture because there is an incomplete sealing or exclusion of the aneurysm sac which is evident on an imaging modality.

Although EVAR is associated with other complications such as, stent migration, infection, limb thrombosis leading to embolisation, separation of limbs and endotension, it is the complication of endoleak that is the most common and most troublesome. Thus patients whom have had endovascular repair need to undergo lifelong surveillance.

3.6.2 Classification of Endoleaks

Endoleaks are typically classified into one of four categories:

i. *Type 1*

Type 1 endoleaks represent an inadequate seal of the graft ends and thus the blood flow into the sac originates at one of the attachment sites.

Type 1 endoleaks can be further divided into *Type 1a* (flow originating from the proximal sealing zone) and *Type 1b* (flow originating from the distal sealing zone). Separation of the graft from the arterial wall causing flow into the aneurysm sac ultimately means the aneurysm has not been excluded from the systemic circulation and thus is at risk of rupture.

Type 1 endoleaks may occur as a consequence of unsuitable anatomy such as an angulated neck proximally or tortuous iliac arteries distally. They require immediate attention. Figure 3.17 and 3.18 demonstrate a *Type 1a* and *Type 1b* endoleak. A CDU image of a *Type 1b* endoleak is illustrated in a figure 3.22.

Extra stent flow originating from the proximal attachment site
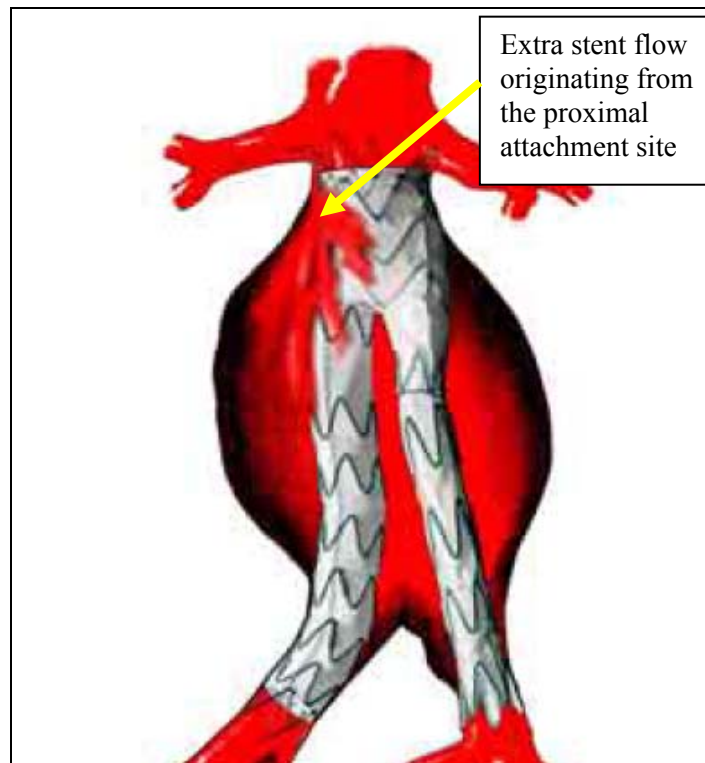
Figure 3.17: Diagrammatic representation of a type 1a endoleak. Extra stent flow can be seen originating from the proximal attachment site

Extra stent flow originating from the distal anastomosis site
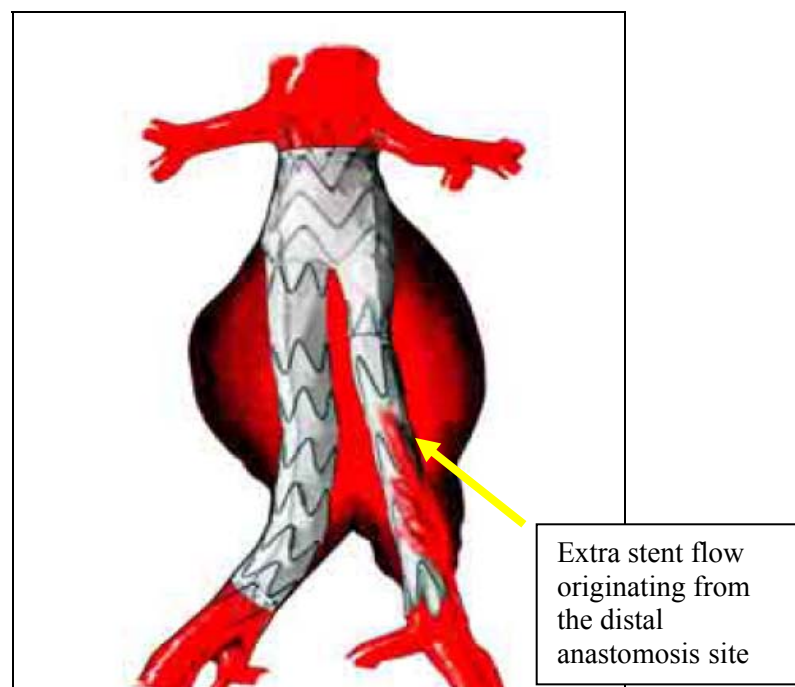
Figure 3.18: Diagrammatic representation of a type 1b endoleak. Extra stent flow can be seen originating from the distal anastomosis site

ii. *Type 2*

Type 2 endoleaks (figure 3.19 & 3.23) represent persistent flow into the aneurysm sac from collateral circulation such as lumbar arteries or a patent inferior mesenteric artery.

Flow is retrograde and these endoleaks are not graft related so a complete seal around the attachment sites is maintained. However, as with *Type 1* endoleaks a direct communication with the systemic circulation is present when a *Type 2* endoleak exists.

Type 2 leaks are the most common type of endoleak to occur following endovascular repair and have been reported to occur in up to 20% of patients following EVAR (Jones et al., 2007).

 In the majority of cases they do not require immediate intervention, quite often close monitoring for a residual sac size with the presence of a patent *Type 2* endoleak is appropriate management.

Flow originating from a patent collateral vessel which is feeding the residual sac
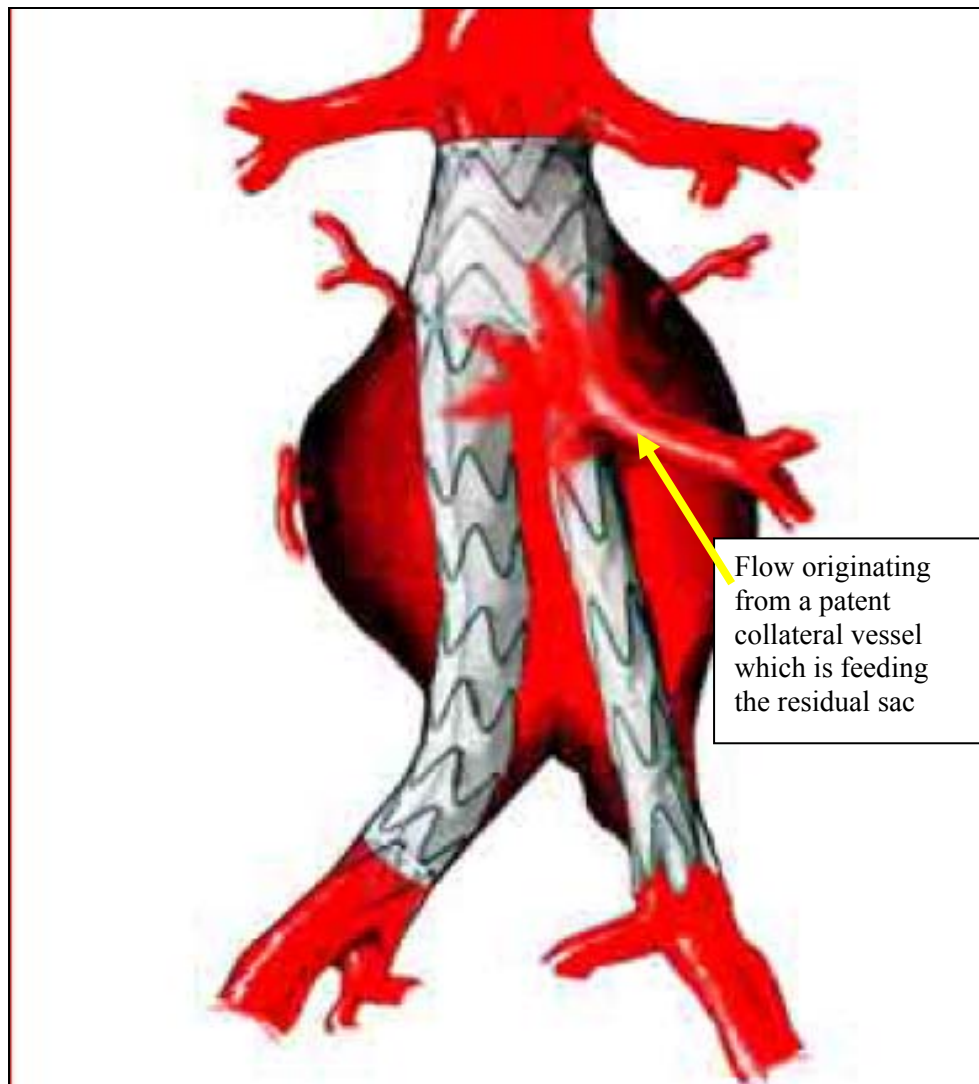
Figure 3.19: Diagrammatic representation of a type 2 endoleak

Flow can be seen originating from a patent collateral vessel which is feeding the residual sac. Figure 3.23 demonstrates the appearance of a Type 2 endoleak on a CDU image.

iii. Type 3

Type 3 endoleaks occur when there has been a structural failure in the graft such as stent fracture, the development of holes within the stent walls or junction separations between the components of the modular device. Like *Type 1* endoleaks, *Type 3* are high pressure leaks and require urgent correction, otherwise they are likely to lead to aneurysm sac expansion and rupture. *Type 3* endoleaks are rare however they may be become more apparent over time as more information is gathered. Figure 3.20 below demonstrates a type 3 endoleak; flow into the aneurysm sac can be seen originating from the left iliac limb attachment site.

Flow into the aneurysm sac can be seen originating from the left iliac limb attachment site
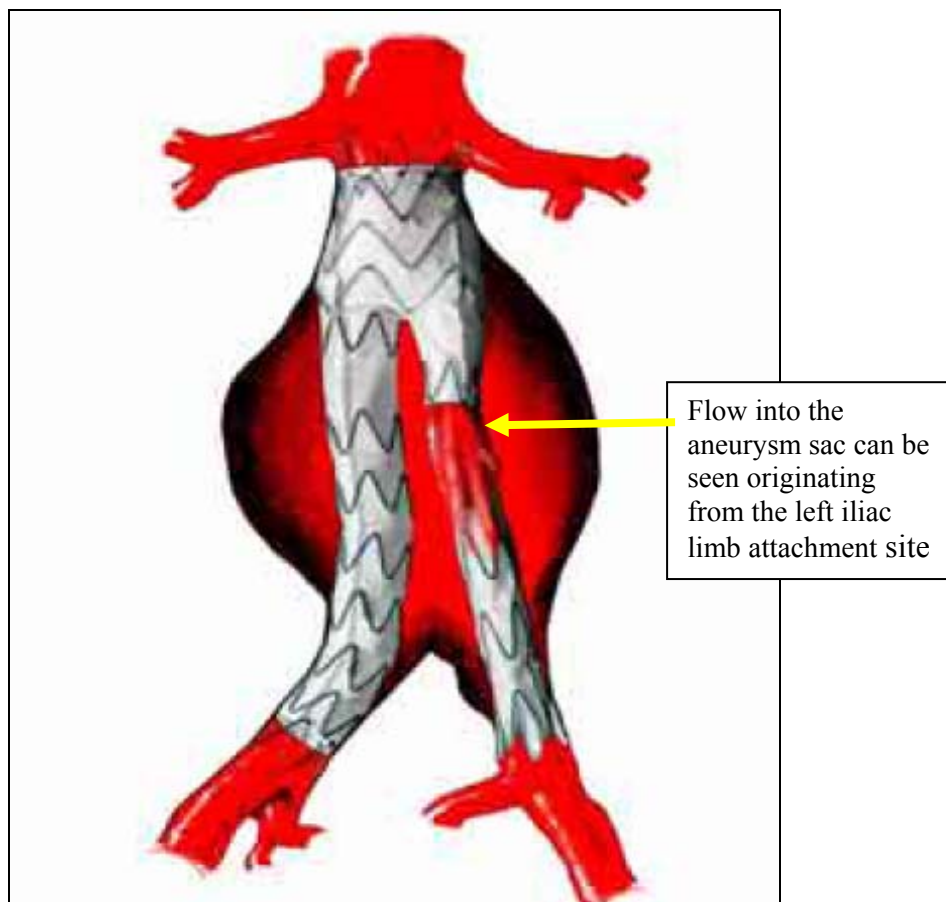
Figure 3.20: Diagrammatic representation of a type 3 endoleak

iv. ***Type 4***

Type 4 endoleaks (figure 3.21) are related to the porosity of the graft within 30 days. Opacification of the aneurysm sac instantly after stent placement without an apparent source of leakage is designated a type 4 endoleak. They occur during the procedure and are transient, resolving after removal of anticoagulation (Bashir et al., 2008)

Opacification of the aneurysm sac
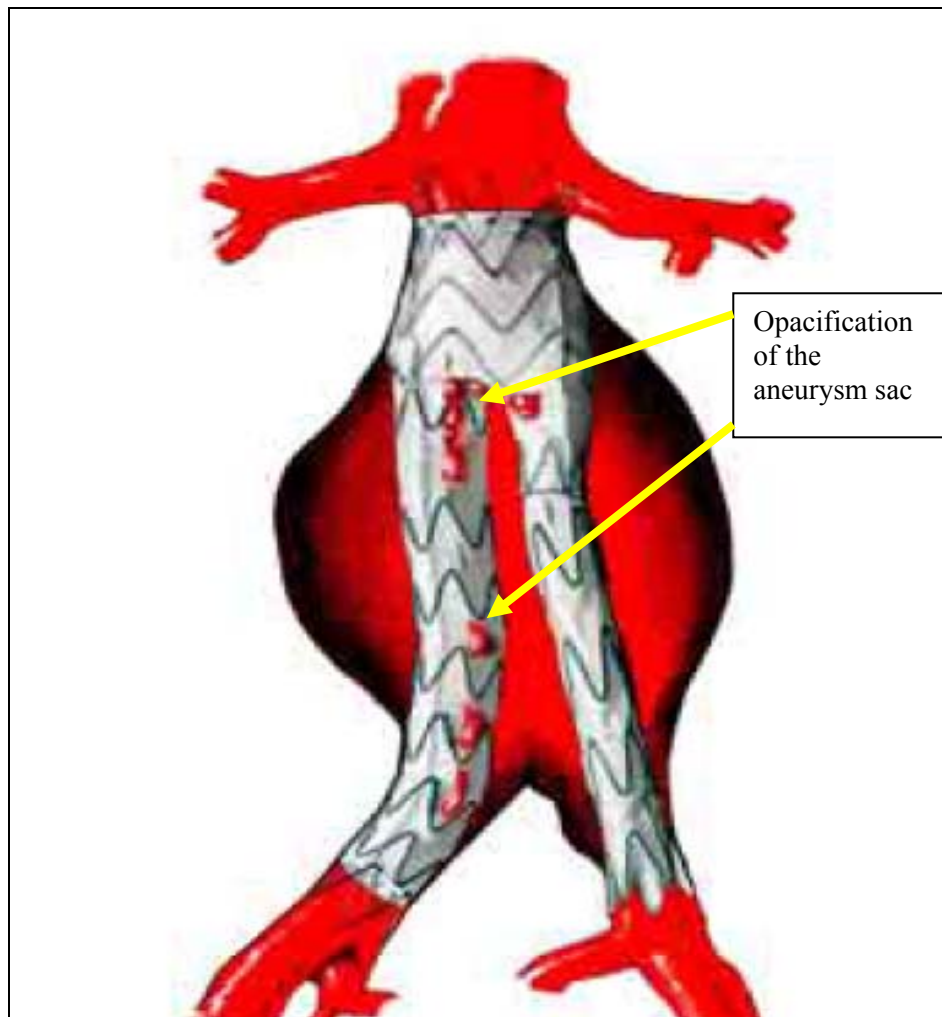
Figure 3.21: Diagrammatic representation of a type 4 endoleak

v. **Type 5**

Type 5 endoleaks are more commonly referred to as "endotension". This may cause a continued expansion of the graft without the presence of a documented endoleak on any imaging modality. While the true nature of endotension has never been documented, it may be due to the presence of a *Type 1, 2 or 3* endoleak that has not been detected on an imaging modality. It is the state of elevated pressure within the aneurysm sac (Veith et al., 2002).
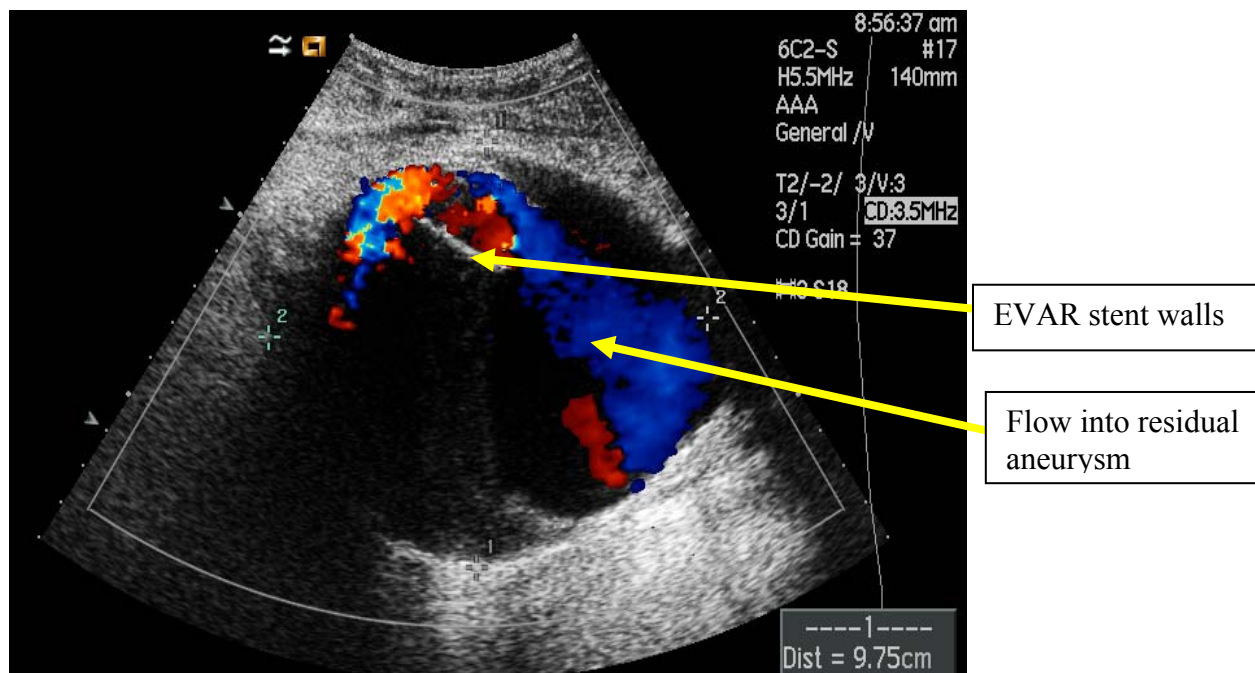
Figure 3.22: A patent residual aneurysm sac on CDU as a result of a type 1b endoleak
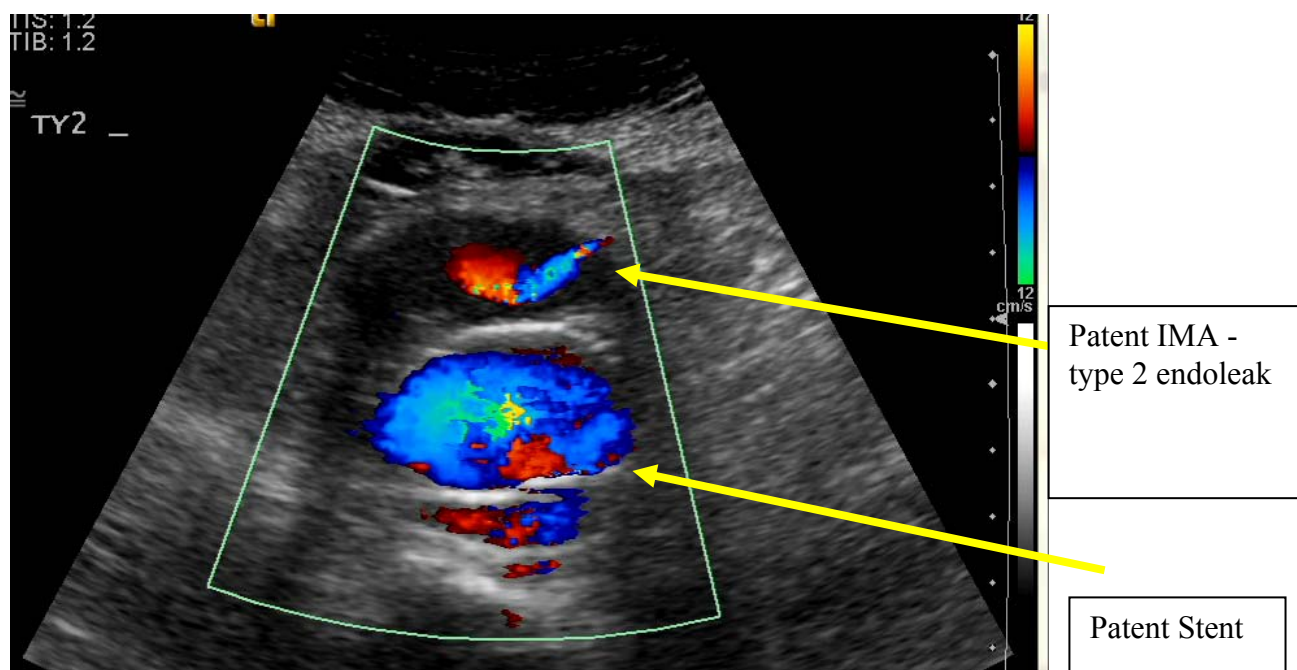
Figure 3.23: A type 2 endoleak on CDU. The residual aneurysm sac is being fed by a patent IMA

3.6.3 Endoleak Detection

Following EVAR, CT is considered by many to be the gold standard imaging modality for the detection and classification of endoleaks. However, other imaging modalities such as CDU are growing increasingly more popular for surveying patients post EVAR for practical reasons.

It has been proven to be a practical, non-invasive and accurate method of monitoring this particular group of patients over a long period of time. CT is a static imaging system that requires the precision timing of contrast injections to obtain optimal imaging results. It is for this reason that CT may not be sensitive enough to detect the low flow that is present in many of the type two endoleaks such as small patent lumbar arteries. CDU has the advantage of real time imaging so the low volume flow present in these endoleaks can be detected more readily.

Both CT and CDU confirm the presence of an endoleak by detecting flow present in the residual aneurysm sac. They both have the ability of measuring the residual aneurysm sac over a period of time. CDU achieves this at a limited risk to the patient. Aneurysms that have been successfully excluded from systemic circulation should naturally decrease over a period of time or at least remain stable. In the presence of an endoleak some residual aneurysms will increase over a period of time, it is for this reason that the residual aneurysm size should be monitored on a regular basis to ensure there is a decrease in size or at least no change in size. Any aneurysm that increases significantly between follow up exams should raise suspicion of an endoleak even if one is not present on an imaging modality.

3.6.4 Treatment of Endoleaks

Endoleaks are managed according to their classification either by observation, further endovascular intervention, surgical ligation of the aneurysm neck or conversion to open surgical repair of the aneurysm.

The presence of a type 1a or 1b endoleak may lead to further endovascular procedures such as a cuff endograft for a type 1a leak (figure 3.17) or an extension endograft for a distal type 1b endoleak (figure 3.22). An intersegment endograft may be used for distraction of component parts of a modular graft. Surgical band ligation of the proximal neck involves a laparotomy and open exposure to place an external ligature around the proximal graft to achieve a seal. Conversion to open repair is usually only indicated when further endovascular procedures have failed.

Type 2 endoleaks are more commonly observed. Some type 2 endoleaks seal spontaneously over time. However, if there is a significant increase in the aneurysm sac observed over time they may be treated by coil embolisation of the feeding vessel. Laparoscopic clipping of the source vessel has also been described.

3.6.5 Complications with Endovascular Aneurysm Repair

Other complications can occur with endovascular grafts, both immediately post operatively and in the late follow up period. Kinking of the graft body or limb can occur post operatively or in the follow up period. Consequences include lower limb ischaemia due to decreased flow or complete thrombosis of one or both of the iliac limbs. Some studies have actually documented the superiority of CDU over other imaging techniques in the detection of limb occlusion (Berdejo et al., 1997). Limb thrombosis may lead to dislocation of the limb of the endograft from the native iliac vessel, kinking and thrombosis of the endograft are amenable to endovascular correction thus avoiding the need to convert to open repair (Rutherford, 5th edition, page 1289).

When complete shrinkage of the residual AAA is achieved, the endovascular graft is subjected to stress at the limb junctions and the proximal and distal anastomosis sites. This may ultimately lead to a type 3 endoleak in the late follow up period however; further information on this will only become apparent as time goes on.

Chapter 4

The Physics of Ultrasound

4.0 Introduction

This chapter examines the background behind the physics involved in Doppler ultrasound and the use of Doppler ultrasound to measure blood flow. It gives a brief introduction to the physics of blood flow, arterial stiffness and pulse wave velocity. Several texts were used to compile this chapter all of which are documented in the reference section (Gibbs, Cole and Sassano. 2009. Hoskins, Thrush and Whittingham. 2003 and Hussey. 1985).

4.1 Sound Waves

Sound is a mechanical disturbance in the air initiated by the vibration of the sound source, which then travels through the air, impinges on and is received by the ear. It consists of local disturbances in the air which propagates from the source to the receiver. This type of phenomena is referred to as a wave.

A wave (figure 4.0) is a disturbance with a regularly repeating pattern which travels from one point to another.
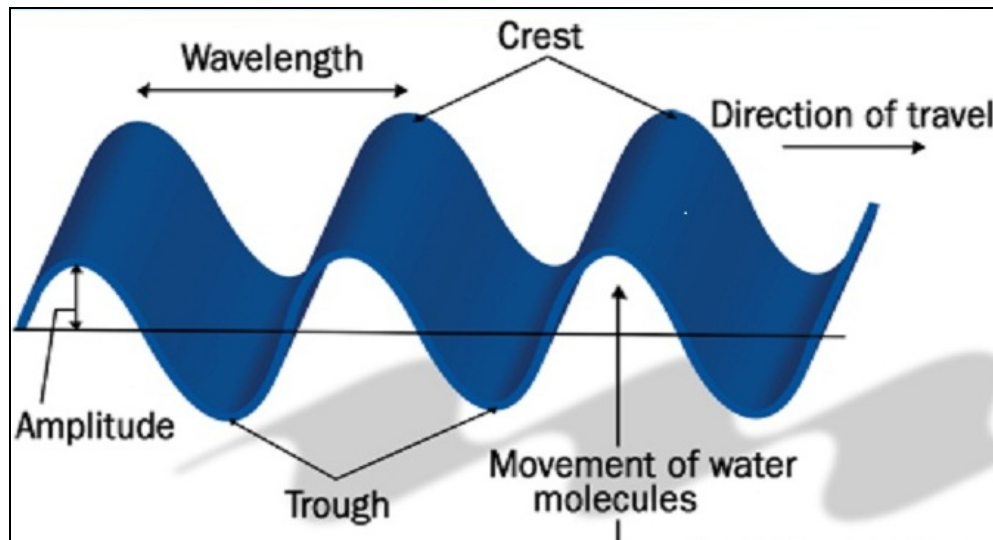
Figure 4.0: A transverse wave

The simplest example of a wave is the one created on the surface of a pond when a stone is thrown into the water. The stone cause's some of the water to be displaced and in turn there is a change in the height of the water. This change in height is transferred to the adjoining region, and so the energy is transported across the water from stone to shore.

This type of wave that travels across the surface of the pond is called a transverse wave (figure 4.0). The movement of the water surface is at 90 degrees (transverse) to the direction of travel of the wave.
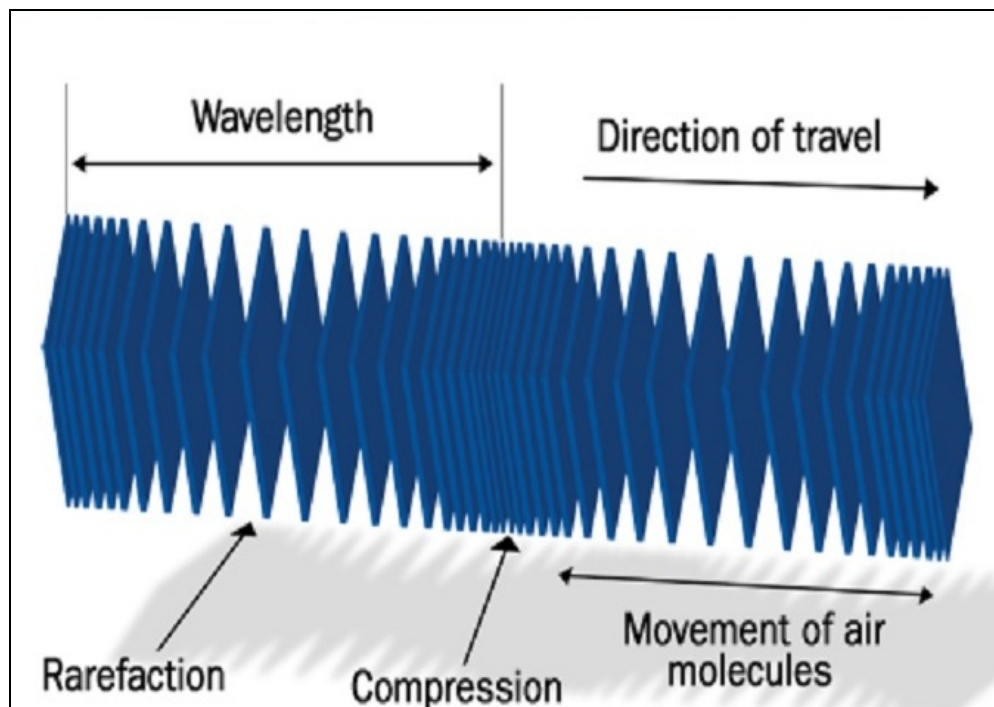
Figure 4.1: A longitudinal wave

The sound waves used to form a medical image are longitudinal waves (figure 4.1). The particles that are closest to the source of vibration are the first to vibrate. The direction of vibration of the particles and the direction of motion of the wave are the same; hence the wave is a longitudinal wave.

Within the medium the particles move backwards and forwards, as the particles in adjacent regions move towards each other they develop a region of compression (increased pressure) however, when the particles move away from each other a region of rarefaction (reduced pressure occurs) as described in figure 4.2. There is no movement of the medium itself, only the disturbance and the associated energy is transported.

The most common sound waves are those that travel in air from sources of sound such as from a bell to the human ear. The surface of the bell when struck vibrates causing the air molecules adjacent to it to push and pull against each other setting the neighbouring air molecules in motion and thus the disturbance travels through

the air as a sound wave. When the sound wave reaches the human ear it causes the ear drum to vibrate giving the sensation of sound. Thus, energy from the bell is transported by the wave to the ear drum causing it to move.
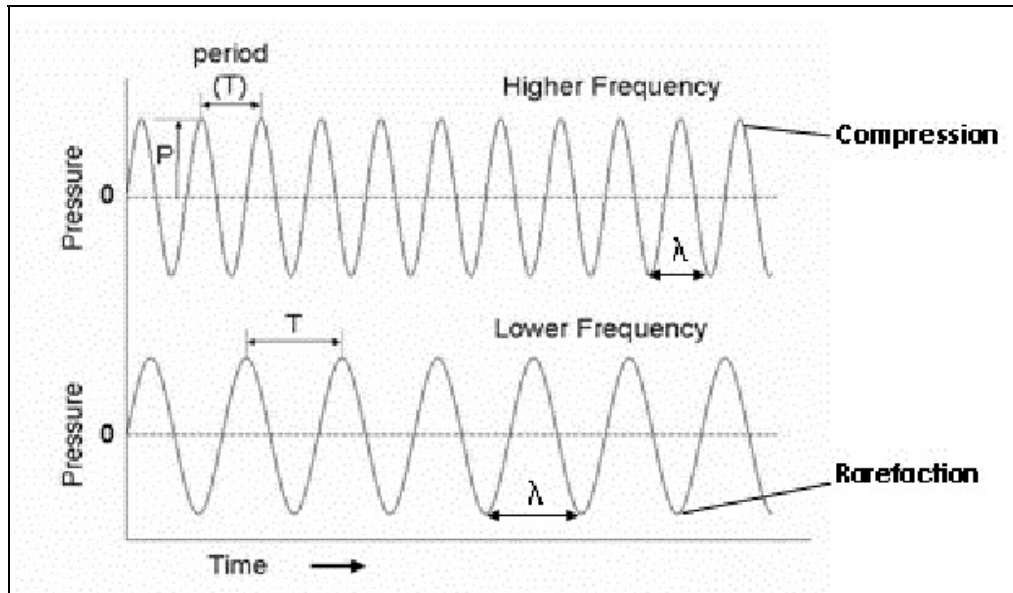
Figure 4.2: Changes in pressure that occur in a medium through which a sound wave is travelling

4.2 Properties of Sound Waves

4.2.1 Frequency

The number of complete cycles occurring at a point each second is called the Frequency (f) (figure 4.2). The units of frequency are hertz (Hz). Frequency is determined by the sound source and not the medium through which it is travelling.

Frequency ranges

Sound can be broken up into three major frequencies. The first one being the *audible sound* range, this is the sound range that a human ear can hear, it varies

with age but can be described as being between 20Hz-20000Hz. ***Ultrasound*** is a high frequency sound wave which is not within the human hearing range, it has a frequency greater than 20000Hz. The third category of sound ranges is ***infrasound*** which includes all frequencies below 20Hz.

4.2.2 Wavelength

Wavelength (figure 4.2) is the length of one cycle of a wave; it is represented by the symbol lambda (λ). The unit of measurement for the wavelength is the meter (m). With an increase in the frequency the wavelength decreases. The wavelength is inversely proportional to the frequency. Wavelength is determined by both frequency and velocity and by both the sound source and the medium through which it is travelling.

$$V = f \times \lambda$$ **Equation 4.0**

V = Velocity
F = Frequency
λ = Wavelength

4.2.3 Period

The period (equation 4.1) is the time taken for one wavelength to pass a particular point. The period is equal to one divided by the frequency and its units of measurement are time.

This relationship may be defined as:

$$Period\ (s) = \frac{1}{Frequency\ (Hz)}$$ **Equation 4.1**

4.2.4 Amplitude

Amplitude is defined as the maximum amount of variation that occurs in an oscillation, or the height of the wave (figure 4.2). It is determined only by sound source and not the medium through which it is travelling. It is equal to the maximum value of the oscillation minus the normal value.

4.2.5 Power and Intensity

Power is the rate at which work is done or energy is converted. The parameter which measures the rate of energy transfer is the intensity, defined as the amount of energy in joules, transported each second through each square meter of the medium perpendicular to the direction in which the sound is travelling. The intensity is the power in watts per square meter. The more intense the sound wave, the more energy that is transported each second through each square meter. It is determined by the source of the sound and not the medium through which it is travelling. Equation 4.2 describes the relationship between intensity, power and beam area.

$$Intensity \left(\frac{W}{cm^2} \right) = \frac{Power (W)}{Beam\ Area (cm^2)}$$ **Equation 4.2**

4.3 Propagation of Sound Waves

The speed at which a sound wave travels is determined by the medium in which it is travelling. The speed of sound has units of meters per second (ms^{-1}). The properties of a medium which determine the speed of sound are Density (ρ), measured in kgm^{-3} and Stiffness denoted by the symbol Kappa (k), units of Pascal (Pa).

Dense materials are composed of large molecules which are difficult to move, these molecules are closer together making it easier for oscillations of individual particles to be transmitted to their neighbouring molecules. Gases have molecules that are far apart when compared to liquids therefore it is more difficult for sound to travel from one particle to another. Increasing stiffness therefore increases transmission speed. The speed of sound in air is $333ms^{-1}$, in soft tissues (human flesh) the speed of sound is 1540 ms $^{-1}$; most medical devices are calibrated for this speed.

Table 4.0 describes the relationship of the velocity of sound to the stiffness of the medium through which it is travelling. The lowest speed occurs in gases such as air, with increasing velocities in liquid such as blood and the highest velocities in solids such as bone.

Material	Speed of Sound (ms^{-1})
Air	331
Lung	650
Mercury	1460
Fat	1460
Water	1520
Blood	1560
Muscle	1580
Bone	2700-4100

Brass	4490
Quartz	5470
Aluminium	6400

Table 4.0: Relationship between velocity of sound and stiffness of a medium

It is important to note that with the exception of bone all body tissues behave like liquids due to their high concentration of water. Therefore they all transmit sound at a similar velocity, approximately 1540m/sec.

Low density and high stiffness lead to high speed sound waves, high density and low stiffness lead to a reduced speed of sound. The speed of sound is expressed in equation 4.3.

$$Speed \ of \ sound \ (c) = \sqrt{\frac{k}{\rho}} \qquad\qquad\qquad \textbf{Equation 4.3}$$

Propagation speed is the speed at which a sound wave moves through a particular medium. It is determined by the density and the stiffness of the medium.

$$Propagation \ speed \ (^m/_{sec} = Frequency \ (Hz) \times Wavelength \ (m))$$

Equation 4.4

In ultrasound the range equation (equation 4.5) is a method of measuring the distance from the sound source to any reflector of interface within the transmission medium. It relates reflector distance to echo arrival time. The propagation speed of the transmission medium must be known and the time for the ultrasound pulse to make a complete round trip from the transducer element to the interface and back to the transducer element again.

The Range Equation:

$$D = \frac{1}{2} \left[Propagation\ speed\ \left(mm/\mu s\right) \times Pulse\ round\ trip\ (\mu s) \right]$$

Equation 4.5

D= the distance from the reflector

4.4 The Interaction of Ultrasound with Tissue

4.4.1 Attenuation

Attenuation describes the reduction in intensity of the sound wave as it propagates. Once a sound wave enters the body, the longer the path it has to travel the greater the effect of attenuation. This decrease in the intensity of the wave is due to multiple factors such as absorption, scattering, reflection and beam divergence.

Absorption of the sound by body tissue accounts for the largest losses. Scattering, occurs when an ultrasound wave strikes a boundary between two media that have surface irregularities of the order of magnitude of the wavelength or less, the reflected wavelength is fragmented into random directions relative to the boundary.

Both absorption and scattering are dependent on frequency and the overall attenuation is also frequency dependent.

Every tissue type has its own attenuation coefficient (MHz^{-1}). Tissues with high attenuation coefficient absorb sound more efficiently than those with a low attenuation coefficient. For example, blood has an attenuation coefficient of 0.2 MHz^{-1} and bone has an attenuation coefficient of 10 MHz^{-1}. Therefore transmission in bone is at a much higher level than blood making it impossible for the sound wave to be transmitted in bone within the diagnostic ultrasound range. This is why bone causes regions of shadowing on an ultrasound image.

4.4.2 Acoustic Impedance

Acoustic impedance (Z) of a material is a measure of the response of the particles of a medium, to a wave of given pressure (equation 4.6). It is determined by the density and the stiffness of the material. An echo is generated when a sound beam crosses into a tissue which is composed of differing acoustic impedances. The amplitude of the echo is dependent on the difference in the acoustic impedances of the two tissues involved. Acoustic Impedance describes the relationship between excessive pressure (P) and particle velocity (Uo).

Substances such as bone whose particles are densely packed have high acoustic impedance so it will take excessive pressure for all the particles to be moved at the same velocity. In contrast, the particles in air are loosely packed. Therefore, it takes a much lower pressure for all the particles to be moved at the same velocity. Therefore air has lower acoustic impedance than bone. Acoustic impedance increases if either the density or the stiffness of the material increases, and it is not dependent on the frequency of the applied signal.

$$Acoustic\ Impedance\ (Z) = \frac{Excess\ Pressure}{Wave\ Velocity} = \frac{P}{Uo}$$

Equation 4.6

4.4.3 Reflection

When an ultrasound beam strikes a particular interface, it is the acoustic impedance of the two mediums that determines whether reflection (figure 4.3) occurs. Several things may happen to the beam depending on whether the beam strikes the interface perpendicularly or at an angle.

If the sound wave strikes the interface at an angle perpendicular to the incident of sound, the wave may be reflected or transmitted, or both. The reflected portion of the beam returns to the transducer and is detected as an echo. The amplitude of the returning echo depends on the intensity of the incident beam and the difference in the two acoustic impedances of the mediums forming the interface.

If the tissue interface is oblique not perpendicular, the reflected sound wave will travel along a different path. The greater the difference in the acoustic impedances of the two mediums the greater the reflected energy and thus a larger echo is received by the transducer. When there is only a small difference in the acoustic impedances of the two mediums only a small amount of energy is reflected back.
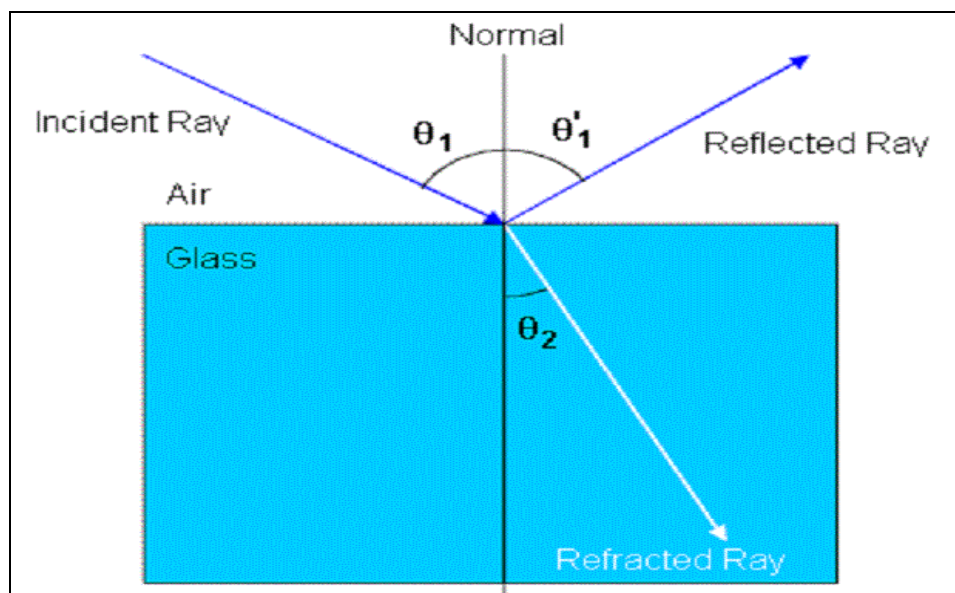
Figure 4.3: Reflection and Refraction

4.4.4 Refraction

Refraction (figure 4.3) of the sound wave occurs when the speeds of sound are different on each side of the tissue interface. If the angle of incidence is not perpendicular to the interface, then the path of the beam will be refracted. Refraction of a beam up to 10% can lead to missregistration of the echoes. This may lead to displaying some of the returned echoes as artefacts.

The degree of missregistration is dependent on the angle of the incident wave and the difference in the speed of sound of the tissues.

Snell's Law (4.7) describes the degree of refraction that occurs with oblique incidence of an ultrasound beam at the boundary of two mediums with differing propagation speeds.

$$\frac{sin\varnothing i}{sin\varnothing r} = \frac{C_1}{C_2}$$
                                                                    Equation 4.7

$\varnothing i$ = angle of incidence

$\varnothing r$ = angle of refraction

C_1 and C_2 = the speed of sound in the two mediums

If the propagation speed through medium two is greater than the propagation speed through medium one, then the transmission angle will be greater than the incidence angle and vice versa.

4.4.5 Scattering

Scattering occurs at large interfaces, for examples between organs were there is a change in acoustic impedances. When an ultrasound wave is incident on such targets, it becomes scattered over a large range of angles (figure 4.4). The sound beam is scattered or diffused by tiny reflectors such as red blood cells, this scattered energy is radiated in all directions, and this phenomenon is referred to as Rayleigh scattering. These backscattered echoes allow for the imaging of tissues. The intensity of the backscattered echoes varies with the size of the scatter and the frequency of the transducer. The backscattered echoes as in the case of red blood cells may also be received by the transducer and then analysed.

In the case of Rayleigh scatter the returning sound intensity is not entirely dependent on the angle of incidence. It is also dependent on the dimension of the scatter, the number of scatters present and the frequency of the ultrasound. More scattering will be noted at higher frequencies. Some of the echoes will be returned to the transducer and displayed. However, the majority will be scattered non-uniformly in all directions and not recorded.
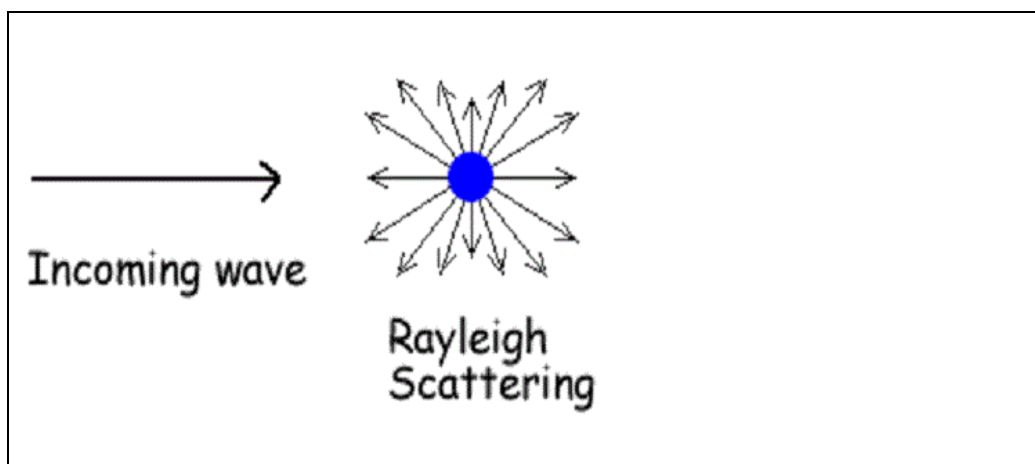
Figure 4.4: Rayleigh scattering of a wave

4.5 Ultrasound Transducers

4.5.1 The Piezoelectric Effect

The Piezoelectric effect is the ability of a material to generate an electrical charge in response to applied pressure. When a piezoelectric material is compressed a potential difference is generated across opposite faces, one becomes positive and the other becomes negative. Conversely, if an electric field is applied across the crystal it changes its shape.

A transducer converts one form of energy into another. An ultrasound transducer converts electrical energy into ultrasound energy and vice versa, using the piezoelectric effect. When a voltage is applied to the ultrasound transducer a mechanical wave is generated, when the wave returns to the transducer an electrical voltage is generated. The transducer serves as both the emitter of sound and the receiver of the returning sound waves.

Due to their mechanical nature sound waves require a medium for their transmission. The mechanical wave produced by the transducer travels away from the source causing displacement of the particles within the medium.

Ultrasound transducers are usually described by their type and operating frequency which can range from as low as 2,000,000Hz (2MHz) to as high as 20,000,000Hz (20MHZ). They can operate in a continuous mode or in a pulsed mode with the voltage being applied in a pulsed fashion.

An ultrasound transducer should be chosen to best suit the purpose it is intended for; image resolution will not be as good with a transducer that operates at deeper frequencies. For example a 15MHz transducer will give excellent resolution of

superficial structure such as the cephalic vein but would not be suitable to image deeper structures such as the aorta.

As a continuous alternating voltage is applied to the transducer element, the element produces a continuous alternating pressure wave that propagates as a sound wave. The frequency of the sound produced by the transducer is directly related to the frequency of the voltage applied to the transducer element as well as the thickness and propagation speed of the element itself.

Pulsed ultrasound is used in medical ultrasound imaging, the pulse repetition frequency (PRF) is the number of pulses occurring in one second (figure 4.5), and its units are hertz (Hz). The amount of time between each pulse is measured in seconds and is referred to as the pulse repetition period (PRP). Pulse duration is the time taken for one complete pulse to occur and is equal to the period multiplied by the number of cycles in the pulse.

$$PRP = \frac{1}{PRF\ (kHz)}$$

Equation 4.8

$$Pulse\ duration\ (\mu s) = \frac{The\ number\ of\ cycles\ in\ the\ pulse}{Frequency\ (MHz)}$$

Equation 4.9
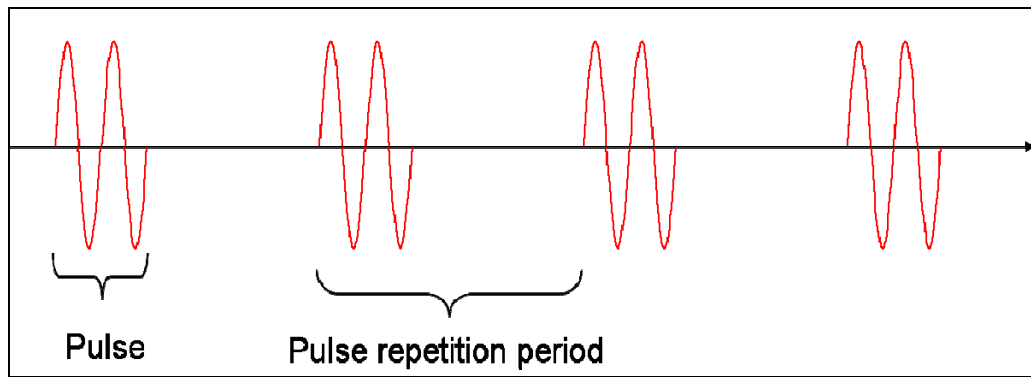
Figure 4.5: Pulse repetition period

Equation 4.9 is derived from equation 4.8. Both equations describe the following relationships. As the PRF increases, PRP decreases. As the period increases, pulse duration decreases. As the number of cycles in the pulse increases, pulse duration increases. And finally, as the frequency increases, pulse duration decreases.

4.6 Ultrasound Transducer Construction

Ultrasound transducers are composed of several major components, the piezoelectric crystal, the backing material, a matching layer, and a case to house the components.
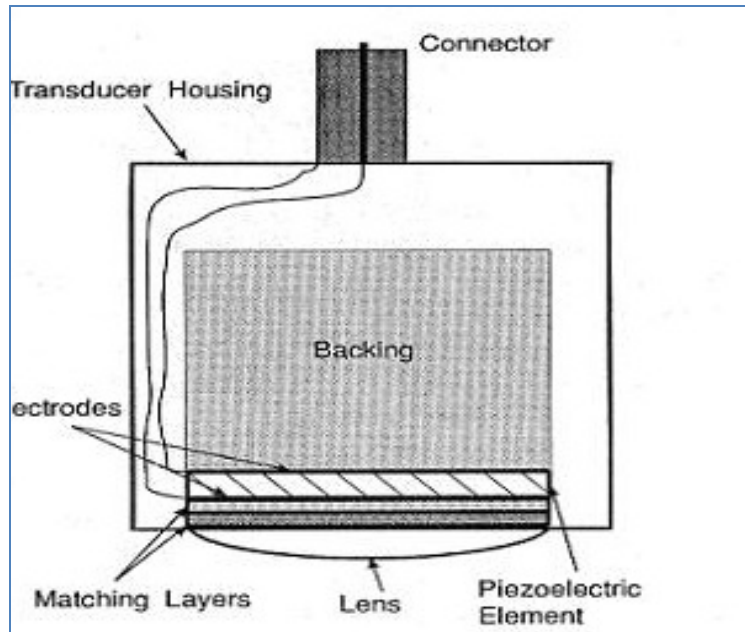
Figure 4.6: A single element ultrasound transducer

i.   *The Crystal Element*

The piezoelectric effect is responsible for the production of a pressure wave when a piezoelectric material is deformed by an electric voltage. Most transducers are composed of ceramic material such as lead zirconate titanate which following a procedure called polarisation is made piezoelectric.

Piezoelectric materials are crystalline materials composed of dipolar molecules which have a random arrangement within the material. These dipolar molecules

have an inability to arrange themselves in an applied electrical field. However, when the material is heated above the Curie temperature (365 degrees Celsius) in the presence of an electrical field the molecules align within the field. When the material is cooled below the Curie temperature the molecules will remain aligned while an electric field is removed. The piezoelectric crystal can now be used in an ultrasound transducer to transmit and detect sound.

For pulsed ultrasound the thickness of the transducer element as well as the propagation speed of the material that the element is composed of determines the operating frequency of that transducer. The operating frequencies of the ceramic crystal will increase with the increasing propagation speed of the transducer element.

ii. Damping Material

This layer is applied to the back of the crystal element to reduce the duration of the pulse and thus the number of cycles in the pulse. This is necessary as the transducer will continue "ringing" at its resonant frequency following excitation by the pulse transmitter.

iii. Matching Layer

This is applied to the face of the crystal element and is composed of a material which has an acoustic impedance value that is between the transducer element and the tissue interface to which the transducer is being applied. This reduces the reflection that occurs at the transducer skin interface due to the difference in their acoustic impedances. The matching layer is further enhanced when acoustic gel is applied to the transducer before applying the transducer to the patient. This gel

acts as a coupling agent and eliminates the air interface that is present between the transducer and the patient thus interfering with sound transmission.

4.6.1 Ultrasound Beam Profiles

The ultrasound beam is the area through which the sound energy emitted from the ultrasound transducer travels. The beam is a three dimensional emission and is symmetrical around its central axis. It can be divided into two regions (figure 4.7), the near field (Fresnel Zone) and the far field (Fraunhofer Zone).

The near field is cylindrical in shape and will increase as the frequency of the transducer increases and with an increasing transducer diameter. The area between the near field and the far field is called the transition zone.

The far field is the region beyond a distance of one near field length away from the transducer face. It is where the beam diverges and becomes cone shaped (figure 4.7). The shape of the beam depends on factors such as the diameter of the crystal, the frequency and the wavelength. The design of the transducer will also be a factor in the shape of the beam. Increasing the frequency of the transducer will create a longer near field and a shorter far field. A narrow crystal results in the beam being narrow in the near field.
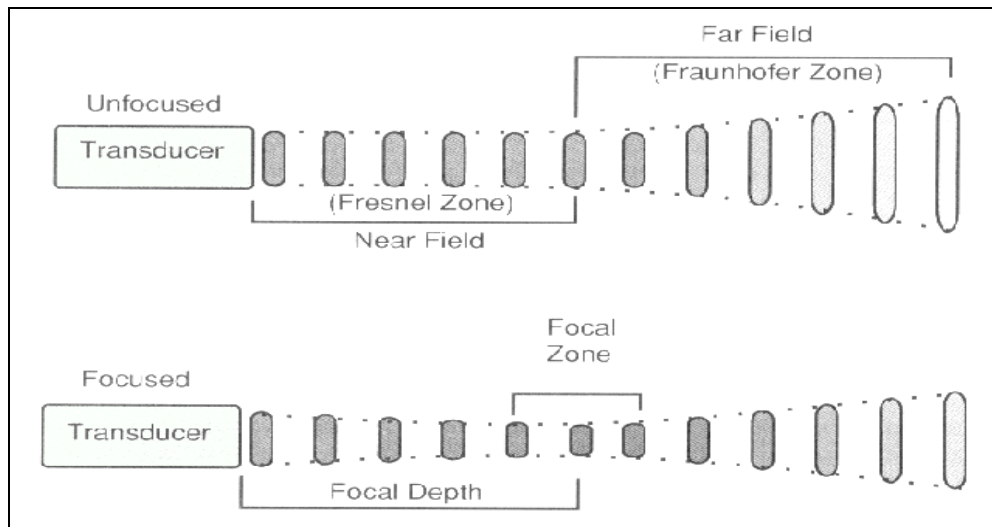
Figure 4.7: Near and far zones of an ultrasound beam

4.6.2 Side Lobes

Side lobes describe the energy that radiates at various angles from the transducer face (figure 4.8). They are not part of the main ultrasound beam, they are three dimensional and there may be one or more of them. They return echoes from any interface they encounter. These returning echoes will be incorrectly placed on the image as the ultrasound machine assumes they are from the main beam. They result from continued excitation of the piezoelectric crystal. The number of side lobes can be reduced by energising the crystal in a pulsed pattern.

Grating lobes are at various angles to the main beam and also have the same effect as side lobes (figure 4.9). Grating lobes are caused by the regular, periodic spacing of the small array elements. Both can lead to artefact on the image.
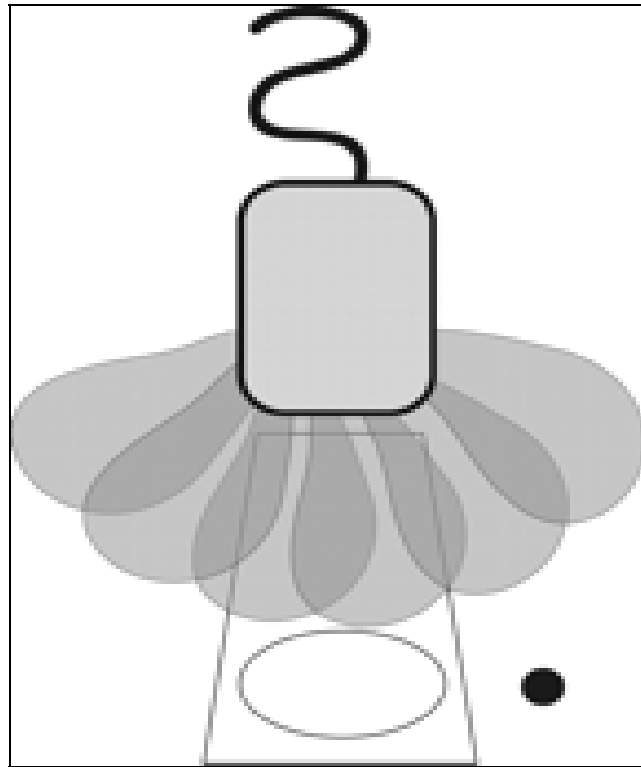
Figure 4.8: Side lobes of an ultrasound beam
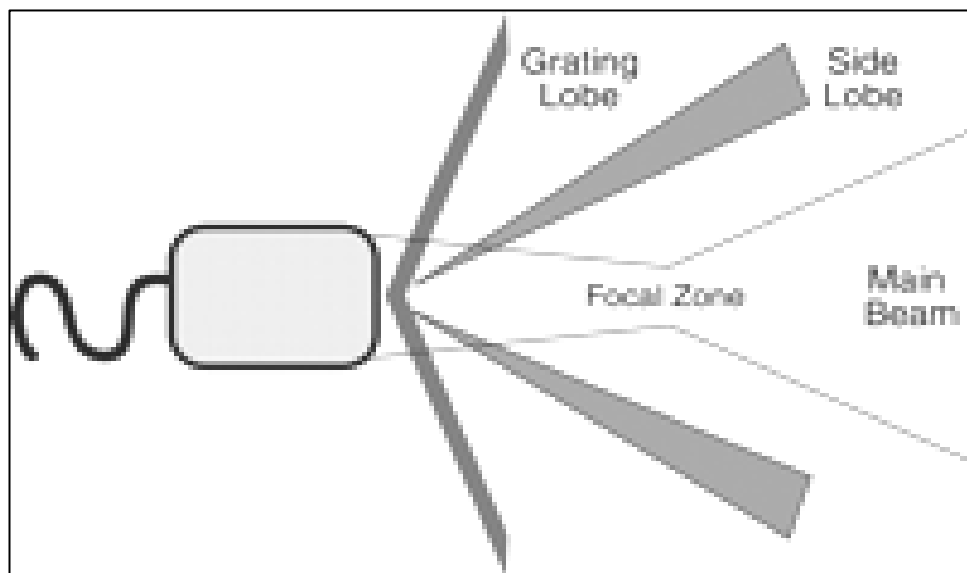
Figure 4.9: Grating lobes of an ultrasound beam

4.6.3 Beam Focusing

The diameter of the ultrasound beam at any given point determines the lateral resolution of the transducer. The focal zone of the transducer is the distance between the centre of the ultrasound beam at which the intensity remains within 25% of the peak intensity of the focus of the transducer (figure 4.10). The width of the ultrasound beam is the dimension of the beam in the scan plane and it will vary accordingly when focusing of the beam is being conducted. The width of the beam will vary with depth and will have an effect on the spatial resolution of the resulting image. In principle, the narrower the beam the better the resolution.

Focusing of the ultrasound beam will improve the quality of the image at that particular point, causing the ultrasound beam to converge at a particular region resulting in a narrower beam at the region of interest. Increasing the number of focal zones will improve resolution; however, because the transducer is now sending out multiple sets of echoes with a focus at each of the focal zones, this takes more time and will result in a slower frame rate.
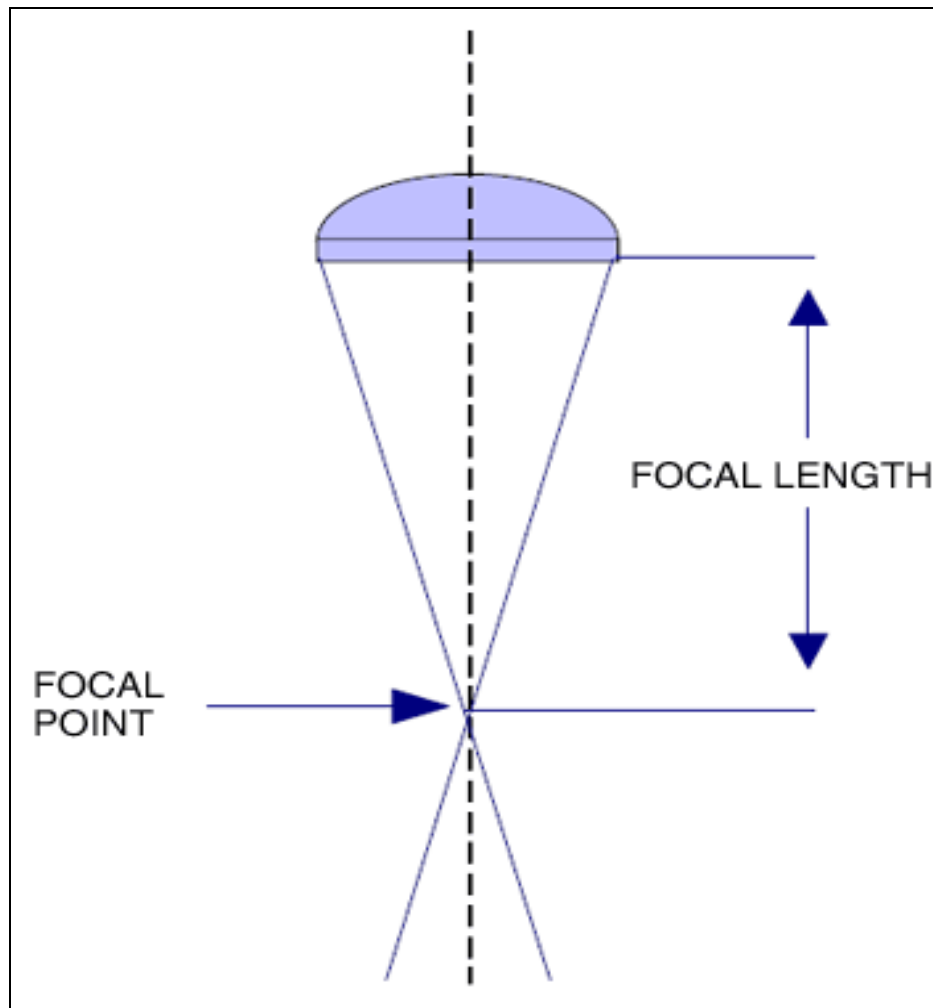
Figure 4.10: Focal zone of an ultrasound beam
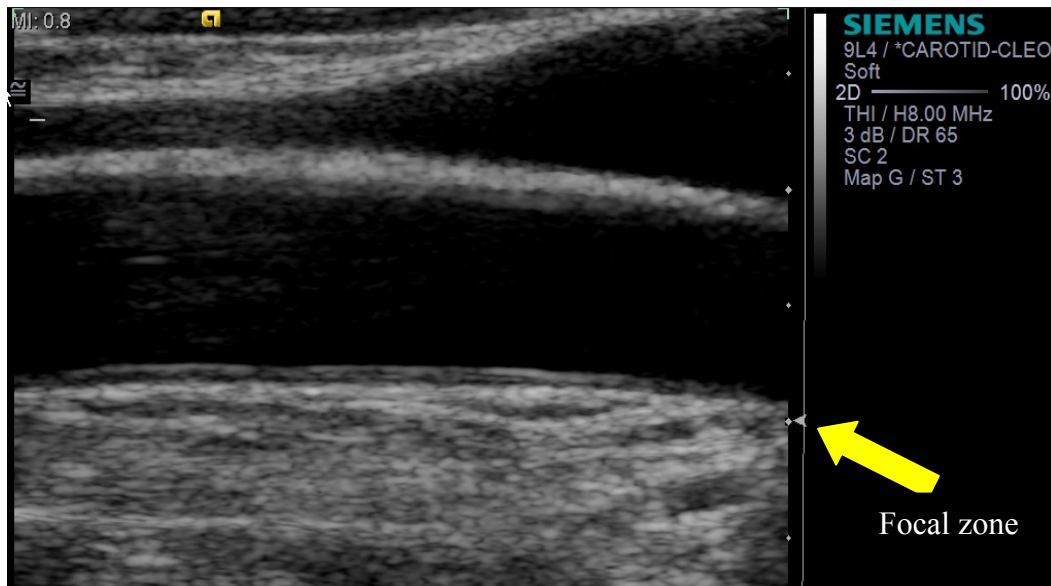
Figure 4.11: A B-Mode Duplex image with one focal zone
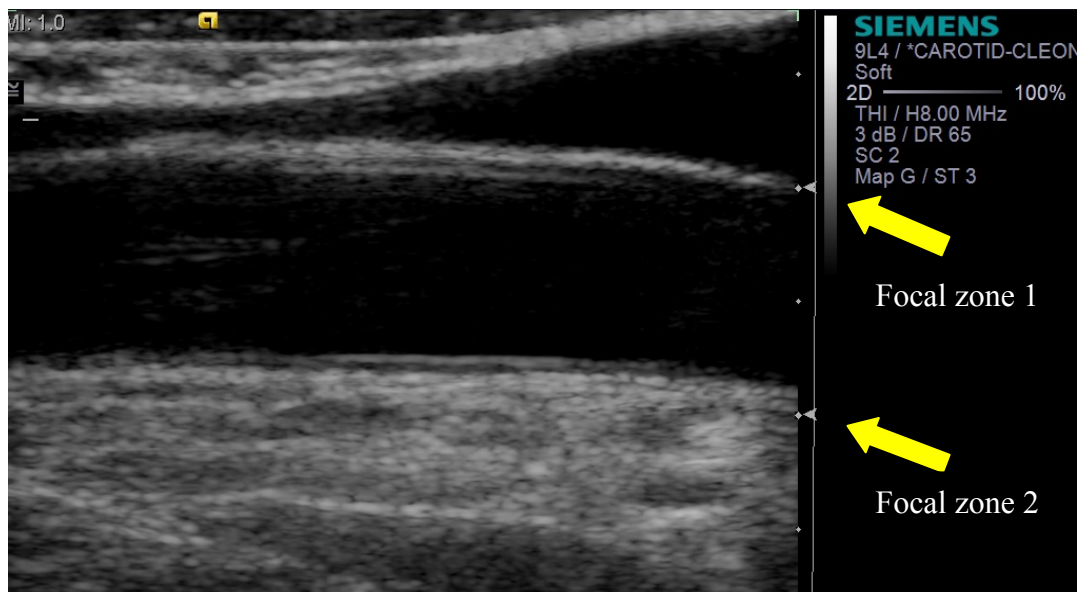
Figure 4.12: A B-Mode Duplex image using two focal zone

4.7 Image Resolution

Detailed resolution is composed of two components, axial resolution and lateral resolution.

i. Axial Resolution

This is the resolution along the axis of the beam; it is dependent on the spatial pulse length (figure 4.12) and can be defined as the minimum distance separating two different reflectors along a longitudinal axis of sound travel thus separate echoes are produced on the display. It is equal to half the spatial pulse length of the ultrasound pulse emitted from the transducer. Axial resolution therefore improves as it reduces.

Frequency and transducer design both affect the spatial pulse and therefore the axial resolution. Ultrasound transducers with a higher frequency for imaging will result in a shorter spatial length and improved axial resolution. The length of the pulse also depends on the amount of dampening applied to the piezoelectric crystal. Increasing the amount of dampening makes the pulse length shorter and therefore the axial resolution will be improved.

ii. Lateral Resolution

Lateral resolution (figure 4.13) is the minimum distance separating two different reflectors lying in a plane that is perpendicular to the direction of sound travel, thus separate echoes are displayed. Lateral resolution is equal to beam diameter at that point in the ultrasound beam and it improves as frequency increases. It is

dependent on the beam width and is the resolution at right angles to the beam. Lateral resolution is generally not as good as axial resolution. The width of the beam determines the size of the echoes that are displayed on the screen. The structures being imaged must be separated by a distance greater than the beam width for them to be resolved into separate structures.

iii. Contrast Resolution

This is the ability of an ultrasound system to assign a different shade of grey to returning echoes of varying amplitudes thus differentiating between body tissues and displaying them on a monitor. Better contrast resolution will result in better axial and lateral resolution. Transducer design, analogue to digital conversion and the control settings of the machine such as gain, time gain compensation and harmonic imaging, all affect the contrast resolution.
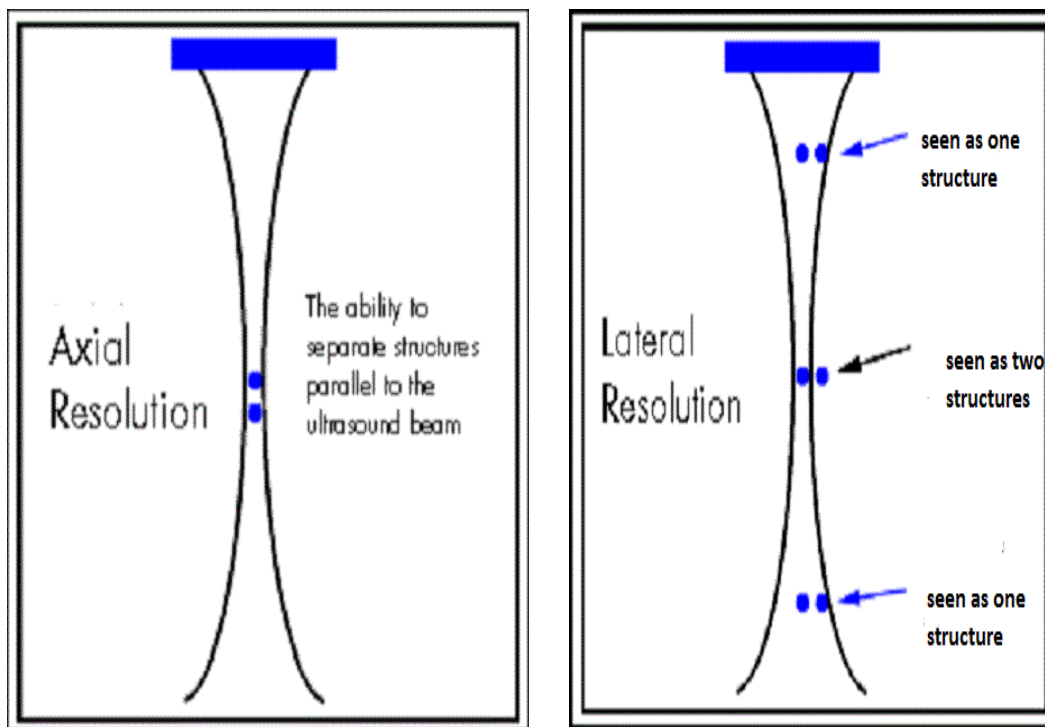
Figure 4.13: Axial and lateral resolution

4.8 Ultrasound Imaging

4.8.1 Introduction

i. *Amplitude Mode*

The earliest and most simple form of presenting returning echoes on a display was to use Amplitude mode (A-Mode). This is where a transducer was placed in the direction of the area of interest and a pulse of ultrasound was directed into the subject. The pulse of ultrasound travels through the medium at the speed of propagation of sound in the medium. After a distance it encounters a reflecting boundary. At the boundary the incident pulsed wave is portioned into the reflected and transmitted components. The reflected components travel back towards the probe at the speed of propagation of ultrasound in the medium. The reflected pulse reaches the transducer as an echo and is detected by the transducer.

By measuring the time taken for the echo to return and knowing the speed of propagation of ultrasound in that medium, the depth of the reflecting boundary producing the echo may be calculated (equation 4.10).

$$L = \frac{c\,\Delta\,t}{2} \qquad\qquad\qquad \textbf{Equation 4.10}$$

A-Mode imaging is not of great importance today it is still however used today in ophthalmology and to some extent in cardiology.

ii. Brightness Mode

Brightness mode ultrasound (B-Mode) displays the returning echoes as a series of dots with the position of each dot corresponding to its distance from the reflector and the brightness of each dot corresponding to the amplitude of the returning signal.

The transducer crystal emits a sound pulse, some of which is reflected back to the transducer or transmitted further into the tissues. At each interface a dot with grey scale brightness proportional to the strength of the signal is placed on the screen. This process continues in real time along the length of the transducer with the result being a B-Mode image. Currently ultrasound systems utilize one hundred or more ultrasound beams to produce a single frame for a B-Mode image.

The development of B-Mode imaging greatly expanded the use of ultrasound in medical imaging. B-Mode scanning techniques required the operator to move the transducer across the area of interest resulting in a slice or a cross sectional image of the patient at that point, this required a method of storing the echoes as well as displaying them on a monitor.

There are two types of B-scan formats that may be used, static scanning and real time imaging. Static scanning is not as commonly used in medical imaging today.

A real time ultrasound machine must have the ability to produce several images per second in order for a moving image to be displayed on a monitor. Each individual scan produced by the transducer is referred to as a frame and each frame is composed of hundreds of scan lines, one scan line for each time the

ultrasound transducer is pulsed. Line density is the number of vertical lines present per field of view, the greater the number of lines the better the resolution of the image. The pulse repetition rate or the frame rate is limited by the speed of ultrasound in the tissue being imaged as a new pulse cannot be generated until the first pulse has returned. Therefore when imaging deeper structures a slower frame rate or pulse repetition rate is used.

4.8.2   Real Time Ultrasound Imaging

The two most common formats of displaying an ultrasound image are rectangular and sector, depending on the type of transducer being used.

Real time ultrasound scanning can be performed in two ways mechanically and electronically. During mechanical scanning one or more transducer elements are mechanically moved to form a real time image. Electronic scanning involves the activation of an array of transducers by electronic means, the transducers do not move. In both methods the ultrasound beam is continually swept or scanned through an area of interest. Electronic array scanning is more commonly used in vascular ultrasound.

Electronic Array Scanning

Electronic muti array transducers have an array of rectangular piezoelectric crystals etched side by side within the transducer housing. There around 128-256 elements across the face of these transducers which are individually connected through an ultrasound port on the machine. Electronic array transducers emit a series of small narrow beams along the transducer face which travel along adjacent paths through the patient to generate a cross sectional image. By

introducing a set of time delays to the individual elements the shape of the ultrasound beam and direction can be electronically manipulated to focus and steer the ultrasound beam. None of these transducers have moving parts; they simply focus the ultrasound beam by introducing a time delay to a crystal when it emits its pulse of energy. By varying the location and the sequence of each pulse it is possible to focus more ultrasound signal at a given point of interest or depth and thus improve the resolution of the image from this depth. This ability to achieve focusing by applying the order in which the elements of the array are fired is referred to as phasing.

The electronic array ultrasound transducers available for today's applications can be classified into one of three groups, linear array transducers, curvilinear or sector array transducers and phased array transducers. Linear array transducers and sector array transducers are widely used in vascular ultrasound.

i.   *Linear Array*

Linear array transducers (Figure 4.14) are commonly used to image the more superficial structures and vessels. They are composed of between 128 – 256 piezoelectric crystals in a row which produce parallel scan lines and transmit perpendicularly to the transducer face thus resulting in a rectangular field of view (figure 4.15).

Linear transducers traditionally operate at frequencies above 4 MHz and usually produce an image about the length of the transducer head. They can operate at frequencies as high a 15MHz.
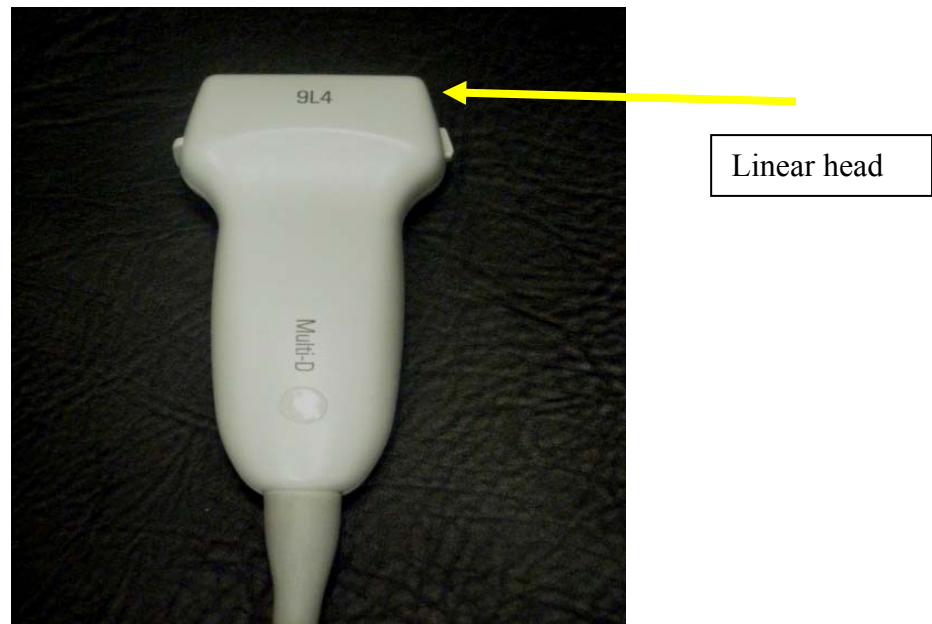
Figure 4.14: A Siemens linear array transducer
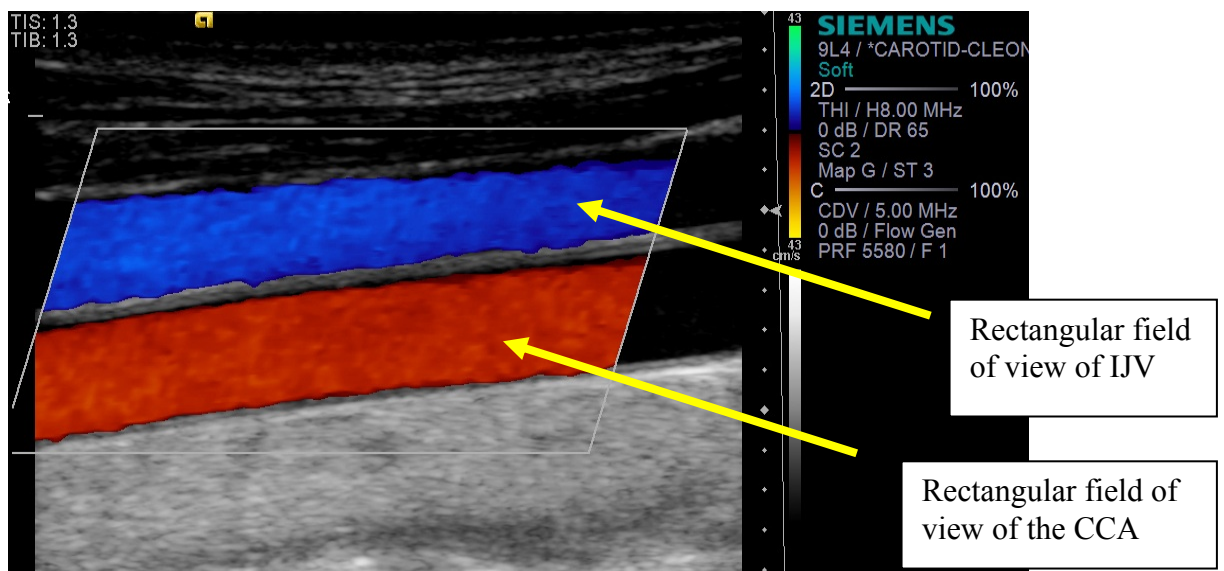
Figure 4.15: A rectangular field of view produced by a linear array

transducer

ii. Curvilinear Array

These transducers are sometimes referred to as sector array transducers. They traditionally operate at lower frequencies than linear array transducers and are therefore good at imaging deeper structure within the body. They operate around 3.5MHz and provide a wide field of view (figure 4.16) due to the transducer head being curved in shape (figure 4.17).
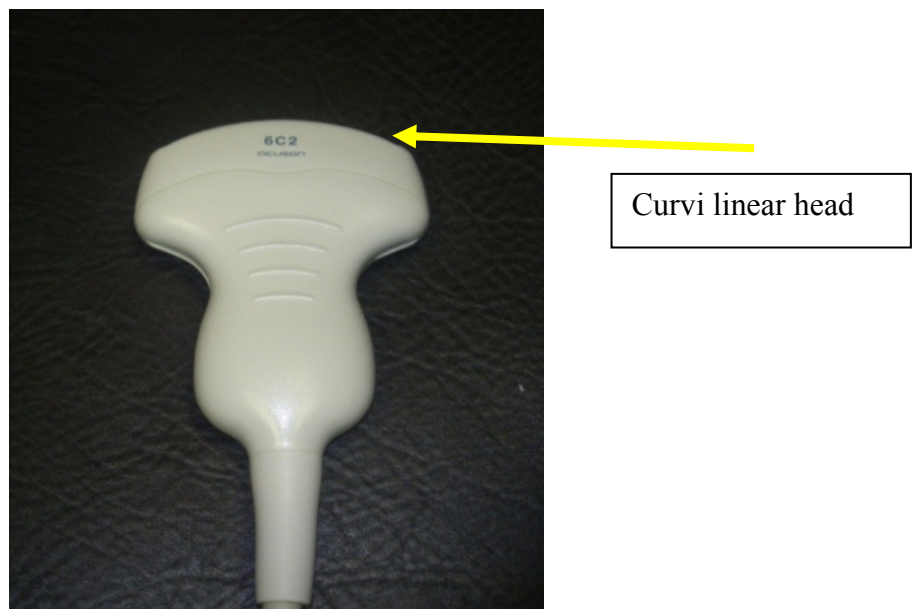
Curvi linear head

Figure 4.16: A Siemens curvi linear array transducer

Wide field of view produced by a curvilinear transducer

Figure 4.17: A wide field of view produced by a sector array transducer

4.9 Doppler Ultrasound

4.9.1 Introduction

The Doppler Effect was first described by Christian Andreas Doppler in 1842; the acoustical Doppler Effect was first demonstrated in 1845 by Buys Ballot using a trumpeter riding on a steam locomotive. However, the use of Doppler in the clinical investigations of peripheral vasculature was not accomplished until the 1960's after the development of the first Doppler probe by Satomura in 1959.

Today Doppler ultrasound is routinely used as a non invasive test to examine and evaluate the movement of blood flow through arteries and veins and thus giving us the ability to diagnose multiple conditions such as arterial narrowing, heart valve defects, deep venous thrombosis, varicose veins and arteriovenous malformations.

4.9.2 The Doppler Effect

The Doppler Effect is the occurrence of a shift in the observed frequency of a sound or ultrasound wave when there is relative movement between the sound source and the observer.

In medical imaging this occurs when the ultrasound beam that has been produced by the transducer encounters a moving target rather that the stationary interface. It is defined as a change in the perceived frequency of sound emitted by a moving wave source, receiver or reflector.

Doppler ultrasound is used in vascular imaging to identify changes in the frequency or the velocity of moving reflectors, red blood cells. This frequency shift is known as the Doppler Effect and applies to both light and sound waves.

The Doppler Effect is used in ultrasound to examine blood flow through a vessel. It gives us information on the direction of flow within the vessel, the presence of flow and the absence of flow within the vessel. The transducer is the emitter and the receiver of the ultrasound beam. The returned echoes are detected by the transducer and are processed by the ultrasound system to detect the frequency shift when compared to the emitted signals. The frequency shift detected in the emitted and the received signals depends on the magnitude and the direction of blood flow within the vessel.

4.9.3 Doppler shift

The Doppler shift is defined as the reflected frequency minus the incident frequency, thus we get the frequency of the moving red blood cells. This is called the Doppler shifted frequency and can be positive or negative depending on whether the blood flow is going towards or away from the transducer.

In vascular ultrasound the Doppler shift frequency provides the basis for calculating the velocity of flow in the vessel under investigation. The Doppler shifted frequency falls within the audible hearing range of the human ear and so the pitch is heard by the Technologist.

4.9.4 The Doppler Equation

The Doppler equation describes the relationship between the speed of the moving target and the change in frequency that occurs when the sound beam encounters the moving target.

$$f(d) = \frac{2f(o)v\cos\theta}{C}$$
Equation 4.11

f(d) = Doppler shifted frequency
f(o) = Transducer operating frequency
C = Velocity of sound1540mms^{-1}
V = Velocity of the moving red blood cells
θ = The angle between sound beam and blood flow.

4.9.5 The Doppler Angle

When the Doppler beam is pointing towards the direction of blood flow a positive Doppler shifted signal is detected however, once the Doppler beam is pointed away from the direction of flow a negative beam is observed. The smaller the angle between the Doppler beam and the blood vessel, the larger the Doppler shifted frequency. No signal is produced at an angle of 90 degrees. For a constant flow velocity (V), the maximum value of cos θ and the maximum value of the Doppler shifted signal is at an angle of zero degrees. This corresponds to a Doppler beam which is at an angle parallel to the vessel. In practice we take Doppler measurements at an angle of between 45-60 degrees to ensure reliable Doppler shifted frequencies. Angles above 90 degrees are always avoided as greater flow velocities and smaller angles produce larger Doppler shifted frequencies.

In clinical use sound approaches the moving targets somewhere between 0 and 90 degrees. Due to the variability of the angle between the ultrasound beam and the direction of blood flow, angle correction must be applied using the Doppler angle. The Doppler angle may be defined as the angle between the direction of flow and the direction of sound propagation.
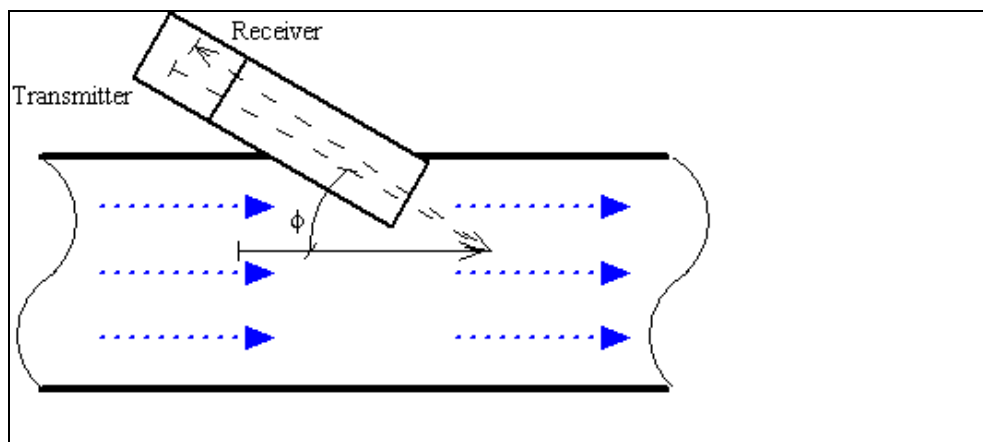
Figure 4.18: The Doppler effect

4.10 Doppler Instruments

In clinical practice Doppler techniques can be either imaging or non-imaging. Non imaging techniques include the traditional hand held continuous wave Doppler units used in detection of peripheral pulses and in obstetrics (figure 4.20). Imaging techniques widely include colour Doppler, power Doppler and spectral pulsed wave Doppler and are always used in conduction with B-Mode image.

4.10.1 Continuous Wave Doppler

These are the simplest Doppler devices available. They are typically a hand held unit with a pencil probe attached (figure 4.20). The pencil probe (transducer) consists of two piezoelectric elements. One element acts as the emitter and one the receiver (figure 4.19). The two elements are set at angles to each other so that the emitted and received beams over lap (figure 4.19). The overlap region is known as the active or sensitive area which is where the Doppler signal can be detected. The detected signal is obtained by comparing the emitted and received signal.

Continuous wave devices are still widely used today and have many clinical applications such as fetal heart monitoring and detection of peripheral pulses. However, their main disadvantage is that any sound detected in the crossover region can be heard by the operator. For example flow from more than one vessel may be heard at the same time such as an artery and a vein, resulting in a mixed arterial and venous signal being detected. The biggest advantage is that they are inexpensive and easy to use.
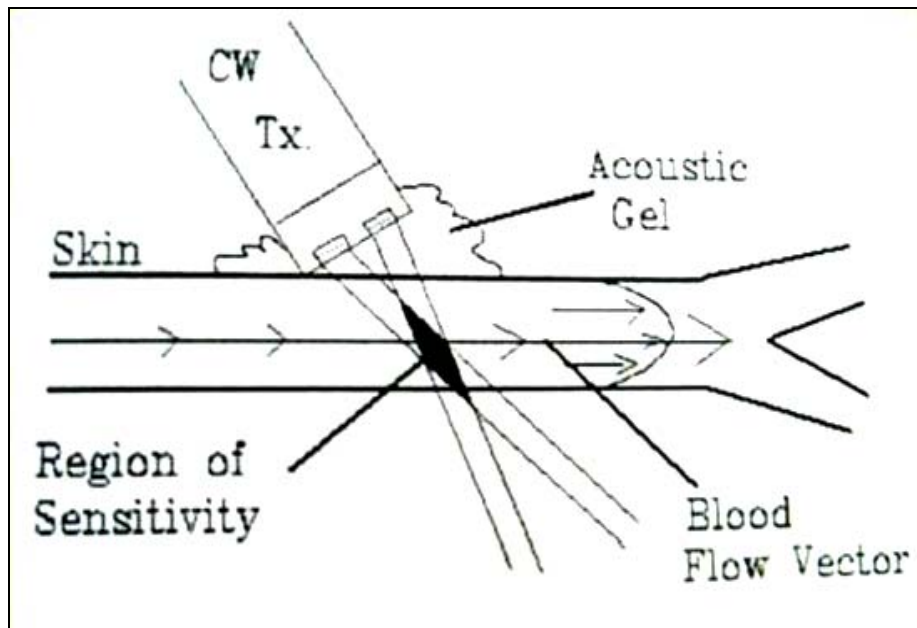
Figure 4.19: A continuous wave Doppler probe

Figure 4.20: A handheld continuous wave Doppler unit

4.10.2 Duplex Systems

Duplex ultrasound systems are devices that have a dual capacity, usually B-Mode imaging and a Doppler blood flow detector in the same unit. The idea is to obtain a B-Mode image of a blood vessel (figure 4.21) then a line representing the path of the ultrasound beam from the Doppler unit can be inscribed on the image, so that the angle of incidence of the ultrasound beam relative to the flowing blood cells can be measured directly (figure 4.24).

4.10.3 Colour Flow Doppler Imaging

Colour flow Doppler imaging enables us to quickly and effectively identify the presence and direction of flow within a vessel as the colour quickly highlights abnormalities within a vessel such as a narrowing.

Colour flow imaging is always used alongside B-mode imaging, it is operated using a colour box (figure 4.22) which highlights an area of interest. This colour box is superimposed onto the B-Mode image and its position and size can be adjusted to give the operator a wider field of view. The colour box is made up of hundreds of lines which are further subdivided into smaller sample volumes. For each sampler volume the mean Doppler shifted velocity is calculated and is assigned a colour depending on weather it is positive or negative which is then mapped onto a colour scale consisting of two primary colours red for positive and blue for negative.

This is the direction information and once it has been assessed the sample volume is assigned a shade depending on the calculated velocity. Doppler angle is again of

extreme importance. The appearance of the colour flow image is dependent on the operator's ability to maintain a sufficient angle between the beam and the vessel.
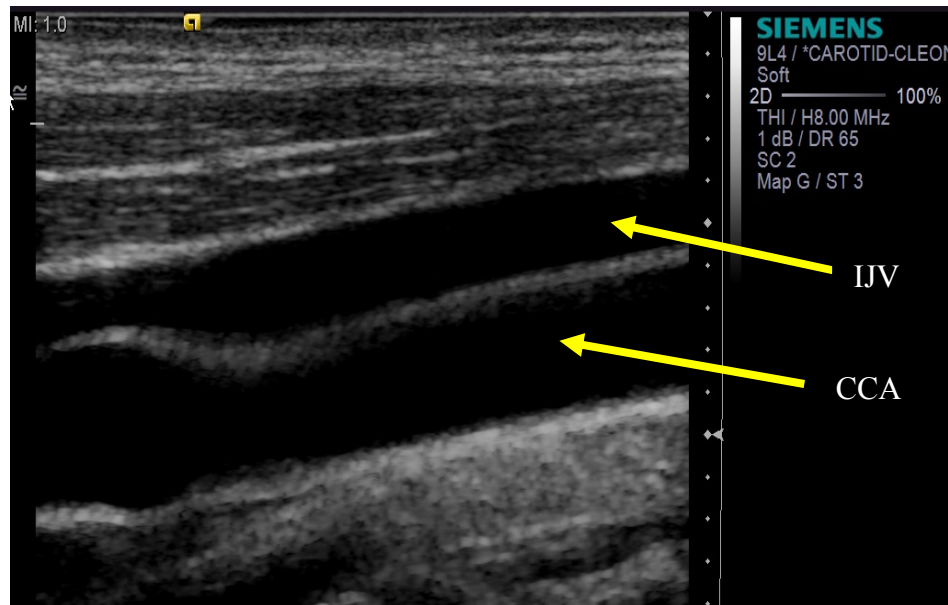
Figure 4.21: B-mode image of a common carotid artery and jugular vein
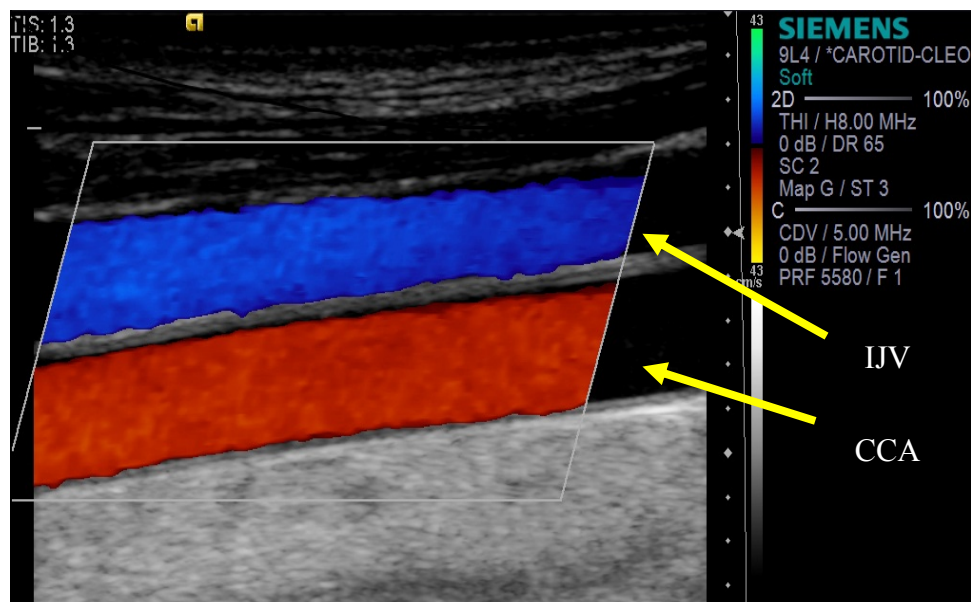
Figure 4.22: B-mode image of the common carotid artery and the jugular

vein with colour flow superimposed showing the different direction of blood

flow in both vessels in red and blue

4.10.4 Formation of Colour Flow Images

Colour flow imaging is carried out by estimating and displaying the mean velocity relative to the ultrasound beam direction of scatters and reflectors in a scanned region. The echo signals from the returning echoes are displayed so the colour hue, saturation or the brightness indicates the relative velocity. The colour flow data is then superimposed onto the B-mode image from stationary structures to create a composite image.

To produce colour flow images there are several methods that have been described. Some operate on the signal produced after Doppler signal processing, few process Doppler signals directly. For each method a series of pulsed echo sequences are produced along a signal beam axis. Echo signals from each succeeding transmit pulse are compared with signals from the previous pulse, and phase shifts in the succeeding signals are estimated. When this is carried out for all pulse echo sequences along the beam line a mean Doppler frequency shift is calculated. The process is completed for all locations along the beam line and estimated velocity is displayed using a colour scale.

Frame rate tends to be lower than that of normal B-mode images as data for each acoustic line that forms a colour velocity image are acquired using multiple pulse echo sequences. The direction of blood flow is coded by the colour display. Red may indicate towards the transducer and blue may indicate flow away from the transducer. The colour process displays motion relative to the ultrasound beam direction for each beam line, forming a new image. Different parts of a vessel are often interrogated using different beam directions, usually due to the orientation of the vessel.

4.10.5 Pulsed Spectral Doppler

Pulsed wave Doppler is a process where the transducer is excited with regular short bursts of pulses rather than a continuous pulse. It uses signals that are much longer than those used in other imaging systems in order to properly determine the Doppler shift of the returning echoes. After being reflected form the tissue interface, the ultrasound waves received by the transducer are converted to voltage pulses which are sent to the receiver. The receiver compares the frequencies of the pulses detected by the transducer with the original transmitted frequency and determines the difference. The result being the Doppler shifted frequency which is then sent to a loudspeaker for audible analysis as well as display.

To detect a signal from a given depth within the tissue a "range gate" is placed within the sample area (figure 4.23). The system will only detect a signal from within this range gate. The Doppler sample is therefore only detected from a specific volume within the body known as the sample volume.

Sample volume within the region of interest
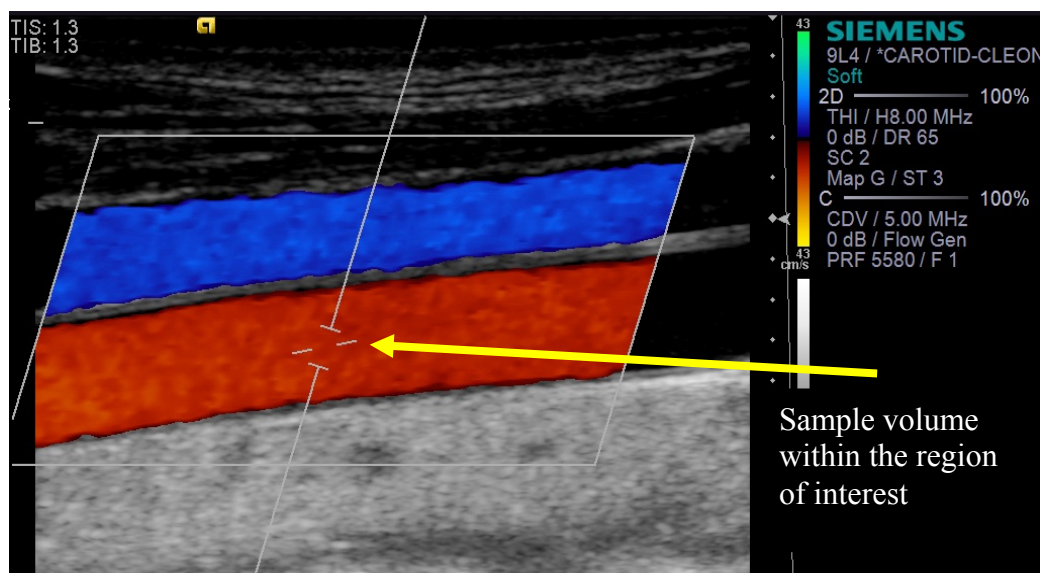
Figure 4.23: A sample volume from the region which the Doppler signal is detected

Duplex systems use Doppler ultrasound in conjunction with imaging to provide an overall picture. It enables the precise location of the Doppler sample volume in the centre of the vessel were the flow is fastest (figure 4.24).

It is also possible to choose the angle of insonation of the Doppler sample and the vessel using angle correction, thus ensuring that the Doppler sample is obtained at an angle as close to 60 degrees as possible. Ideally the vessel walls should be imaged with the beam at right angles to the vessel wall, were as the optimal measurements are obtained parallel to the vessel wall so a compromise has to be made. Linear transducers have the ability to steer the Doppler beam allowing the Doppler beam to set an angle to the imaging beam enabling both the imaging and the Doppler recording to be made in a vessel that runs parallel to the skins surface. Curvilinear transducers do not have this ability to steer the beam so compromise has to be made by angling the transducer and not the beam.
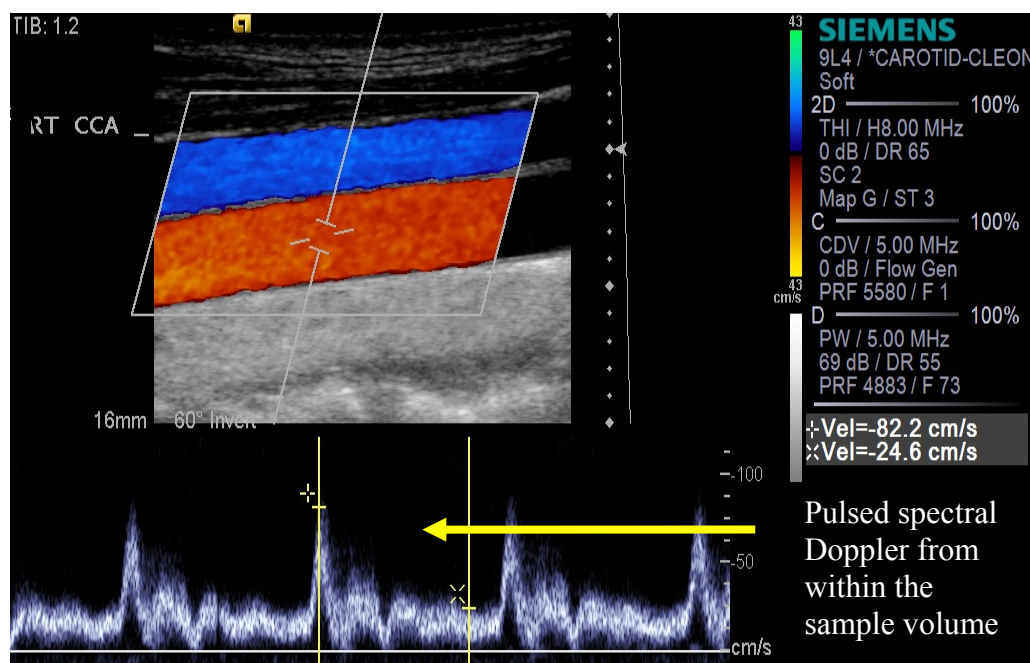
Figure 4.24: Pulsed spectral Doppler obtained from a specific sample volume within the artery

The Doppler sample obtained can be analysed into its frequencies using a process called the Fourier transform. The range of frequencies obtained relates to the range of velocities within the sampled blood flow. The brightness of the display at each point indicates the amplitude of each of the component frequencies which in turn is an indication of the backscatter power for each value of Doppler frequency shift. If the angle of insonation is known then the vertical frequency can be converted to a velocity scale.

4.10.6 Doppler spectral analysis

The Doppler signal is in the audible frequency range and clinical interpretation can be made by listening to the signal. A complex signal may be composed of many single frequency signals each with a particular amplitude and phase, when added together they form the original signal. Spectral analysis is a way to separate a complicated signal into its individual components. The majority of systems use a Fast Fourier Transform to carry out the spectral analysis of a Doppler signal. The Doppler signal is fed into the spectral analyser in small time segments and then displayed along a line were the height represents the frequency and the brightness represents the power. The intensity of the Doppler signals depends on the amount of blood generating that signal, so the brightness represents the amount of flow at the velocity corresponding to that Doppler frequency.

As the spectral signals from a segment are being displayed, a subsequent segment is being analysed and thus a continuous display is produced. Duplex instruments produce a B-mode image along with a Doppler spectral display (figure 4.25).
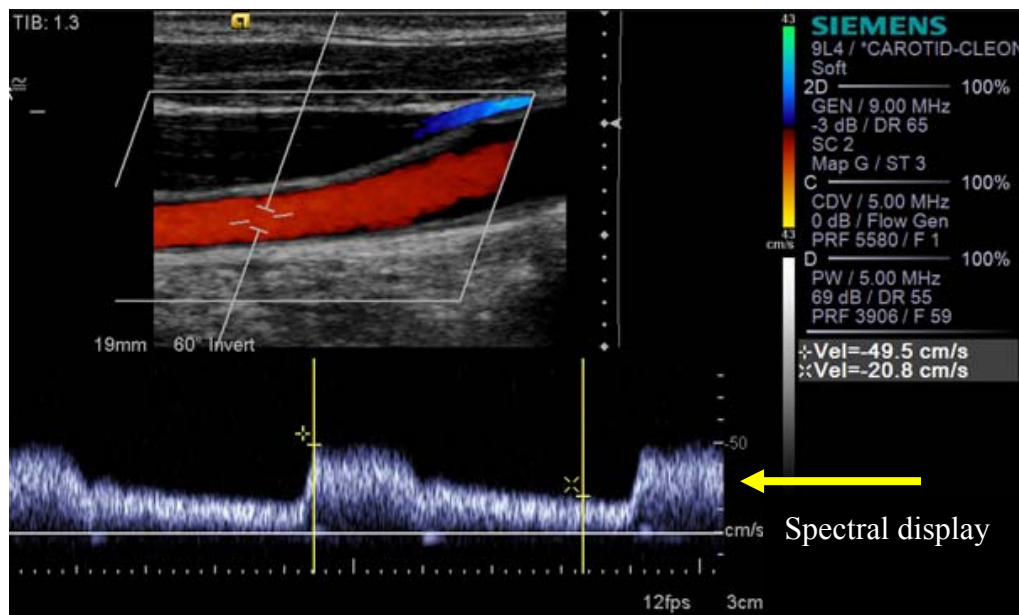
Figure 4.25: The Doppler spectral display from a selected sample volume at an accurate Doppler angle

4.10.7 Power Doppler Ultrasound

Also referred to as energy Doppler or amplitude Doppler, power Doppler is a colour flow imaging technique that maps the magnitude or the power of the backscattered Doppler signal rather than the shifted flow velocities. The strength of the Doppler signal is calculated and superimposed onto a B-mode (figure 4.26). It is a measure of the amplitude of the red blood cells in one area. It does not display the velocity or the direction of the blood flow in the sampled area. It uses single colour strength and maps increasing signal strengths to increased luminosity. It has several advantages over colour flow in that it is more sensitive to flow and detecting very low velocity flow. It is independent of angle and it is not subject to imaging artefacts such as aliasing as it does not use a sampling technique. The obvious disadvantages of power Doppler are its inability to determine flow velocity and direction, it has poor temporal resolution and it is

extremely sensitive to motion so the transducer needs to be very steady in order to obtain high quality images.

Carotid bifurcation imaged with power doppler
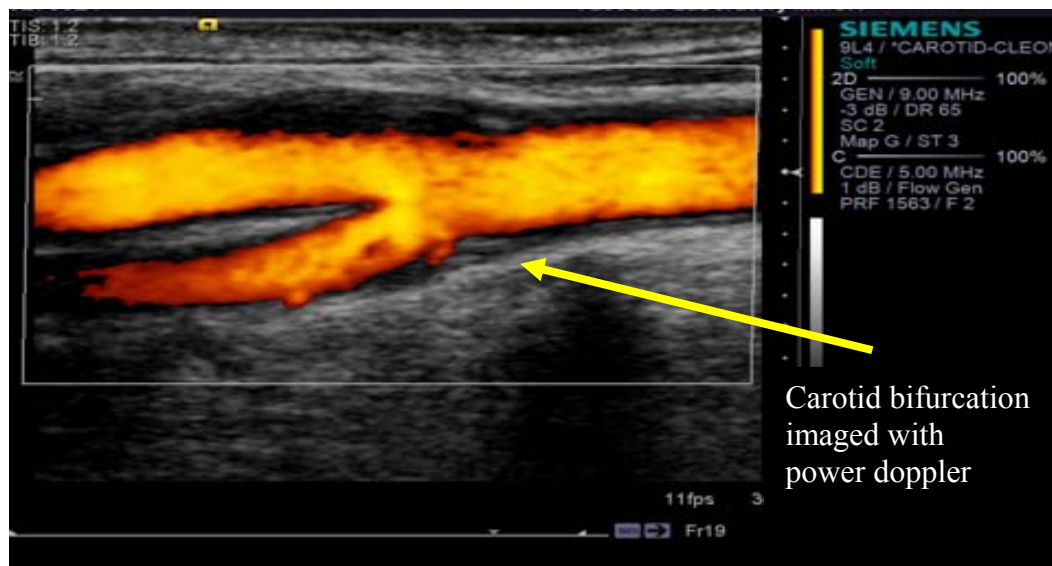
Figure: 4.26: Imaging of the carotid bifurcation using power Doppler

4.10.8 Ultrasound Artifacts and Limitations

An ultrasound artifact is a structure in an image which does not correlate with the tissue being scanned. They can exist in many forms including, structures present on an image that are not actually present, objects that should be represented but are not and structures that are miss registered.

Misinterpretation of results is possible when an operator is not aware of the presence of an artefact. Only some of the more common artifacts that we come across daily are described here.

i. Reverberation

This is the production of false echoes due to repeated reflections between two structures with a high acoustic impedance mismatch. This can occur for example behind bowel gas when the sound reverberates between the gas surface and the transducer and can be differentiated from real echoes due to lack of breathing movement.

ii. Acoustic Shadowing

This is one of the biggest limitations of vascular ultrasound. It appears as an area of low amplitude echoes behind an area of strongly attenuating tissue. It will occur at interfaces with a large acoustic mismatch such as bone or in the internal carotid artery due to the presence of calcified plaque obscuring a portion of the artery and thus imitating its assessment. Figure 4.27 demonstrates the acoustic shadowing caused by the vertebral bodies thus obscuring the assessment of the vertebral artery or vein.
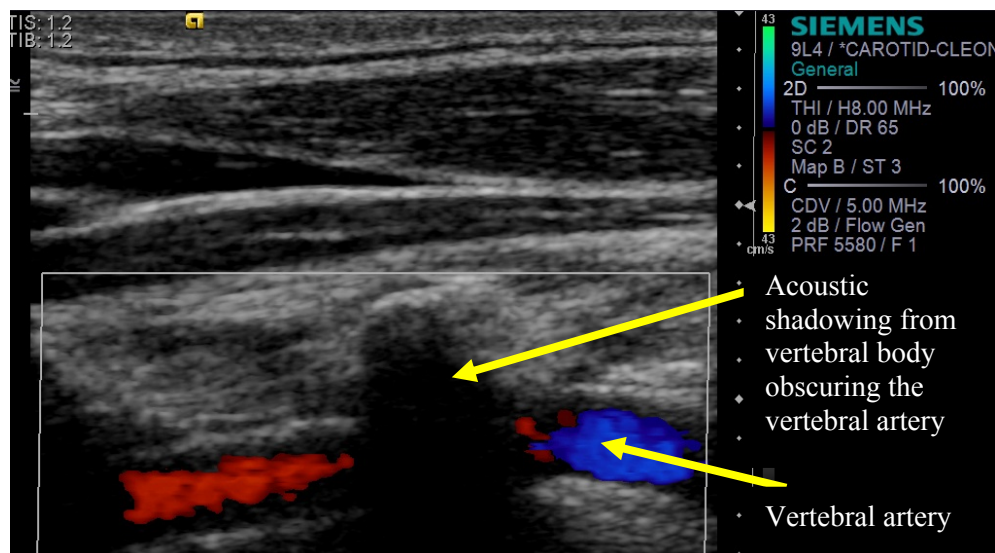
Figure 4.27: Acoustic shadowing caused by vertebral body

iii. Aliasing

Aliasing can occur with all pulsed Doppler instruments because they employ a sampling method to build the Doppler shifted signals. It is incorrect estimation of Doppler shifted signals. The displayed Doppler shifted signals wrap around the Doppler velocity scale and the Doppler shifted signals change from the maximum velocity in one direction to the maximum velocity in the other direction.

Colour velocity images are also subject to aliasing as the colour velocity image is produced using pulsed Doppler techniques. Altering the colour baseline can shift the allowable Doppler frequency range and thus reducing the aliasing.

4.11 Blood Flow within the Human Body

4.11.1 Introduction

Like all other fluids, blood flow in the circulatory system has to obey the laws of physics. In the human circulatory system arterial haemodynamics begins with the heart. It consists of two pumps in series, one to pump blood through the lungs for oxygen and carbon dioxide exchange and the other to pump the oxygenated blood to all the tissues of the body.

Cardiac output (the volume of blood being pumped out of the heart) varies however; the continuous flow to the peripheral vessels is maintained after distention of the aorta and its branches following ventricular systole. The elastic recoil of the wall of the larger arteries propels blood forward as the heart relaxes. With the continued repeated contraction and relaxation of the heart, the blood moves rapidly forward into the smaller arteries which in turn branch and become progressively narrower as they approach the periphery.

4.11.2 Factors Affecting Blood Flow

　　i.Pressure

There must always be a pressure gradient present in order for blood to flow from one region to another. The circulatory system consists of high pressure, high energy arterial reservoir and a low energy, low pressure venous system. These two systems are connected by vessels of varying size and are intimately related by the

resistance vessels that make up the microcirculation, arterioles, capillaries and venules.

Arterioles are the principle point of resistance to blood flow in the circulatory system. Adjustment in the degree of contraction of the muscle walls of the arterioles allows regulation of tissue blood flow and helps control the arterial pressure.

In addition to the change in pressure that occurs across the arterioles there is also a change in the type of flow. The blood flow changes from pulsatile to steady.

ii.   Energy

The main form or energy present in flowing blood is the pressure distending from the vessel walls. This is a form of potential energy which is created by the continued pumping action of the heart followed by the immediate contraction of the aorta.

Other forms of energy such as hydrostatic pressure and gravitational pressure also exist. Hydrostatic pressure is as a result of the weight of a column of blood when a person is standing upright it increases the pressure on the vessel walls and therefore the degree of distension. Gravitational potential energy is related to the effect of gravity on a moving body. The higher the body part the greater the gravitational energy. For example raising an arm above your head will raise the gravitational energy.

Kinetic energy occurs due to the fact that flowing blood is a moving mass. Increases in kinetic energy occur whenever flow is at a higher state such as during exercise or at high velocity stenotic lesions.

$$Total\ fluid\ energy = Potential\ energy + Kinetic\ energy$$

Equation 4.12

Potential energy - pressure and gravity

Kinetic energy - velocity

4.11.3 Energy Losses in the Circulatory System

As blood flows through the circulatory system there is a continual loss of energy in the form of heat due to the friction that occurs between different layers of blood flow, as well as the frictions that are caused by the vessel walls. Pressure and energy levels naturally fall due to these frictions. The energy required to maintain arterial pressure and blood flow is continually being restored by the pumping action of the heart.

i   *Viscous energy losses*

These are energy losses due to the friction that occurs between the layers of blood flow. Normal blood flow in a non diseased artery is referred to as laminar blood flow (figure 4.28). The flow velocity in a normal non disease artery is identical across the width of the artery. This is referred to as "Plug Flow" and is normally seen in aorta or at vessel origins. A few centimetres down steam the blood flow profile will change to laminar which can be described as successive cylindrical layers.

With laminar flow each red blood cells move in one concentric layer (figure 4.28 A) in a highly organised manner with each layer travelling at a different velocity, the layers adjacent to the vessel wall move at a slower speed to the layers in the centre of the vessel (figure 4.28 B). This creates a "parabolic" or "cone shaped" flow pattern. Laminar flow describes the viscous energy losses that occur between

the layers of blood flow and that of the vessel wall resistance. When there is a significant increase in velocity through an artery due to the presence of a stenosis laminar flow breaks down and the blood flow is referred to as turbulent (figure 4.29). Turbulent flow is when the cells move randomly at all different speeds however; they still maintain an overall forward flow. When turbulent flow is present there is greater energy needed, this may be seen distal to a stenosis and an increase in spectral broadening may occur due to the variety of velocities involved. The blood flow within any vessel may not be moving at the same speed at one particular point in time. Faster flow is normally observed closer to the centre of the vessel, slower flow observed closer to the wall. This variation in the speed of blood flow is referred to as the "blood flow profile". The shape of the profile will affect the appearance of the colour flow image and the Doppler spectrum.
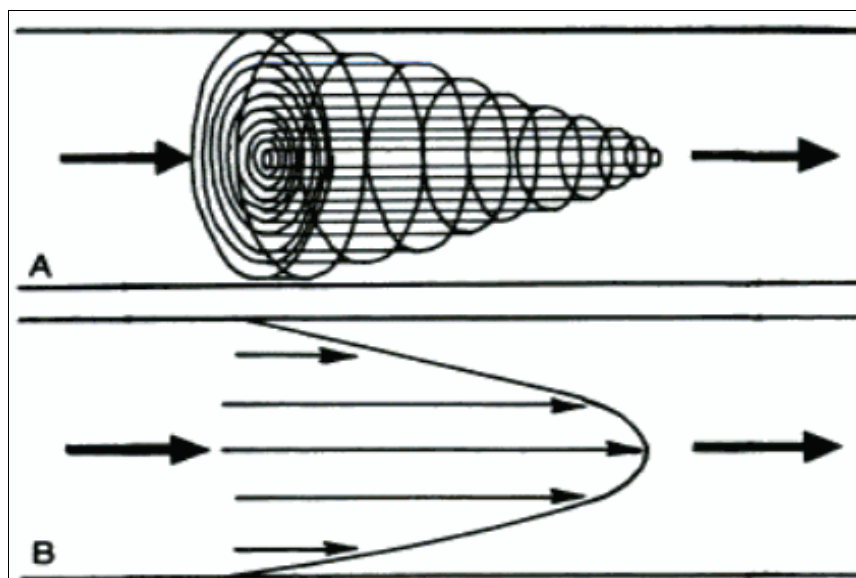
Figure 4.28: Laminar flow profiles within a non diseased artery
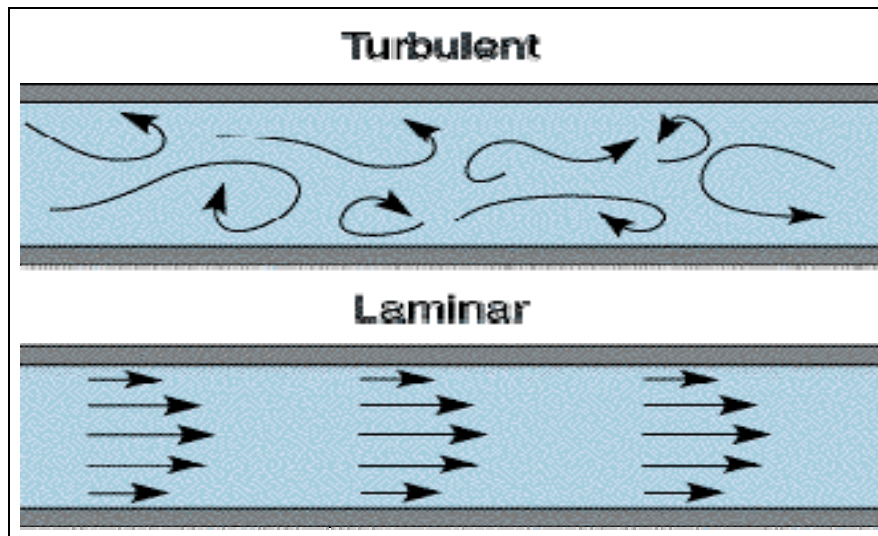
Figure 4.29: Laminar and turbulent flow profiles

ii. Inertial Losses

Inertial losses occur as a result of changes in blood flow velocity or direction. When there is a deviation from the laminar flow pattern resulting in disturbed flow there is an inertial loss of energy. Disturbed flow can be a result of changes in cardiac cycle, change in vessel diameter, a curve or bifurcation of a vessel.
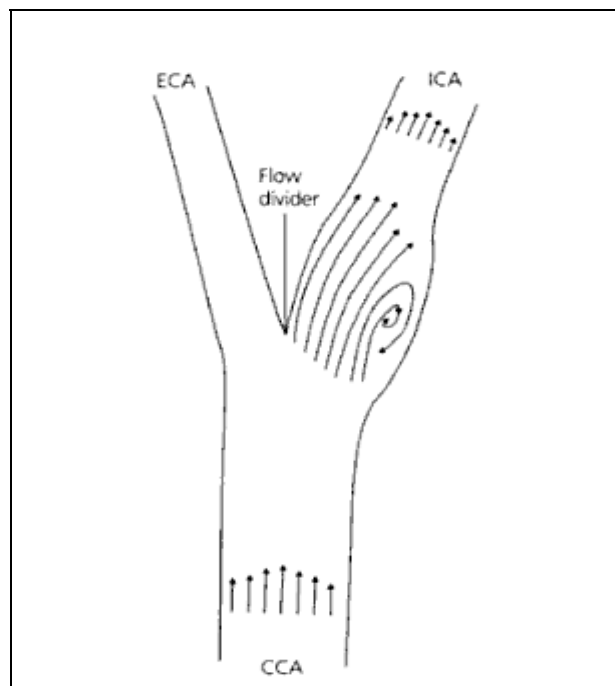
Figure 4.30: Flow patterns observed at a carotid bifurcation

Figure 4.30 describes the blood flow profiles that occur at the carotid bifurcation. There is a change in blood flow profile form the parabolic profile seen in the common carotid artery (CCA) to an asymmetric internal carotid artery (ICA) flow pattern with higher velocities near the flow divider and flow separation opposite the flow divider within the carotid bulb.

Figure 4.31 demonstrates the flow changes that occur at a curve. There is distortion of the parabolic flow pattern caused by centrifugal forces, the highest flow velocities are at the outside wall of the curve. This is commonly observed in a tortuous ICA.
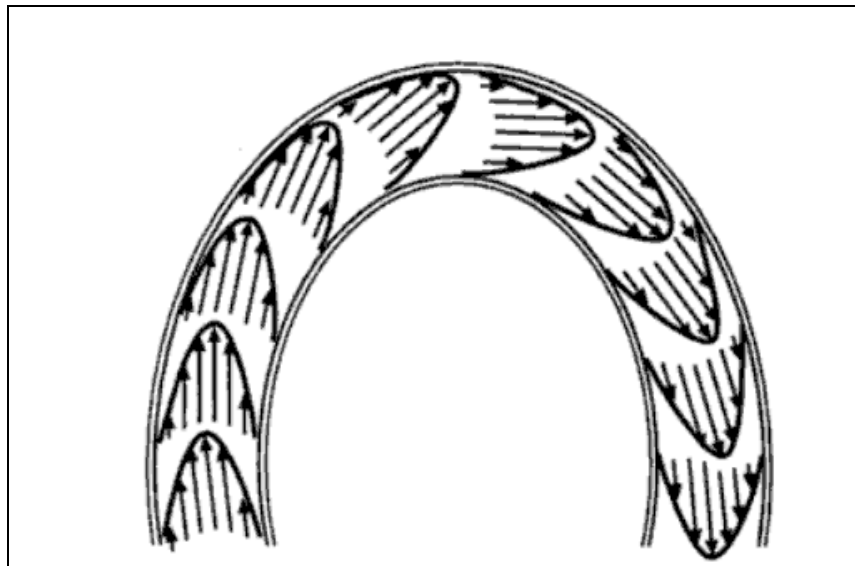
Figure 4.31: Flow profiles in a curved vessel

The final cause of inertial energy losses are the flow changes that occur within a stenosis. The flow profile is always altered within an artery when there is a narrowing or a stenosis present. There is a small amount of flow reversal that can occur distal to vessel constriction. Flow velocity increases as blood moves through a narrowing. As figure 4.28 demonstrates the wide area immediate to the

narrowing, shows an area of flow reversal caused by the sudden changes in pressure which occur when velocity increases through a narrowing.
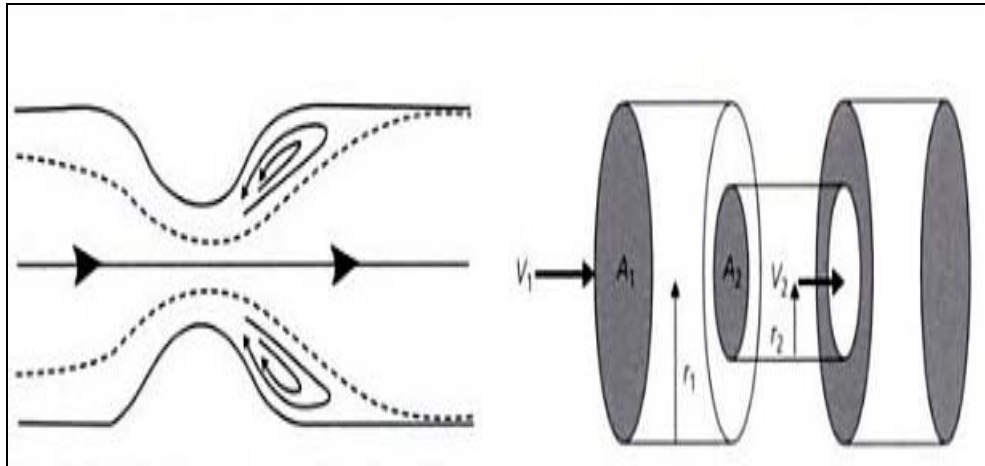
Figure 4.32: Relationship of flow through a tube to cross sectional area

4.11.4 Poiseuille's Law

Relationship of Blood Flow Velocity and Cross Sectional Area

The relationship between steady flow (Q) in a rigid tube of a given cross sectional area A, and the velocity of the fluid V is described by:

$$Q = V \times A$$
                                                                Equation 4.13

Flow throughout the tube will remain constant so long as there are no outlets or branches along it. The mean velocity of flow at any point along the tube will depend on the cross sectional area at a given point. When the cross section area of a tube changes and flow remains constant, then the velocity changes are related to the changes in cross sectional area.

$$\frac{V_2}{V_1} = \frac{A_1}{A_2}$$

                                                                Equation 4.14

This relationship is applied to flow through a rigid tube so it cannot be directly applied to pulsitile flow through an artery however; it gives an indication to how the velocity can change across a stenosed artery.

The velocity at any point in the circulatory system is dependent on the cross sectional area but it is also dependent on the magnitude of blood flow(Q) which depends on many factors such as pressure gradient and the properties of the fluid and dimensions of the entire circulatory system.

Poiseuille's law is an important law governing flow of fluid through cylindrical tubes. In a cylindrical tube the mean linear velocity of laminar flow is directly proportional to the energy difference between the ends of the tubes and the square of the radius and is inversely proportional to the length of the tube and the viscosity of the fluid.

When applied to the circulatory system, volume flow is of more interest than velocity, volume flow is proportional to the forth power of the vessel radius, because it is equal to the product of the mean linear velocity and the cross sectional area of the tube. Poiseuille's law is expressed as follows:

$$Q = \frac{\pi(P_1 - P_2)r^4}{8Ln}$$

Equation 4.15

Q = volume flow rate   r = Radius of the vessel

L = Length of the vessel   n = viscosity of the fluid

$\frac{\pi}{8}$ Is the constant of proportionally

P_1-P_2 = Pressure differential from the proximal to the distal end of the tube

Even small changes in the radius of the vessel will result in large changes in flow. Flow varies directly with the pressure difference and the fourth power of the radius of the vessel, and varies inversely as the length of the vessel and the viscosity of the blood.

Poiseuille's law proves that as the pressure differences increases the flow rate increases, as the diameter of the tube increases the flow rate increases, as the length of the tube increase the flow rate decreases and finally, as the viscosity of the fluid increases the flow rate decreases.

The most import conclusion to be reached from Poiseuille's equation is the relationship between the radius of the vessel and flow, as the diameter increases the flow rate increases, since the volume flow is proportional to the fourth power of the radius; it is evident that very small changes in vessel diameter will result in an increase in flow.

Since the length of the vessel and the viscosity (fluids resistance to flow) of the blood flowing in the vessel remain constant, changes in blood flow occur mainly due to changes in the radius of the vessel and the pressure gradient across the vessel, this phenomenon is known as the Bernoulli Effect.

Turbulent flow can occur in a non diseased vessel due to vessel bifurcations and tortuosity as we have stated. In order to quantify the amount of turbulence that may develop in a non diseased vessel, the elements that may affect turbulence can be related to each other by the Reynolds number.

$$Reynolds\ Number = \frac{Average\ flow\ speed \times Tube\ diameter \times Density}{Viscosity}$$

Equation 4.16

Reynolds number is unitless, as described in equation 4.14 we can derive several relationships from this equation. As flow speed increases the Reynolds number increases, as the vessel diameter increases the Reynolds number increases, as fluid density increases, the Reynolds number increases and finally, as the viscosity of the fluid increases, the Reynolds number decreases. A Reynolds number greater than 2000 results in turbulent flow.

4.11.5   The Bernoulli Effect

The Bernoulli Effect demonstrates the changes in kinetic energy that occur as a result of a stenosis, by converting pressure into velocity and back to pressure. In the circulatory system changes in energy are made by measuring velocity and pressure. When there is a stenosis present there is an increase in velocity at a region of narrowing and thus the pressure decreases. Distal to the stenosis the velocity decreases and the pressure increases.

The pressure never returns to the pre stenotic levels due to the fact that much of the kinetic energy resulting from the increase in blood flow velocity within the narrow portion of the vessel is dissipated in the turbulent jet that occurs after a stenosis. The magnitude of the loss of energy is proportional to the degree of stenosis. The Bernoulli Effect explains why there is a pressure drop distal to a stenosis.

4.11.6   Pressure Changes in Systemic Circulation

As a result of left ventricular contraction, the volume of blood in the arterial tree increases rapidly, rising blood pressure to it systolic peak. However, when cardiac contraction ceases, the outflow of blood through the peripheral resistance vessels exceeds the volume of blood ejected by the heart and the pressure begins to fall. This fall in blood pressure continues during diastole.

This pulsatile variation in blood volume and energy results in a pressure wave that can be detected at any point along the arterial tree. The amplitude and the shape of the wave depends on factors such as the stroke volume of the heart, the left ventricular contraction, the stiffness of the arterial walls and the peripheral resistance.

Thus, an increase in any of these factors will result in an increase in the pulse amplitude.

The arterial pressure wave travels from the heart through the peripheral arteries. The pulse wave's velocity increases as the vessel walls become stiffer due to the increasing muscle content and the ratio of wall thickness to vessel diameter. Therefore, the speed of the propagation of the wave increases as it courses further into the arterial tree. Pressure changes also occur as the pulse wave travels distally. The mean systolic and diastolic pressure in the arterial tree falls between the aorta and the peripheral resistance (figure 4.33). The amplitude of the pressure wave and the systolic pressure actually increases as the wave travels distally. This is referred to as systolic amplification and it occurs as the stiffness of the vessel

walls increases as the wave travels distally and also due to the presence of reflected waves by increasing peripheral resistance.
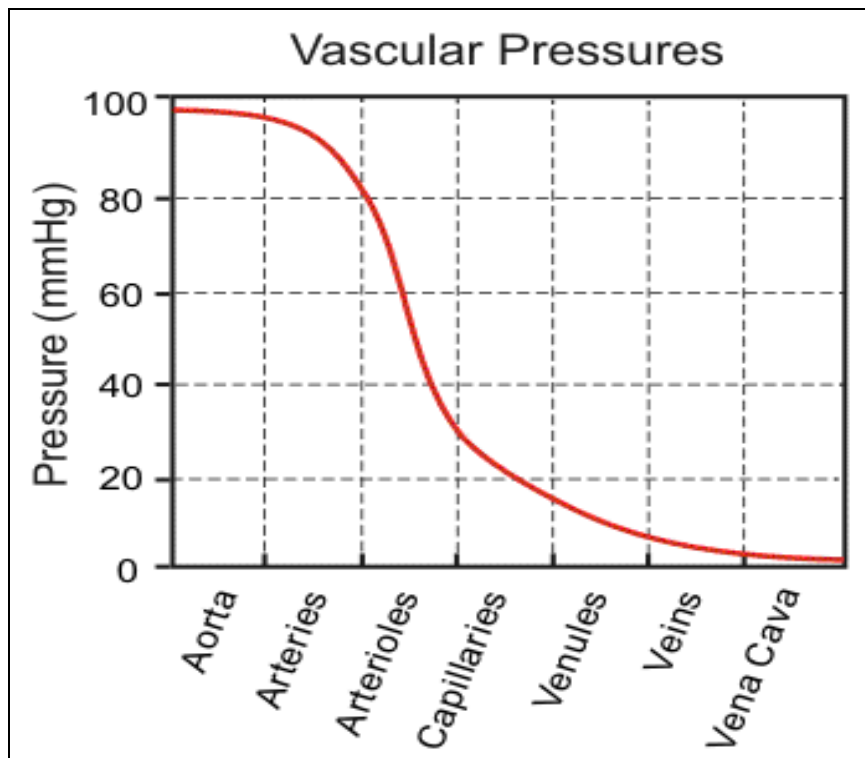
Figure 4.33: Normal pressure changes that occur in systemic circulation

Reflected waves occur at a site where vessel walls change in diameter, vessel walls bifurcate or where vessel walls change in stiffness. In extremities the reflected waves are enhanced by the increase in peripheral resistance.

4.11.7 Velocity Changes in Systemic Circulation

In the extremity arteries of the peripheral arterial circulation there is forward flow of blood noted during systole, but temporary flow reversal occurs during early diastole, this is referred to as diastolic flow reversal. This may occur due to the negative pressure gradient and peripheral resistance which causes a reflection wave proximally. Late in diastole flow again returns to a forward direction as the

reflected wave encounters the proximal resistance caused by the next oncoming wave and therefore reverts. In general, diastolic flow reversal exists in the vessels that supply the vascular beds with a high peripheral resistance such as the extremities. Flow reversal decreases with vasodilation and increases with vasoconstriction.

4.11.8 The Effect of Exercise on Arterial Flow

In a normal resting position, blood flow to the peripheries is sufficient to supply the metabolic needs of the muscles. The skin and the peripheral nerves have the highest metabolic needs at rest and so demand a large percentage of the blood flow. Muscle at rest has a much lower metabolic need.

Exercises causes a large increase in cardiac output related to the increase in stroke volume (the volume of blood pumped from one ventricle of the heart with each heart beat) and heart rate as well as large increase in the volume of blood supplied to the peripheral vascular bed and muscles. This flow increase is as a result of the increased metabolic needs of the peripheral muscles secondary to exercise. Blood flow increases as a result of the dilation of arterioles in response to the by-products of increased metabolism.

The metabolic demands of exercise increase arterial flow to the muscular beds by as much as five times the normal resting levels. When diseased arteries are present, blood flow increase to the muscles is limited by the proximal resistance of the arterial stenosis. A pressure drop also occurs across the stenosis, this pressure drop can be measured at the level of the ankle.

4.11.9   The Critical Stenosis

This is described as a narrowing of the arterial lumen resulting in a haemodynamically significant reduction in volume, pressure and flow.

Blood flow within a stenosis will vary with the degree of reduction in the diameter of the vessel. When a reduction is less than 70-80% the flow will remain relatively unchanged, as the diameter of the vessel reduces the stenosis that is present will limit the flow. Figure 4.34 shows that as the diameter of a vessel decreases the velocity within the vessel will increase. It is for this reason that velocity changes are considered a more sensitive method of detecting vessel lumen reduction. A point will be reached on the graph were flow will drop to such a huge extent that the velocity will be described as "Trickle Flow" within the vessel.
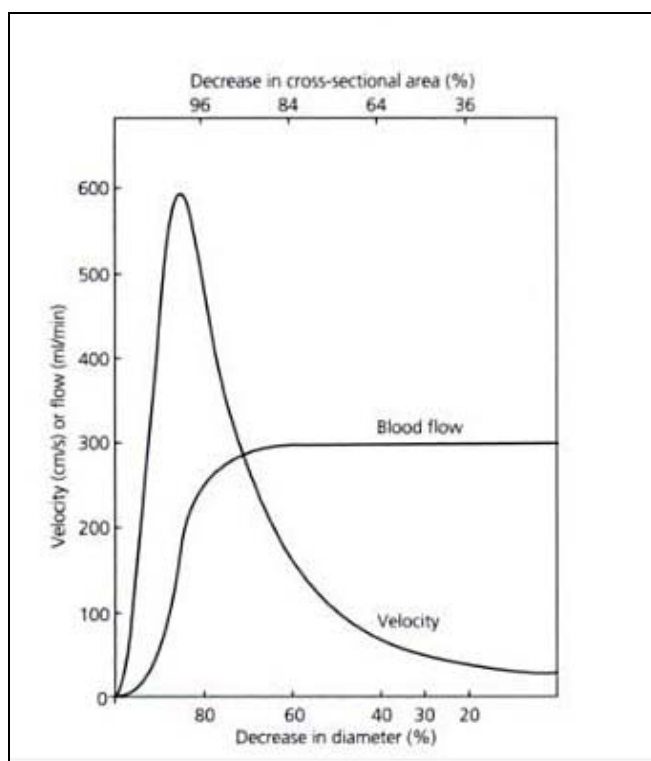
Figure 4.34: Altered flow velocities with a decrease in diameter reduction

4.12 Arterial Stiffness

The pulsatile changes in blood volume and energy in each cardiac cycle is manifested in a pressure wave that can be detected throughout the arterial system. The amplitude and the shape of the arterial pressure wave depends on many factors such as stroke volume, the time course of ventricular ejection, peripheral resistance and the stiffness of the arterial walls. An increase in any of these factors can cause an increase in the pulse amplitude i.e., the pulse pressure (a difference between the systolic and the diastolic pressure).

Increase in the stiffness of the arteries tends to occur with many risk factors such as age, diabetes, renal disease and other cardiovascular disease. The arterial pressure wave is propagated along the arterial tree distally away from the heart. The speed propagation of the wave (pulse wave velocity) increases with the stiffness of the artery wall and with the wall thickness. Arteries become progressively stiffer towards the periphery and therefore the speed of propagation of the wave should increase as it moves peripherally.

Arterial stiffness can be assessed non-invasively by many indirect measurements of pulse wave velocity (PWV) based on the time it takes the pulse wave to travel a specific distance along the peripheral vasculature.

Critical points of these methods are the precise measurements of the pulse transit times and the path length. PWV is being used more commonly now as a diagnostic tool in the clinical setting to assess a patients cardiovascular risk. The relationship

between the pulse wave and the elasticity of a thin walled elastic tube filled with an incompressible fluid is expressed by Moen's Kortweg equation (4.17).

$$PWV = \sqrt{\frac{Eh_v}{2\rho_b r_{vi}}}$$

Equation 4.17

ρb = Density of blood

E = elastic modulus

h_v = thickness of the arterial wall

r_{vi} = the internal radius of the artery

We take from this equation that the PWV is related to the square root of Young modulus of elasticity (E) so measuring PVW is a method of measuring the stiffness of the tube. Higher velocities are equal to higher values of arterial stiffness. Blood density (ρ) should be constant and h and D may be estimated from the B-mode image of the artery.

4.12.1 Factors affecting Pulse Wave Velocity

There are many factors and physiological parameters that affect pulse wave velocity and can alter its end value such as age and cardiovascular health. It is well known that arterial stiffness increases with age therefore, PWV will also increase with age and cardiovascular disease. Some studies have shown that pulse wave velocity can vary with respiration. The observed differences between inspiration and expiration were less than 0.5m/sec. Typical common carotid pulse wave velocity is between 6.8m/s and 8.3m/s. some studies have shown however that eating prior to testing increases pulse wave velocity of the peripheral vessels.

Chapter 5

Methodology

5.1 Assessment of Lower Limb Arterial Disease

5.1.1 Introduction

The measurement of Ankle Brachial Indices (ABI's) is a rapidly performed, reproducible and quantitative method of assessing arterial blood flow to the lower limbs. This is a non invasive investigation and is useful as a screening tool to assess the presence and severity of peripheral arterial disease (PAD). In the context of patients undergoing endovascular abdominal aortic aneurysm repair (EVAR) ABI's provide an objective measurement of the adequacy of lower limb arterial inflow. This is an important aspect of EVAR surveillance as both the introduction of a large delivery sheath to the ilio femoral vessels during stent delivery or the presence of the graft itself may alter the haemodynamics of the lower limb blood supply.

5.1.2 Patient Preparation

No specific preparation is necessary for this test. The patient was required to remove their shoes, socks and any bulky clothing for the purpose of the test. The test was then explained in full to the patient and any questions were answered.

5.1.3 Ankle Brachial Index Equipment

All ABI measurements were carried out using a Vasogard Scimed Microlite automated system (figure 5.0). Four blood pressure cuffs in total were used during the test, one on each ankle and one on each arm (figure 5.2). An 8 MHz continuous wave Doppler probe (figure 5.1) was used to insonate to the Doppler waveform from the brachial artery (BA) in each arm, the posterior tibial artery (PTA) and the dorsalis pedal artery (DPA) in each leg.

Figure 5.0: Scimed microlite automated ABI system

Figure 5.1: 8 MHz continuous wave pencil probe

5.1.4 Performance of Ankle Brachial Indices

1. Patients are examined while supine. Those patients who are unable to lie supine are examined in the seated position with their legs elevated and this is documented in the patient's report.

2. A pneumatic cuff is then carefully placed around each of the patient's ankles and each of the patient's arms (figure 5.2). The end of an 8MHz continuous wave Doppler probe is covered in ultrasound gel and the BA in the right arm is then insonated.

Figure 5.2: Placement of pneumatic cuffs for ABI measurement

3. While the probe is held static and the technologist listen's to the BA Doppler signal, the pneumatic cuff is inflated until the signal is inaudible, indicating occlusion of the artery.

4. The cuff is then slowly deflated until the BA Doppler signal returns sharply. The systolic pressure reading at this point is recorded and the remainder of the air in the cuff is rapidly deflated.

5. Steps 4 to 6 are repeated for the left arm.

6. Using the 8 MHz continuous wave Doppler probe the Doppler signal in the PTA in the right foot is insonated.

7. The probe is adjusted until the best Doppler signal could be heard, at which point the cuff is inflated until the PTA is occluded and the Doppler signal is inaudible. The cuff is then slowly deflated until the signal sharply returns, this systolic pressure is recorded.

8. The Doppler signal in the DPA in the right foot is then insonated. The cuff is inflated until the artery is occluded and the DPA Doppler signal is inaudible. The cuff is slowly deflated until the Doppler signal returns and the systolic pressure at this point is recorded. The remainder of the air in the cuff is rapidly deflated.

9. Steps 8 to 10 were repeated for the left leg.

5.1.5 Interpretation of Ankle Brachial Index Measurements

ABI's are expressed as the ratio of blood pressure in the ankle to the blood pressure in the arms (equation 5.1).

$$ABI = \frac{Highest\ ankle\ systolic\ pressure\ DPA\ or\ PTA}{Highest\ brachial\ systolic\ pressure}$$

Equation 5.1

In a normal healthy resting individual, lying supine, the ankle systolic pressure should be equal to or slightly greater that the brachial systolic pressure. However, in all patients with PAD of the lower extremities, the systolic pressure of the lower limbs will be less than the systolic pressure in the BA and the degree of this reduction will correlate with the severity of the PAD present in that limb. Thus, a normal ABI at rest should be greater than or equal to 1.0.

Resting ABI	Severity of disease
>1.4	Incompressible arteries
>1.0	No arterial disease at rest
1.0-0.8	No significant arterial disease at rest
0.8-0.5	Moderate disease at rest
<0.5	Severe disease at rest
<0.3	Critical ischemia at rest

Table 5.1: Interpretation of ankle brachial pressure index

(Cole, Norris and Walker. 2001)

Table 5.1 summarises the interpretation of ABI measurements currently used in the MMUH vascular laboratory as recommended by the Society of Vascular Technology of Great Britain and Ireland (SVT).

5.1.6 Limitations of Ankle Brachial Indices

Like all investigations ABI's are not 100% sensitive of specific. The principle limitation is in the assessment of patients with incompressible arteries, such as those patients with diabetes or those with chronic renal failure. In these groups of patients the ankle pressures obtained may be falsely elevated due to the inability of the pneumatic cuff to occlude the rigid diseased arteries. In some cases the arteries will not occlude even with an ankle pressure of >250mmHg. In these patients the

measurement of the toe brachial pressure index (TBI) is a more accurate and reliable method of assessing blood flow to the lower limbs as these smaller arteries are less likely to suffer from calcification.

5.1.7 Toe Brachial Indices

Toe brachial indicies are performed using the same automated Vasogard Scimed machine used for measuring ABI's (figure 5.0). Four cuffs are used in total, one on each of the patient's arms and one on each of the patient's great toes (figure 5.4). It is important to ensure that the patient's feet are warm before carrying out this test as the digital arteries are prone to vasoconstriction.

All toe pressures are performed by photoplethysmography (PPG) as follows.

1.   All patients should be preferably lying supine for this test. A toe cuff is applied to each of the patient's great toes and the PPG sensor (figure 5.3) attached to the toe above the cuff (figure 5.4). The pressure in both great toes can be recorded simultaneously.

2.   When a steady arterial waveform is displayed on the screen. The cuff is inflated until the waveform is obliterated indicating occlusion of the digital artery

3.   The cuff is then slowly deflated until the waveform reappears. The arterial waveform at the point of return is recorded.

4.   This BA pressures are measured as in method section 5.4 steps 1-5.

Figure 5.3: A photoplethysmography sensor used for performing TBI's

Figure 5.4: Blood pressure cuff and PPG sensor attached to a patients great

toe

5.1.8 Interpretation of Toe Brachial Measurements

In the normal limb the baseline digital index should be greater than or equal to 0.6 (Cole, Norris and Walker. 2000). TBI are calculated as described in equation 5.2.

If PAD is present this value will drop accordingly. A systolic toe pressure measurement of < 30mmHg indicates the presence of critical ischemia.

$$TBI = \frac{Great\ toe\ systolic\ pressure}{Highest\ brachial\ systolic\ pressure}$$

Equation 5.2

5.2 Assessment of Carotid Artery Disease

5.2.1 Introduction

Colour Duplex ultrasound (CDU) of the carotid and vertebral arteries is a reliable non-invasive method of screening for extracranial vascular disease. The accuracy of carotid Duplex scanning in the assessment of the degree of internal carotid artery (ICA) stenosis is approximately 90% if performed with proper technique and interpreted by experienced clinicians with established and validated criteria (Brown et al., 2004).

Carotid artery Duplex scanning combines B-mode imaging and CDU to give a high resolution anatomical picture as well as accurate flow velocities through the vessel, which allows the determination of the degree of narrowing to be accurately calculated.

Multiple screening programmes use CDU successfully to diagnose extracranial vascular disease quickly and effectively in the community thus, reducing the risk of stroke in a high-risk population. Qureshi and colleagues in 2001 screened an unselected patient population for carotid artery disease and discovered that smoking, hypercholesterolemia, coronary artery disease (CAD) and age greater than 65 years were associated with an ICA stenosis of >60% by standard Duplex scanning. Jacobowitz et al., 2003 documented that 9.3% of patients screened for CAD were found to have a unilateral or a bilateral carotid artery stenosis, the absence of risk factors such as smoking, hypertension, cardiac disease and hypercholesterolemia was associated with a 1.8% incidence of carotid artery stenosis. When one risk factor was present this increased to 5.8%, rising to 13.5%

if there were two present and 16.7% if three risk factors were identified. The authors concluded that the presence of carotid artery stenosis increases significantly in the presence of one or more risk factor and that carotid artery screening is justified in a select group of patients where treatment of carotid artery disease is fundamental to stroke prevention.

5.2.2 Patient Preparation

No specific preparation is necessary for this investigation. The patient is required to lie supine on the examination table and loosen the clothing around their neck to allow the technologist to gain access to the vessels to be interrogated (figure 5.5).

Figure 5.5: Patient positioning for carotid and vertebral artery Duplex

5.2.3 Equipment

All carotid Duplex scans were performed using one of 3 high resolution ultrasound machines was used a Siemens Sequoia 512 Ultrasound System, a Siemens S2000 Ultrasound System (figure 5.6) or, a Phillips IU22 Ultrasound System. All CDU scans were performed using a multi frequency linear array transducer (figure 5.7).

Figure 5.6: A Siemens S2000 ultrasound system

Figure 5.7: A 7MHz linear array probe

5.2.4 Procedure for Carotid and Vertebral Artery Duplex

1. All patients are scanned in the supine position with their head rotated initially to the left to allow assessment of the right carotid and vertebral arteries and then to the right to scan the contralateral vessels.

2. Beginning at the base of the right side of the neck with the transducer placed transversely across the neck in an anterolateral approach the common carotid artery (CCA) is initially assessed in B-mode in a transverse plane (figure 5.8).
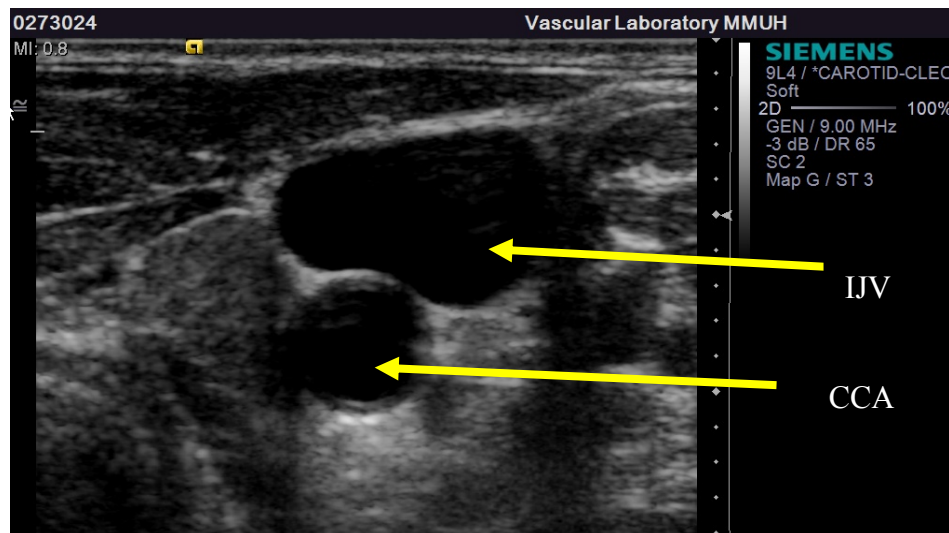
Figure 5.8: The CCA in a transverse plane in B-Mode

3. The transducer is slowly advanced towards the earlobe making note of any plaque, thrombus or any wall abnormality.

4. The transducer is gradually moved towards the jaw bone until the bifurcation appears as two round structures in the centre of the image, the internal jugular vein (IJV) will also be imaged at this level (figure 5.9). One being the ICA and the other being the external carotid artery (ECA). The ECA may be identified at this stage by its branches. The ICA does not branch extracranially.
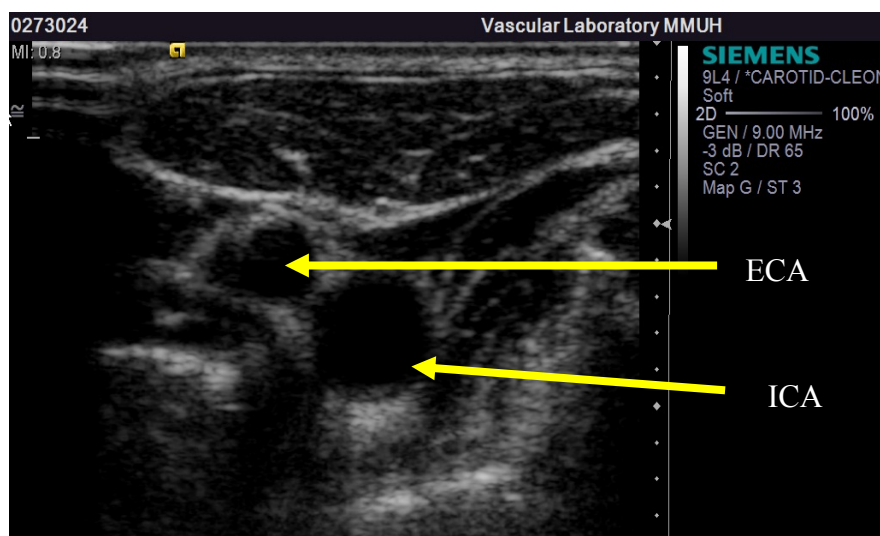
Figure 5.9: The carotid bifurcation in transverse plane in B-Mode

5. A note is made of any plaque, thrombus or wall abnormality that is present.

6. Steps 2-7 are then repeated this time using colour Doppler imaging.

7. Returning to the base of the neck the transducer is placed in a longitudinal orientation (figure 5.10) and slowly moved towards the ear lobe making note of any plaque, dilations or any abnormalities.
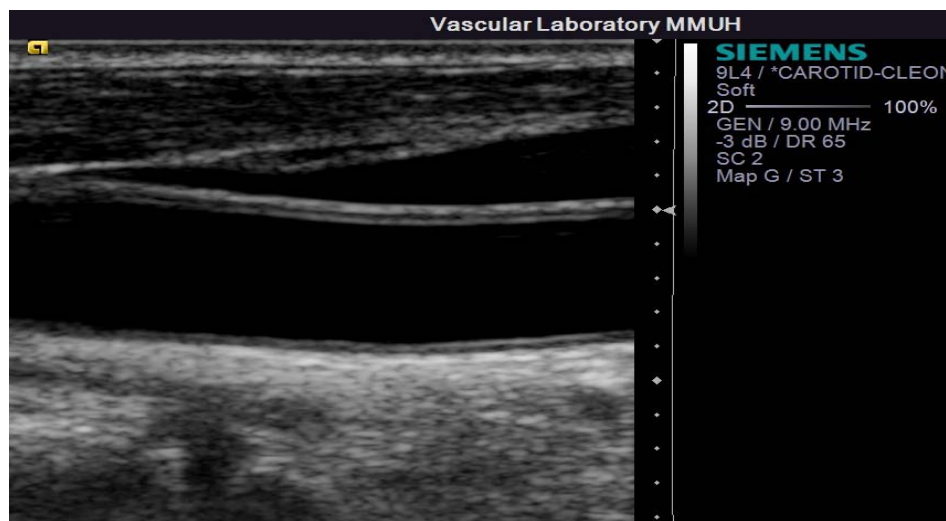
Figure 5.10: The CCA in a longitudinal plane in B-Mode

8. The bifurcation eventually becomes evident. It is important to identify two vessels at the bifurcation (figure 5.11). Both vessels may not be imaged on the same plane.
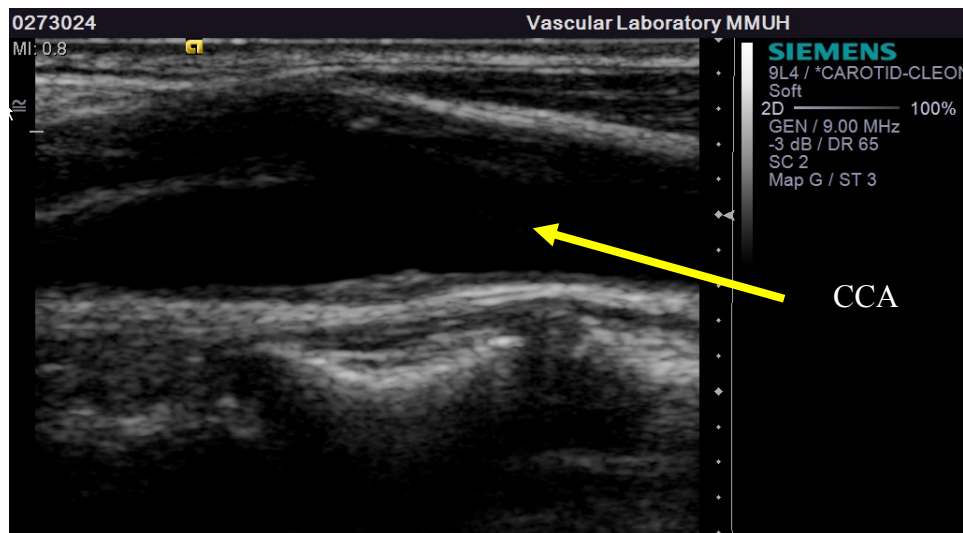
Figure 5.11: The carotid bifurcation in longitudinal plane in B Mode

9. Steps 1-4 are repeated in longitudinal orientation with the colour flow on (figure 5.12).
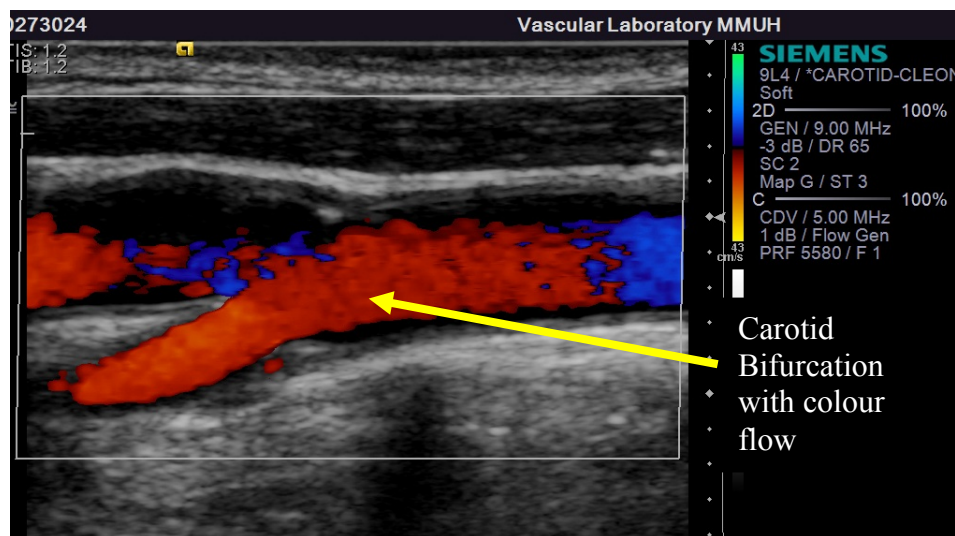
Figure 5.12: The carotid bifurcation in a longitudinal plane in colour flow

10. Returning to the base of the neck the CCA is assessed in a longitudinal plane, with colour flow on and the Doppler sample volume placed in the centre of the vessel (figure 5.13).
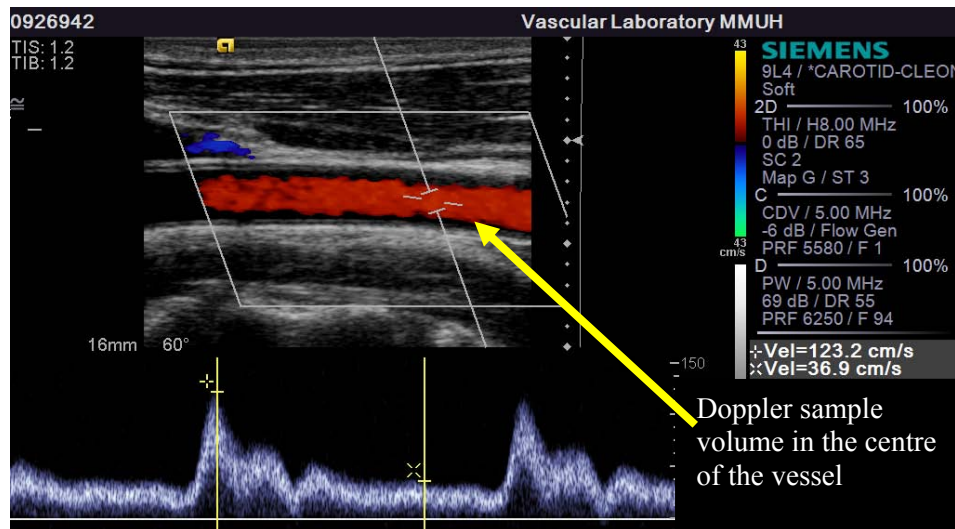
Figure 5.13: Assessment of the CCA with the Doppler sample volume placed in the centre of the vessel

11. The Doppler spectral waveform is recorded at several points in the CCA, taking note to record the increase in velocity proximal to, at and distal to any plaque.

12. The transducer is then moved to the bifurcation and the ECA is identified and assessed with the Doppler sample volume (figure 5.14).
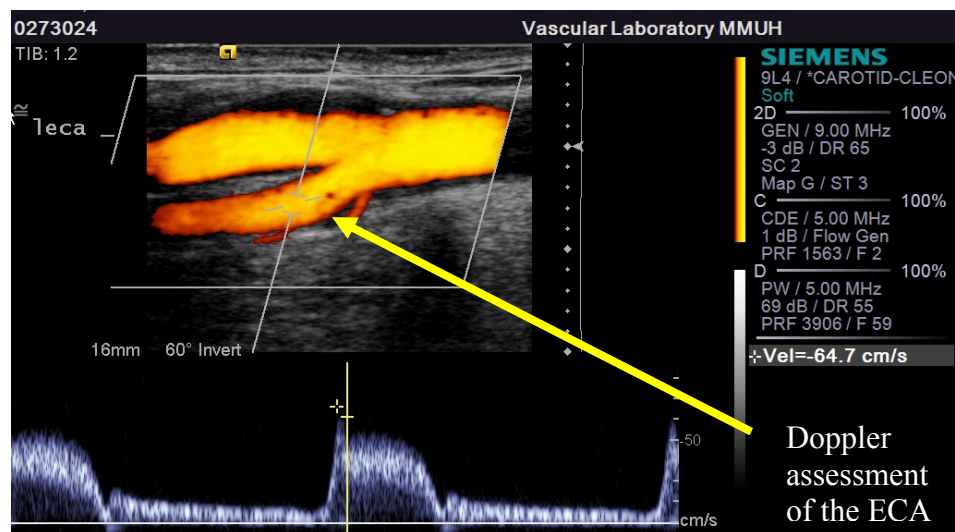
Figure 5.14: Assessment of the external carotid artery

13. The ICA is then identified and assessed with the Doppler sample volume. The maximum peak diastolic velocity (PSV) and end diastolic velocity (EDV) throughout the ICA are recorded (figure 5.15). Care is taken around plaques to ensure the maximum velocities proximal to, at and distal to the plaque are gained and recorded.
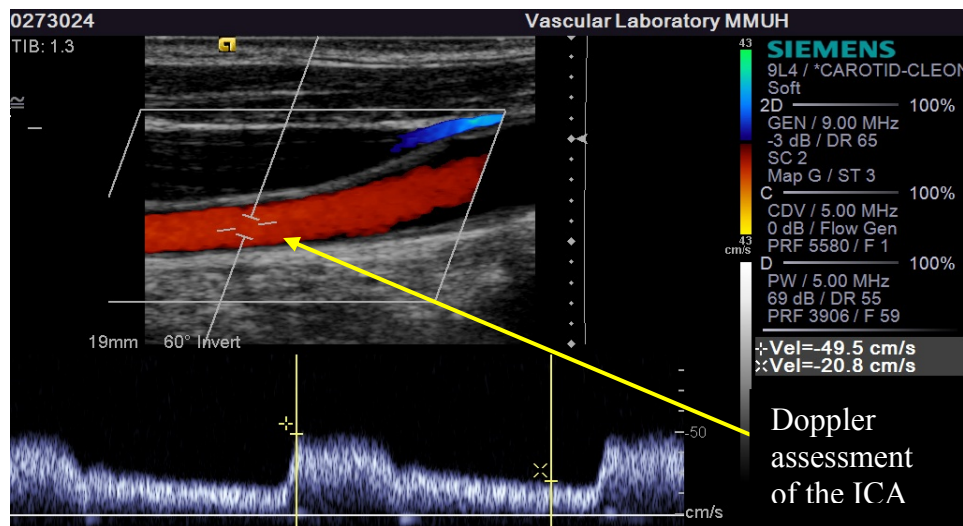
Figure 5.15: Assessment of the internal carotid artery

14. Steps 1-13 above are all repeated with the patients head turned to their right in order to assess the left carotid and vertebral arteries.

5.2.5 Interpretation of Carotid and Vertebral Artery Duplex

The relationship between the progressive increases in flow velocity which occurs in accordance with the degree of stenosis is used as the basis for estimating the degree of narrowing in the ICA.

The degree of ICA stenosis is based on the analysis of the maximum PSV and the EDV obtained within the ICA and the relationship of the PSV in the ICA to the PSV in the CCA. Plaque can be identified in both B-Mode and colour Doppler imaging. However, as the degree of visible lumen depends on the view used, a

stenosis can often be overestimated or underestimated if this is the sole method employed. Therefore, flow velocities are a more accurate way of quantifying the level of stenosis present.

When there is a greater than 50% stenosis present the flow velocities will rapidly increase. Measurement of the PSV, EDV and the ratio of the PSV in the ICA to the PSV in the distal CCA are the most commonly used measurement. Using these measurements the velocity increase is classified into one of six stenosis categories. The velocity criteria employed in the MMUH is recommended by the Society of Vascular Technology (Oates CP et al., 2008).

Stenosis Category	Velocity Criteria
0-29%	PSV <100cm/sec in the presence of plaque
30-49%	PSV >100cm/sec <125cm/sec in the presence of plaque
50-69%	PSV >125cm/sec EDV <140cm/sec
70-80%	PSV > 125cm/sec ICA/CCA ratio of 4
80-90%	PSV >125cm/sec EDV >140cm/sec
90-99%	PSV >125cm/sec EDV >200cm/sec
Occlusion	No colour flow or Doppler signal

Table 5.2: Interpretation of internal carotid artery velocities

(Oates CP et al., 2008)

A very high grade stenosis of the CCA or the ICA on one side may lead to increased compensatory flow in the contralateral carotid arteries. This creates an increase in flow velocities on the other side which may be wrongly interpreted as representing a degree of disease more extensive than that which actually exists. Thus a carotid artery stenosis can appear to reduce in severity on ultrasound following a carotid endertrectomy (CEA) that has been performed on the opposite side.

All Doppler waveforms should be obtained in a longitudinal plane with colour Doppler on and with an angle of insonation as close to 60 degrees as possible. All PSV and EDV values obtained with an angle greater than 60 degrees are inaccurate and may lead to over or underestimation of a stenosis. When there is plaque present a Doppler sample should be obtained proximal to the plaque, within the area of stenosis and distal to the plaque. In all cases the highest PSV and EDV are used to derive the percentage value of the stenosis.

Colour flow is used in all cases as it enables us to quickly and accurately identify the area of narrowing and the region at which the highest velocities will be obtained, this region is commonly referred to as the "jet" (figure 5.16). It also enables us to diagnose an occlusion of the vessel quickly and accurately (figure 5.17).
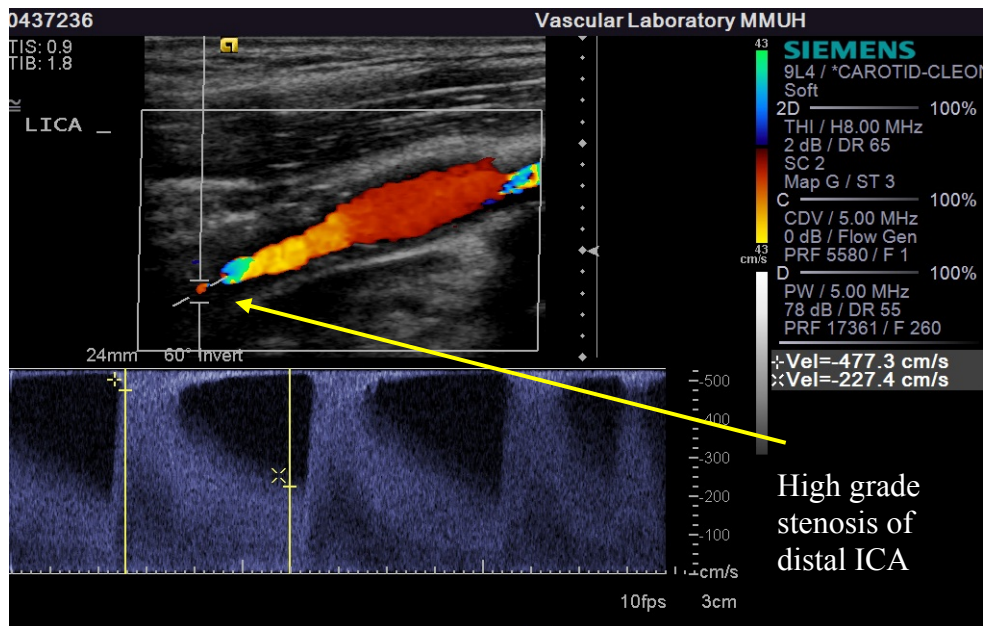
Figure 5.16: A high grade stenosis in the distal internal carotid artery
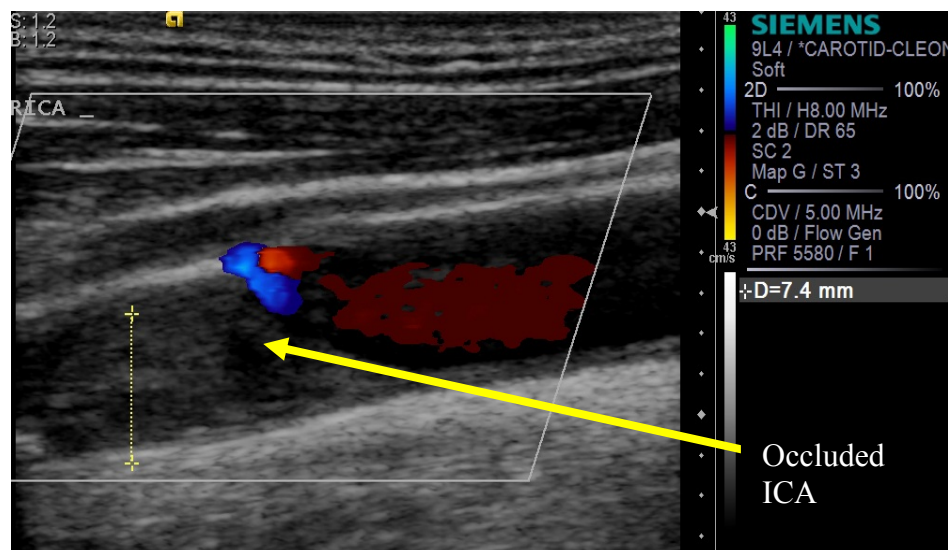
Figure 5.17: A total occlusion of the internal carotid artery

5.2.3.1 Vertebral Artery Analysis

All standard carotid Duplex scans should routinely involve examination of the vertebral arteries. Figure 5.18 represents the vertebral artery in B-mode with the shadowing from the cervical vertebrae obscuring portions of the image.
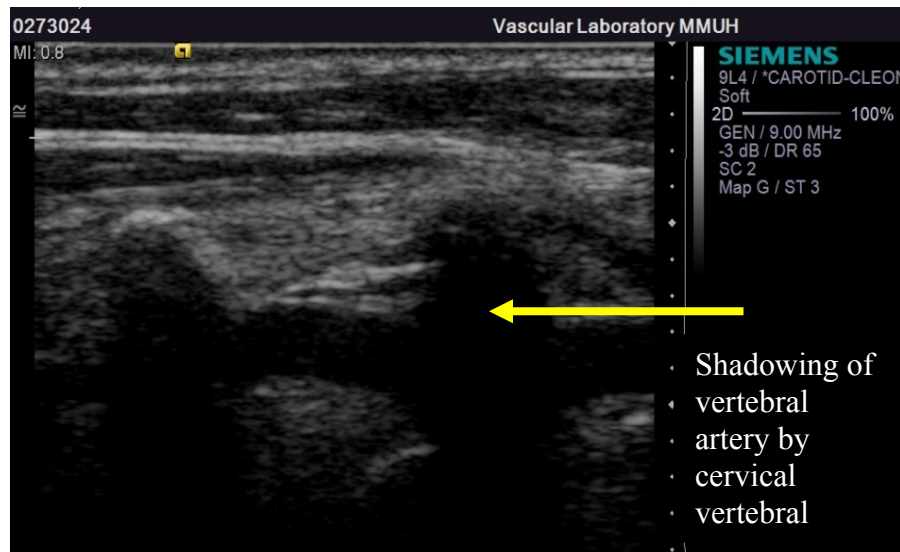
Figure 5.18: Shadowing from the cervical vertebrae

Patency of the vertebral arteries and flow direction should be documented. Figure 5.19 demonstrates a widely patent vertebral artery and assessment of flow through the portion of the artery imaged. However, assessment of stenotic lesions may be difficult due to the shadowing from the cervical vertebrae which only permits assessment of the segmental portions of the arteries see figure 5.19. Reversal of flow in the vertebral arteries indicates a stenosis or occlusion of the proximal subclavian arteries or the innominate artery. When there is only a partial occlusion of these arteries there will be a drop in the systolic portion of the waveform.
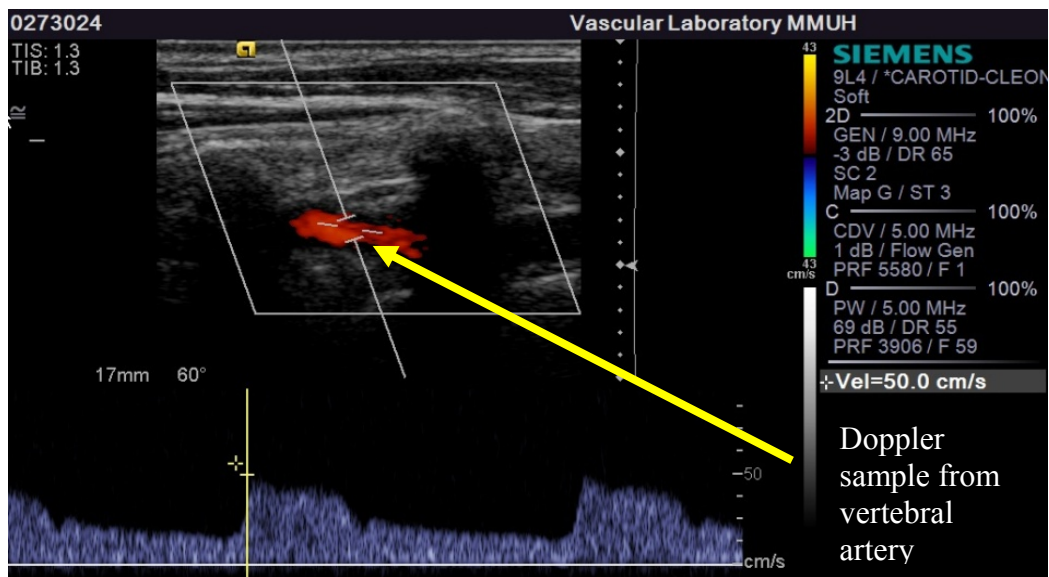
Figure 5.19: Doppler spectral analysis of the vertebral artery

5.3 Abdominal Aortic Aneurysm Surveillance

5.3.1 Introduction

Ultrasound has been used in the diagnosis of abdominal aortic aneurysms (AAA) since the 1960's. An AAA was first demonstrated on ultrasound by Donald and Brown in 1961. Using, Amplitude-Mode (A-Mode) ultrasound they were able to demonstrate a one dimensional view of the aneurysm. Multiple studies have long since demonstrated the accuracy of ultrasound in determining the maximum AAA diameter (Bernstein et al., 1976). The United Kingdom small aneurysm trial (UKSAT) highlighted the use of Duplex ultrasound as a tool for the surveillance for AAA's.

All patients that have been diagnosed with an AAA in the MMUH vascular laboratory are followed up routinely according to the standard follow up protocol for AAA (Chaikof et al., 2009), Table 5.3.

5.3.2 Patient Preparation for Abdominal Aortic Duplex Scanning

All patients are required to fast for at least 6 hours prior to the examination to minimise the effects of bowel gas on the imaging. Where possible all routine surveillance scans are carried out in the morning as bowel gas is naturally less in the morning. The patient is then asked to loosen or remove any constrictive clothing from their abdomen and loosen the waist band on their trousers (figure 5.20).
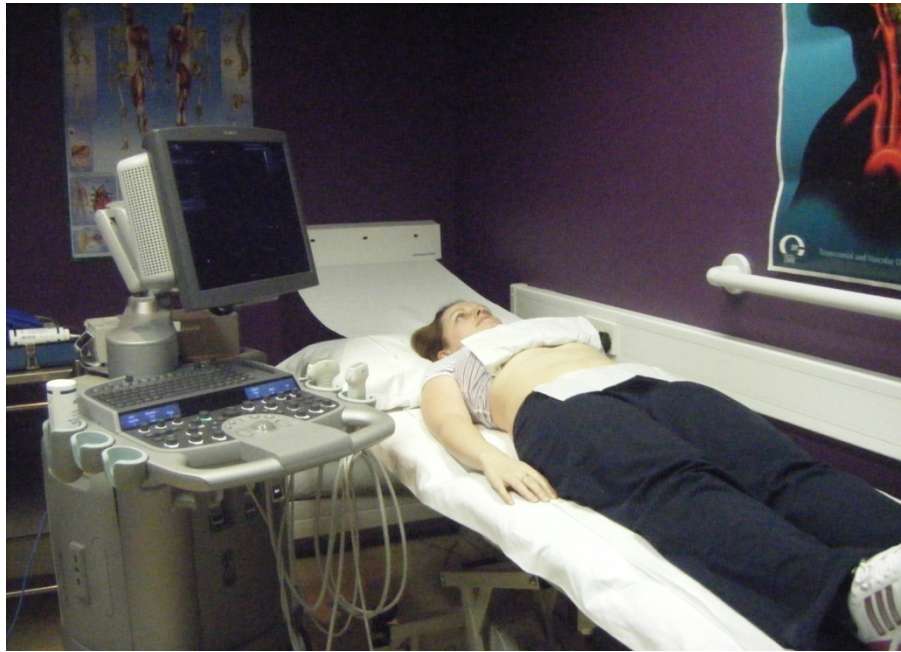
Figure 5.20: Patient positioning for abdominal scanning

5.3.3 Equipment used in Abdominal Aortic Duplex Scanning

All abdominal aorta scans are performed by a qualified vascular technologist on one of two machines a Siemens Sequoia 512 ultrasound system (figure 5.6) or, a Phillips IU22 ultrasound system both using a curvi linear array transducer (figure 5.21) operating at the optimum frequency (2-5MHz).

Figure 5.21: A multi frequency curvi linear ultrasound transducer

5.3.4 Procedure for Duplex Ultrasound of Abdominal Aortic Aneurysms

1.   The patient lies supine on the bed with their hands either by their side or placed behind their head.

2.   Ultrasound gel is applied to the patient's abdomen and beginning in B-Mode and transverse orientation the abdominal aorta is imaged from the diaphragm to the level of the iliac bifurcation (figure 5.22).
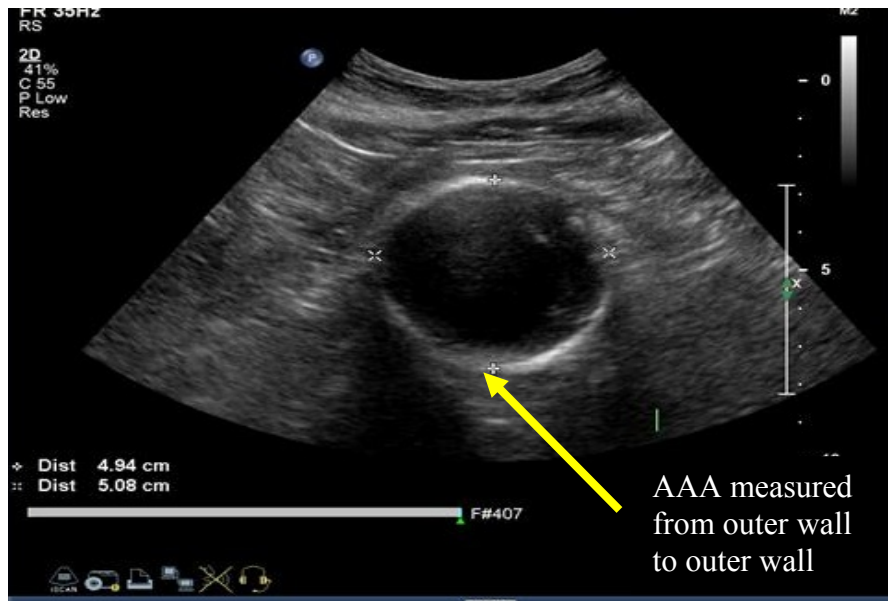
Figure 5.22: An AAA measured from outer wall to outer wall

3.   The presence of any aneurysmal dilatation or thrombus is noted and the maximum diameter is recorded at multiple sites along the aorta (figure 5.22).

4.   All measurements are taken from the outer wall to the outer wall and the maximum measurement obtained was recorded and used for comparison in the next follow up scan.

5.   The iliac arteries are then imaged in a transverse plane in B-Mode from the level of the iliac bifurcation to the common femoral arteries (CFA) where possible (figure 5.23).
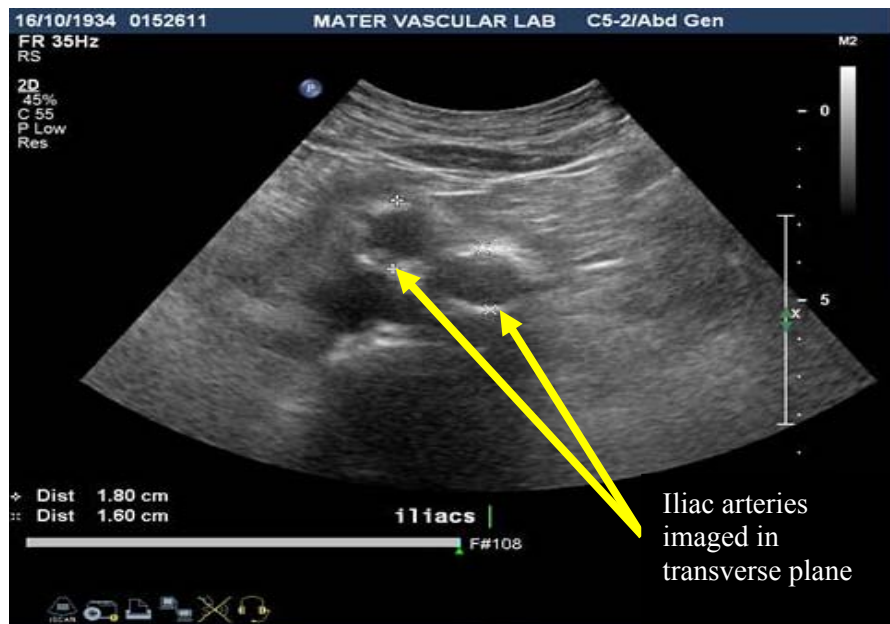
Figure 5.23: A transverse image of the iliac arteries in B-Mode

6. The maximum anterior to posterior wall (AP) and maximum transverse diameters are obtained at multiple sites along the artery and the maximum of the two measurements is recorded.

7. The aorta is then imaged in a longitudinal plane in B-Mode from the diaphragm to the level of the iliac bifurcation.

8. The location of the aneurysm to the renal arteries is examined, the extent and the presence of thrombus is noted.

9. The Iliac arteries were also imaged in B-Mode in a longitudinal plane and the extent of an iliac artery aneurysm if present was noted.

10. Using colour flow and spectral Doppler, the aorta and the iliac arteries are examined in a longitudinal plane for the presence of a stenosis.

5.3.5 Interpretation of Abdominal Aortic Duplex Scanning

With much debate as to the exact definition of an aneurysm in the literature the most widely accepted definition is "an artery is considered aneurysmal when its diameter equals or exceeds 1.5 times the normal diameter of the artery in question. The normal diameter of the aorta in the majority of adults does not exceed 2cm and so it is considered aneurymsal at 3cm" (Zweibel. 2005).

Iliac artery aneurysms can occur in conjunction with an AAA or in isolation. As well as determining the maximum diameter of the aorta when following up a patient with an AAA it is also important to determine the aneurysm's relationship to the renal arteries. The majority of AAA's occur more than 1.5cm below the renal arteries terming them "infra renal", however they can also occur at the level of the renal arteries "juxta renal" or above the renal arteries "supra renal". Approximately 95% of all aneurysms of the abdominal aorta are localised to the infra renal segment and are due to atherosclerosis of the aorta (Winterstein and Baxter, Chapter 34, page 449, Essential Practices of Surgery).

Aneurysms of the aorta are termed "true aneurysms"; they are permanent dilations and involve all three layers of the artery wall. They can be fusiform or saccular and this should be documented on the report.
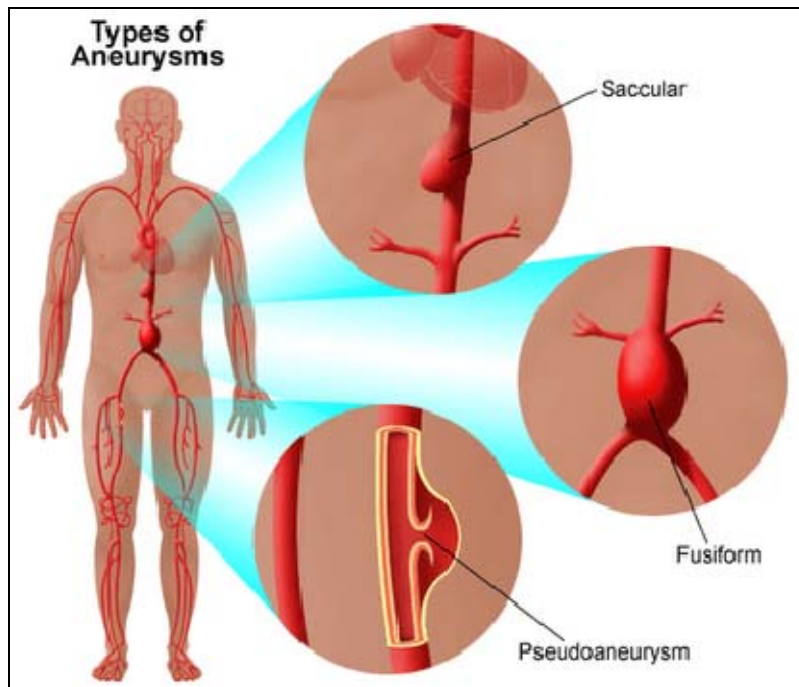
Figure 5.24: Different forms of abdominal aortic aneurysms

The vascular laboratory in the MMUH routinely follows up all AAA's according to a standard protocol summarised in Table 5.3.

Aneurysm Size	Follow up period
2.5cm - 3.0cm	2 Years
3.0cm - 4.0cm	Yearly
4.0cm - 4.5cm	6 monthly
>4.5cm	3 monthly

Table 5.3: Protocol for surveillance of small AAA's in the MMUH

(Chaikof et al., 2009)

5.4 Colour Duplex Ultrasound Surveillance of Patients Post Endovascular Aneurysm Repair

5.4.1 Introduction

The surveillance of patients post EVAR is essential due to a number of complications that can occur. Endovascular grafts are a relatively new and evolving technology and thus require lifelong surveillance to monitor for unforeseen complications. CDU is a non invasive and reproducible method of surveying this particular group of patients.

There are three main objectives in CDU assessment of patients following EVAR.

1. Ensuring that the residual aneurysmal sac is not increasing in size

2. Ensuring that there is no perigraft blood flow

3. Ensuring that there is no evidence of a stenosis or occlusion in the graft, leading to a reduction in flow to the extremities.

5.4.2 Patient Preparation

The patient is required to fast for at least six hours prior to the exam, with the majority of all surveillance scans being carried out in the morning to minimise the effect of bowel gas on imaging. The patient is asked to loosen or remove any restrictive clothing from their abdomen and the waist to ensure the abdomen is visible (figure 5.20).

The patient's personal details are correlated with records before proceeding to the exam room. A brief history is taken from the patient noting any new symptoms since their last visit. It is extremely import to note any new onset of symptoms such as claudication as this may indicate a new occlusion or stenosis of a graft limb.

5.4.3 Duplex Ultrasound Equipment

All CDU scans on EVAR patients are performed by the same accredited vascular technologist using a Siemens Sequoia 512 ultrasound system with a wideband curved linear array transducer (6C2, figure 5.21).

5.4.4 Procedure for CDU surveillance of patients post EVAR

1. The patient is required to lie supine on the bed with their hands by their side (figure 5.20).

2. ABI's are performed on all patients on both lower limbs prior to their ultrasound exam following the protocol documented in section 5.1.4.

3. Each exam commences with imaging of the residual aneurysm in a transverse plane in B-mode from the diaphragm to the iliac bifurcation. Multiple measurements are obtained of the residual aneurysm sac in the transverse plane (figure 5.25).
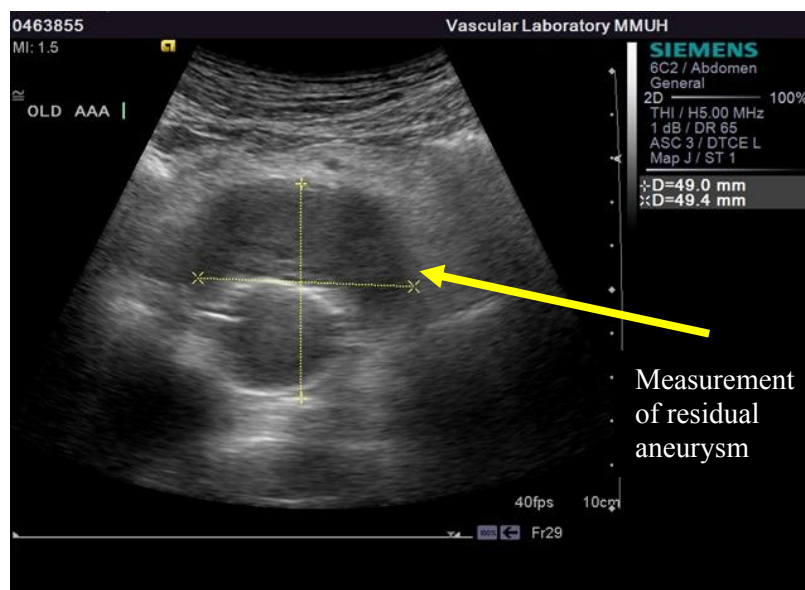
Figure 5.25: Measurement of the residual aneurysm

4. The maximum measurements of the residual aneurysm sac are recorded and compared to the last scan report measurements to ensure that there has been no significant increase in sac size.

5. Careful note is made in B-mode of the stent walls to ensure that there is no evidence of obvious defects or kinking of the metal exo-skeleton.

6. The iliac arteries are imaged in B-mode throughout their entire length. Multiple Transverse and AP measurements are obtained (figure 5.26) and the maximum of the two measurements recorded for follow up purposes.
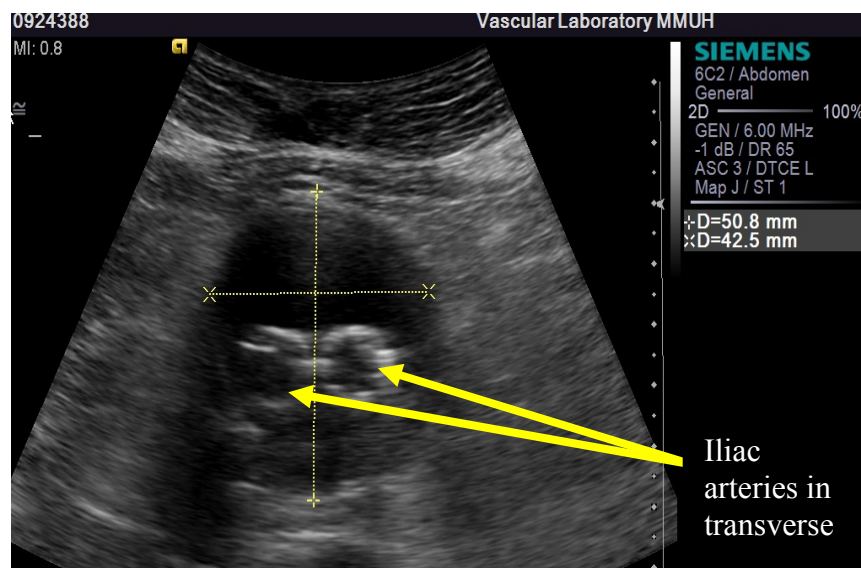
Figure 5.26: Transverse imaging of the residual aneurysm in B-Mode

7. Careful attention is given to the iliac limbs of the stent in B-mode to ensure there is no evidence of graft compression or separation of modular junctions or kinking (figure 5.26).

8. The stent and residual aneurysm sac are then assessed using colour flow and spectral Doppler to rule out the presence of an endoleak. This required the use of very sensitive colour flow scale settings to determine the presence of low velocity leaks which may have been present within the residual aneurysm sac (figure 5.27).
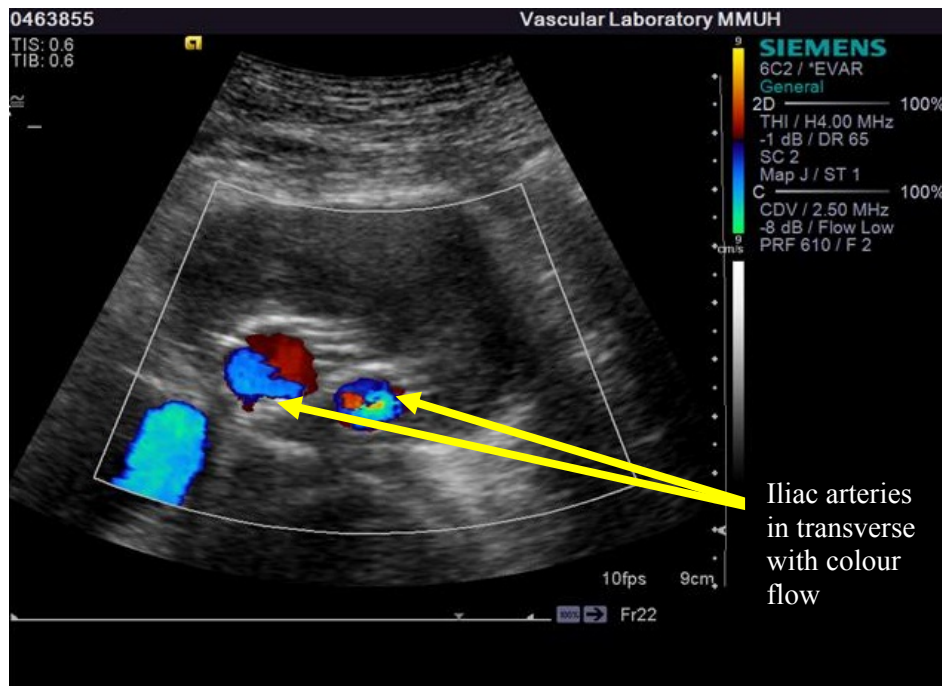
Figure 5.27: Assessment of the residual AAA with colour flow

9. The stent is then assessed, again beginning at the diaphragm and continuing to the iliac bifurcation, careful attention is given to both the proximal and the distal anastomosis sites to ensure that there was no evidence of high jet flow indicating a Type 1 endoleak.

10. Low velocity flow within the old aneurysm sac demonstrating forward and reversed flow indicates the presence of a Type 2 endoleak which may represent patent lumbar arteries or a patent inferior mesenteric artery.

11. Careful note is given to the iliac bifurcation to ensure that there is no evidence of a Type 1 of Type 3 endoleak at the iliac junction.

12. Finally, the iliac limbs are assessed using both colour flow and Doppler ultrasound to ensure that both the limbs were patent and that there is no increase in flow indicating that there may be a stenosis resulting from graft compression or kinking.

5.4.5 Interpretation

i   *Residual Aneurysm Size*

A successful EVAR results in complete exclusion of the aneurysm from the systemic circulation. An aneurysm that has been successfully excluded should naturally decrease in size or remain stable. The residual aneurysm sac size should be compared to the previous exam to ensure that there is no growth in the aneurysm as an increase in size may indicate the presence of an endoleak from the graft or the phenomenon of endotension (Chapter 3, section 3.6.2).

Any patient with a significant increase in sac size between each visit should be investigated thoroughly, if there is a documented endoleak on CDU they should be referred for further imaging such as CT or angiography. Any examination that does not completely visualise the entire residual sac should be documented as limited or inconclusive and the scan should be repeated or an alternative imaging modality should be recommended.

ii   *Endoleaks*

An endoleak is identified by detecting the presence of colour flow outside of the stent walls, within the residual aneurysm sac. When an aneurysm has been excluded from the systemic circulation the blood flow within the residual sac tends to clot naturally over time and will appear echogenic on a B-Mode image. A residual aneurysm that contains echolucent regions within the residual aneurysm over time should raise suspicions for the presence of an endoleak. The Doppler waveform obtained from an endoleak should be reproducible in all cases.

Endoleaks can be classified in to four categories as explained previously in Chapter 3.0.

5.5 Measurement of Pulse Wave Velocity Using CDU

5.5.1 Introduction

Pulse wave velocity (PWV) is universally regarded as the gold standard method of determining arterial stiffness in individuals. The PWV of arteries naturally increases with age and increased arterial stiffness is thought to be an indicator of underlying cardiovascular disease (Blancher et al., 1999, Laurent et al., 2000).

PWV is a non invasive method of determining arterial stiffness. The traditional method of measuring PWV utilises an ECG trace as a timing reference, sensors are applied aver the carotid and the femoral arteries sequentially. The transit time between the upstroke of the carotid arteries and the femoral arteries can then be determined. It can however also be determined by the transit time between the Doppler velocity signal in the common carotid and the common femoral arteries (Jiang et al,. 2007).

There are many commercially avaible systems on the market today to measure PWV however, a standard Vascular Ultrasound system can also be used. Jiang and colleagues in 2007 compared the measurements made by a commercially avaible PWV system and a standard vascular ultrasound system demonstrating no significant statistical difference between the two systems.

Vascular ultrasound scanners are available in all vascular laboratories thus making the measurement of PWV practical in a clinical setting without the acquisition of additional equipment

5.5.2 Patient Preparation

No specific preparation is required for this procedure. The patient is required to remove the clothing from their chest area, loosen the clothing around their groin and lie supine for 10 minutes prior to the exam to allow their blood pressure to normalise.

5.5.3 Ultrasound Equipment

All PWV ultrasound scans were carried out using a Phillips IU22 Ultrasound System utilizing a 7-10MHz linear array transducer by the same accreditated vascular technologist in a temperature controlled room of 20 degrees. The ECG was attached to the patient appropriately and adjusted until a steady waveform was obtained.

5.5.4 Procedure

1.   The patient is required to lie supine and rest for 20 minutes prior to commencement.

2.   Using a standard commercial tape measure the distance between the sternal notch and the femoral arteries was measured. This is the path length (L).

3.   Ultrasound gel and the linear probe was applied to the right side of the patient's neck and the probe was adjusted until a clear image of the right CCA proximal to the bifurcation was obtained in a longitudinal plane.

4.   The Doppler sample gate was placed in the right CCA approximately 2 cm proximal to the bifurcation and the Doppler spectral waveform and the ECG trace were then recorded simultaneously for several cycles.

5.   The time interval between the R waves of the ECG to the foot of the Doppler waveform was determined using the onboard computer and callipers. The foot of

the waveform was identified by the intersection of the upstroke of the wave with the base line of the zero frequency (figure 5.28).

Figure 5.28: Measurement of time interval between the R-wave of an ECG trace to the foot of the Doppler waveform in the right CCA

6. The femoral arteries were then identified by applying ultrasound gel and the linear probe to the patient's groin area and the probe adjusted until a clear image of the CFA 1-2cm proximal to the bifurcation was obtained in a longitudinal plane.

7. The sample gate was place in the right CFA and a Doppler spectral waveform and the ECG trace were recorded for several cycles (figure 5.29).
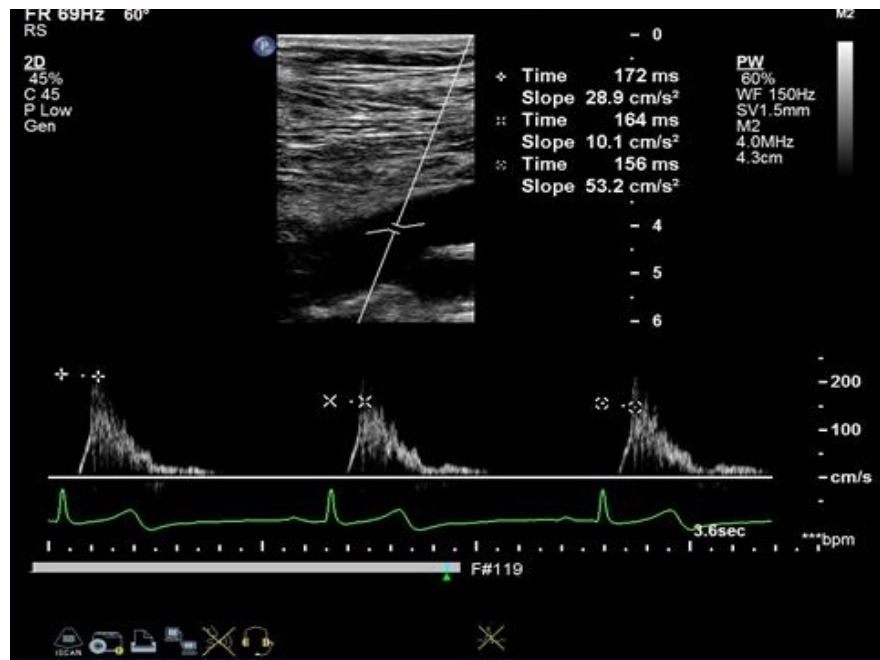
Figure 5.29: Measurement of time interval between the R-wave of the ECG trace to the foot of the Doppler waveform in the right CFA

5.5.5 Interpretation

The PWV was calculated for each patient using the following formulae as described previously by Jiang et al., 2007.

$$PWV = \frac{Length}{Pulse\ transit\ time\ common\ carotid - common\ femoral\ artery}$$

Equation 5.3
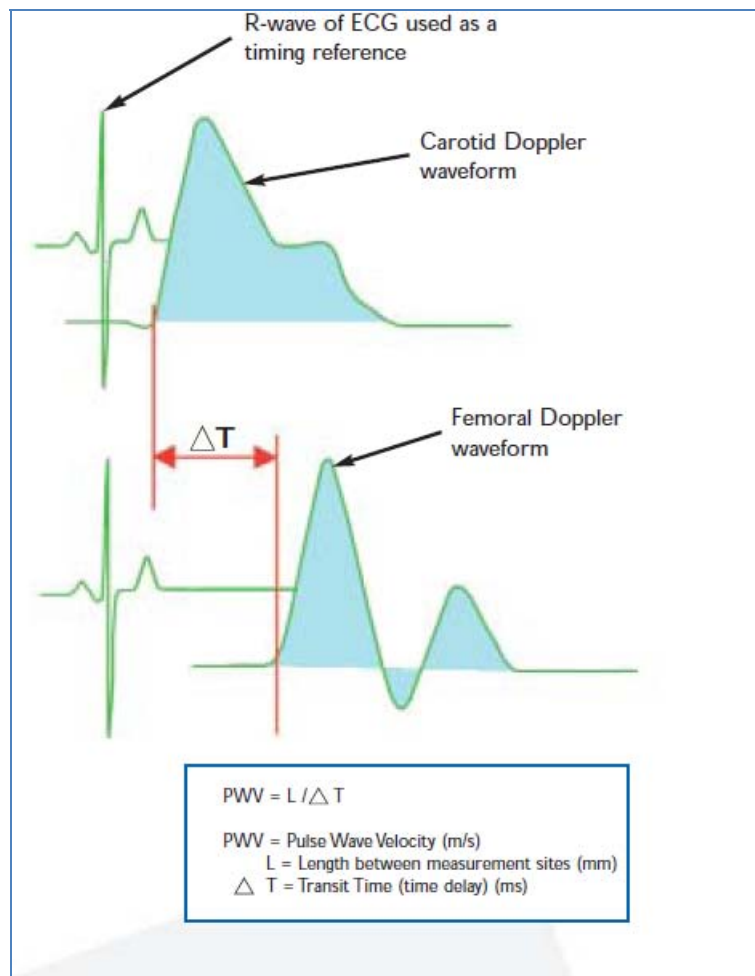
Figure 5.30: Measurement of PWV using the R-wave of the ECG trace as a timing reference

Chapter 6

Colour Duplex Ultrasound as a Screening Tool for

Peripheral Arterial Disease and Carotid Artery

Disease in Patients with Abdominal Aortic

Aneurysms

6.1 Introduction

Atherosclerosis is a systemic disease, with peripheral arterial disease (PAD), carotid artery disease (CAD) and coronary artery disease often co-existing together (Sukhija et al., 2004). A relationship between CAD, PAD and coronary artery disease has long been established. Kallikazaros et al., in 1999 examined the relationship between coronary artery disease and CAD; they concluded that CAD was significantly related to the presence and severity of coronary artery disease. And the presence of CAD in patients with chest pain reflects the presence of coronary artery disease. Klop and colleagues in 1991 demonstrated that PAD and CAD co exist, suggesting that patients presenting with symptoms of PAD should also be screened for CAD. In patients with overt cardiovascular disease, the presence of PAD is associated with an increased risk of myocardial infarction (MI), ischemic stroke, and vascular death (Hiatt and Krantz. 2006). Occlusive PAD of the lower extremities is a common but often overlooked condition. Its age adjusted prevalence is 12% and the risk of developing PAD more than doubles each decade after the age of 40 years (Hiatt and Krantz. 2006). Patients with PAD also show a 2 to 6 fold increase in the incidence of cardiovascular death (Cimminiello et al., 2010). Criqui et al in 2008 demonstrated that after a 5 year follow up of 100 patients with PAD, 16 had died of cardiovascular causes, 4 of cerebrovascular causes, 3 of other vascular causes and 7 of non vascular causes, equating to 30% mortality at 5 years. Carotid artery intima medial thickness (IMT)

has also been widely described as a marker of the presence of CAD (Kallikazaros et al., 1999) and has been previously correlated with the severity of coronary artery disease (Adams et al., 1995). The exact causes of the degenerative process remain unclear. Patients with AAA's commonly have manifestations of atherosclerotic cardiovascular disease (Hultgren., et al 2007) yet there is little in the literature to suggest that screening this select group of patients for other vascular disorders is a worthwhile exercise.

Colour Duplex ultrasound (CDU) is a non invasive, safe, reliable and inexpensive method of screening patients for CAD. The sensitivity of CDU for the detection and grading of carotid artery lesions has been reported to be as high as 90% (Wain et al., 1998). However, despite the advantages of CDU, identifying candidates for carotid endarterectomy (CEA) with mass screening costs more per quality life adjusted year than is usually considered acceptable (Kurvers et al., 2003). The identification of a group at high risk of having occult CAD to allow more focused screening is paramount. Carotid artery disease is associated with a risk of stroke that increases with the severity of the internal carotid artery (ICA) disease that is present (Busuttil et al., 1996).

Asymptomatic carotid disease, defined as the presence of internal carotid artery stenosis, carotid bifurcation stenosis or occlusive lesions in patients with no signs or symptoms of cerebrovascular disease (Halliday et al., 1994) may progress to symptomatic disease within a mean time of 3-4 years. Thus there is merit in identifying and treating patients with an asymptomatic stenosis prior to it becoming symptomatic. The difficulty lies in identifying a population to screen for asymptomatic carotid disease. The frequency of stroke in asymptomatic patients

with a haemodynamically significant ICA stenosis is 2-5% (Rancic et al., 2002). The asymptomatic carotid surgery trial (ACST) demonstrated that at 5 years the risk of stroke or death in patients that underwent CEA was found to be 6.4% compared to the 11.8% in the patients treated medically. The ACST also demonstrated that patients with an asymptomatic carotid artery stenosis who have undergone CEA are less likely to have a disabling stroke (3.5% in the surgical group compared to the 6.1% in the non surgical group).

Identifying patients with an asymptomatic carotid artery stenosis usually occurs in one of 2 ways, either identification of a bruit during routine physical exam, or during an ultrasound screening programme. The current known rate of TIA or stroke in patients with asymptomatic carotid artery disease of 5-18% is dependent on the severity of the stenosis present and the nature of the plaque itself.

PAD of the lower limbs is thought to be a marker of cardiovascular ischemic events. It is easily detected by the measurement of Ankle Brachial Indices (ABI's) yet it still remains widely unrecognised by clinicians and the general population (Cimminiello et al., 2010). The ABI is a ratio of the ankle to brachial systolic pressure with a value of less than 0.9 at rest indicating the presence of lower limb arterial disease. ABI's have an inter observer variability as low as 7%, a sensitivity of 90% and specificity of 98% for detection of arterial lesions greater than 50% in the lower limbs (Quriel et al., 1982). Despite this, PAD is still thought to be an under diagnosed lifestyle limiting disease that can be an indicator of atherosclerosis in other vascular territories such as the carotid and coronary arteries (Dooby and Anand. 2005). Under diagnosis of PAD is largely due to the

fact that patients suffering with this disease initially present with symptoms of intermittent claudication. Early detection of PAD in some patients may be limited due to their inability to walk as they may suffer from other illnesses. There is evidence to suggest that PAD is a strong predictor of future cardiovascular outcomes such as myocardial infarction (MI), stroke and death (Vogt et al., 1993).

Similar to CAD, identification of a high risk group to screen for occult asymptomatic PAD is an important step in cardiovascular risk reduction in the population.

The objective of this study was to determine the presence and severity of asymptomatic CAD and PAD in patients with known AAA's who are perhaps an unscreened population for atherosclerotic disorders in other vascular territories in order to determine if this would be a reasonable focus group to screen for occult CAD and PAD.

6.2 Patients and Methods

Following approval from the hospital ethics committee, a retrospective audit of all patients attending the vascular laboratory of the Mater Misericordiae University (MMUH) hospital between the 1st of January 2007 and the 31st of December 2009 was performed.

All patients that had a known AAA who had either a CDU or ABI's to determine the presence of CAD and PAD as part of their surveillance were included in the study. The patients pre-existing risk factors were obtained from the patient's clinical notes. The risk factors variables that were examined in the study included age, gender, diabetes mellitus, history of coronary artery disease, hypertension, hypercholesterolemia, smoking status and family history of an AAA.

In this time frame 389 patients were identified on the aneurysm surveillance programme in the MMUH with a mean ($\pm$ SD) age of 76 ($\pm$ 8) years. There were 305 (78.4%) male patients and 84 (21.6%) female patients. The mean male age was 75.4 ($\pm$ 7.8) years and the mean female age was 77($\pm$ 11) years.

6.2.1 Patient Demographics

The patient's risk factors and demographics are summarised in figure 6.1 below. Of the 389 patients included in the study demographics were not available in 27 (6.9%) patients due to deficiencies in the patient's notes.
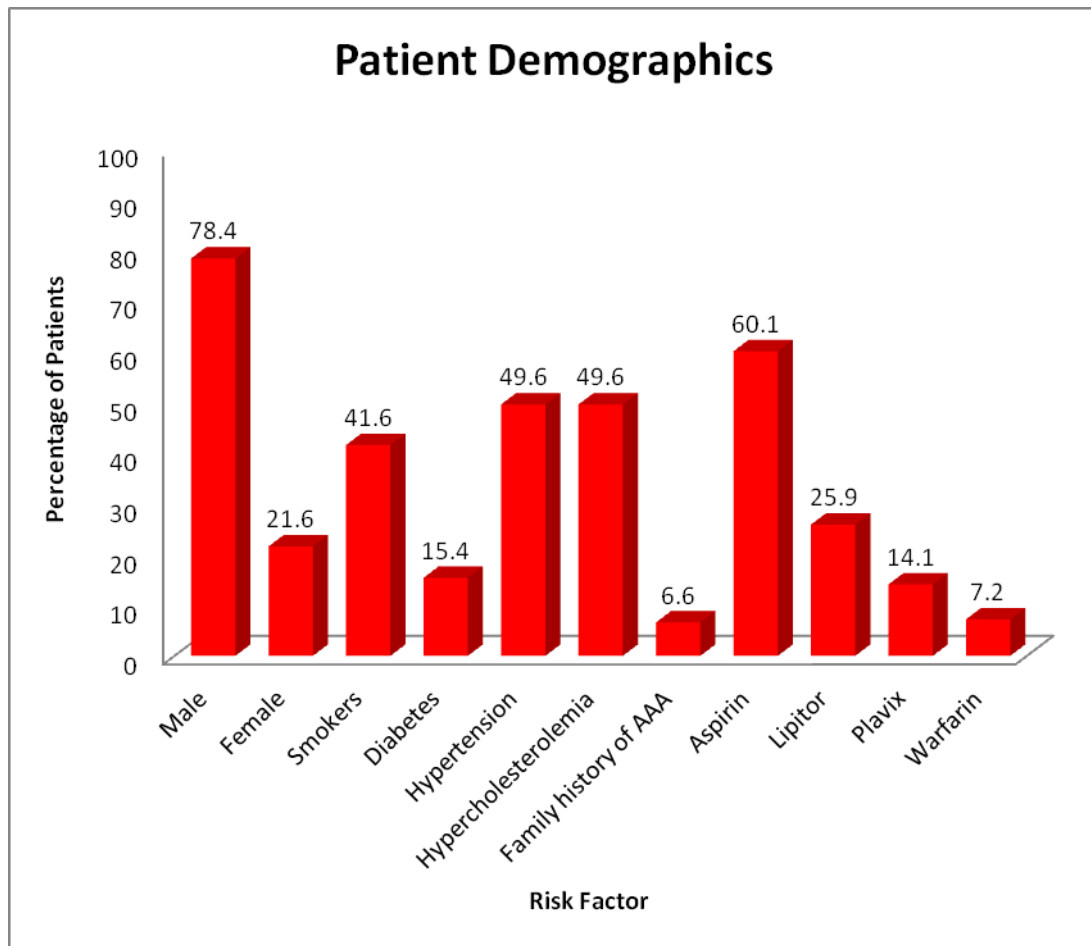
Figure 6.1: Patient demographics

Of the 26 (6.6%) patients with a known family history of AAA, the mean ($\pm$ SD) age was found to be 74 ($\pm$ 7) years. Twenty two (84.6%) of the 26 patients were male with a mean ($\pm$ SD) age of 74 ($\pm$ 7) years. Four (18.2%) were female with a mean ($+$ SD) age of 78 ($\pm$ 4.5) years.

6.2.2 Carotid Artery Disease

Of the 389 patients included in this study, 332 (85.4%) patients had a CDU scan performed to determine the presence of CAD at the time of study completion. The mean ($\pm$ SD) age of this group was found to be 76 ($\pm$ 7.6) years.

Colour Duplex Ultrasound

All CDU scans were carried out by a qualified vascular technologist using one of three machines, a Siemens Sequoia 512 ultrasound system, a Siemens S200 ultrasound system (Chapter 5.0, figure 5.6) or a Phillips IU22 ultrasound system all using a multi frequency linear transducer (Chapter 5.0, figure 5.7).

All patients were scanned in the supine position in a darkened temperature controlled room following the standard clinical measurement protocol for carotid and vertebral artery Duplex as previously described in Chapter 5 section 5.2.4. Carotid artery stenosis was graded according to the maximum peak systolic velocity (PSV) and end diastolic velocity (EDV) and interpreted as previously described in Chapter 5.0 section 5.2.5.

A haemodynamically significant stenosis was defined as a greater than 50% internal carotid artery (ICA) stenosis. Patients with a carotid artery stenosis of less than 50% were taken to have no significant CAD.

6.2.3 Peripheral Arterial Disease

Of the 389 patients included in the study 289 (74.2 %) of patients had either ABI's or TBI's performed at the time of study completion to determine the presence of PAD at rest. The mean ($\pm$ SD) age of the 295 patients was found to be 76 ($\pm$ 8) years.

Ankle Brachial Indices and Toe Brachial Indices

All ABI's and TBI's were performed in a temperature controlled room with the patient lying supine using an automated Vasogard Microlite system (Chapter 5.0, figure 5.0) following the standard clinical measurement protocol for measurement of ABI's and TBI's as previously described in Chapter 5 section 5.1.4 and 5.1.7. All results were interpreted as previously described in Chapter 5.0 section 5.1.5 and 5.1.8. TBI's were only performed in patients who were known diabetics and patients with falsely elevated ankle pressures (>220MMHg).

PAD was defined as having an ABI less than 0.9 at rest or a TBI of less than 0.6 at rest. The severity of the PAD at rest was classified into mild, moderate and severe as described in Table 6.1 and 6.2 (Vascular Laboratory Practice Part III, First Edition, Cole, Walker and Norris).

ABI	Severity of PAD at rest
>0.9	Normal
0.8-0.9	Mild
0.5-0.8	Moderate
<0.5	Severe

Table 6.1: ABI classification of PAD

TBI	PAD Classification
>0.6	Normal
0.5-0.6	Mild
0.3-0.5	Moderate
0.2 or 30mmHg	Severe

Table 6.2: TBI classification of PAD

6.3 Results

6.3.1 Carotid Artery Disease

Of the 332 patients that had a CDU for the detection of CAD, 101 (30.4%) patients had a significant carotid artery stenosis (>50%) in either the right or the left ICA or both. The remaining 231 (69.5%) patients had no significant CAD (<50%) on either side.

Of the 101 (30.4%) of patients with significant CAD, 56 (55.4%) patients had bilateral disease and 45 (44.6%) patients had unilateral disease. The total of 202 ICA's in these 101 patients were classified into one of 5 categories according to the severity of the CAD present (figure 6.2).

	Number of Patients
Patients screened for CAD	332
Significant CAD (>50% ICA stenosis)	**101(30.4%)**
No significant CAD (<50% ICA stenosis)	231(69.5%)

Table 6.3: Summary of 332 AAA patients screened for carotid artery disease

Stenosis Category	Number of ICA's
<50%	48 (23.7%)
50-69	83 (41.1%)
70-80	22 (10.9%)
80-90	10 (4.9%)
90-99	17 (8.4%)
Occluded	22 (10.9%)

Table 6.4: Distribution of the 202 ICA's in 101 patients with significant CAD
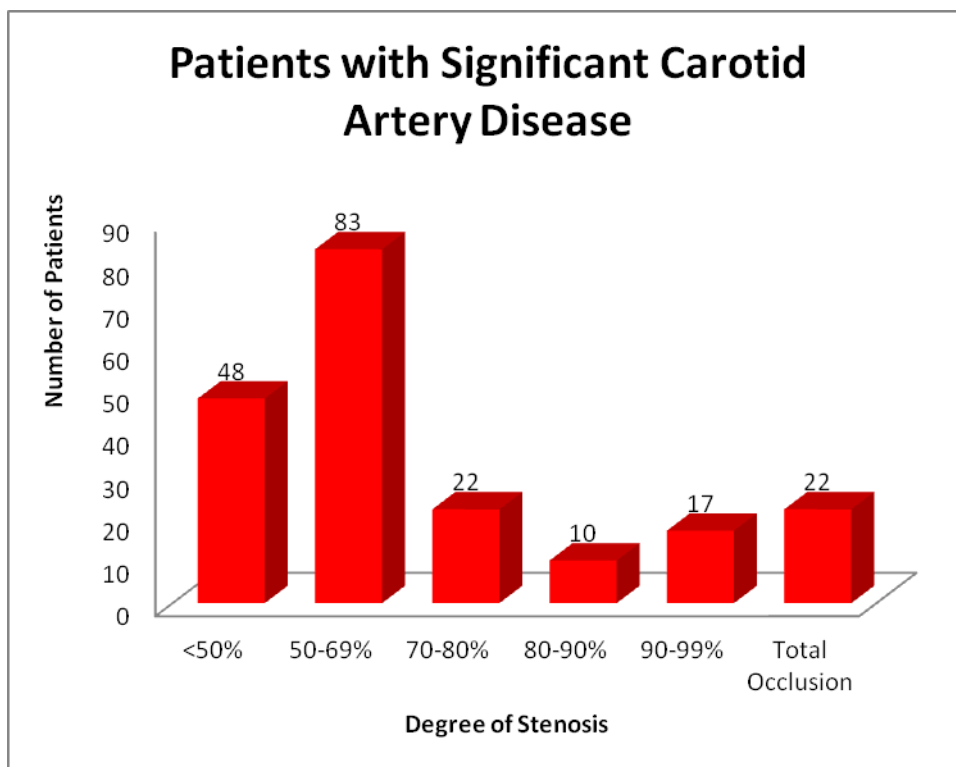
Figure 6.2: Bar chart illustrating distribution of patients with significant CAD

6.3.2 Peripheral Arterial Disease

Of the 289 patient included in this group 131 (45.3%) were found to have PAD at rest. The remaining 158 (54.7%) patients had an ABI greater than 0.9 or a TBI greater than 0.6 at rest and were therefore determined to have no PAD at rest (figure 6.3).

	Number of Patients
Total patients screened for PAD	289
Significant PAD at rest	**131 (45.3%)**
No significant PAD at rest	158 (54.7%)

Table 6.5: Summary of 289 AAA patients screened for PAD at rest
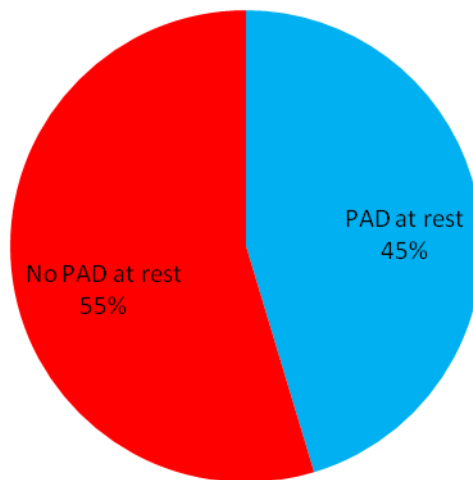
Figure 6.3: Summary of 289 AAA patients screened for PAD at rest

Of the 131 patients with PAD at rest 60 (45.8%) were found to have unilateral PAD and 71 (54.1%) were found to have bilateral disease (figure 6.4).
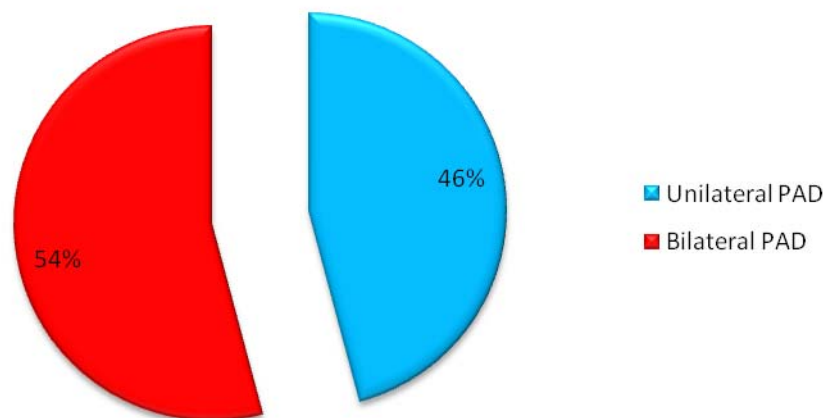
Figure 6.4: Breakdown of patients with significant PAD

	Mild	**Moderate**	**Severe**	**Mixed**
Unilateral PAD	24 (40%)	33 (55%)	3 (5%)	0 (0%)
Bilateral PAD	5 (7%)	31 (44%)	0 (0%)	34(48%)

Table 6.6: Division of patients with unilateral and bilateral disease
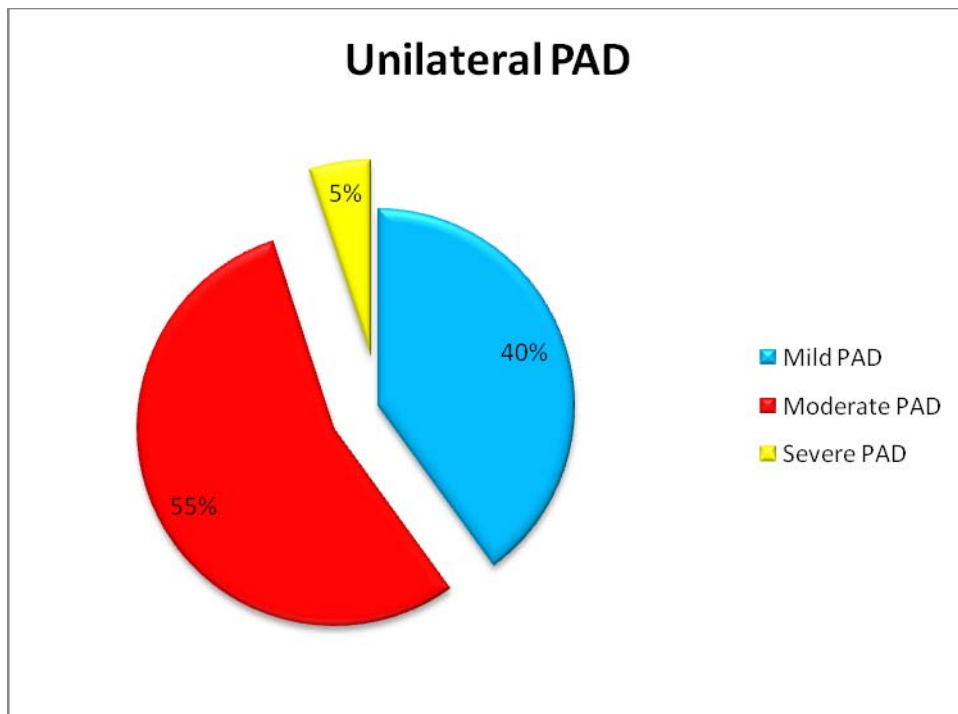
Figure 6.5: Division of patients with unilateral PAD
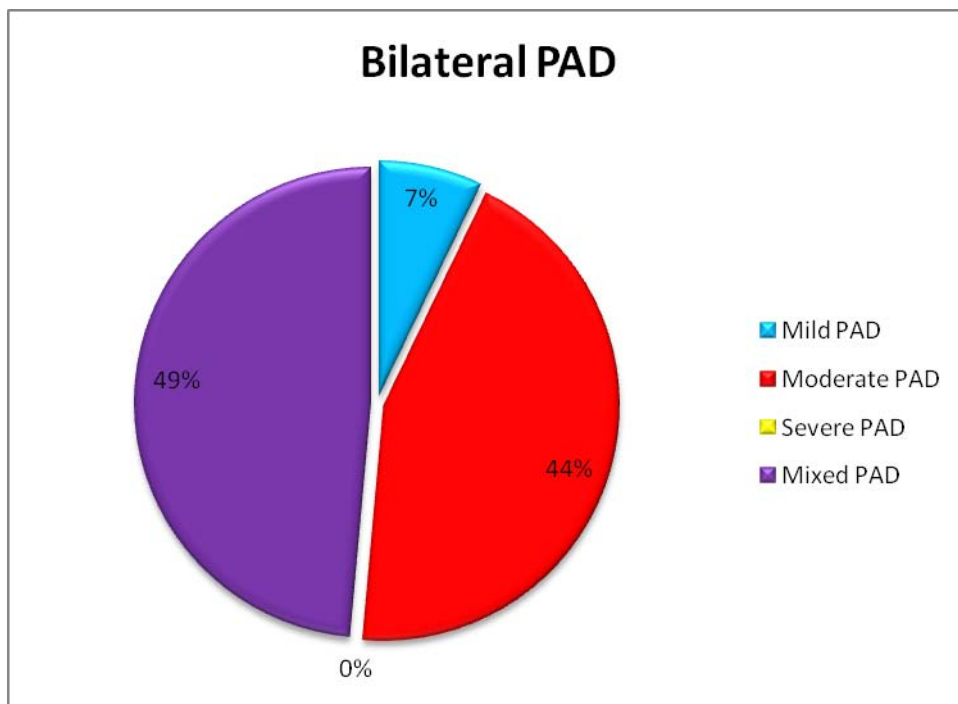
Figure 6.6: Division of patients with bilateral PAD

6.3.3 PAD and CAD

Of the 389 patients on the current aneurysm surveillance programme 289 patients had both a CDU scan for detection of carotid artery disease and ABI for the detection of PAD. 59 (20.4%) patients had both significant PAD and CAD. The mean ($\pm$ SD) age in this group was found to be 76 ($\pm$ 8). Eleven (18.6%) of the 59 patients were female and 48 (81.4%) were male.

6.3.4 Summary

Group	Number of Patients screened	Number of patients with significant disease	Mean Age
CAD	332	**101 (30.4%)**	76 ± 7.6
PAD	289	**131 (45.3%)**	76 ±8
CAD and PAD	289	**59 (20.4%)**	76 ±8

Table 6.7: Summary of the incidence of CAD and PAD in patients with AAA's
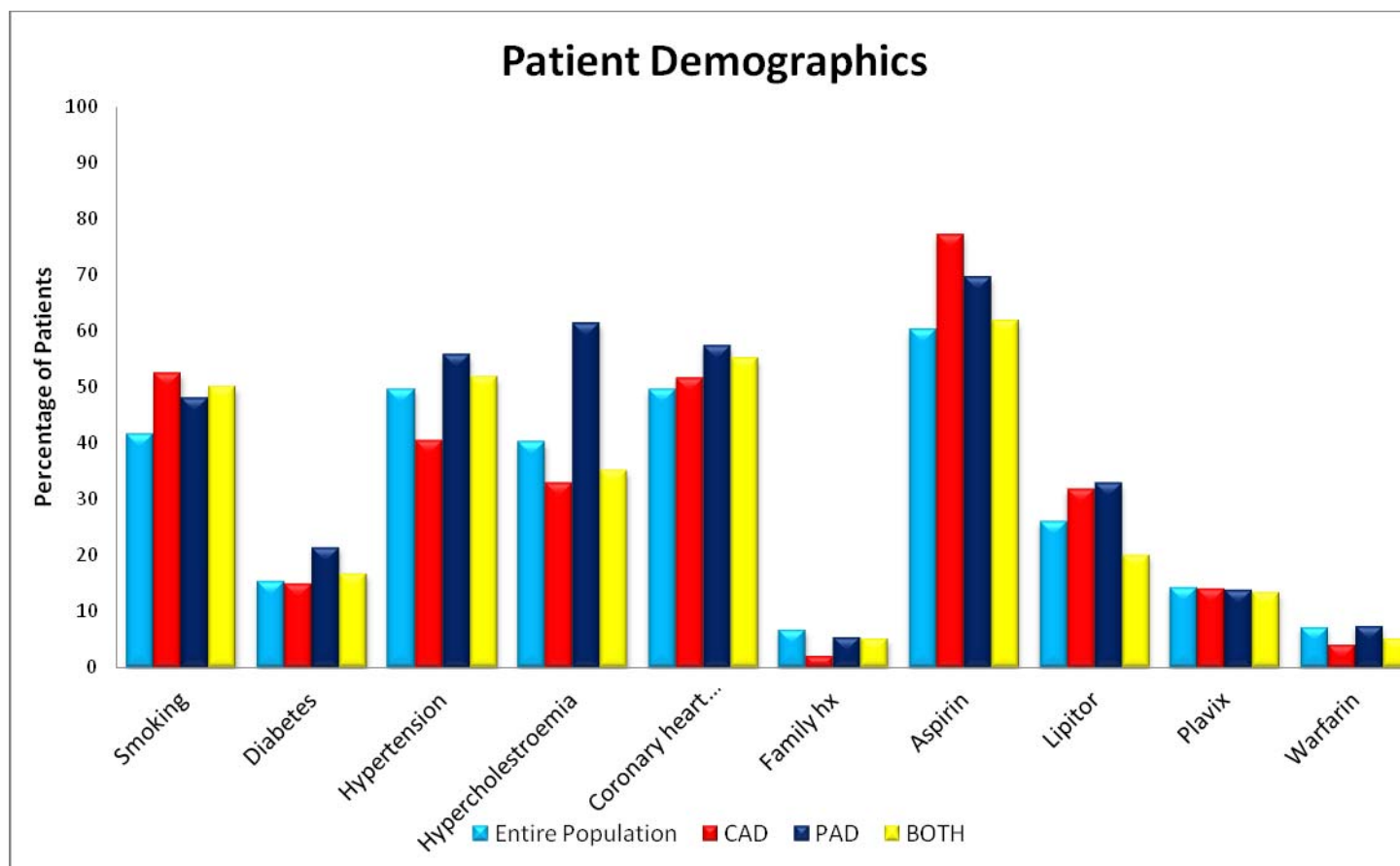
Figure 6.7: Patient demographics by subgroup

Group	Mean Age	Smoker (%)	Diabetic (%)	Hypertension (%)	Hypercholesterolemia (%)	Coronary disease (%)	Family History (%)	Aspirin (%)	Lipitor (%)	Plavix (%)	Warfarin (%)
Entire	76±8	41.6	15.4	49.6	49.6	49.6	6.6	60.1	25.9	14.1	7.2
CAD alone	76±7.6	52.5	14.9	40.5	32.8	51.5	1.9	77.2	31.7	13.9	3.9
PAD alone	76±8	48	21.4	55.7	61.4	57.3	5.3	69.5	32.8	13.7	7.3
CAD and PAD	76±8	50	16.7	51.7	35	55	5	61.7	20	13.3	5

Table 6.8: Patient demographics by subgroup

6.4 Discussion

It is widely accepted that patient's atherosclerotic conditions such as PAD, CAD and coronary artery disease co exist. However, there is little in the literature to suggest that patients with AAA's should be screened for other asymptomatic vascular disorders. This study assessed the prevalence of CAD and PAD in a population of patients with known abdominal aortic aneurysmal disease in order to determine if screening this group of patients for other vascular disorders might be advisable.

When compared to other published series this study demonstrates a much higher incidence of significant CAD (30.4%) than the 6% in the cardiovascular health study and the 8% in the Framingham study. The United States preventative task force (USPTF) estimates of the prevalence of carotid artery stenosis in general population based studies ranges from 0.5%-0.8%. Weerd in 2010 performed an individual participant data meta analysis of 23,706 participants of 4 population based studies and concluded that the presence of severe carotid artery stenosis in the general population ranged from 0% to 3.1%. However, Pilcher and colleagues in 2000 examined the prevalence of asymptomatic carotid artery stenosis in 200 patients with known PAD. They determined that 50 patients (25%) had an ICA stenosis of greater than 50% similar to the 101 (30.4%) patients that demonstrated a greater than 50% stenosis in this study. Fassiadis and colleagues in 2008 examined the prevalence of CAD in patients undergoing coronary angioplasty. They examined 117 patients with a male to female ratio of 3.2:1 and demonstrated a much lower prevalence of CAD (12.8%). Kiernan in 2009 also demonstrated a lower incidence of CAD (7.7%) when screening patients undergoing coronary artery bypass grafting. They examined multiple various risk

factors that might be associated with a severe carotid artery stenosis and concluded that the presence of PAD and a carotid bruit predicts the likelihood of a greater than 70% carotid artery stenosis.

A total of 289 (74.3%) were screened for PAD of which 131 (45.3%) demonstrated an ABI of less than 0.9. These findings are similar to that of Sukhija et al, 2004 who examined the presence of coronary artery disease, PAD and cerebrovascular disease in 110 men with an AAA. Despite their small sample size and limiting their study to males they demonstrated a 46% prevalence of PAD and a 27% prevalence of cerebrovascular disease compared to the 45.8% and 30.4% presented here. They also documented a similar combined PAD and cerebrovascular disease prevalence of 24%, compared to the 20.4% obtained in this study. Of note the mean age ($\pm$ SD) of patients in their study was much younger at 66 ($\pm$ 10) years compared to the higher mean age of 76 ($\pm$ 8) years in this study.

In 2003 Kakisis et al documented that a reduced ABI was a significant predictor of cardiovascular mortality in patients. An ABI of less than 0.9 showed a 2.8 fold increase in the risk of a patient having cardiovascular disease compared to patients that had an ABI of greater than 0.9. They also discovered that a carotid artery stenosis greater than 50% was a strong predictor of cardiovascular mortality with a 3.6 fold increase in the chance of cardiovascular death. The exact role of atherosclerosis in the pathogenesis of the growth of an AAA is widely disputed. However, it is clear that patients with a known AAA are at a greater risk of developing other atherosclerotic occlusive disease.

To screen the general population for asymptomatic CAD is an expensive and time consuming task however; vascular surgeons have been known to perform CEA in asymptomatic patients with a low morbidity and mortality rate of 0-3% (Moore et al., 1995). The ASCT trial reported a risk of stroke or death within 30 days post CEA of 3.1%.

When examining the risk factors present in each group a higher incidence of diabetes was found in the group of patients with significant PAD (21.4%) compared to the 15.4% in the CAD group and the 14.9% in the group as a whole. Hypercholesterolemia was also more prevalent in the PAD group at 61% compared to the 32% in the CAD group and the 49.6% in the entire group. Family history of AAA was more prevalent in the PAD group (5.3%) compared to the 1.9% in the CAD group. The mean age of patients on the AAA surveillance programme with a known family history of AAA was lower at 74 ($\pm$ 7) years compared to the overall mean age of 76 ($\pm$ 8) years.

6.5 Conclusion

The incidence of CAD and PAD in this study is higher than previously found in other screening studies performed on patients with selective atherosclerotic disorders. This study suggests that patients with abdominal aortic aneurysmal disease are at a higher risk of atherosclerotic disorders in other vascular territories and therefore this is a group which should be targeted for screening.

Chapter 7

Comparison of Colour Duplex Ultrasound with

Computed Tomography as a Determinant of

Maximum Abdominal Aortic Aneurysmal diameter

prior to intervention

7.1 Introduction

Annual abdominal aortic aneurysm (AAA) expansion and rupture rates correlate significantly with maximum aneurysm diameter (Lederle et al., 1995 and Sprouse et al., 2003). Hence, the decision to repair an asymptomatic AAA is usually based on an evaluation of its maximum diameter as obtained by a selected imaging modality. In the majority of cases the modality of choice to determine the maximum diameter prior to intervention is computed tomography (CT).

CT provides a detailed anatomical image of the organ of interest; it has capabilities such as 3 dimensional imaging which immediately enhances surgical planning prior to EVAR and thin slicing of images which facilitate the correct diagnosis of anatomical abnormalities. AAA size is most accurate when measured using 3D reconstruction of CT images and by measuring the maximal aortic diameter perpendicular to the central line of flow (Chaikof et al., 2002). CT is considered to be more reproducible than CDU, with more than 90% of re-measurements being within 2mm of the initial figure (Chaikof et al., 2009). Indications for intervention in asymptomatic AAA are a maximum transverse wall or anterior to posterior (AP) diameter of greater than 5.5cm or an expansion of 0.5cm or greater in a 6 month period (Hollier et al., 1992). The United Kingdom Small Aneurysm study concluded that surgical repair of an AAA in the early stages of dilation was of no benefit to mortality or outcome (Manning et al., 2002)

Contrast enhanced CT imaging has been reported to have a sensitivity of 90% and specificity of 91% when imaging symptomatic AAA's (Chaikof et al., 2009).

Despite its advantages CT is both expensive and associated with certain risks to the patient in terms of radiation exposure and intravenous contrast administration. The need for multiple scans for AAA surveillance increases this risk. The majority of intravenous contrast agents currently in use are iodine based and adverse reactions such as contrast nephropathy (renal damage after intravascular injection of the contrast agent) or the rare occurrence of anaphylaxis can have a detrimental effect on the patients health.

Colour Duplex Ultrasound (CDU) is widely accepted as a safe modality for the surveillance of patients with small AAA's (United Kingdom Small Aneurysm Trial participants). It is a non invasive imaging modality that has a sensitivity of 95% and a specificity approaching 100% when performed in a setting with adequate quality assurance (The U.S. Preventative Service Task Force, 2005). CDU is less expensive than CT and is also widely available with no exposure to radiation or intravenous contrast. The investigation can also be conducted as a portable examination, allowing the scanner to travel to the patient, rather than the patient travel to the scanner, if necessary.

Evidence from large clinical trials such as the United Kingdom Small Aneurysm trial (UKSAT participants) and The Multi Centre Aneurysm Screening Study (MASS) demonstrated the safety and cost efficacy of CDU in the surveillance of small AAA. Lindholt and colleagues reported that ultrasound screening is not only cost effective but is also reduces AAA related deaths. The

principal disadvantages of CDU are that it is operator dependent and the presence of excessive bowl gas or the patient's body habitus may affect the quality and resolution of images making it difficult for the technologist to accurately identify the defining walls.

This study sought to compare the two imaging modalities of CDU and CT in assessment of the maximum aneurysm diameter in patients under surveillance for AAA.

7.2 Patients and Methods

Following approval from the hospital ethics committee, all patients attending the vascular laboratory of the Mater Misericordiae University Hospital (MMUH) between the 1st of January 2007 and the 31st of December 2009 were recruited if they had both a CDU and a CT scan for assessment of their AAA within 90 days of each other.

During the study period 389 patients attended the vascular laboratory for aortic aneurysm surveillance. Of these, 126 (32.4%) had both a CDU scan and a CT scan within 90 days of each other. The remaining 263 (67.6%) patients were excluded as they did not have comparable scans within the 90 day period. In all cases this was because these aneurysms fell below the standard threshold for intervention of 5.5cm and thus a CT was not warranted. Of the 126 patients included, 3 (2.4%) patients had two CDU and CT scans within the required time frame and 1 (0.8%) patient had 3 CDU and CT scans within the required time frame, giving a total of 130 pairs of tests available for comparison.

Ninety nine patients (78.6%) were male and twenty seven (21.4%) were female with an overall mean age of 76.1 (± 7.1) years. The mean male age was 76.1 (± 6.5) and the mean female age was 76.2 (± 9.0) there was no statistical difference found between the two (p= 0.98).

7.2.1 Colour Duplex Ultrasound Imaging

All CDU scans were performed by a qualified Vascular Technologist proficient in abdominal imaging using one of 3 machines, a Siemens Sequoia 512, a Siemens S200 (Chapter 5, figure 5.6) or a Phillips IU22. All CDU scans were performed using a wideband curvi linear transducer (Chapter 5, figure 5.21) capable of harmonic imaging. All patients were scanned in the supine position in a darkened temperature controlled room following the standard clinical measurement protocol for surveillance of patients with an AAA as previously described in chapter 5, section 5.3.4.

The maximum anterior to posterior (AP) wall diameter and the maximum transverse wall diameter was recorded and documented for each patient with the greater of the two measurements taken as the maximum aneurysm diameter and used for comparison in this study.

7.2.2 Computed Tomography

All CT scans were carried out in the Radiology department of the MMUH following their standard protocol for abdominal imaging. The maximum aneurysm diameter documented on the final report was used for comparison in this study.

7.3 Statistical Analysis

Statistical analysis included calculation of the Pearson correlation coefficient and Students paired *t*- tests. A p value of less than 0.05 was considered significant. All calculations for Pearson coefficient correlation and paired t-tests were performed using Windows Microsoft Excel 2007.

Correlation between the CDU and CT was performed using the Pearson's coefficient correlation analysis. This method measures the strength of the relationship between the two measurements not the agreement. The value obtained may be anywhere between -1 and +1. It is used as a measure of strength of linear dependence between two variables and may be interpreted as presented in table 7.1.

Pearson's Coefficient Correlation Value	Level of Correlation
0-0.09	None
0.1-0.3	Small
0.3-0.5	Medium
0.5-1.0	Large

Table 7.1: Interpretation of Pearson correlation coefficient

(Cohen. 1998)

As correlation alone does not consider the absolute agreement between the two measurements, limits of agreement (LOA) was performed with the method described

246

by Bland and Altman (Bland and Altman., 1986). LOA comprises of two values, a positive (LOA-P) and a negative (LOA-N), that define the range in which 95% of the differences between the methods of measurements fall (Sprouse et al., 2003). In this study the LOA was calculated using MedCalc statistical software and was calculated as the mean difference ± 1.96 times the standard deviation of the differences. The accepted value for LOA is between -0.5 and 0.5cm, which are the values between which 95% of the measured differenced are expected to fall.

The Pearson's correlation coefficient, paired t-test and LOA were calculated for the group of patients as a whole. Patients were then divided into three subgroups small, medium and large aneurysms (figure 7.1) based on the study reported by Sprouse et al in 2003.
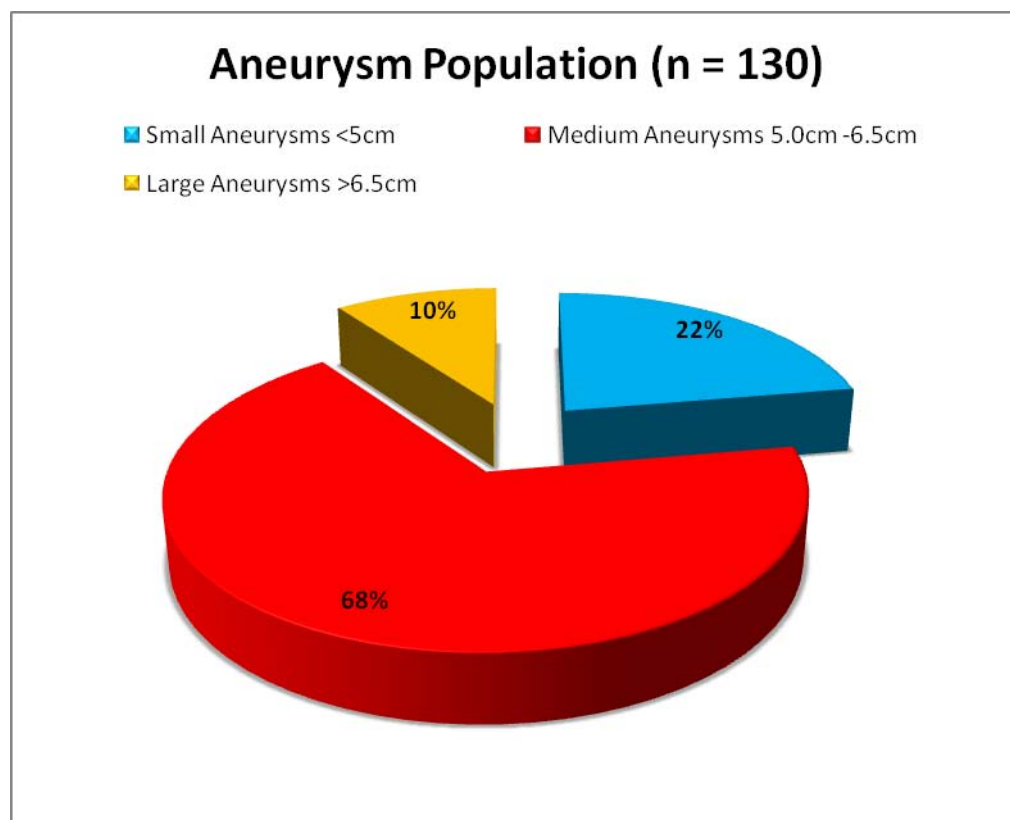
Figure 7.1: Aneurysm subgroup population

7.4 Results

7.4.1 Pearson Coefficient Correlation

i.   *Entire Group*

Mean ($\pm$ SD) AAA diameter on CDU was 5.4 (+1.0)cm and on CT was 5.4 ($\pm$ 1.0)cm. The Pearson Coefficient correlation (*r*) for the entire group and was found to be 0.95, demonstrating a large degree of correlation between the two modalities (figure. 7.2). There is no statistical difference (p = 0.1) between the mean CT and mean CDU aneurysm diameter when the paired *t* test was performed.
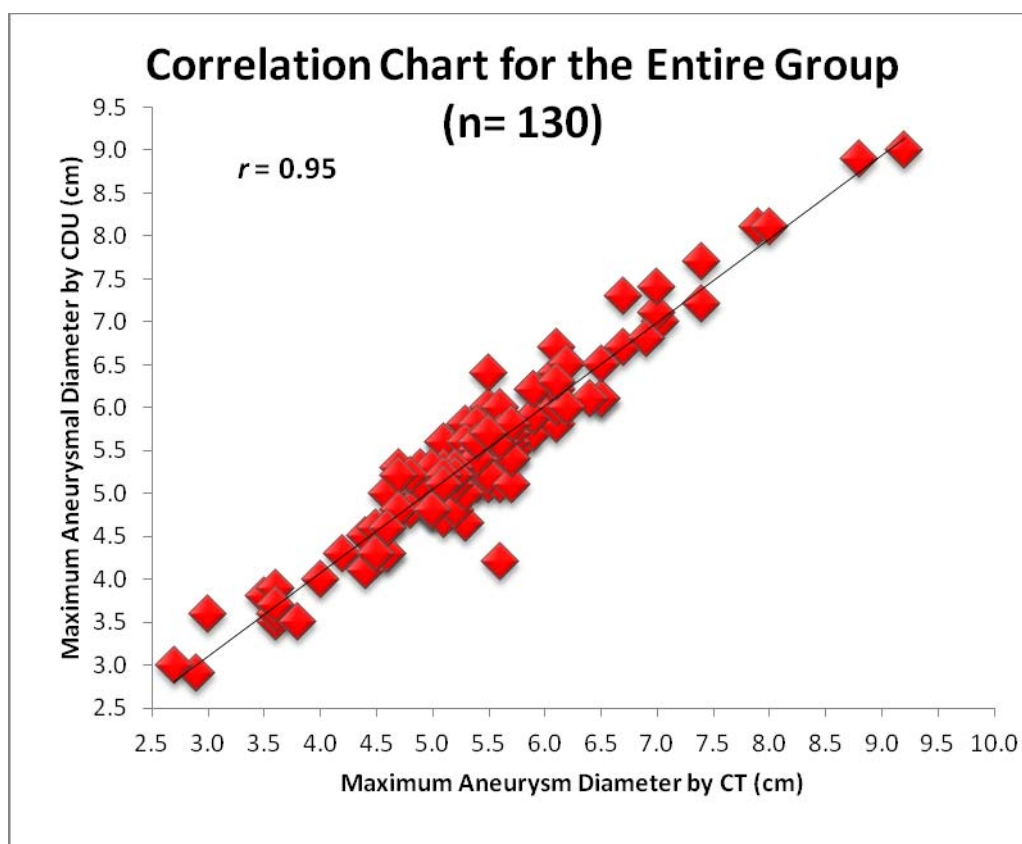
Figure 7.2: Correlation chart for the complete group (n=130) indicating a large degree of correlation between CDU and CT ($r = 0.95$)

ii. *Small Aneurysms (AAA <5.0cm)*

Twenty nine (23.0%) pairs of scans fell into this group. Mean ($\pm$SD) AAA diameter on CDU was 4.2 ($\pm$0.68) cm and 4.2 ($\pm$0.58)cm on CT, which was not statistically different (p = 0.4). The Pearson's Coefficient Correlation (*r*) was found to be 0.94 indicating a large degree of correlation between CDU and CT when imaging aneurysms less than 5.0cm.
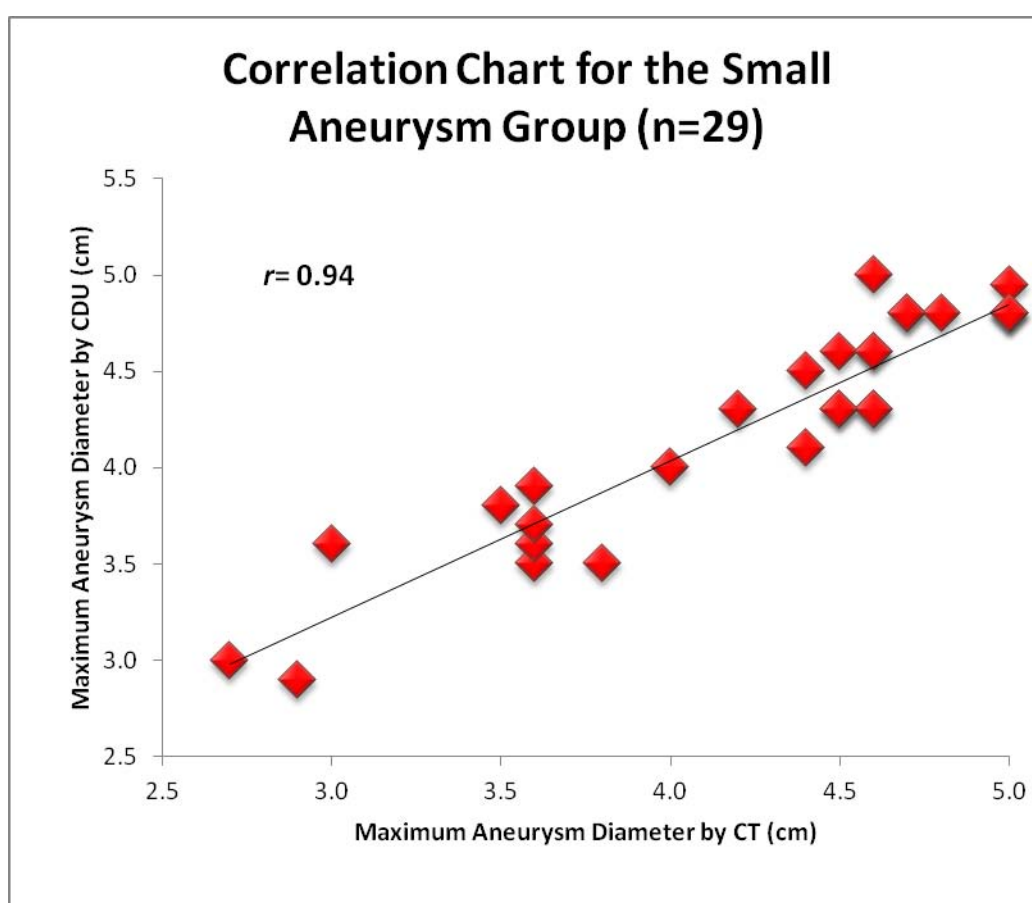
Figure 7.3: Correlation chart for the small aneurysm group (n=29) indicating a large degree of correlation between CDU and CT when imaging aneurysms <5.0cm (*r* = 0.94)

iii. *Medium Aneurysms (AAA 5.0>-<6.5cm)*

Eighty eight (69.8%) pairs of scans fell into this category. Mean (± SD) AAA size on CDU was 5.5 (+ 0.39) cm and on CT was 5.0 (± 0.43) cm there was no statistical difference between the measurements (p = 0. 2) when the paired *t* test was performed. Pearson's coefficient correlation (*r*) for this group was 0.69, indicating a large degree of correlation between CDU and CT for medium size aneurysms.
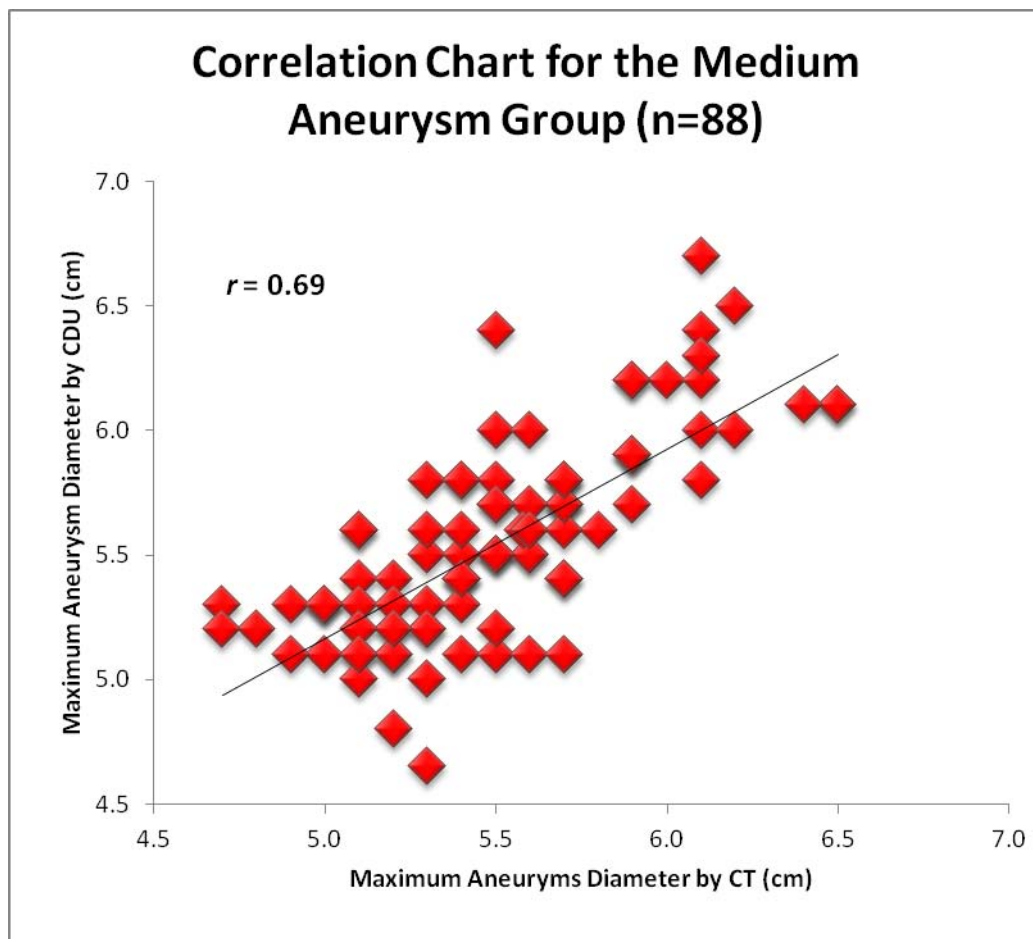
Figure 7.4: Correlation chart for the medium aneurysm group (n=88),

Indicating a large degree of correlation between CDU and CT *(r = 0.69)*

iv. Large Aneurysms (>6.5cm)

Thirteen (10.3%) pairs of scans for comparison fell into this group. Mean ($\pm$ SD) AAA diameter on CDU was 7.4 ($+0.83$) cm and 7.5 ($+0.79$) cm on CT. There was no statistical difference between the two measurements (p = 0.1). Pearson Coefficient Correlation (*r*) was found to be 0.96, indicating a large degree of correlation between the two modalities for larger aneurysms.
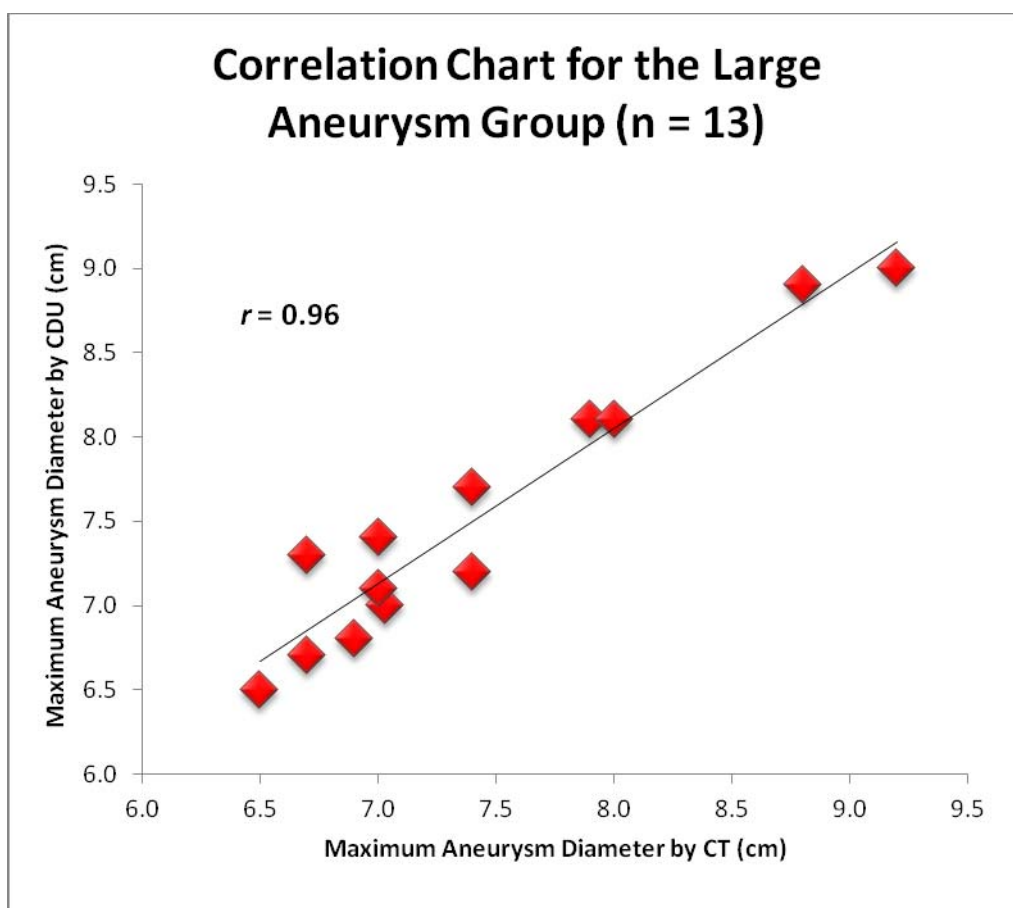
Figure 7.5: Correlation chart for the large aneurysm group (n=13) indicating a large degree of correlation between CDU and CT (*r* = 0.96)

7.4.2 Limits of Agreement

i. *Limits of Agreement for the Entire Group*
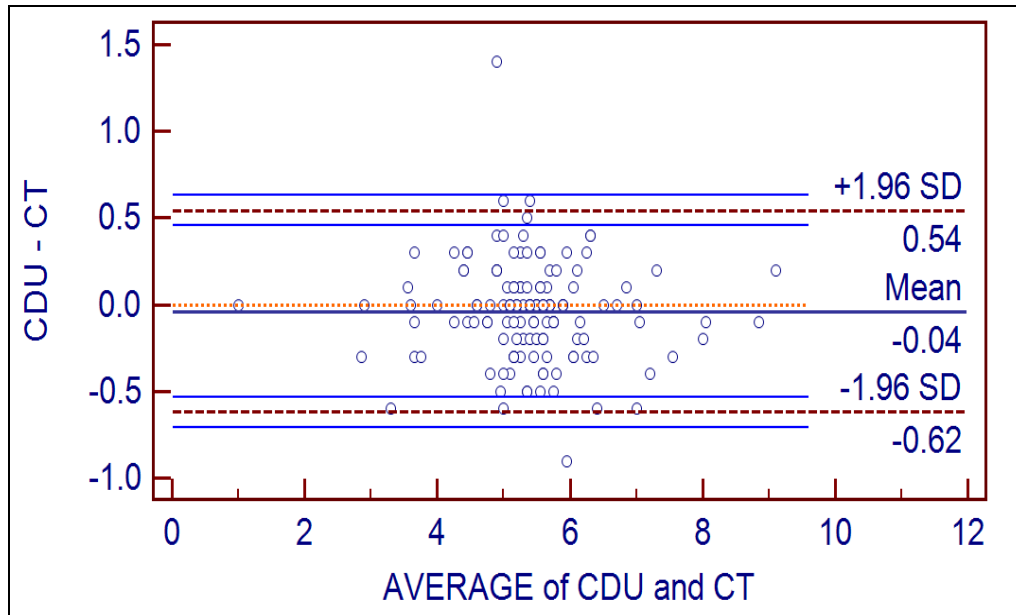
Figure 7.6:Bland and Altman plot for the entire group

Figure 7.6 is the Bland and Altman plot for the measurement of AAA's by CDU and CT for the entire group (n =130). The mean differences between the two measurements are plotted against the mean aneurysmal diameter. The limits of agreement were found to be -0.62 – 0.54, indicating, a 95% confidence level that the error between the two techniques is within this range. However the LOA are outside to accepted range of between -0.5 and 0.5.

ii. ***Small Aneurysms***
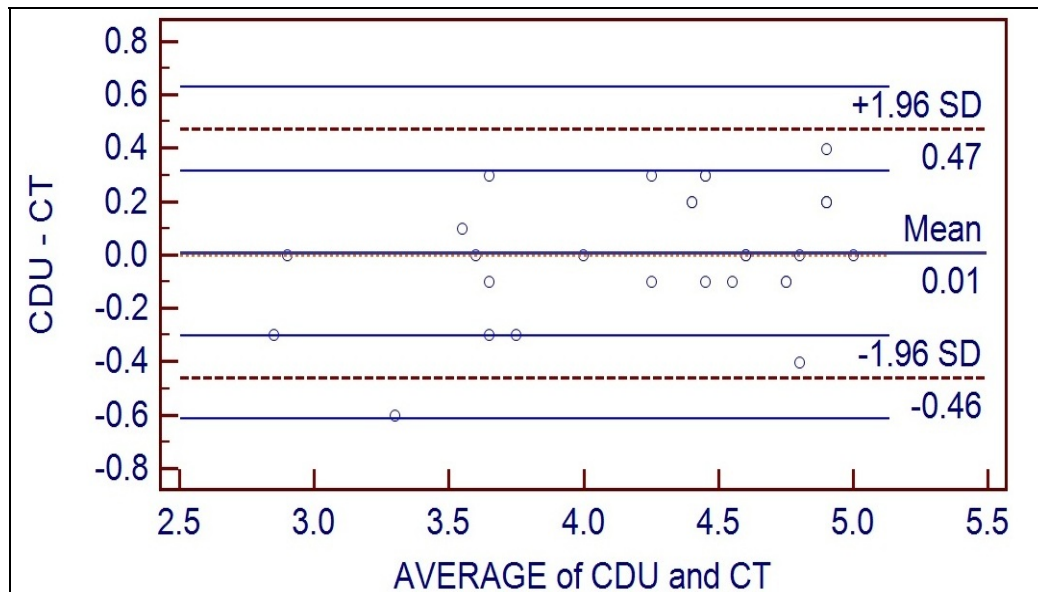
Figure 7.7:Bland and Altman plot for the small aneurysm group

Figure 7.7 is the Bland and Altman for the measurement of small aneurysm by CDU and CT (n=29). The mean differences between the two measurements are plotted against the mean aneurysmal diameter. The limits of agreement were found to be between -0.46 – 0.47 which represents the range within 95% of the differences fall and were calculated as the mean $\pm$ 1.96 times the standard deviation of the differences. Indicating, a 95% confidence level that the error between the two techniques is within this range. These are acceptable LOA as they fall within the acceptable range of between -0.5 and 0.5.
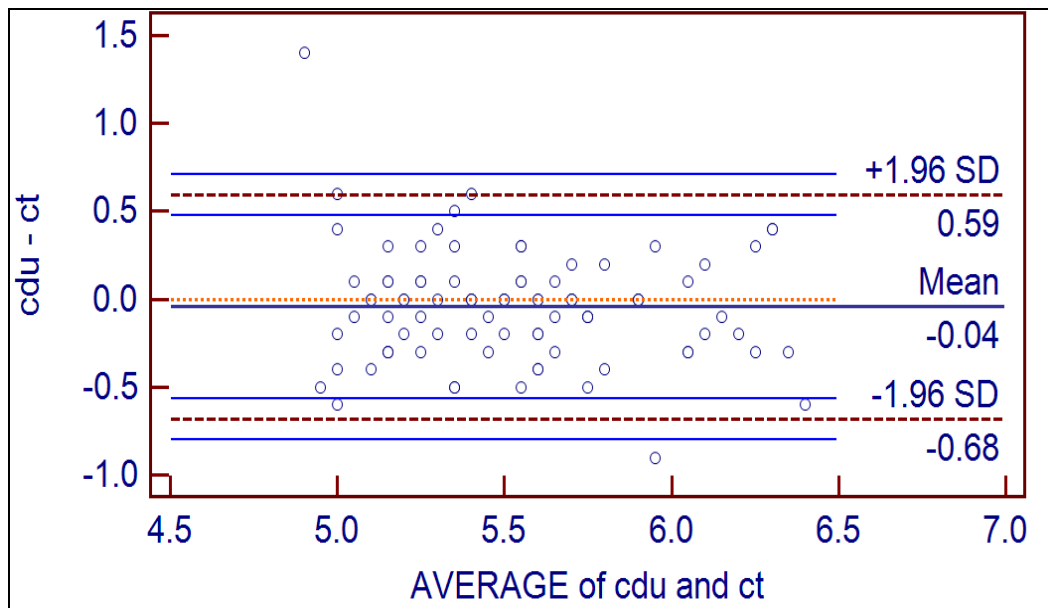
Figure 7.8:Bland and Altman plot for the medium aneurysm group

Figure 7.8 is the Bland and Altman plot for the measurement of medium aneurysms by CDU and CT (n=88). The mean differences between the measurements are plotted against the mean aneurysmal diameter. The limits of agreement (-0.68 – 0.59) represents the range within 95% of the differences fall and were calculated as the mean $\pm$ 1.96 times the standard deviation of the differences, indicating, a 95% confidence level that the error between the two techniques is within this range. However the LOA are outside the accepted range of between -0.5 and 0.5.
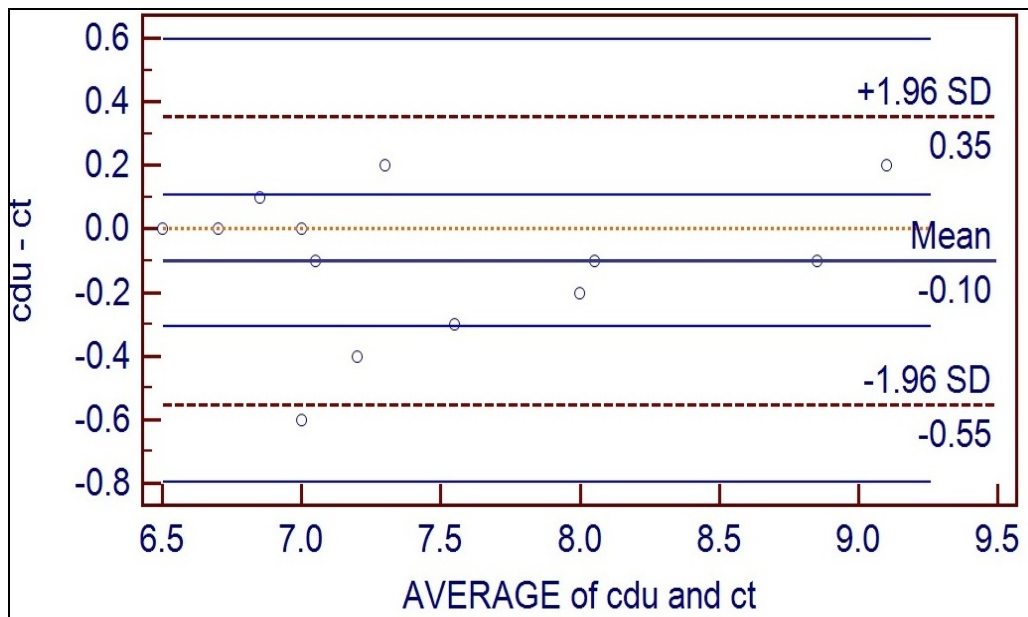
Figure 7.9:Bland and Altman plot for the large aneurysm group

Figure 7.9 is the Bland and Altman plot for the measurement of large aneurysms by CDU and CT (n=13). The mean differences between the measurements are plotted against the mean aneurysmal diameter. The limits of agreement (-0.55 – 0.35) represents the range within 95% of the differences fall and were calculated as the mean $\pm$ 1.96 times the standard deviation of the differences. Indicating, a 95% confidence level that the error between the two techniques is within this range.

7.5 Discussion

This study evaluated the accuracy of CDU in assessing maximum AAA diameter prior to intervention compared to the gold standard method of CT. CDU demonstrated a large overall degree of correlation ($r = 0.95$) when compared to CT for measuring the maximum AAA diameter. A large degree of correlation was also achieved in all in all three subgroups (small, medium and large aneurysms) verifying that measurement of aneurysm size prior to surgery can be accurately measured by either imaging modality.

LOA in the entire group was found to be (-0.62 to 0.54), in the small aneurysm group (-0.46 to 0.47) in the medium aneurysm group (-0.68 to 0.59) and in the large aneurysm group was found to be (-0.55 to 0.35). These results indicate a 95% confidence level that any error between the two techniques will be within these ranges. In general the narrower the LOA, the smaller the expected error between the two measurements. The accepted value for the LOA was defined as between -0.5 and 0.5, which are the values between which 95% of the measured differences are expected to fall. Despite achieving excellent correlation and small limits of agreement between the two imaging modalities in all groups, the small aneurysm group (<5cm) were found to have better agreement with 95% of the differences in the two measurements falling between -0.46 and 0.47.

The patient demographics of this series differ significantly from those of Huber et al., 2001 who reported a 6:1 male to female ratio, compared to 3.6:1 ratio of male to female obtained in this study. The mean age of patients in this study was 76.1 (± 7.1) years whereas those in Huber's series were slightly younger with

a mean age of 72 years. This increase in mean age may be due to the increase in the number of endovascular repairs being carried out now on patients that would have otherwise been unfit for open AAA repair or may simply be explained by an increase in life expectancy since Huber's study was published in 2001.

Discordance in measurements between various imaging modalities when measuring the maximal AAA diameter have been reported previously. Several authors have reported that maximal AAA diameter on CT is smaller than that obtained on Duplex (d'Audiffret et al 2001 and Lederle et al 1995), while Meier documented that AAA diameter with ultrasound is usually larger than CT (Meier et al 2003). In a study by Manning the mean CT measurement was significantly larger than of ultrasound with Lederle (1995) and Sprouse (2003) reporting that ultrasound measurements are consistently smaller than that found on CT. Measurement of maximal aneurysm diameter on CT is considered the most accurate method (Veith et al., 2004). The reporting standards for endovascular aneurysm repair from the Society of Vascular Surgery recommended that AAA size be measured in three dimensional reconstructions. However, amongst asymptomatic patients ultrasound detects the presence of an aneurysm accurately, reproducibly and at a low cost with a sensitivity and specificity approaching 100%, with 1-3% of ultrasound scans being inconclusive due to the patient's body habitus or the presence of bowel gas. CT has, in the past been more reproducible than ultrasound however the other advantages of ultrasound make it the method of choice for surveillance, with CT being the primary modality of choice for pre operative assessment.

The discordance between imaging modalities has been explained by the variation in techniques used to determine maximum aneurysm diameter, together with the presence of interobserver error. The United Kingdom Small Aneurysm Trial (UKSAT participants) used the maximal anterior to posterior wall measurements as obtained by ultrasound and recommended that surgical repair should take place on aneurysms greater than 5.5cm in AP measurements. This study employed the method similar to that used in the Multi Centre Aneurysm Screening Study (MASS) which measured both the maximal AP and transverse diameter, with the higher of the two measurements being reported as the AAA size.

The high degree of correlation achieved in this study may be explained by the improved grey scale resolution and harmonic imaging achieved by currently available ultrasound machines. Sprouse demonstrated an overall high correlation of 0.70 compared to the overall correlation of 0.95 found in this study. They also found that despite obtaining a good degree of correlation their LOA was clinically unacceptable at (-0.45 to 2.36cm) compared to the (-0.62-0.54) achieved in this study. Their subgroup analysis also demonstrated poor LOA in all cases.

7.6. Conclusion

AAA's less than 5cm in diameter can be accurately measured using CDU. On the basis of these results it is reasonable to suggest that CDU is the surveillance tool of choice for small AAAs, but cannot hope to supplant CT as the definitive planning tool prior to Aortic intervention.

Having demonstrated the reliability of CDU as a surveillance tool prior to intervention, the next logical investigation was to identify its role in postoperative surveillance of patients who had undergone endovascular aneurysm repair.

Chapter 8

A Comparison of Colour Duplex Ultrasound with

Computed Tomography in the Post Operative

Surveillance of Patients Following Endovascular

Aneurysm Repair

8.1 Introduction

Successful endovascular aneurysm repair (EVAR) has been defined previously as the exclusion of the aneurysm from circulation with absence of endoleak, limb occlusion, graft migration, late rupture or the need for secondary intervention (Sternberg et al., 2003).

Randomised control trials such as the United Kingdom Endovascular Aneurysm Repair Trials (EVAR -1 trial) and the Dutch Randomised Endovascular Aneurysm Repair trial (DREAM trial) have both established the superiority of EVAR in the management of abdominal aortic aneurysmal disease. In the short term, benefits such as decreased mortality, reduced blood loss, shorter hospital stay and improved quality of life post procedure have all been documented (EVAR -1 trial and DREAM trial). Long term follow up data and concerns regarding EVAR specific complications such as, the durability of stent grafts, endotension and the presence of endoleaks have necessitated lifelong surveillance programmes in order to ensure continued exclusion of the aneurysm from the circulation.

Contrast enhanced computed tomography (CT) is currently the standard imaging modality for EVAR surveillance (Chaer et al., 2009). Concerns exist regarding the use of CT as the primary surveillance modality due to the administration of high doses of ionising radiation and the nephrotoxicity of the

contrast used (Sandford et al., 2006). In addition the increased demand for CT scanning by virtually all hospital disciplines means the avaibility of scanning time is becoming an issue. As the number of patients in the EVAR surveillance programme in the Mater Misericordiae University Hospital (MMUH) has increased, the ongoing need for CT scanning has risen exponentially (figure 8.1 & figure 8.2). The identification of a safer, non invasive and less harmful method of adequately imaging the aorta with a high sensitivity and specificity following EVAR is desirable.
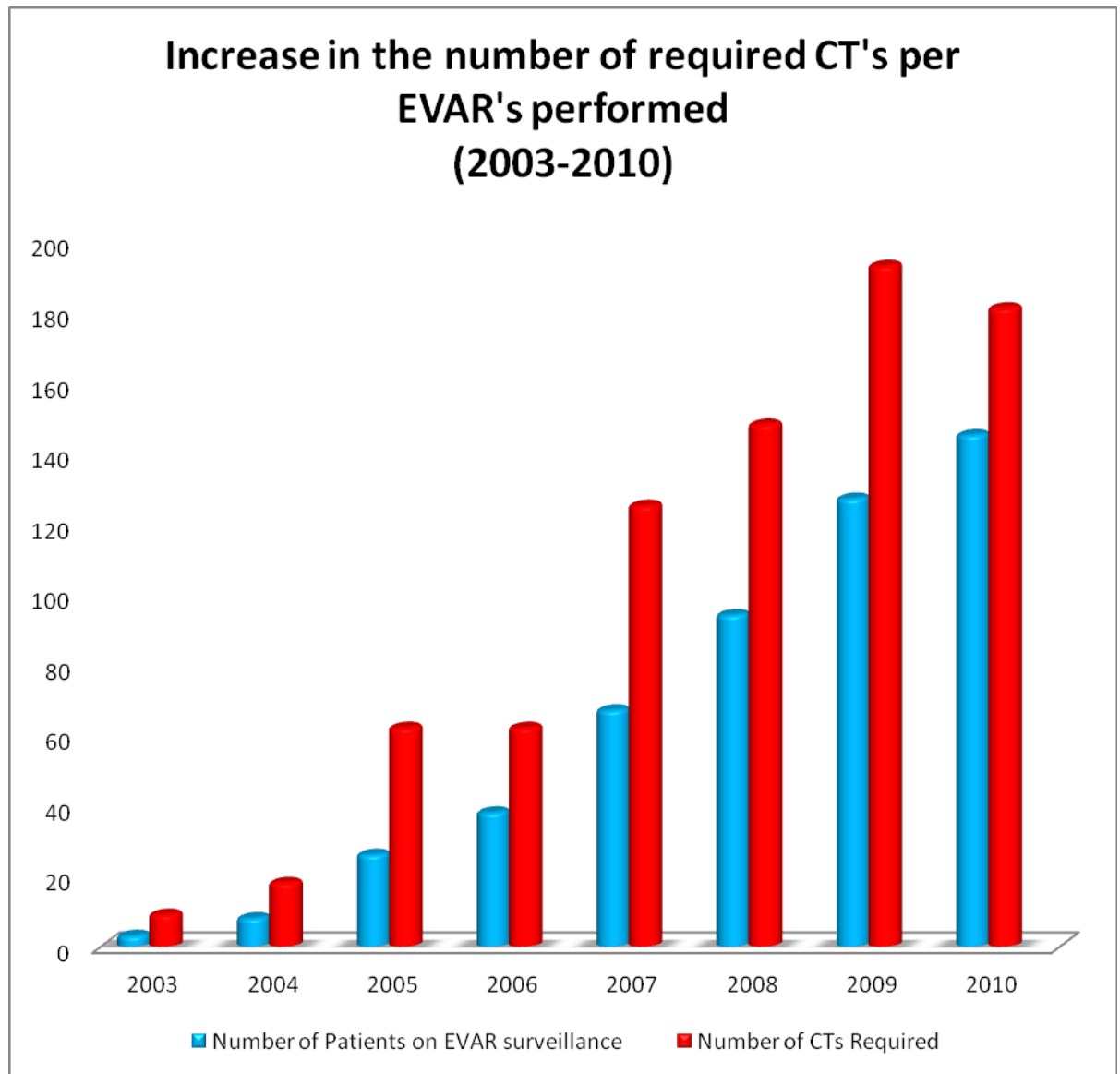
Figure 8.1: Increase in the number of CT scans required as the number of

EVAR's increase

Figure 8.1 summarises the increased in the number of CT's required per year as

the number of EVAR procedures increases, assuming that each patient has a CT

post surgery at 6 months and 1 year and annually thereafter.

Colour Duplex Ultrasound (CDU) is an inexpensive, harmless, non-invasive

and widely available imaging modality which is the investigation of choice for the

ongoing surveillance of AAA's prior to undergoing intervention (UKSAT and

MASS trial). CDU allows the measurement of aneurysm sac size over time and the detection of blood flow within the residual aneurysm and thus should be capable of supplanting CT as the primary surveillance tool in patients that have undergone EVAR. CDU is more operator dependent than CT (Chaer et al., 2009) and there is a perception that CDU scanning lacks reliability and reproducible results (Arko et al., 2004).

There is much controversy in the literature with regard to the use of CDU as the method of choice for post operative EVAR surveillance. Several studies have established the ability of CDU to detect endoleaks and have documented good correlation with CT in measuring the residual aneurysm diameter following repair (Chaer et al., 2009). However Sandford concluded that although CDU was a valuable method for follow up after EVAR, it was not as sensitive as CT in the detection of endoleaks. Raman found that CDU had a high degree of correlation with CT in aneurysm diameter measurement following EVAR but a low sensitivity and positive predictive value in endoleak detection and concluded that CDU could not effectively replace CT as a post operative surveillance modality. Chaer and Beeman suggested that CDU surveillance alone following EVAR is safe and can be initiated early after treatment in patients with shrinking and stable aneurysms (Chaer et al., 2009 and Beeman et al., 2009).

Following the successful validation of CDU as a method of assessing patients prior to undergoing EVAR as outlined in Chapters 6 and 7, the aim of this study was to evaluate the role of CDU in the postoperative surveillance of such patients, comparing it to the standard surveillance modality of CT, to determine if CDU

could supplant CT as the first line surveillance tool following EVAR thus altering

the existing post operative follow up algorithm (figure 8.3).

8.2 Patients and Methods

Following approval from the hospital ethics committee, all patients who underwent EVAR of their AAA in the MMUH between the first of June 2003 and the first of July 2010 (n=145) were retrospectively reviewed.

Figure 8.2 summarise the increase in the number of EVAR carried out over this time frame.
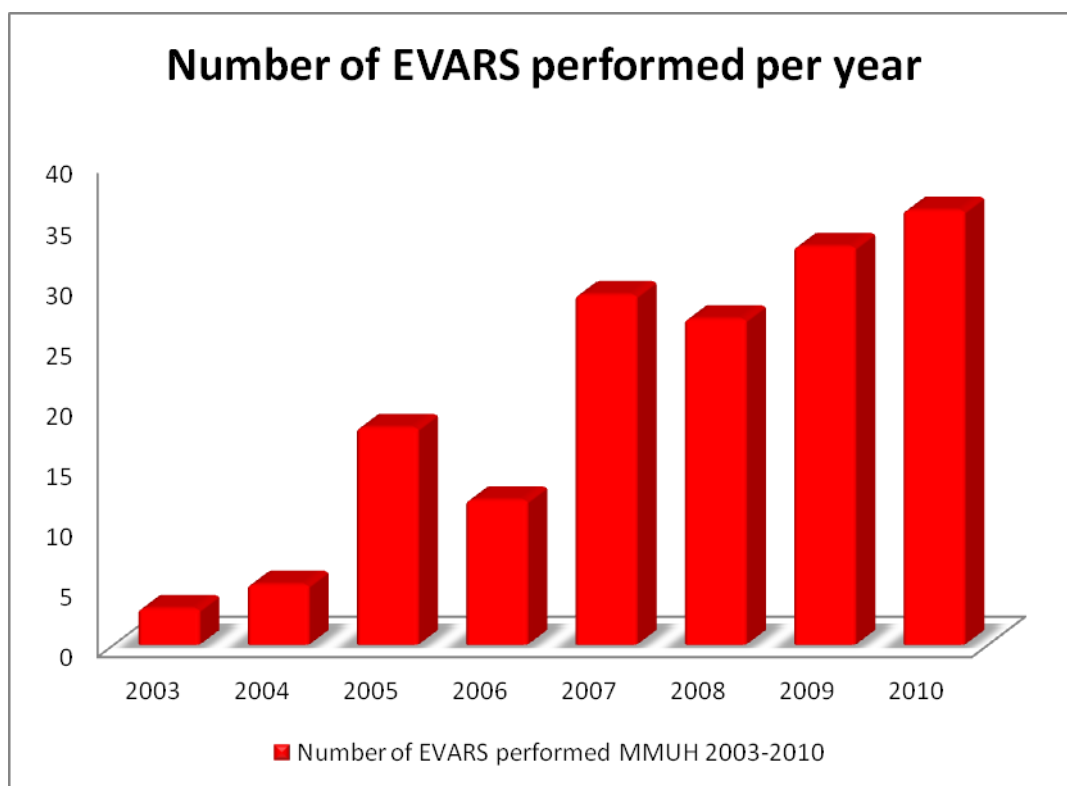
Figure 8.2: Increase in the number of EVARs per year

Following graft implantation all patients underwent regular post operative surveillance (figure 8.3). This included a CDU scan of the aorta, ankle brachial indices (ABI's), a CT scan and an abdominal plain film within 7 days of surgery. After discharge from the hospital, all patients had both a CDU scan and ABI at 1 month and then a CDU scan, ABI's and a CT scan, at 6 months, 12 months and

annually thereafter if there was no documented endoleak on either CDU or CT (figure 8.3).
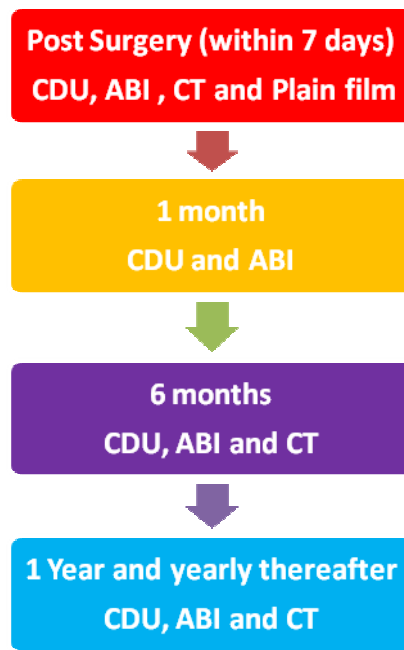
Figure 8.3: Current follow up algorithm

Patients with a documented endoleak post implantation of their graft underwent more rigorous follow up to closely monitor for an increase in the residual aneurysm sac size.

The CDU scans and CT scans of all 145 patients were retrospectively reviewed. All scans carried out more than 90 days apart from each other were excluded from the study.

There were 122 (84.1%) male and 23 (15.8%) female patients with a mean ($\pm$ SD) age of 77.1 (± 7.9) years. The age range was 53-93 years. There was no statistical difference found between the mean male age 76.6 ($+8.2$) years and the mean female age of 79.3 (± 5.2) years (p=0.99).
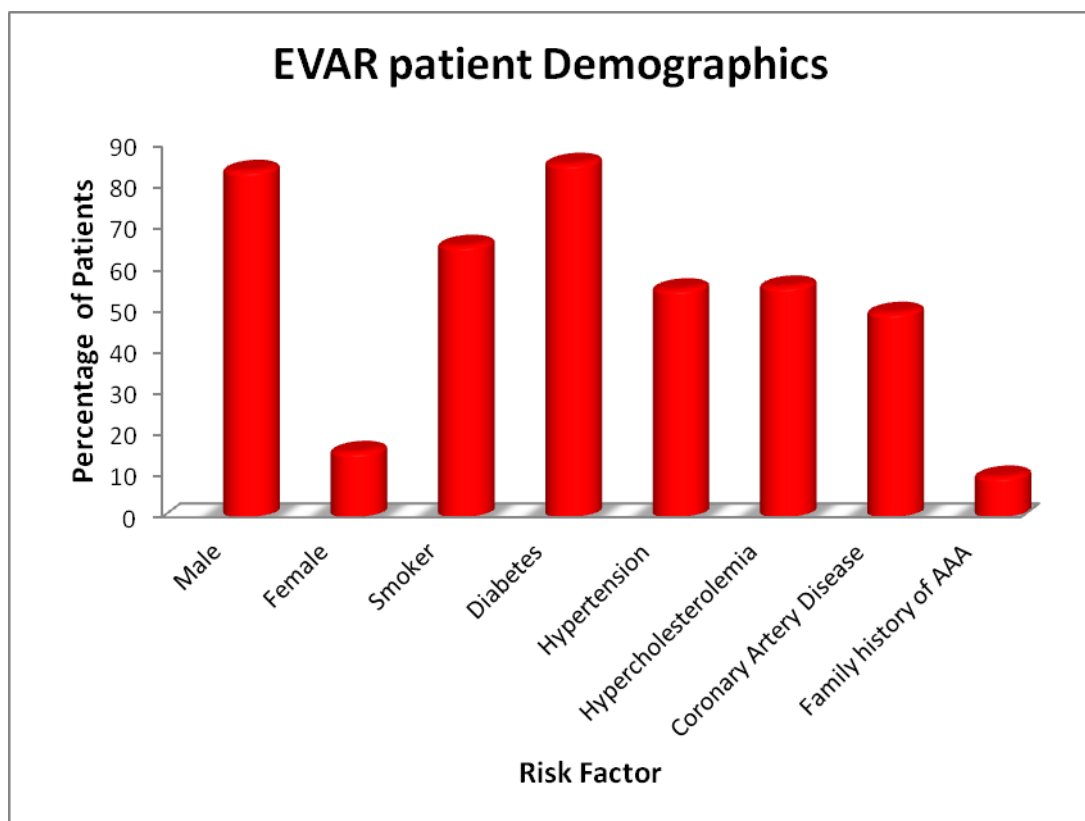
Figure 8.4: Patient demographics and co morbidities

Complete patient demographics and risk factors were available in 141 (97.3%) patients (figure 8.4). The remaining 4 (2.8%) patients risk factors were not available due to deficiencies in the clinical notes.

A total number of 715 scans were performed on the 145 patients that were reviewed, of which 426 (59.6%) were CDU scans and 289 (40.4%) were CT scans. The mean ($\pm$ SD) number of CDU scans per person was 2.9 (± 1.9), the mean ($\pm$ SD) number of CT scans per person was 1.9 (± 1.5) scans.

Of the total 715 tests performed there were 484 (67.9%) scans avaible for comparison (242 pairs) in 114 (78.6%) of the 145 patients reviewed.

The CDU and CT scans of the remaining 31 (21.4%) patients were not available for comparison due to reasons such as inconsistent timing of imaging modalities (scans performed greater than 90 days apart were excluded), failure to attend and CT being contraindicated due to i.v. contrast allergy.

Of the 426 CDU scans carried out 26 (6.1%) scans were reported as limited, due to the presence of excess bowel gas and body habitus limiting the capabilities of CDU in determining the residual aneurysm sac size and detection of an endoleak. The maximum residual aneurysm size was documented on the remaining 400 (93.9%) CDU scans.

Of the 289 CT's performed 107 (37%) CT reports did not document the maximum residual aneurysm size. The maximum residual aneurysm size was documented on the remaining 182 (63%) of CT scan reports.

8.2.1 Colour Duplex Ultrasound Scanning

All CDU scans were performed in the Vascular Laboratory of the MMUH by the same Accredited Vascular Technologist using a Siemens Sequoia 512 Ultrasound system (Chapter 5.0, figure 5.6). A wideband curvi linear transducer (Chapter 5.0, figure 5.21), the 6C2 was used to perform all grey scale and Colour Doppler images. All patients were required to fast for at least 6 hours and were scanned in the supine position in a darkened temperature controlled room according to the standard clinical measurement protocol as outline previously in Chapter 5.0 section 5.4.4. In all cases the vascular technologist was blind to the CT results until after the CDU scan was reported.

8.2.2 Ankle Brachial Indices

All ABI's were performed in the vascular laboratory of the MMUH by the same accreditated vascular technologist using an Automated Viasys, VasoGuard peripheral arterial system (Chapter 5, figure 5.0). ABI's were performed to assess the flow to the lower extremities and to rule out graft compression or stenosis in the iliac stents from kinking.

All ABI's were performed in the supine position in a temperature controlled room according to the standard clinical measurement protocol as outline previously in Chapter 5 section 5.1.4.

8.2.3 Computed Tomography

All CT scans were carried out in the radiology department of the MMUH following their standard protocol. The maximum residual aneurysm measurement

and the presence or absence of an endoleak as reported on the final report was used for comparison.

8.3 Statistical Analysis

Both modalities were compared for accuracy in determining the residual aneurysm sac size and detection and classification of endoleaks post EVAR. The sensitivity, specificity, positive predictive value and negative predictive value were calculated for all patients taking CT as the gold standard. The patient was considered a false negative if CDU missed an endoleak that CT detected, a false positive if CDU detected an endoleak that CT did not; a true positive if the endoleak was detected by both CDU and CT and a true negative if CDU and CT documented no endoleak.

The Pearson Coefficient Correlation was performed to assess the strength of the relationship between CDU and CT in the measurement of the residual aneurysm sac size post repair. A paired *t* test was performed also and a p value of less than 0.05 was considered statistically significant. All calculations for Pearson coefficient correlation and paired *t* tests were performed using Windows Microsoft Excel 2007.

A limit of agreement (LOA) was performed with the method described by Bland and Altman (Bland and Altman., 1986). LOA comprises of 2 values a positive (LOA-P) and a negative (LOA-N) that define the range in which 95% of the differences between the methods of measurements fall (Sprouse et al., 2003). In this study the LOA was calculated using MedCalc statistical software from the means and differences of the two measurements.

8.4 Results

8.4.1 Detection and classification of endoleaks and graft complications

Of the 484 scans available for comparison (242 pairs) an endoleak was documented on 87 (36%) CDU scans and 25 (10.3%) CT scans.

i. Type 1 endoleaks

There were 5 (2.1%) type 1 endoleaks noted on CDU, 3 (1.2%) were detected on CT. There were no type 1 endoleaks noted on CT that were missed on CDU.

Of the two patients who had a type 1 endoleak on CDU and not on CT, one was an anatomical abnormality which was misinterpreted on the CDU scan. The second patient was documented as a type 2 endoleak on CT.

Four out of the five patients who had a type 1 endoleak detected on CDU underwent further intervention.

ii. Type 2 endoleaks

Of the 242 pairs of scans available for comparison within the 90 day time frame, type 2 endoleaks were detected on CDU in 82 (33.9%) scans and on CT in 22 (9.0%) cases.

In no case was a type 2 endoleak detected on CT and not detected on CDU. Three patients with a documented type 2 endoleak on both imaging modalities underwent further intervention.

iii. Type 3 endoleaks

There were no type 3 endoleaks detected in this series on either CT or CDU.

iv. Type 4 endoleaks

There were no type 4 endoleaks detected in this series on either CT or CDU.

v. Endotension

One patient underwent further intervention for "endotension". Both imaging modalities documented a significant increase in residual aneurysm sac size. CDU documented the presence of a type 2 endoleak originating from a lumbar artery; no patent vessel was noted on CT or selective angiography. The patient underwent an elective laparotomy were the aneurysm sac was opened but no patent feeding vessel was identified and the sac was plicated over the endograft.

vi. Limb occlusion

Of the 145 patients in the study 2 patients underwent secondary intervention for limb occlusion. In both cases the limb occlusion was documented on CDU first, both patients then underwent a CT scan which confirmed the diagnosis and underwent further surgery.

vii. Late Rupture

One (0.7%) patient experienced rupture at a late stage in the follow up and underwent emergency conversion to an open repair. The patient had no endoleak on either imaging modality at any stage during follow up and had a no significant

increase in residual aneurysm sac size over time. The reason for rupture is unknown as the patient underwent emergency surgery at another institution.

viii. Secondary Intervention

Eleven (7.5%) of the 145 patients in total underwent secondary intervention. Four patients had further intervention for a type 1 endoleak, 3 for a type 2 endoleak, 2 for limb occlusion, 1 for endotension and 1 patient suffered late rupture.

8.4.2: Sensitivity, specificity, positive predictive value and negative predictive value

CDU was found to have a sensitivity of 100% and a specificity of 85% in the detection of endoleaks. The positive predictive value was 28% and negative predictive value 100%.

8.4.3 Residual Aneurysm Measurement

Of the 242 pairs of scans available for comparison, the residual AAA size on CDU was not documented on 15 (6.1%) scans due to limited imaging. The residual AAA diameter was not documented on 91 (37%) of the 242 CT scan reports.

This gave us a total of 142 (58%) pairs of scans where both the CDU scan and the CT scan could be compared for accuracy in determining the residual AAA diameter post EVAR.

Of the 142 pairs of scans for comparison the mean ($\pm$ SD) residual AAA diameter on CDU was 5.5 ($\pm$ 1.4) cm and on CT was 5.6 ($\pm$1.3) cm there was no statistical difference noted between the two measurements (p=0.99). The Pearson Coefficient correlation was found to be 0.96 indicating a high degree of correlation (Chapter 7.0, Table 7.1) between CDU and CT when measuring residual aneurysm size post EVAR (figure 8.5).
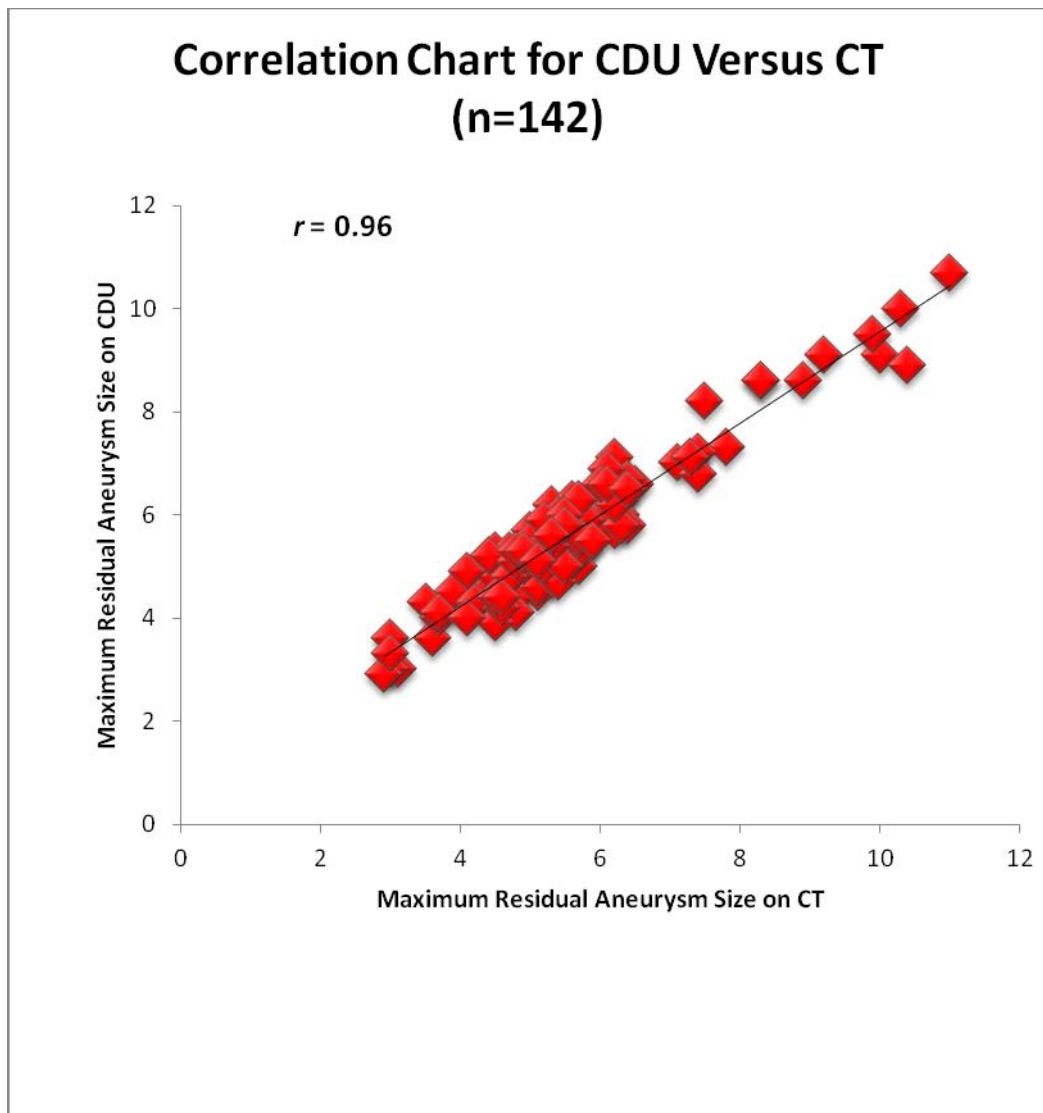
Figure 8.5: Scatter plot showing correlation (*r*) of residual aneurysm sac size by CDU and CT (n=142) with a line of equality showing a clear trend in the bias
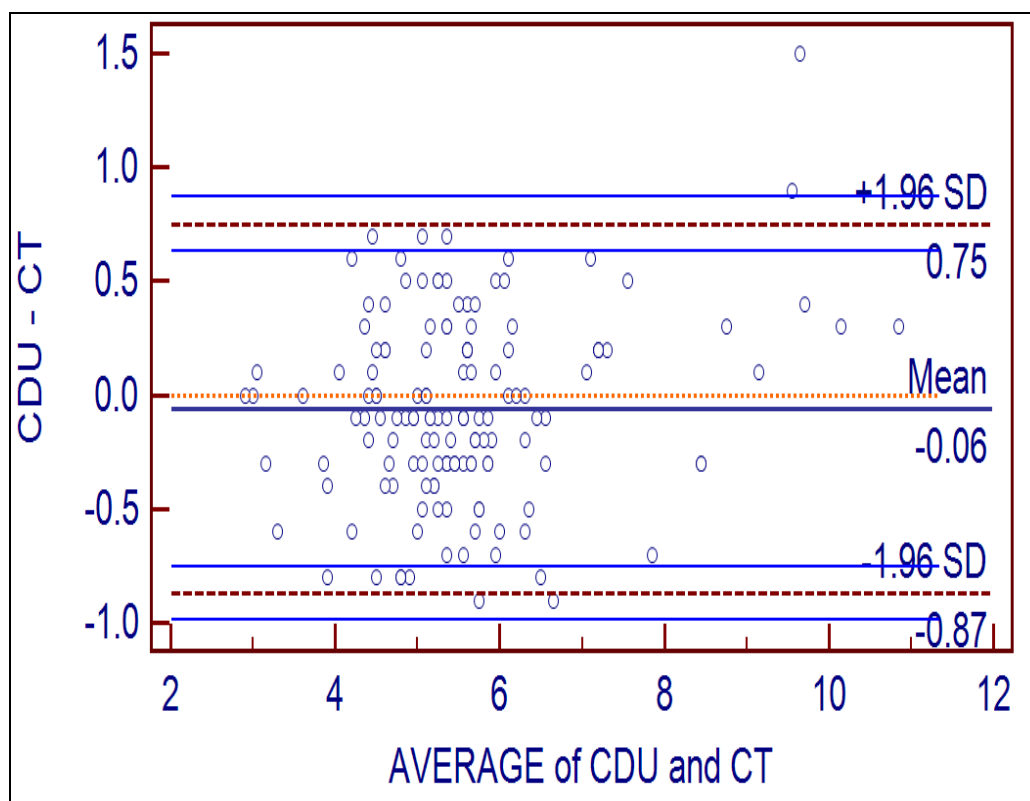
Figure 8.6: Bland and Altman plot for CDU versus CT in the measurement of the residual aneurysm size post EVAR

Figure 8.6 is a Bland and Altman plot of the differences against the average of the two measurements of residual aneurysm size post EVAR. The mean differences between CDU and CT are plotted against the mean aneurysmal diameter. The limits of agreement (-0.87-0.75) represents the range within 95% of the differences would be expected to occur, and were calculated as the mean $\pm$ 1.96 times the standard deviation of the differences. Indicating a 95% confidence level that the error between the two techniques is within this range. However the LOA are outside to accepted range of between -0.5 and 0.5.

8.5 Discussion

These results show an excellent degree of correlation ($r = 0.96$) between CDU and CT in measuring the residual aneurysm sac size over time demonstrating that either imaging modality could be safely utilized to determine an alteration in the residual aneurysm size during post operative surveillance. The high proportion of CT scans (37%) were the maximum residual aneurysm diameter was not made simply highlights the poor awareness of the importance of this measurement by radiologists. Our results compare favourably to previous results reported by Raman et al., 2003 who demonstrated a correlation of $r = 0.65$ and Arko et al who reported a correlation of $r = 0.93$. The LOA however was not satisfactory with 95% confidence interval ranging from -0.87- 0.75 which falls outside the accepted range of between -0.5 and 0.5.

CDU scans were documented as limited in 26 (6%) patients, for reasons such as bowel gas and body habitus. This figure is lower than other studies which documented that CDU was limited in up to 25% of scans performed (Elkouri et al., 2004). This could simply be due to the prolonged fasting time required (> 6 hours) for the CDU scan.

Ultrasound sensitivity was found to be 100% and specificity was found to be 85% for the detection of endoleaks, these values differ somewhat to those reported in the literature. Sandford and colleagues reported 67% sensitivity and 91% specificity for CDU versus CT in the detection of endoleaks with a positive predictive value of between 33-100% and negative predictive value of between 91-100%. The positive predictive value and negative predictive value in this study

was similar at 32% and 100% respectively. Arko et al in 2004 demonstrated that CDU had a sensitivity of 81%, a specificity of 95%, a positive predictive value of 94% and a negative predictive value of 90% when compared to CT, However, they documented that a small number of endoleaks were missed on CDU and detected on CT. In comparison there were no endoleaks missed on CDU in this study and detected on CT.

Manning and colleagues, in a series of 132 patients reported values similar to our own. They documented a 45% positive predictive value and 94% negative predictive value for CDU when compared to CT for postoperative surveillance following EVAR. Specificity of CDU for endoleak detection was 67% when compared with CTA and sensitivity for CDU was 86%, both lower than our own findings. Their conclusions however were broadly similar to our own, suggesting CDU as a first line screening tool which allowed selection of a smaller cohort of patients in whom CT was necessary (Manning et al., 2009).

Long term follow up of patient post EVAR is currently required due to the unique unforeseen set of complications that may occur with the rapidly advancing technology involved in is technique. The desired outcome of EVAR is shrinkage of the residual aneurysm sac without the presence of an endoleak. Despite the multiple imaging modalities available to carry out this surveillance many institutions continue to avail of CT angiography despite the risk to patients from both radiation and contrast related nephrotoxicity also the obvious disadvantage of cost.

CDU is universally accepted as the method of choice for the surveillance of patients with small AAA. It has advantages over CT angiography that make it a

more desirable imaging modality for the long term surveillance of patients. It has no risk of radiation exposure and nephrotoxicity as well as the obvious advantage of being readily avaible, non invasive and being a much cheaper imaging modality. However, as with all imaging modalities it too has disadvantages, such that is largely operator dependant and the quality of CDU images is largely affected by the patient's body habitus and excess bowel gas.

Noll et al., 2007 report that almost one-third of the cost of postoperative EVAR was attributable to radiology imaging costs. In a series of 20 patients, Henao and colleagues in 2006 described how CT failed to recognize three type II endoleaks seen by contrast-enhanced ultrasound. A study performed by Civitello and colleagues in 2003 concluded that contrast enhanced CDU is more accurate than standard CDU for the detection of endoleaks following AAA repair. As our current scanning protocol has already detected all clinically significant endoleaks it is difficult to see how patient care would be optimised by the use of contrast enhanced ultrasound.

Our results suggest that CDU could be employed as the primary postoperative surveillance tool in patients who have undergone EVAR. Certain findings could be indications for proceeding to CT such as increase in sac size, the detection of high velocity flow within the aneurysm sac suggestive of an endoleak, structural abnormalities in the graft or inability to obtain adequate pictures of the graft with CDU. The resultant effect of this would be a dramatic reduction in the number of CT scans being ordered for patients in post op EVAR surveillance programmes with resultant less exposure to both ionising radiation and intravenous contrast. As the number of patients in the EVAR programme has

increased, thus the ongoing demand on CT scanning has risen exponentially. Figure 8.2 summarised the increase in the number of EVARS performed per year in the MMUH. Each patient undergoes 3 CT's in their first year of surveillance (post surgery, at 6 months and 1 year). Figure 8.7 demonstrates the increase in the number of new CT's required each year with the current surveillance programme. If each patient underwent only 1 CT post surgery this would lead to a drastic reduction in the number of new CT's required per year (figure 8.7). The average cost of a CT scan varies between hospitals. Assuming that each CT scan cost €500 (Lifescan, United Kingdom Screening Services), Figure 8.8 demonstrates the reduction in expenditure on new CT scans alone per year. The total expenditure on new CT's alone to date is approximately €244,500. If the new EVAR patients underwent just one CT post surgery this would have cost approximately €81,500 a reduction of €163,000 between 2003 and 2010.
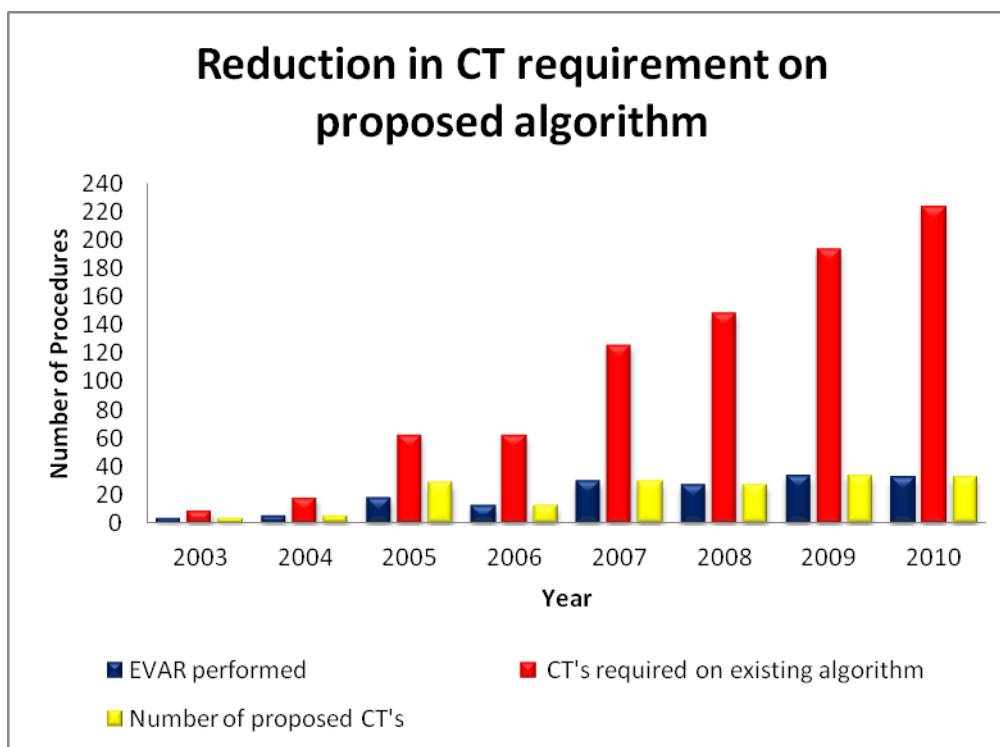
Figure 8.7: Current CT's requirement per year and proposed CT requirement per year
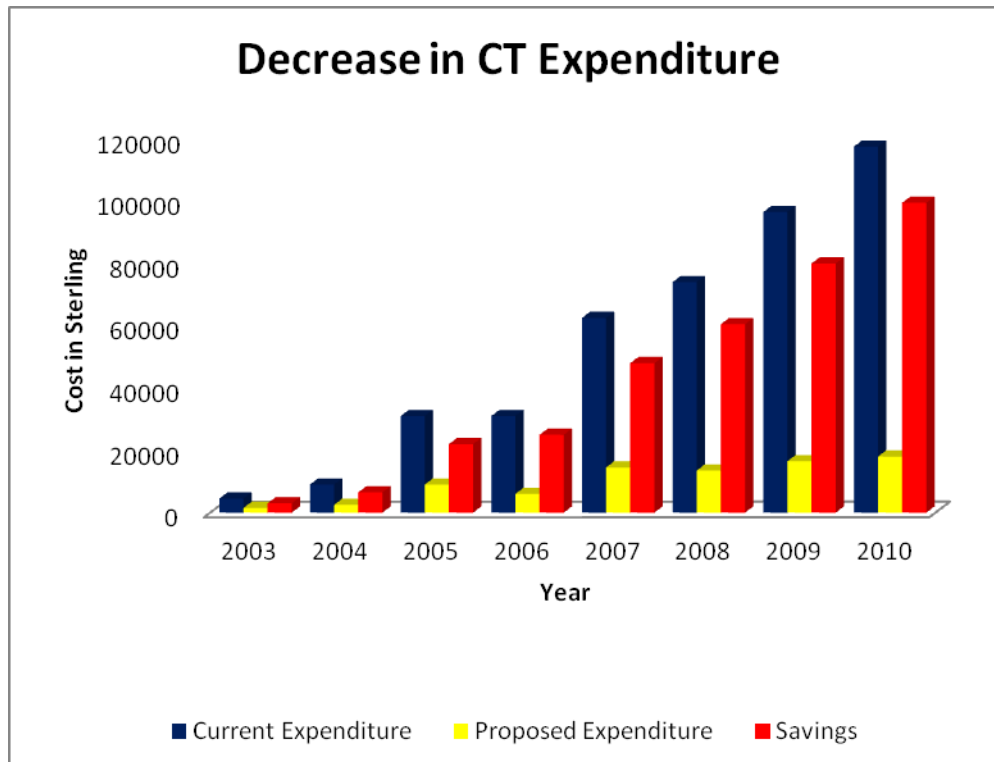
Figure 8.8: Decrease in expenditure on new CT' required per year

(MMUH Series 2003-2010)

284

8.6 Conclusion

Based on the results obtained in this study we propose that CDU replace CT as the primary long term surveillance imaging modality for patients post EVAR of their AAA. However, if abnormalities occur on the CDU scan, then further investigation of the endovascular stent by CT should be performed at the earliest convenience (figure 8.9).
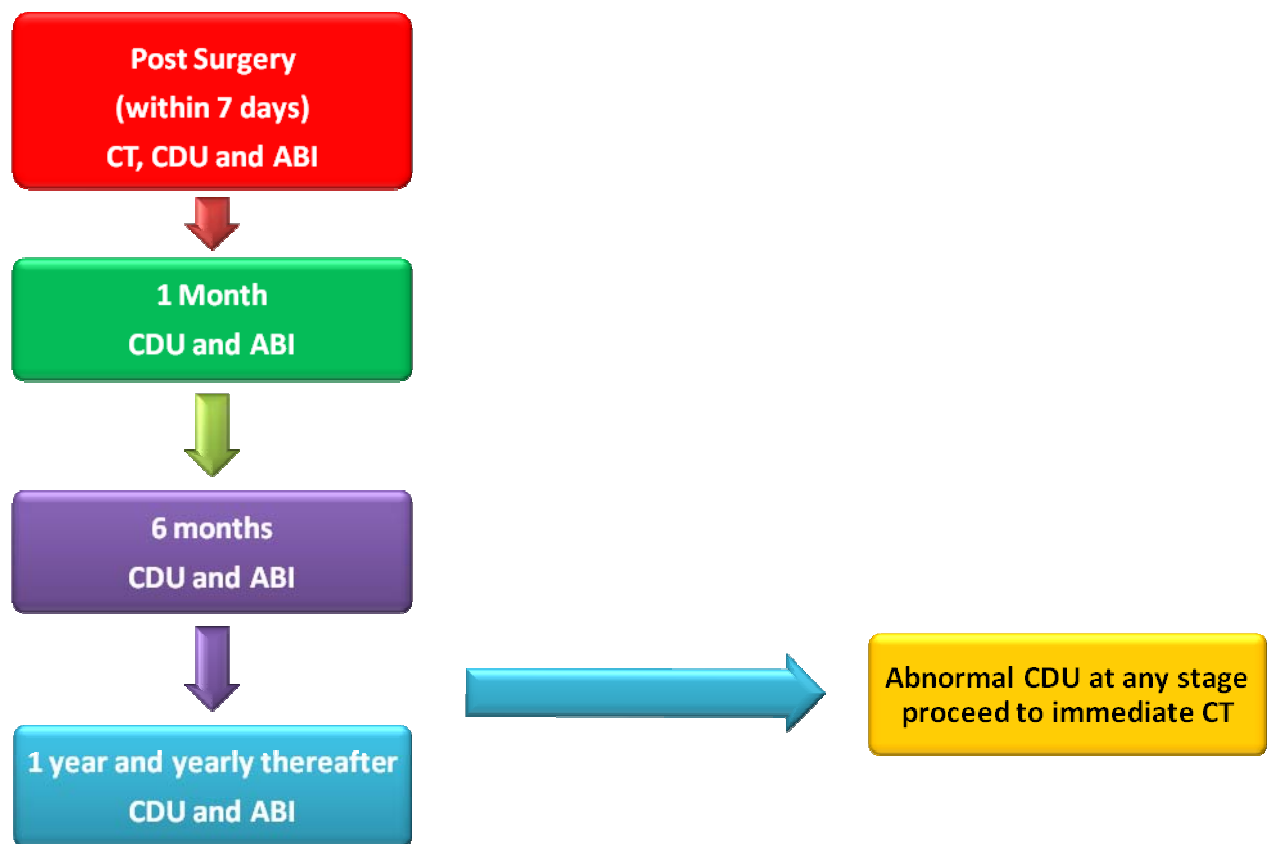
Figure 8.9: Proposed algorithm for the surveillance of patients post EVAR

Having demonstrated a high degree of correlation between CDU and CT in measuring aneurysm size prior to undergoing intervention and following implantation of an endovascular stent. We sought to extend this research to examine the natural history of aneurysm sac behaviour following EVAR as measured by CDU presented in the following chapter.

Chapter 9

Natural History of Aneurysmal Sac Size

Following Endovascular Aneurysm Repair as

Assessed by Colour Duplex Ultrasound

9.1 Introduction

Regression of the residual aneurysm sac around an implanted aortic graft is indicative of successful repair, demonstrating exclusion of the aneurysm from the systemic circulation.

Two large randomised control trials have shown many short term benefits with EVAR compared to open surgery. The EVAR 1 trial and the DREAM trial demonstrated a two thirds reduction in the 30 day post procedure mortality in patients with aneurysms treated by EVAR compared to those undergoing open repair, with advantages such as reduced blood loss and lower perioperative morbidity and a shorter hospital stay (Makaroun et al., 2001). However, as EVAR continues to evolve it is important to identify factors that are predictive of long term success.

Exclusion of the residual aneurysm sac from the systemic circulation is a fundamental component of EVAR as persistent arterial pressurisation of the sac will lead to continued expansion with the risk of eventual rupture and catastrophic haemorrhage. Regression of the residual aneurysm sac following endovascular repair is taken as a marker of a successful procedure while continued expansion implies failure due to the presence of an endoleak or endotension. Multiple imaging techniques such as digital subtraction angiography (DSA), computed tomography (CT) and colour duplex ultrasound (CDU) have been employed to demonstrate morphological characteristics and aneurysm size prior to surgery and are routinely used to monitor the residual aneurysm sac post repair.

Several authors have reported regression of the residual aneurysm at an early stage based on measurements made with CT, some suggesting that

regression is linked to graft type and make (Sternberg et al, 2003). Some have linked regression to pre repair factors such as aneurysm size and neck thrombus (Fairman et al., 2006). Wolf in 2000 concluded that aneurysm regression was unpredictable and the presence of an endoleak did not determine the rate of regression. The EURO STAR registry indicated that 16% of aneurysms failed to decrease in size after repair despite the absence of an endoleak on CT (Gilling-Smith 1999).

Having demonstrated in Chapter 7 and 8 that CDU has an excellent correlation with CT for measuring aneurysm sac size pre and post endograft implantation, I sought to define its role in determining the natural history of the residual aneurysm sac following EVAR. The aneurysm change was calculated as the difference from the maximum pre operative aneurysm size to the maximum aneurysm change observed during surveillance following EVAR.

The aneurysm change was calculated and its relationship to pre existing risk factors, pre operative aneurysm size and the presence or absence of a type 2 endoleak was determined.

9.2 Patients and Methods

Following approval from the hospital ethics committee, all patients who underwent elective EVAR from 1st of January 2003 to the 1st of July 2010 (n=145) in the Mater Misericordiae University Hospital (MMUH) were recruited. Patients were considered eligible for the study if they had at least two consecutive measurements of their residual aneurysm sac following graft implantation on CDU.

There were 122 (84.1%) male and 23 (15.8%) female patients with a mean ($\pm$ SD) age of 77.1 (± 7.9) years. We examined the various risk factors present in each patient, the presence or absence of an endoleak and the original aneurysm size prior to repair. Patient demographics and risk factors were retrieved from the patient's admission record and included smoking status, diabetes; hypertension, statin theraphy, a history of coronary artery disease, family history of AAA, and drug history.

Patients were considered to be diabetic if they were actively being treated for type 1 or 2 diabetes, to be hypertensive if they were being treated with anti hypertensive's and to have a history of coronary artery disease if they had previous cardiac stenting or surgery.

The change in the residual aneurysm sac size on consecutive CDU examinations was recorded over time. A significant change in aneurysm sac size was taken to be a change of $\pm$ 0.5cm between consecutive visits (Sternberg et al., 2003, Fairman et al., 2006 and Rhee et al., 2000). Patients were followed up post operatively until one of the end points of rupture, death or most recent scan was reached.

All patients underwent routine post operative surveillance as previously described in Chapter 8; figure 8.3. The maximum preoperative measurement obtained on CDU was considered the base line measurement for this study.

Of the 145 patients that underwent EVAR, 106 (73.1%) patients had at least 2 consecutive CDU measurement post device implantation making them eligible for the study.

Thirty nine (26.9%) patients were excluded due to failure to attend for follow up at the appropriate times and patients who underwent recent EVAR only had one available CDU scan for analysis post implantation. The demographics and co morbidities of the 106 patients included in the study are summarised in figure 9.1.
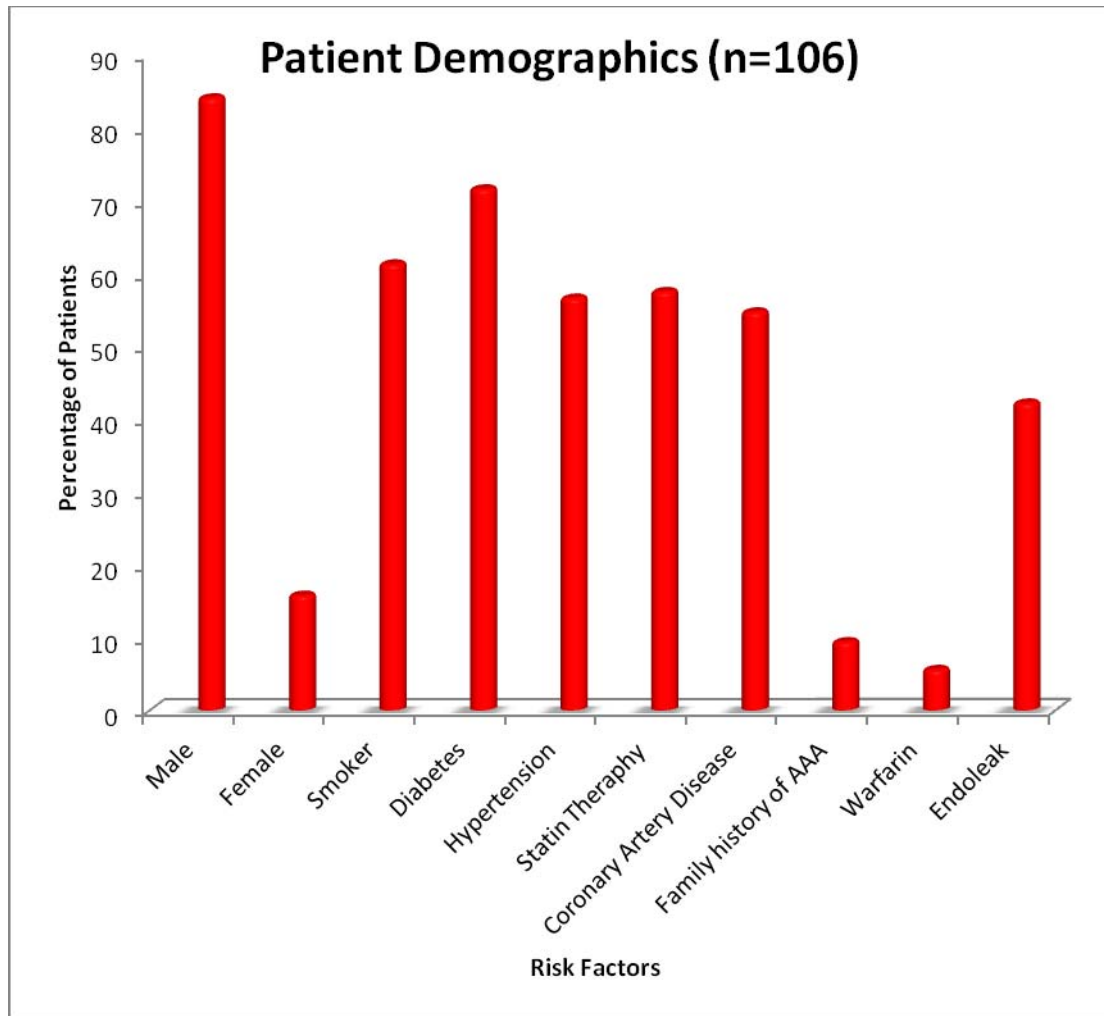
Figure 9.1: Patient demographics

Of the 106 patients included in the study the mean ($\pm$ SD) number of CDU scans per person was 4.6 (± 1.4) scans.

9.2.1 Colour Duplex Ultrasound

All CDU scans were conducted by the same accredited vascular technologist using a Siemens Sequoia 512 Mountain View system and a curvilinear 6C2 transducer (Chapter 5.0 figure 5.6), following the standard clinical measurement protocol for surveillance of patients post EVAR as previously described in Chapter 5.0, section 5.4.4.

The maximum anterior to posterior (AP) wall measurement and the maximum transverse wall diameter was documented in each CDU scan and the larger of the two measurements was used to determine the residual aneurysm size. The presence or absence of a type 2 endoleak was also documented.

9.3 Statistical Analysis

The patient's aneurysm change at each point in their surveillance was calculated (equation 9.1). The percentage aneurysm change at each point in their surveillance was also calculated (equation 9.2).

$$\text{Aneurysm Change (cm)} = \text{Baseline measurement} - \text{Follow up measurement}$$

Equation 9.1

$$\text{Percentage Aneurysm Change (\%)} = \frac{\text{Baseline measurement} - \text{Follow up measurement}}{\text{Baseline measurement}} \times 100$$

Equation 9.2

A univariate and multivariate risk factor analysis was performed using statistical analysis system software (SAS) to determine if any of the pre existing risk factors assessed prior to graft implantation or the presence of a type 2 endoleak were predictive of aneurysm change. A statistical difference was defined as a p value of <0.05 in all cases.

292

This analysis was performed for the group as a whole (n =106). A subgroup analysis was also performed; patients were allocated to subgroups of decreasing aneurysms, increasing aneurysms and stable aneurysms based on the maximum aneurysm change observed during their surveillance.

9.4 Results

9.4.1 Entire Group

All 106 patients with a mean ($\pm$ SD) age of 75.6 ($\pm$7.2) years were included in this analysis, 23 (21.6%) female and 83 (78.3%) male patients. The mean ($\pm$ SD) aneurysm size pre surgery was 5.8 ($\pm$ 0.9) cm.

Table 9.1 summarises the mean aneurysmal change and the mean percentage aneurysmal change at each time point and the number of patients that had complete follow up to that time point.

Time Frame (Months)	Number of Patients Assessed	Mean Aneurysmal Change (cm)	Mean Percentage Aneurysmal Change (%)
0	106	-0.17	-3.0
1	106	-0.24	-4.31
7	77	-0.59	-9.87
12	55	-0.73	-12.4
18	27	-0.92	-15.8
24	10	-0.48	-16.6
36	3	-1.0	-16.6

48	1	-2.1	-28

Table 9.1: Summary of residual aneurysmal change for the entire patient group

The mean aneurysmal change at 1 month was a decrease of 0.24cm equating to a percentage aneurysm change of 4.3%. At 7 months post surgery the mean aneurysmal change was a decrease of 0.59cm (9.8%), at 12 months, a decrease of 0.73cm (12.4%). At 18 months, a decrease of 0.92cm (15.8%) and at 36 months, a decrease of 1.0cm (16.6%). One patient had follow up at 4 years; their mean aneurysm change at this point was a decrease of 2.1cm, (28%). Figure 9.2 demonstrates the mean percentage change at each time point and the number of patients who had follow up to that point.
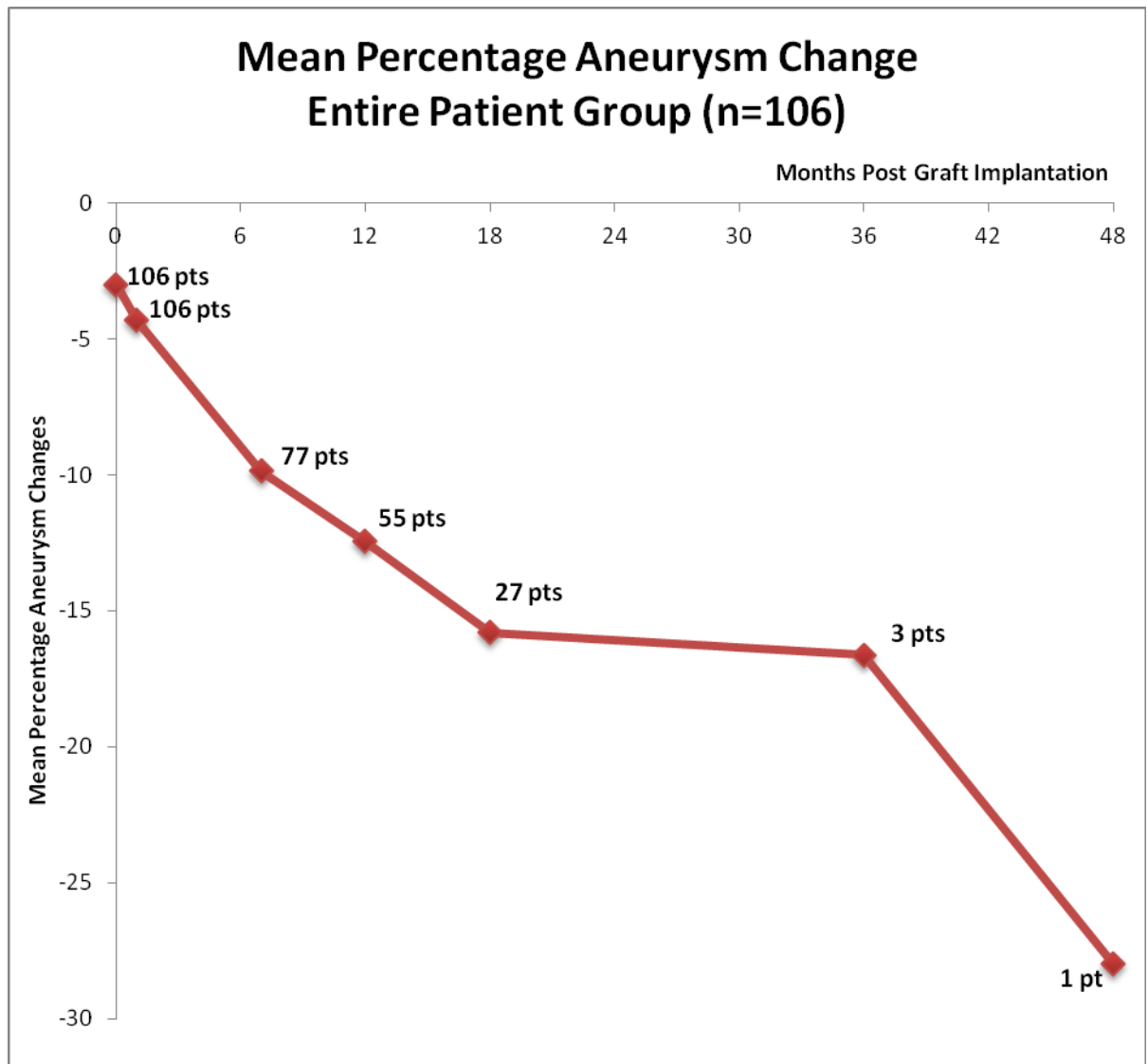
Figure 9.2: Mean percentage aneurysm change for the entire patient group

9.4.2 Subgroup Analysis

The study population was then sub divided into stable, decreasing and increasing aneurysms on the basis of the maximum change observed in residual AAA sac size during postoperative surveillance (Equation 9.2).

Stable aneurysms were defined as having a less than 0.5cm increase or decrease in aneurysm sac size. Decreasing aneurysms were defined as having a greater than 0.5cm reduction in aneurysm sac size and increasing aneurysms were defined as aneurysms that increased in size by 0.5cm or greater.
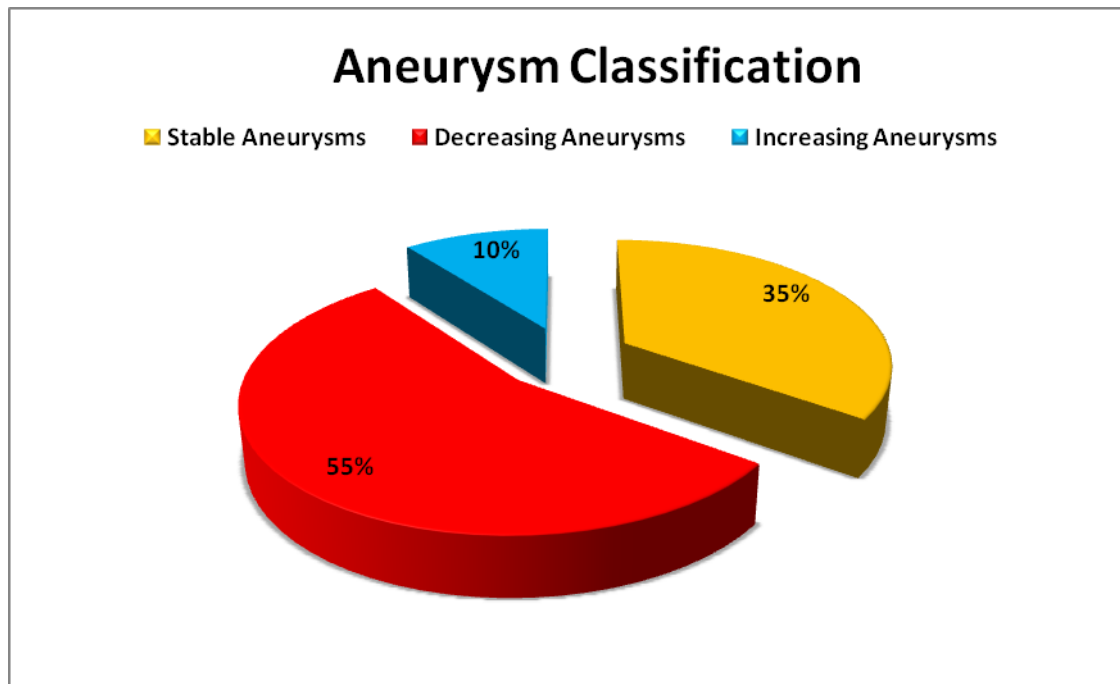
Figure 9.3: Aneurysm classification

Group	Increasing Aneurysms	Decreasing Aneurysms	Stable Aneurysms
Number of Patients	11 (10.4) %	58 (54.7) %	37 (34.9) %
Mean Age	74.8 (±9.6) years	77 (±6.9) years	73 (±7) years
Mean pre op AAA size	6.4 (±1.3) cm	5.9 (±0.9) cm	5.6 (±0.6) cm
Mean Aneurysm change	+1.06(±0.6) cm	-1.3 (±0.7) cm	-0.06 (±0.27)cm
Mean percentage change	+16.5(±7.9) %	-22.7 (±10.2)%	-1.2(±5.0)%

Table 9.2: Summary of residual aneurysm change by subgroup

i. *Increasing Aneurysms*

Eleven patients (10.4%) patients had a significant increase in residual aneurysm size (0.5cm or greater) with a mean age (± SD) of 74.8 (± 9.6) years. All the patients in this group were male. The mean (± SD) pre operative AAA size was 6.4 (± 1.3) cm (range 5.1- 9cm).

The mean (± SD) aneurysmal change observed in this group was an increase of 1.06 (± 0.56) cm, a percentage (± SD) change of an increase of 16.5 (± 7.9) %.

ii.   Decreasing Aneurysms

There were 58 (54.7%) patients who were found to have a significant decrease in residual aneurysm size (a decrease of ≥ 0.5cm) with a mean (± SD) age of 77 (± 6.9) years. There were 12 (20.6%) female and 46 (79.3%) male patients in this group.

The mean (± SD) pre operative AAA size was 5.9 (± 0.9) cm (range 4.8-8.8cm). The mean (± SD) aneurysmal change was a decrease of 1.3 (± 0.7) cm and the mean (± SD) percentage change was a decrease of 22.7 (± 10.2) %.
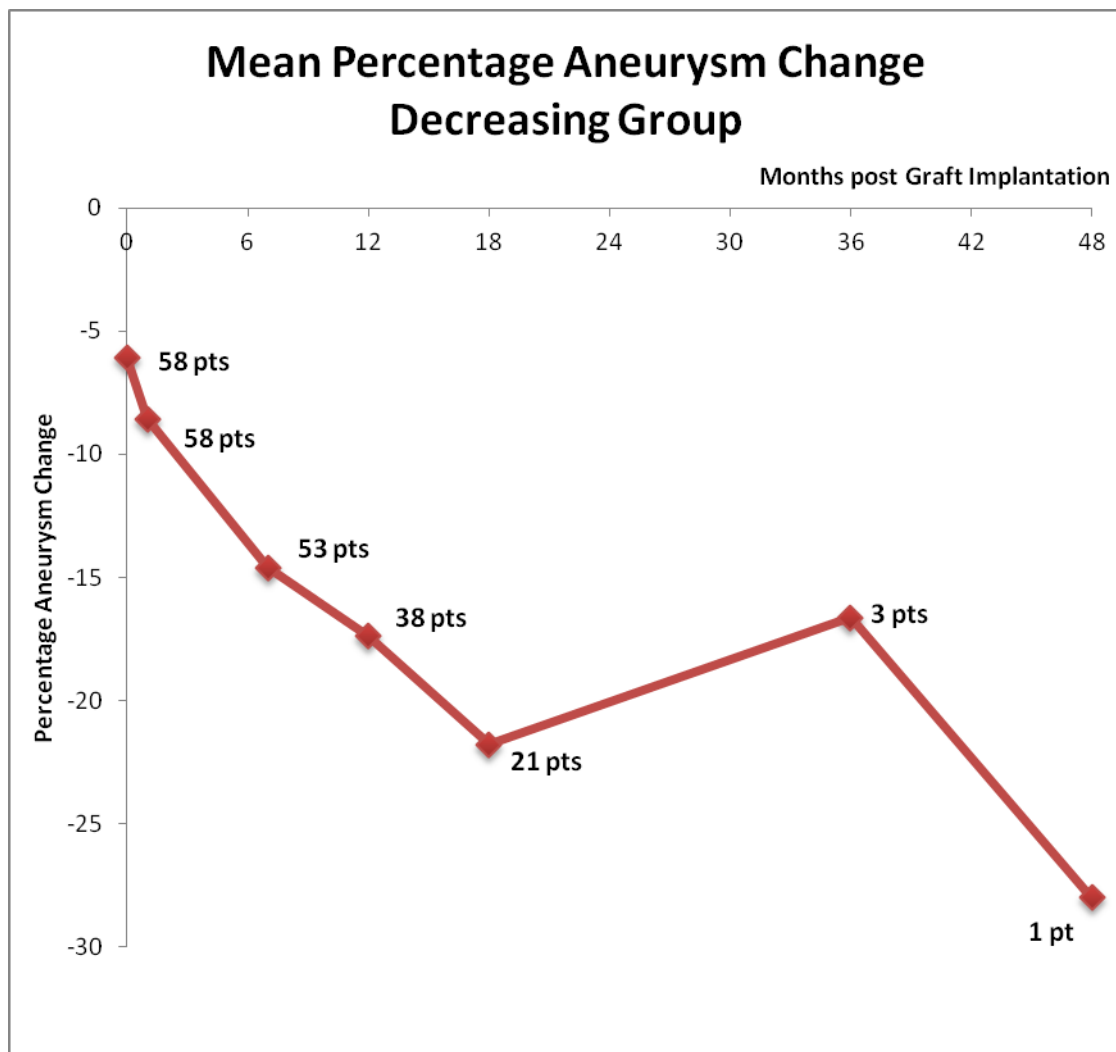
Figure 9.4: Mean percentage aneurysm change decreasing aneurysm group

iii. *Stable Aneurysms*

Thirty seven patients (34.9%) were found to have no significant alteration in residual aneurysm size and were therefore termed stable aneurysms. There were 7 (18.9%) female and 30 (81.1%) male patients with a mean (± SD) age of 73.9 (± 7.0) years. The mean (± SD) pre operative AAA size was 5.6 (± 0.65) cm (range 5.1- 9cm).

The mean (± SD) aneurysmal change was a decrease of 0.06 (± 0.27) cm and the percentage change (⊥ SD) was a decrease of 1.2 (⊥ 5.0) %.
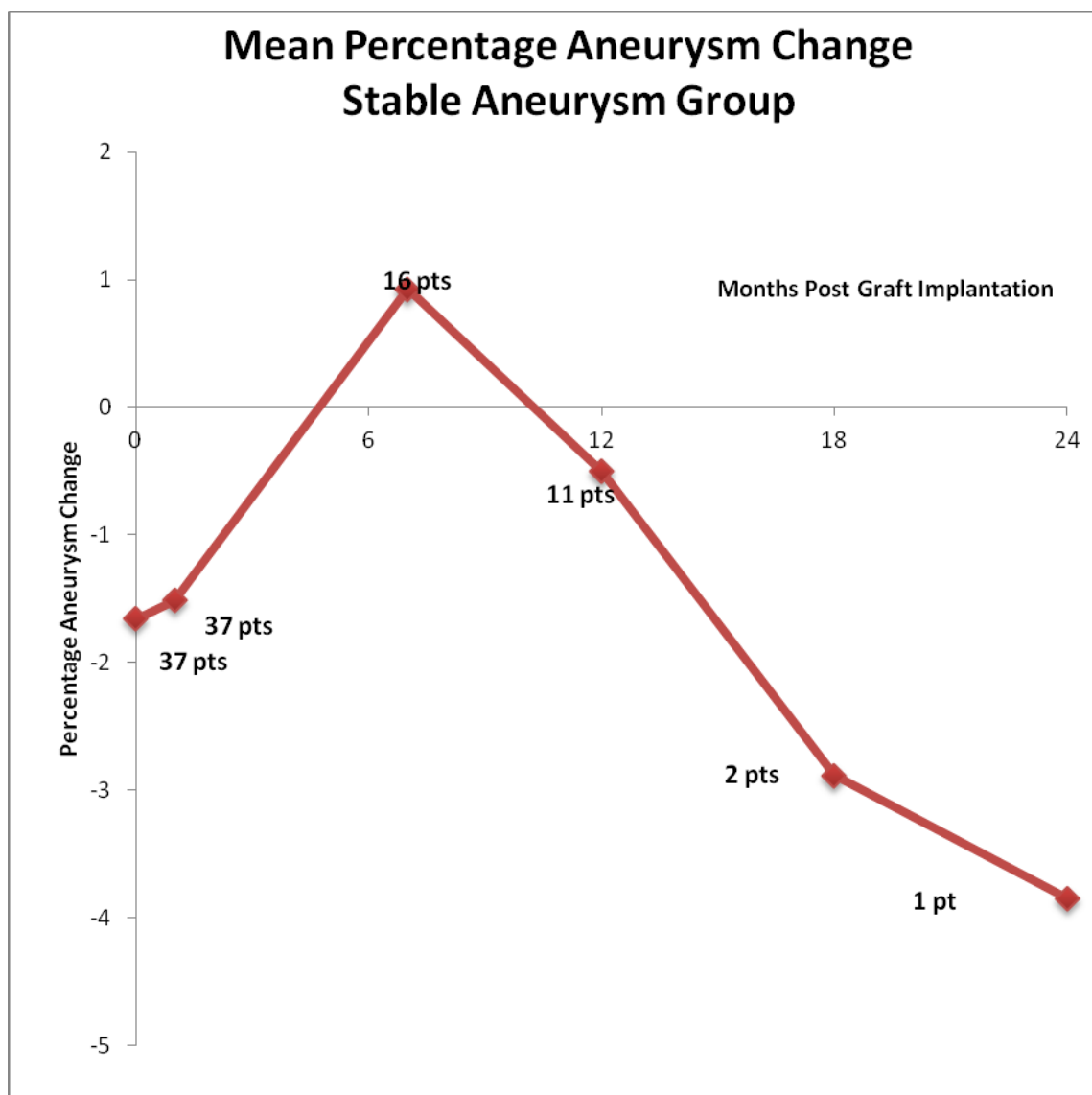
Figure 9.5: Mean percentage aneurysm change stable group

9.4.2 Risk Factor Analysis

The patient demographics in each subgroup were are summarised in Figure 9.6 and Table 9.3.
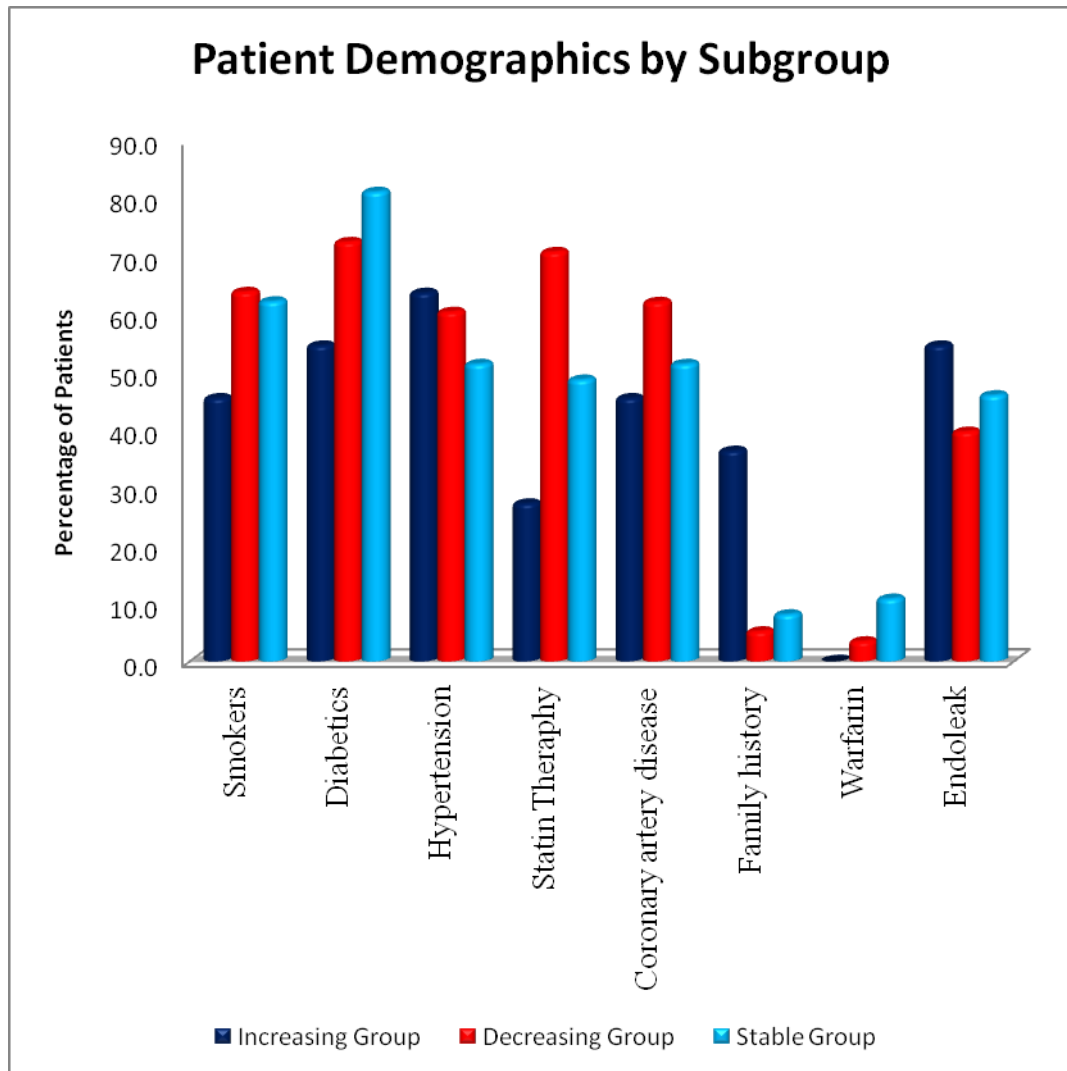
Figure 9.6: Patient demographics by subgroup

Risk Factor	Entire Group (n = 106)	Increasing aneurysms (n = 11)	Decreasing Aneurysms (n = 58)	Stable Aneurysms (n = 37)
Mean Age	75.6 (±7.2) years	74.8 (±9.6) years	77.9 (±6.9) years	73 (±7) years
Mean Pre op AAA size	5.8 (±0.9) cm	6.4 (±1.3) cm	5.9 (±0.9) cm	5.6 (±0.6) cm
Smoker	61.3 %	45.5 %	63.8 %	62.2 %
Diabetic	72.6 %	54.5 %	72.4 %	81.1 %
Hypertension	56.6 %	63.6 %	60.3 %	51.4 %
Statin Therapy	57.5 %	27.3 %	70.7 %	48.6 %
Coronary Disease	55.7 %	45.5 %	62.1 %	51.4 %
Family History	9.4 %	36.4 %	5.2 %	8.1 %
Warfarin	5.7 %	0 %	3.4 %	10.8 %
Endoleak	42.5 %	54.5 %	39.7 %	45.9 %

Table 9.3: Patient demographics by subgroup

Table 9.3 summarises the distribution of patient demographics in the entire population and in each subgroup. The increasing aneurysm group demonstrated a lower percentage of smokers (45.5%) and diabetics (54.5%) than the 62.2% smokers and 81.1% diabetics in the stable aneurysm group and the 63.8% smokers and 72.4% diabetics in the decreasing aneurysm group.

There was a higher percentage (70.7%) of patients in the decreasing aneurysm group on statin therapy compared to the 48.6% in the stable aneurysm group and 27.3% in the increasing aneurysm group.

The stable aneurysm group demonstrated a lower percentage of patients with hypertension and coronary artery disease. A higher proportion of the stable aneurysms patients were on Warfarin (10.8%) compared to the other groups. Family history of AAA was more prevalent in the increasing aneurysm group (36.4%).

9.5 Statistical Analysis

Univariate and multivariate analysis were performed to assess the influence of various risk factor variables on aneurysm change. The predicative values assessed in this series included age, pre operative aneurysm size, smoking status, diabetes, hypertensive, statin therapy, coronary artery disease, family history of AAA and the presence of a type 2 endoleak.

Univariate and multivariate analysis was performed for the entire patient population and each subgroup.

9.5.1 Entire Patient Group (n = 106)

i. Univariate Analysis

Univariate analysis was performed to assess if aneurysm change was influenced by any one variable.

Predictive Factor Variable	Parameter Estimate	Standard Error	t Value	p Value
Age	**-0.42**	**0.21**	**-2.02**	**0.045**
Pre operative size	0.54	1.7	0.31	0.76
Smoking status	-0.001	3.2	-0.00	0.99
Diabetes	12.6	2.96	1.42	0.16
Hypertension	-2.48	3.15	-0.79	0.43
Statin therapy	**-10.66**	**2.99**	**-3.56**	**0.0006**
Coronary artery disease	-2.35	3.14	-0.75	0.46
Family history of AAA	9.09	5.27	1.72	0.087
Warfarin	3.17	6.76	0.47	0.64
Endoleak	**7.2**	**3.07**	**2.36**	**0.01**

Table 9.4: Univariate analysis entire patient population

Univariate analysis for the entire population (n=106) determined that an increasing age (p=0.04) and statin therapy (p = 0.0006) were positively associated with aneurysm regression. The presence of an endoleak was determined to be inversely related to aneurysm regression (p= 0.01).

Multivariate analysis was performed on the entire patient population to determine if aneurysm change was influenced by multiple variables or combinations of variables.

Predictive Factor Variable	Parameter Estimate	Standard Error	t value	p value
Age	-0.28	0.20	-1.35	0.17
Pre operative size	0.21	1.6	0.13	0.89
Smoking status	1.5	3.18	0.48	0.63
Diabetes	3.7	3.5	1.05	0.29
Hypertension	1.3	3.2	0.42	0.67
Statin therapy	**-11.1**	**3.5**	**-3.16**	**0.002**
Coronary artery disease	0.16	3.11	0.05	0.95
Family history of AAA	4.2	5.22	0.81	0.41
Warfarin	1.4	6.4	0.23	0.82
Endoleak	**7.3**	**2.9**	**2.47**	**0.01**

Table 9.5: Multivariate analysis entire patient group

Multivariate analysis for the entire patient population (n=106) demonstrated that statin therapy (p=0.002) was the only risk factor variable positively associated with aneurysm regression. The presence of a type 2 endoleak was determined to be inversely related to aneurysm regression (p = 0.01).

Predictive factor	Parameter Estimate Univariate	Parameter Estimate Multivariate	t value Univariate	p value Multivariate
Age	**-0.42**	-0.28	**0.045**	0.17
Pre operative size	0.54	0.21	0.76	0.89
Smoking status	-0.001	1.5	0.99	0.63
Diabetes	12.6	3.7	0.16	0.29
Hypertension	-2.48	1.3	0.43	0.67
Statin therapy	**-10.66**	**-11.1**	**0.0006**	**0.002**
Coronary artery disease	-2.35	0.16	0.46	0.95
Family history of AAA	9.09	4.2	0.087	0.41
Warfarin	3.17	1.4	0.64	0.82
Endoleak	**7.2**	**7.3**	**0.01**	**0.01**

Table 9.6: Comparison of univariate and multivariate analysis for the entire patient group

9.5.2 Subgroup Analyses

i. Decreasing Aneurysm Group (n=58) Multivariate Analysis

Predictive Variable	Parameter Estimate	Standard Error	t Value	p Value
Age	-0.05	0.17	-0.31	0.76
Pre operative size	-1.53	1.3	-1.18	0.25
Smoking status	-1.29	2.60	-0.50	0.62
Diabetes	**9.65**	**2.84**	**3.39**	**0.001**
Hypertension	-2.67	2.5	-1.06	0.29
Statin therapy	**-9.4**	**2.9**	**-3.23**	**0.002**
Coronary artery disease	**6.01**	**2.52**	**2.38**	**0.02**
Family history of AAA	-7.90	5.2	-1.5	0.14
Endoleak	**6.2**	**2.4**	**2.59**	**0.01**

Table 9.7: Multivariate analysis decreasing aneurysm group

Multivariate analysis was performed on patients in the decreasing aneurysm group. A history of Diabetes (p= 0.001) a history of coronary artery disease (p= 0.02) and the presence of an endoleak (p = 0.01) were found to be inversely related to aneurysm regression. Statin therapy (p = 0.002) was found to be positively associated with aneurysm regression in this group.

ii. Stable Aneurysm Group (n= 37) Multivariate Analysis

Multivariate analysis on the stable aneurysm group demonstrated no significant results as there was no significant change (<0.5cm) in aneurysm size in this group.

iii. Increasing Aneurysm Group (n=11) Multivariate Analysis

Predictive Variable	Parameter Estimate	Standard Error	t Value	p Value
Age	0.34	0.19	1.73	0.33
Pre operative size	0.22	1.9	0.12	0.92
Smoking status	-13.45	7.9	-1.7	0.34
Diabetes	-7.22	8.17	-0.88	0.53
Hypertension	1.1	5.99	0.20	0.87
Statin therapy	9.7	10.48	0.93	0.52
Coronary artery disease	-6.8	4.13	-1.65	0.35
Family history of AAA	-1.55	8.5	-0.18	0.88
Endoleak	7.63	6.79	1.12	0.46
Warfarin	1.4	6.4	0.23	0.82

Table 9.8: Multivariate analysis increasing aneurysm group

Multivariate analysis on the increasing aneurysm group revealed that no variables were associated with aneurysm change.

9.6 Discussion

Endovascular aneurysm repair of abdominal aortic aneurysms has become increasingly employed as the method of choice for repair of abdominal aortic aneurysms. However, unlike patients who undergo open surgical repair, EVAR patients are at continued risk of aneurysm rupture if there is incomplete aneurysm exclusion from systemic circulation. Regression of the residual aneurysm sac is perhaps the most important observation following EVAR as it implies successful exclusion of the aneurysm from the systemic circulation.

An alteration in AAA sac size of 0.5cm or more has previously been described by others (Sternberg et al., 2003, Fairman et al., 2006 and Rhee et al., 2000) as being significant and thus was the measurement used for the purpose of defining subgroups for analysis in this study.

Using repeated CDU measurements, we observed a significant (>0.5cm) decrease in sac size in 54.7% of patients who underwent EVAR. A significant reduction in residual aneurysm size was noted at 7 months following surgery (0.59cm), which continued at 12 (0.73cm) and 18 months (0.92cm) but slowed at 2 years (0.48cm). Rhee and colleagues in 2000 reported a similar progressive decrease in residual aneurysm sac size in a series of 123 patients in the first year of endograft implantation. Eleven patients (10.4%) demonstrated a significant (>0.5cm) increase in aneurysm sac size while thirty seven (34.9%) showed no significant change in size.

Multivariate analysis performed on the entire patient group (n=106) demonstrated that statin therapy (p=0.002) was the only variable associated with aneurysm regression following EVAR. Univariate analysis revealed that statin

therapy (p =0.0006) and an increasing age (p = 0.04) were associated with aneurysm regression whereas the presence of an endoleak (p = 0.01) was inversely related to aneurysm change. These results therefore would suggest that stains play an active role in aneurysm regression.

Further subgroup analysis revealed that diabetes (p = 0.001) the presence of an endoleak (p =0.05) and a history of coronary artery disease (p = 0.02) were all inversely related to aneurysm change in the decreasing aneurysm group. Statin therapy in the decreasing aneurysm group was found to be positively associated with regression (p = 0.002). There were also no predisposing factors associated with aneurysm change in either the stable or the increasing aneurysm group.

The mean (±SD) preoperative age in the entire group of 75.6 (±7.2) years was slightly older than the 73 (±8) years reported by Fairman (2006) and 72 (±0.8) years described by Rhee (2000). Patients in the increasing aneurysm group had larger mean diameters pre operatively 6.3cm (±1.3) than the 5.8cm (±0.9) and 5.6 cm (±0.6) seen in the decreasing and stable aneurysm groups respectively and in the entire group 5.8cm (± 0.9). Preoperative aneurysm size was not found to be statistically significant following univariate and multivariate analysis on the entire patient population or following multivariate analysis on any of the subgroups (P= >0.05 in all cases).

Fairman and colleagues in 2006, in a series of 351 patients examined aneurysm change at 1, 6 and 12 months post EVAR and the effect of factors such as graft type, age, gender, smoking status and variables such as pre procedure neck thrombus on sac shrinkage they monitored regression with repeat CT measurements. At 1 month none of their independent variables were predictive of

sac shrinkage. At 12 months they demonstrated that pre operative AAA size, the presence of an endoleak, preoperative neck thrombus and gender was indicative of aneurysm regression. In our series following univariate and multivariate analysis aneurysm size prior to intervention was not found to be associated with aneurysm change in any of the groups (p = >0.05 in all cases).

In contrast to Fairmans series, gender was not found to be a predictor of aneurysm regression in this study with only 12 female patients in the decreasing group and 7 in the stable group. However, in Fairmans series only 7 % of the study population were female, in contrast to the 17.9% presented here, which might explain these findings.

Multivariate analysis in all groups demonstrated no statistical significant association between age and aneurysm change (p= >0.05 in all cases). Univariate analysis however, on our entire patient population demonstrated that an increasing age was positively associated with aneurysm regression (p=0.04).

Our results are comparable to Rhee (2000), who, in a series of 123 patients, found that significant sac shrinkage occurs at 6 months after graft implantation. They also demonstrated a steady decrease in residual aneurysm sac from baseline to 6 months and 12 months.

Wolf and colleagues in 2000 sought to determine the rate of aneurysm regression after EVAR using repeated CT measurements in a series of 110 patients. They concluded that the rate of aneurysm decrease in individual aneurysms is unpredictable and the presence of an endoleak is unreliable in predicting aneurysm change. In contrast, univariate analysis in our series demonstrated that the presence of a type 2 endoleak was inversely related to

aneurysm regression (p =0.01) in the entire patient population. Multivariate found the presence of a type 2 endoleak to be inversely related to aneurysm regression (p= 0.01) in the entire patient group and the decreasing aneurysm group (p = 0.01). Indicating that the presence of a type 2 endoleak does affect aneurysm change. Wolf and colleagues pre operative aneurysm diameter was similar to our own at 5.9 (± 0.84) cm. Their mean aneurysmal decrease for their entire group at 6 months (0.34cm) and 12 months (0.59cm) was also similar to our own at 6 months (0.24cm) and 12 months (0.59cm).

Bobadilla and colleagues in 2010 assessed the effect of warfarin therapy in the development of type 2 endoleaks after EVAR and concluded that warfarin was linked to an increased risk of endoleak development. The effect of Warfarin on aneurysm regression was assessed in this study and demonstrated no statistical significance (p= 0.64 univariate analysis and p = 0.84 multivariate analysis) however, as only 5.7% of patients were warfarinised, this series is not sufficiently powered to assess its effect. There were a higher percentage of patients in the stable aneurysm group (10.8%) on warfarin therapy than in the decreasing aneurysm group (3.4%).

Of the 11 patients in the increasing aneurysm group 6 (54.6%) patients had a documented endoleak during surveillance with 5 (45.5%) ultimately requiring treatment. Multivariate analysis revealed that the presence of an endoleak (p = 0.46) was not statistically significant. However, the small sample numbers in this group is a limitation. This study demonstrates a much higher percentage of aneurysms that failed to decrease significantly (34.9% in the stable aneurysm group) compared to the EUROSTAR registry which indicated that 16% of

aneurysms failed to decrease in size after repair despite the absence of an endoleak on CT (Gilling-Smith 1998).

There are several limitations of this study such as the small sample size, the retrospective nature of the study and the failure of a proportion of patients to attend for follow up. Also, despite the multiple variables evaluated in this series, the effect of endograft type was not taken into account. Sternberg examined aneurysm sac shrinkage in a series of 169 patients after endovascular aneurysm repair using repeat CT measurements at 6 months and 12 months using two different graft types and concluded that aneurysm regression was graft specific. The presence of graft type was not taken into account in this study as two different endograft types were employed with ~95% of the endografts being the same type, therefore making any meaning full analysis of the effect of endograft type biased.

9.7 Conclusion

This study further defines the role of CDU in the postoperative surveillance of patients who have undergone endovascular repair of an abdominal aortic aneurysm. Maximum aneurysmal sac reduction occurs in the first year following EVAR.

Aneurysm change is clearly influenced by treatment of predisposing risk factors that can be determined prior to undergoing intervention. Our key finding is that there is a highly significant statistical association with decreasing aneurysms size following EVAR and patients on statin therapy, suggesting that statins play a key role in the regression process. However, to suggest that patients with a known history of hypercholesterolemia be selected for altered follow up based on the numbers in this series is unreasonable. A larger more prolonged study to examine

313

the effect of statin therapy on the mechanics of aneurysm regression should be undertaken.

This study also demonstrates that the presence of an endoleak is inversely related to aneurysm change in the entire patient group and the decreasing aneurysm group following EVAR, indicating that patients with persistent endoleaks should undergo more rigorous imaging to monitor aneurysm change and perhaps a more aggressive intervention approach should be employed.

Chapter 10

The Effect of Endovascular Aortic Stent Graft

Placement on Arterial Stiffness

10.1 Introduction

Atherosclerotic coronary artery disease is one of the leading causes of death worldwide and is the leading cause of early and late mortality following abdominal aortic aneurysm (AAA) repair (Ballard et al., 1998). Early detection of risk factors associated with increased cardiovascular risk should therefore be of upmost importance in patients being considered for elective AAA repair. Having established the role of CDU in pre and post operative surveillance following EVAR, we sought to identify a role for CDU in assessment of this risk.

Pulse wave velocity (PWV) is a measure of arterial stiffness and an increase in PWV has been identified as an independent risk factor for increased cardiovascular morbidity and mortality (Alecu et al., 2008). Aortic pulse wave velocity is an indicator of the stiffness of large arteries and is an independent predictor of morbidity and mortality especially in the elderly population (Alecu et al., 2008). PWV is the time taken for the arterial pulse to propagate from the common carotid artery (CCA), to either the radial or the femoral artery.

There is a clear link in the literature to support the relationship between increased PWV and outcomes in groups with other atherosclerotic disorders. However there is little to support a link between elevated PWV and the outcome of patients post Endovascular Aneurysm Repair (EVAR). Despite the improvement in 30 day mortality associated with EVAR, adverse cardiac events

are still the leading cause of long term mortality following AAA repair (Virgillio et al., 2006).

There have been several large randomised trials to date which demonstrate an improved 30 day survival rate for EVAR versus the open aneurysm repair but no difference in the quality of life at 1 year. All cause mortality rates were similar between the open group and EVAR group at 4 years, suggesting that the initial survival benefit associated with the reduction in perioperative mortality does not persist (EVAR 1 trial and DREAM trial). Schouten et al in 2006 demonstrated that the major adverse events affecting long term morbidity and mortality following EVAR were cardiac in origin (Schouten et al., 2006).

According to the Moens Korteweg equation (Equation 10.1) the PWV, which is related to the square root of the elastic modulus, rises in stiffer arteries (Blacher et al., 1999).

$$PWV = \sqrt{\frac{E h_v}{2 \rho_b r_{vi}}}$$

Equation 10.1: Moens Korteweg Equation

ρb: density of blood
E: the elastic modulus
h_v: the thickness of the arterial wall
r_{vi}: internal radius of the artery

The elastic properties of the aorta and the larger arteries in the body are important due to their need to expand to accommodate large volumes of blood during systole.

Arterial wall stiffness can be measured non-invasively by measuring the speed of arterial pressure wave transmission through the arterial tree. It can be measured using several reference points such the common carotid artery and the femoral artery by a simple reproducible method using many commercially available devices.

Measurement of PWV is simple and, unlike other imaging methods for determination of arterial stiffness, does not require the evaluation of blood pressure at the site of imaging. It has become widely regarded as the gold standard method of measuring of arterial stiffness (Jiang et al., 2007). PWV is calculated by dividing the distance between two measurement points by the transit time delay from both points and may be described by the following equation (Zhang and Greenleaf. 2005)

$$PWV = \frac{Length}{Pulse\ Transit\ Time\ Carotid - Femoral}$$

Equation 10.2: PWV Equation

PWV is usually determined by arterial tonometery using one of two commercially available systems, the SphygmorCor (AtCor Medical, Sydney, Australia) and the Complior system (Conlson, Gorges les Genosse, France). PWV uses pressure sensors that are applied over the carotid and femoral arteries either simultaneously or sequentially using an electrocardiogram (ECG) as a timing reference to determine the time delay between the upstroke of the carotid and the femoral pulse waveforms (Jiang et al., 2007).

Jiang and colleagues in 2007 compared the carotid femoral PWV measured by tonometery (the SphygmoCor system) with a standard vascular ultrasound system using a linear transducer and concluded that there was no mean difference between the mean values of PWV obtained by the two techniques, indicating that a commercially available ultrasound scanner such as is available in our department can be used to accurately and reproducibly measure PWV.

Carotid-femoral PWV is a recognisable index of aortic stiffness and has been proven to be an important predictor of cardiovascular events in many disorders (Villacorta et al., 2006). This method of measuring aortic PWV has emerged as the only reliable measure of arterial stiffness that is able to predict outcomes in individuals with such risk factors (Smith et al., 2005).

PWV can increase with various risk factors such as age; hypertension and diabetes. There are no accepted normal reference values, however on the basis of previous prospective morbidity and mortality studies values greater than 12m/sec are considered elevated (Rajzer et al., 2001). This value varies depending on the method of measurement used. In 2008 Cosmin Alecu et al., 2008 defined

reference values for aortic PWV in the elderly using the commercially available pulse pen device. They used an apparently healthy group of both males and females aged between 60-75 years. Individuals with hypertension and diabetes were excluded from the study. They concluded that in this age group a PWV of below 10m/sec measured with the pulse pen was considered normal. Values above 13m/sec were considered elevated.

The primary aim of this study was to determine if the implantation of an endovascular aortic graft altered the patients PWV compared to the patients who underwent the traditional open surgical repair. An increase in PWV following EVAR could explain the absence in long term survival benefit in patients who had EVAR of their aneurysms compared to those who survived open surgery.

10.2 Patients and Methods

Following approval from the hospital ethics committee, commencing on the 1st of July 2008, 34 patients being worked up for elective repair of their Abdominal Aortic Aneurysm (AAA) in the Mater Misericordiae University Hospital (MMUH) gave their consent to have their PWV calculated using a standard vascular ultrasound system.

Of the total number of patients examined there were 31 (90%) male and 3 (10%) female patients with an overall mean ($\pm$ SD) age of 73 (± 6.8) years.

Fifteen (44.1%) patients underwent open surgical repair with a mean ($\pm$ SD) age of 72 (± 7.7) years and 19 (55.8%) patients underwent EVAR with a mean ($\pm$ SD) age of 73 (± 6.2) years. Both groups had their PWV recalculated post procedure within 4 weeks.

Patient demographics and co morbidities in the two groups are detailed in table 10.1 and figure 10.1.

Risk Factor	EVAR Patients (%) (n = 19)	Open Repair Patients (%) (n =15)
Male	84.2	100
Female	15.8	0
Smoker	35.3	40
Diabetic	23.5	6.6
Hypertension	41.2	46.6
Hypercholesterolemia	52.9	20.0
Coronary Disease	52.9	13.3
Family History of AAA	11.7	6.6
Aspirin	47.0	53.3
Lipitor	29.4	13.3
Plavix	11.7	13.3
Warfarin	0	6.6

Table 10.1: Patient demographics by group
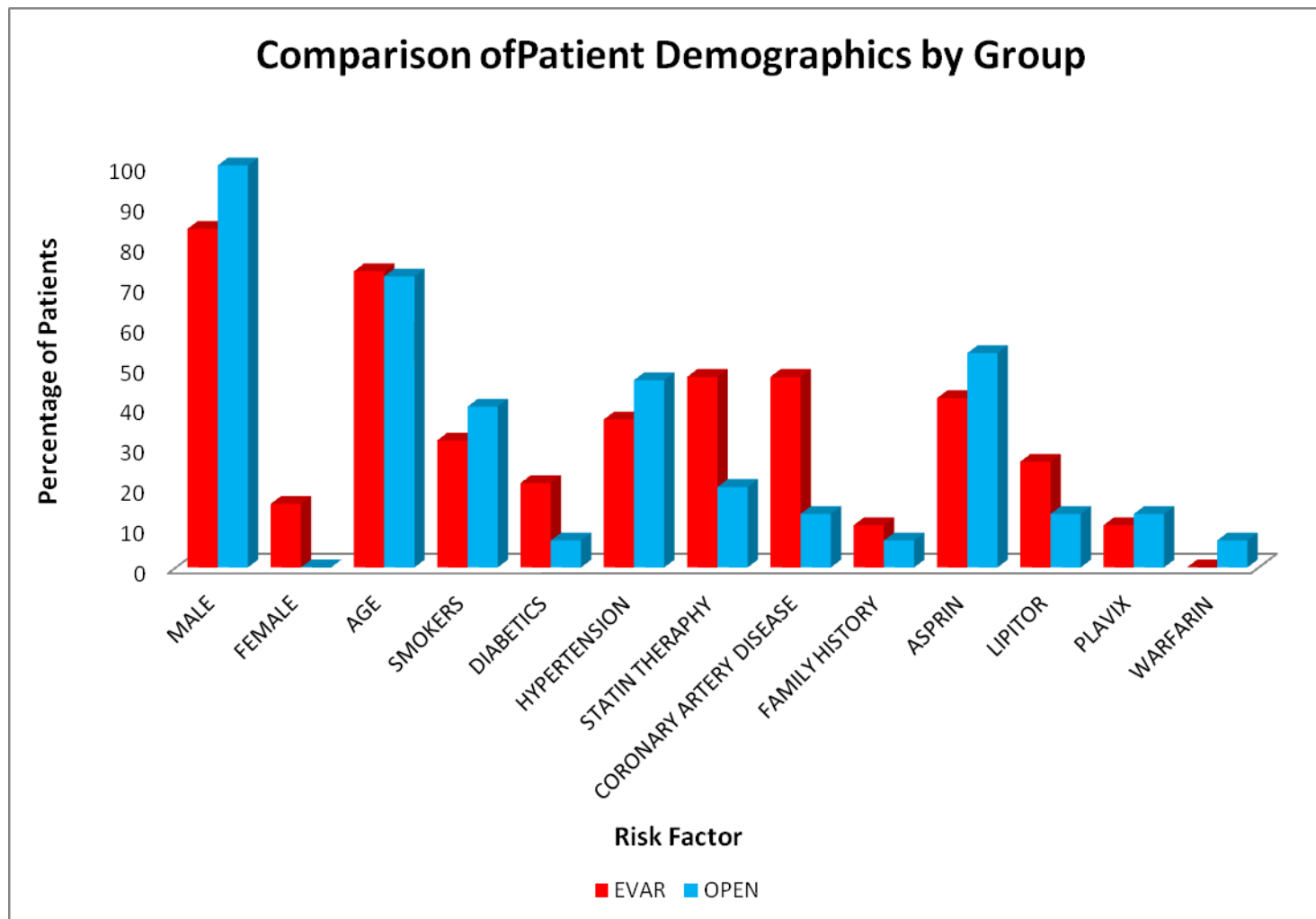
Figure 10.1: Patient demographics by group

10.2.1 Measurement of PWV

All patients were scanned in the vascular laboratory of the MMUH by the same accreditated vascular technologist. A Phillips IU22 vascular ultrasound system was used to perform all colour Duplex ultrasound (CDU) measurements utilising a 7-10MHz linear array transducer. All scans were performed in a darkened temperature controlled room following the clinical measurement protocol as previously described in Chapter 5, section 5.5.4. All CDU scans were performed within a week prior to undergoing intervention, and repeated within four weeks following intervention.

The two reference points used for the purpose of this study were the right common carotid artery (RCCA) and the right common femoral artery (RCFA). All values for PWV were calculated as previously described in Chapter 5.0 section 5.5.5.

10.3 Results

Of the 34 patients included in this study the mean (± SD) PWV prior to undergoing intervention was found to be 9.3 (±2.6) m/sec .

Open surgical repair group

Fifteen patients in total underwent open surgical repair. Their mean PWV prior to undergoing intervention was found to be 9.9 (±3.1) m/sec. After intervention the mean PWV in this group decreased to 9.7 (±4.5) m/sec. The mean change was found to be a decrease of 0.2 (±4.9) m/sec. No statistical difference was found between the PWV pre surgery and post surgery in the open group when the student paired *t*- test was performed (p = 0.88).

Endovascular Aneurysm Repair

Nineteen patients underwent EVAR. Their PWV prior to undergoing graft implantation was found to be 8.8 (±2.1) m/sec. Post implantation of endovascular graft the mean (± SD) PWV in this group of patients increased to 12.2 (±4.5) m/sec. The mean change in PWV was found to be an increase of 3.3 (±3.7) m/sec. This difference was statistically significant when the student paired *t*- test was performed (p=0.001).
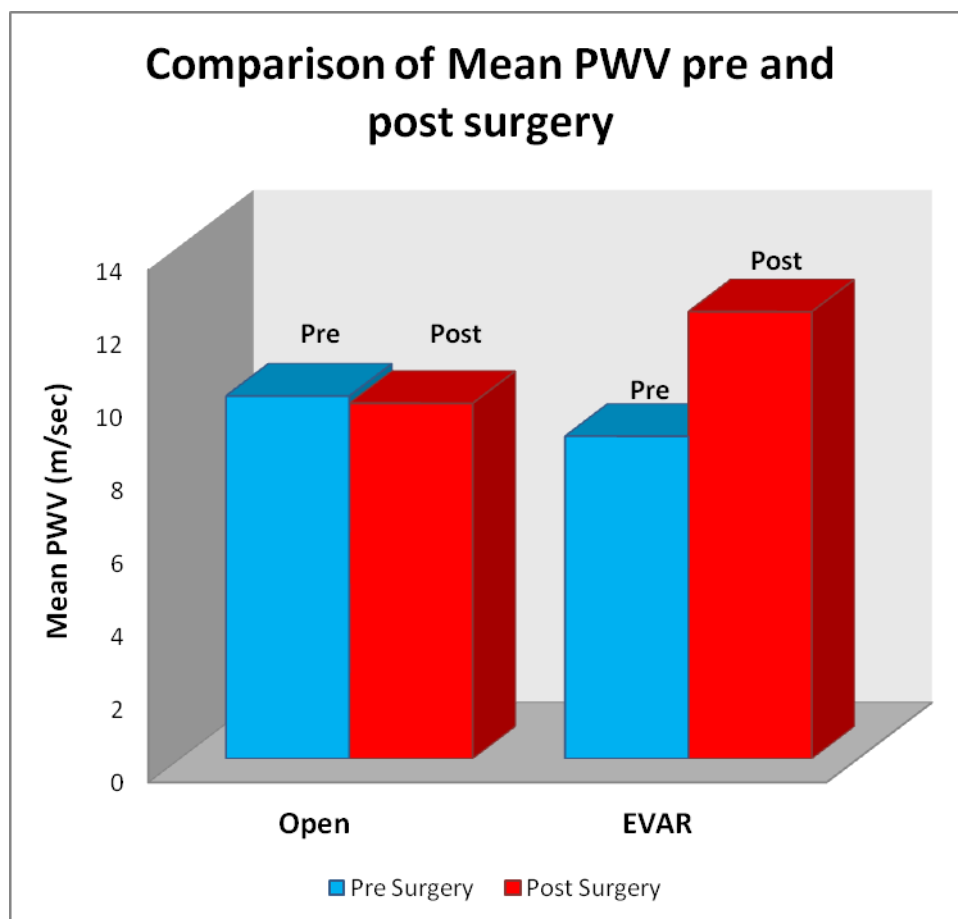
Figure 10.2: Difference in mean PWV pre and post surgery in both groups

10.4 Discussion

This study demonstrates a clear increase in mean PWV in the group of patients who underwent EVAR when compared to the open surgical repair group. The mean post procedure PWV of 9.7 ($\pm$ 4.5) m/sec in the open group was significantly lower than the elevated 12.2 ($\pm$ 4.5) m/sec detected in the EVAR group.

A study carried out by Alecu et al., in 2008 concluded that PWV values below 10m/sec were considered normal, values between 10-13m/sec borderline with values greater than 13m/sec being elevated. Rajzer et al., in 2008 considered 12m/sec to be elevated. Taking this into account, prior to undergoing intervention the mean ($\pm$SD) PWV in the open group was 9.9 ($\pm$ 3.1) m/sec and in the EVAR group was 8.8 ($\pm$ 2.1) m/sec, both within the normal value ranges. After surgery however, the mean ($\pm$SD) PWV in the open surgical group remained within the normal range at 9.7 ($\pm$4.5) m/sec whereas the mean ($\pm$SD) PWV in the EVAR group was elevated at 12.2 ($\pm$4.5) m/sec. This indicates that patients in the EVAR group are at a higher cardiovascular risk post operatively, when compared to the patients in the open surgical group.

PWV is an independent predictor of cardiovascular morbidity and mortality with age, hypertension and diabetes being the primary determinants of arterial stiffness (Alecu et al., 2008). Smith et al in 2005 stated that arterial stiffness is increased by multiple risk factors such as hypertension, and diabetes. Patients that have diabetes and renal disease have a higher PWV than those without diabetes, a condition that leads to a higher all cause and cardiovascular mortality in these patients (Smith et al., 2005). There was no statistical difference noted between the

risk factor variables in each group (p = 0.05) however, there was a higher percentage of patients in the EVAR group with known diabetes, hypercholesterolemia and coronary artery disease. The proportion of patients with known hypertension was lower in the EVAR group (41.2%) than the open surgical group (46%). The mean age of patients 73.7 years in the EVAR group, compared to 72.4 in the open surgical repair group were not significantly different (p =0.9). All patients in the open surgical group were male and only 15.8% in the EVAR group were female.

There are limitations with this study, such as the gender distribution and sample size. There were no female patients in the open surgical group and the EVAR group only contained 3 (15.8%) female patients. As gender is one of the risk factors that affect PWV this is a limitation of the study which could only be remedied with a larger more evenly distributed population. The PWV measurements were obtained within four weeks post surgery. To assess the implication of increased PWV on the long term cardiovascular morbidity and mortality of these patients, a prospective follow up of this population assessing cardiovascular event rate and mortality would be required.

10.5 Conclusion

The initial 30 day mortality results following EVAR demonstrate better survival when compared to open aneurysm repair. This survival rate does not persist when the patients are followed up long term. The findings of this study demonstrate that within the 30 days of graft implantation patients that underwent EVAR have a higher PWV measurement than those who underwent open surgical repair.

An increase in PWV correlates with an increased risk of cardiovascular morbidity and mortality in patients with atherosclerotic conditions and the elevation in PWV observed in the EVAR group in this study could equate to an increased postoperative cardiovascular event rate which could explain the failure of the initial survival benefit seen with EVAR.

To appropriately evaluate the long term implications of arterial stiffness on cardiovascular morbidity and mortality following EVAR, a larger scale study with a longer prospective follow up specifically looking at cardiovascular event rate and mortality would be required.

Chapter 11

Conclusions

Advances in technology and surgical technique have led to the evolution of endovascular aortic aneurysm repair. The minimally invasive nature of the procedure coupled with the concerns regarding durability of the repair have forced a re-evaluation of how aneurysm patients are assessed prior to and following their surgery.

The aim of this thesis was to investigate the role that Colour Duplex Ultrasound (CDU) plays in the detection, diagnosis and management of patients with AAA's, with particular relevance to those undergoing endovascular aneurysm repair (EVAR).

Chapter 6 sought to determine the presence and severity of asymptomatic carotid artery disease (CAD) and peripheral artery disease (PAD) in 389 patients with AAA to determine if this was a reasonable focus group to screen for occult CAD and PAD. The incidence of CAD (30.4%) and PAD (45.3%) was found to be higher in patients with AAA than that documented previously in other similar screening studies. Therefore, it is reasonable to conclude that patients with AAA are a group that should be targeted for screening for atherosclerotic disorders in other vascular territories. Similarly it is logical to suggest screening patients with CAD and PAD for AAA's.

The obvious advantages of screening for occult disease are that advances prior to AAA repair may help anticipate and thus prevent complications which may arise during, or as a consequence of surgery. More importantly, however, is the question of whether identification of these conditions alters the long term clinical outcome for the patient. A larger, more prolonged study of patients with co-incidentally diagnosed PAD and CAD as a consequence of screening during AAA workup, is required to determine what proportion of these patients ultimately

require intervention for their disease and whether the cardiovascular death rate in this screened population is different to the population as a whole.

Chapter 7 assessed the accuracy of CDU in measuring maximum aneurysm sac size in patients with AAA who had not yet undergone intervention. A high degree of correlation between CDU and the commonly accepted gold standard of computed tomography (CT) was established. However, CT scanning is still necessary prior to undergoing EVAR as numerous measurements of the native aorto-iliac segment need to be taken. The obvious next study would be to determine whether or not CDU could be employed as a measurement tool in patients prior to EVAR selection thus obviating the need for preoperative CT completely.

Chapter 8 evaluated the role of CDU in the postoperative surveillance of patients following EVAR, comparing it to the gold standard method of CT. A high degree of correlation between CDU and CT was demonstrated when measuring residual aneurysm sac size post EVAR, with a high sensitivity and specificity also achieved for CDU when compared to CT for the detection of endoleaks. Thus, it is reasonable to conclude that CDU could safely supplant CT as the primary imaging modality following EVAR, with just those patients with abnormal or inconclusive CDU scans requiring a CT. This would produce a sizeable reduction in the number of surveillance CT scans required with an accompanying reduction in radiation and contrast exposure, along with a substantial cost saving.

Having established the efficacy of CDU in the postoperative surveillance of EVAR patients, chapter 9 sought to identify its role in evaluating the residual aneurysm sac following EVAR. Aneurysm change was assessed and its relationship to pre existing risk factors and the presence of a type 2 endoleak

332

examined. Maximum residual sac reduction was found to occur in the first year following EVAR. Following univariate and multivariate risk factor analysis, reduction of the residual aneurysm sac was found to be dependent on risk factors that could be assessed prior to undergoing intervention. One key observation was the highly statistical associated observed between patients on statin treatment and aneurysm regression indicating that statins play a significant role in the regression process following EVAR. Based on this observation a larger more prospective study to clearly identify and outline the role that statins play in the regression process would be recommended.

One potential factor which was not assessed in this series was the influence of endograft type on sac behaviour following implantation and this is perhaps an area which should receive further study.

Chapter 10 demonstrated that within 30 days of graft implantation, patients that underwent EVAR have a higher pulse wave velocity (PWV) measurement than those patients who underwent open surgical repair. An increase in PWV correlates with an increase in arterial stiffness and an associated higher risk of cardiovascular morbidity and mortality in patients with atherosclerotic conditions. This could explain the absence of a long term survival benefit in patients who underwent endovascular repair of their aneurysms compared to those who survived open surgery. The next step in evaluating this finding would entail examining the long term implications of increased arterial stiffness on cardiovascular morbidity and mortality following EVAR. A larger scale study with a longer prospective follow up would be required to compare the postoperative cardiovascular event rate in patients who underwent EVAR with open repair.

References

Abramson, BL. and Huckell, V. (2005). Peripheral Arterial Disease Consensus Document. Canadian Cardiovascular Society Consensus conference 2005; http://www.ccs.ca/download/consensus_conference/consensus_conference_archives/CCFinalPre_CJC_Pub.pdf

Adams, MR. Keech, A. Robinson, J. et al. (1995). Carotid intima media thickness is only weakly correlated with the extent and severity of coronary artery disease. *Circulation*; **92**:2127-2134.

Alec, C. Labat, C. Kearney-Schwartz, A. et al. (2008) References values for aortic pulse wave velocity in the elderly. *Hypertension*; **26** (11):2207-2212.

Altman, DG. and Bland, JM. (1983) Measurement in medicine: The analysis of method comparison studies. *The Statistician*; **32**:307-317.

Arko, FR. Filis, KA. Heikkinen, MA. et al. (2004) Duplex scanning after endovascular aneurysm repair: An alternative to computed tomography. *Seminars in Vascular Surgery;* **17**(2):161-165.

Ballard, DJ. Filardo, G. and Powell, JT. (2008) Surgery for small abdominal aortic aneurysms (Review). *The Cochrane Library*; **4.**

Ballard, JL. Bergen, JJ. Singh, P. et al. (1998) Aorta iliac stent deployment versus surgical reconstruction: Analysis of outcome and cost. *The Journal of Vascular Surgery*; **28**(1):94-103.

Bashir, M. Ferral, H. Jacobs, C. et al. (2008) Endoleaks after endovascular abdominal aortic aneurysm repair: Management strategies according to CT findings. *American Journal of Roentgenology*; **192**:178-186.

Beeman, BR. Doctor, LM. Doerr, KA. et al. (2009) Duplex Ultrasound imaging alone is sufficient for midterm endovascular aneurysm repair surveillance: A cost analysis study and prospective comparison with CT scanning. *The Journal of Vascular Surgery*; **50**(5):1019-1024.

Berdejo, GL. Lyon, RT. and Veith, FJ. et al. (1997) Colour Duplex ultrasonagraphy for the evaluation of endovascular PTFE stented grafts for occlusive disease. *JVT*; **21**(1): 11-15.

Bernstein, EF. Dilley, RB. Goldberger, LE. and Leopold, GR. (1976) Growth rates of abdominal aortic aneurysms. *Surgery*; **80**:765-73.

Blacher, J. Guerin, A. Pannier, B. et al. (1999) Impact of Aortic Stiffness on Survival in End Stage Renal Disease. *Circulation*; **99**:2434-2439.

Blakemore, A. and Voorhees, A. (1954) The use of tubes constructed from Vinyon "N" cloth in bridging arterial defects-experimental and clinical. *Annals of Surgery*; **140** (3):324-333.

Bland, JM. and Altman, DG. (1986) Statistical methods of assessing agreement between two methods of clinical measurement. *The Lancet*; **1** (8476):307-10.

Bobadilla, J. Hoch, J. Leverson, G. and Tefera, G. (2010) The effect of warfarin therapy on endoleak development after endovascular aneurysm repair (EVAR) of the abdominal aorta. *The Journal of Vascular Surgery*; **52**(2):261-271.

Brewster, DC. Cronenwett, JL. Hallett, JW. et al. (2003) Guidelines for the treatment of abdominal aortic aneurysms: report of a subcommittee of the joint council of the American association for vascular surgery and the society for vascular surgery. *The Journal of Vascular Surgery*; **37**(5):1106-1117.

Brown, LC. Epstein, D. Manca, A. et al. (2004) The UK endovascular aneurysm repair (EVAR) trials: Design, Methodology and Progress. *European Journal of Vascular and Endovascular Surgery*; **27**:372-381.

Brown, OW. Bendick, PJ. Bove, PG. et al. (2004) Reliability of carotid artery duplex scanning: Value of vascular laboratory accreditation. *The Journal of Vascular Surgery*; **39** (2): 366-371.

Busuttil, SJ. Franklin, DP. Youkey, JR. and Elmore, JR. (1996) Carotid duplex overestimation of stenosis due to severe contralateral disease. *American Journal of Surgery*; **172** (2):144-7.

Chaer, R. Gushchin, A. Rhee, R. et al. (2009) Duplex Ultrasound as the sole long term surveillance method post endovascular aneurysm repair: A safe alternative for stable aneurysms. *The Journal of Vascular Surgery*; **49**(4): 845-849.

Chaikof, EL. Blankensteijn, JD. Harris, PL. et al. (2002) Reporting standards for endovascular aneurysm repair. *Journal of Vascular Surgery*; **35**:1048-1060.

Chaikof, EL. (2009) The care of patients with an abdominal aortic aneurysm: The society of Vascular Surgery practice guidelines. *The Journal of Vascular Surgery*; **50** (4 supplement):S2-S49.

Cimminiello, C. Borghi, C. Kownator, S. et al. (2010) Prevalence of peripheral arterial disease in patients at non- high cardiovascular risk. Rationale and design of the PANDORA study. *BMC Cardiovascular Disorders*; **10**: 35.

CiVitello, AB. Woodruff, A. Mahmood, H. et al. (2003) Contrast enhanced duplex ultrasound improves endoleak detection following endovascular abdominal aortic aneurysm repair. *Journal of the American College of Cardiology*; **41**(6):39.

Cochrane Review. (2007) Percutaneous transluminal angioplasty and stenting for Cochrane library.

Cole, S. Norris, R. and Walker, R. (2001) Vascular Laboratory Practice Parts 1-6. First Edition.

Cohen, J. (1998), Statistical power analysis for the behavioural sciences (2nd Edition).

Criqui, MH. Ninamija, JK. and Wingard, C. (2008) Progression of peripheral arterial disease predicts cardiovascular disease morbidity and mortality. *Journal American Cardiology*; 52:A36-42.

Cronenwett, J. and Johnston, K. (1999) The United Kingdom Small Aneurysm Trial: Implications for surgical treatment of abdominal aortic aneurysms. *The Journal of Vascular Surgery*; **29**: 191-4.

d'Audiffret, A. Desgranges, P. Kobeiter, et al. (2001) Follow up evaluation of endoluminally treated abdominal aortic aneurysms with duplex ultrasonagraphy: Validation with computed tomography. *The Journal of Vascular Surgery*; **33**(1):42-50.

de Virgillio, C. Toosie, K. Arnell, T. et al. (1997) Asymptomatic carotid artery stenosis screening in patients with lower extremity atherosclerosis: A prospective study. *Annals of Vascular Surgery*; **11**(4):374-377.

DeBakery, M. Cooley, D. Crawford, E. and Morris, G. (1958) Clinical application of a new flexible knitted Dacron arterial substitute. *A.M.A. Archives of Surgery*; 77.

Dennis, M. Bamford, J. Sandercock, P. et al. (1990) Prognosis of transient ischemic attacks in Oxfordshire community stroke project. *Stroke*; **21**(6):848-853.

Dente, C. and Feliciano, D. Alexis, C (1873-1994). *Arch Surgery* 2005; **140.**

Dieter, RS. Chu, WW. Pacanowski. et al. (2002) The significance of lower extremity arterial disease. *Clinical Cardiology;* **25**:3-10.

Dobrin, PB. (1989) Pathophysiology and pathogenesis of aortic aneurysms. Current concepts. *Surgical Clinics of North America* 1989; **69**(4):687-703.

Donald, I. and Brown, TG. (1961) Demonstration of tissue interfaces within the body by ultrasonic echo sounding. *British Journal of Radiology*; **34**:539-46.

Dooby, AV. and Anand, SS. (2005) The sensitivity and specificity of the ankle brachial index to predict future cardiovascular outcomes. A systematic review. *Arteriosclerosis, Thrombosis and Vascular Biology*; **25**(7):1463-1469.

Dubost, C. Allary, M. and Oeconomos, N. (1952) Resection of an aneurysm of the abdominal aorta. *A.M.A Archives of Surgery*; **64** (3):405-408.

Elkouri, S. Glovicszki, P. McKusick, M. et al. (2004) Perioperative complications and early outcomes after endovascular and open surgical repair of abdominal aortic aneurysms. *The Journal of Vascular Surgery*; 39(3):479-507.

European Carotid Surgery Trialists Collaborative Group. (1998). Randomised trial of endarterectomy for recent symptomatic carotid stenosis: final results of the MRC European carotid surgery trial (ECST). *Lancet*; **351**:1379-1387.

EVAR Trail Participants. (2005) Endovascular aneurysm repair versus open repair in patients with abdominal aortic aneurysms. (EVAR Trial 1). *Lancet*; **365**:2179-2186.

Fairman, RM. Notte, L. Snyder, S. et al. (2006) Factors predictive of early or late aneurysm change following endovascular aneurysm repair. *The Journal of Vascular Surgery*; **43**(4):649-656.

Fassiadis, N. Adams, K. Zayed, H. et al. (2008) Occult Carotid artery disease in patients who have undergone coronary artery angioplasty. *Interact Cardiovascular Thoracic Surgery*; **7**: 855-857.

Feiring, AJ. Krahn, M. Nelson, L. et al. (2010) Preventing leg amputations in critical limb ischemia with below the knee drug eluting stents: The PARADISE (preventing amputation using drug eluting stents) trial. *Journal of the American Cardiology*; **55**(15):1580-1589.

Garg, PK. Tian, L. Criqui, MH. (2007). Physical activity during daily life and mortality in patients with peripheral arterial disease. *The Journal of Vascular Surgery;* **45** (2) 437.

Gibbs, V. Cole, D. and Sassano, A. (2009). *Ultrasound Physics and Technology How, Why and When,* Elsevier Health Sciences.

Gilling-Smith, G. Brennan, J. Harris, P. et al. (1999). Endotension after endovascular aneurysm repair: Definition, Classification and strategies for surveillance and intervention. *Journal of Endovascular Surgery*; 6(4):305-307.

Groechenig, E. (2003). Peripheral arterial occlusive disease – an interdisciplinary approach. *Austrian Journal of Cardiology*; **10**(4):139-141.

Guilli, G. Khan, S. and Markus, H. (2009). Vertobasilar stenosis predicts high early recurrent stroke risk in posterior circulation stroke and TIA. *Stroke;* 40:2732-2737.

Haider, S. Najjar, S. Cho, J. et al. (2006). Sac behaviour after aneurysm treatment with the Gore Excluder low permeability aortic endoprosthesis-12- month comparison to the original excluder device. *The Journal of Vascular Surgery*; **44**(4):694-700.

Hallinday, AM. and Mansfield, TD. (1994). The asymptomatic carotid surgery trial (ACST); rational and design. *European Journal of Vascular Surgery*; **8**:703-710.

Henao, EA. Hodge, MD. Felkai, DD. et al. (2006). Contrast enhanced duplex surveillance after endovascular aneurysm repair: Improved efficacy using a continuous infusion technique. *The Journal of Vascular Surgery*; **43**:259-264.

Henry, MH. Amor, M. Klonaris, C. et al. (2000). Angioplasty and stenting of carotid arteries. *Texas Heart Institute Journal*; **27** (2) 150-158.

Henry, RM. Kostense, PJ. Dekker, JM. et al. (2002) Mild Renal Insufficiency is associated with cardiovascular mortality: The Hoorn Study. *Kidney Int*; **62**(4):1402-7.

Hiatt, WR. and Krantz, M. (2006). Masterclass in peripheral arterial disease. *Vascular Medicine*; **11**:55-60.

Higashida, RT. and Meyers, PM. (2006) Intracranial angioplasty and stenting for cerebral atherosclerosis: new treatments for stroke are needed!. *Neuroradiology* 2006; **48**(6):367-372.

High, RM. McDonnell, DE. and Savrin, A. (1984) Critical review of amputation in vascular patients. *The Journal of Vascular Surgery*; **1** (5): 653-655.

Hollier, LH. Taylor, LM. and Ochsner, J. (1992). Recommended indications for operative treatment of abdominal aortic aneurysms. Report of a subcommittee of the joint council of the society of vascular surgery and the North American chapter of the international society for cardiovascular surgery. *The Journal of Vascular Surgery;* **15**(60):1046-1056.

Hoskins, P. Thrush, A. Whittingham, M. (2003) *Diagnostic Ultrasound: Physics and Equipme*nt, Greenwich Medical Media: London.

Huber, TS. Wang, JG. Darrow, AE. et al. (2001). Experience in the United States with intact abdominal aortic aneurysm repair. *The Journal of Vascular Surgery*; **33**(2):304-311.

Hultgren, R. Granath, F. and Swedenborg. (2007) Different disease profiles for women and men with abdominal aortic aneurysms. *European Journal of Vascular and Endovascular Surgery*; **33**(5):556-560.

International Carotid Stenting Study Investigators. (2010). Carotid artery stenting compared with endarterectomy in patients with symptomatic carotid stenosis (International Carotid Stenting Study): An interim analysis of a randomised control trial. *Lancet*; **375**: 985-997.

Irish Heart Foundation Annual Review (2001)

http://www.irishheart.ie/iopen24/pub/positionstatements/heart_for_pdf.pdf

Irish Heart Foundation Annual Review (2009)

http://www.irishheart.ie/media/pub/carolinedocs/ihf%20annual%20report%20200

Jacobowitz, GR. Rockman, CB. Gagne, PJ. et al. (2003). A model for predicting occult carotid artery stenosis; screening is justified in a select population. *The Journal of Vascular Surgery*; **38**(4):705-709.

Jahromi, A. Canddio, C. Liu, Y. et al. (2005). The sensitivity and specificity of colour duplex ultrasound in the estimation of internal carotid artery stenosis: A systematic review and meta analysis. *Journal of Vascular Surgery*; **41**(6):962-972.

Jeffrey, S. (2006). SPACE: Carotid stenting falls short of noninferiority vs endarterectomy. *Medscape Medial News*; October 6.

Jiang, B. Baoming, L. Karen, L. et al. (2007). Measurement of pulse wave velocity using pulse wave Doppler ultrasound: Comparison with arterial tonometry. *Ultrasound in Medicine and Biology*; **34** (3): 509-512.

Johansen, K. Kohler, T. Nicholls, S. Zierler, R. et al. (1991). Ruptured abdominal aortic aneurysms: The Harborview View. *The Journal of Vascular Surgery*; **13** (2): 240-245.

Jones, J. Atkins, M. Brewster, D. et al. (2007). Persistent type 2 endoleak after endovascular repair of abdominal aortic aneurysm is associated with adverse late outcomes. *The Journal of Vascular Surgery*; **46**(1):1-8.

Kakisis, JD. Liapis, CD. Dimitralis, DA. et al. (2003). Carotid ultrasound findings as a predictor of long term survival after abdominal aortic aneurysm repair. A 14 year prospective study. *The Journal of Vascular Surgery*; **38**(6):1220-1225.

Kallikazaros, I. Tsioufis, C. Stefanadis, C. and Toutouzas, P. (1999). Carotid artery disease as a marker for the presence of severe coronary artery disease in patients evaluated for chest pain. *Stroke*; **30**:1002-1007.

Kannel, WB. Skinner, JJ. Schwartz, MJ. et al. (1970). Intermittent claudication. Incidence in the Framingham Study. *Circulation;* **41**(5):875-83.

Kiernan, T. Taqueti, V. Crevensten, G. et al. (2009). Correlates of Carotid stenosis in patients undergoing coronary artery bypass grafting- a case control study. *Vascular Medicine*; **14**: 233.

Klop, R. Eikelboom, B. Taks, A. (1991). Screening of the internal carotid arteries in patients with peripheral arterial disease by colour flow duplex scanning. European *Journal of Vascular Surgery*; **5**(1):41e5.

Kurvers, H. van de Graff, Y. Blankensteijn, JD. et al. (2003). Screening for asymptomatic internal carotid artery stenosis and aneurysms of the abdominal aorta: Comparing the yield between patients with manifest atherosclerosis and patients with risk factors for atherosclerosis only. *The Journal of Vascular Surgery*; **37**(6):1226-1232.

Lederle, F. Wilson, S. Johnson, G. et al. (1995). Variability in measurement of abdominal aortic aneurysms. *The Journal of Vascular Surgery*; **21** (6): 945-952.

Lederle, FA. (2005). Endovascular repair of abdominal aortic aneurysms- Round two. *New England Journal of Medicine*; **352**:23.

Lederle, FA. (2003). Ultrasonographic screening for abdominal aortic aneurysms; *Annals of Internal Medicine*; **139**(6):515-522.

Leiner, T. Jan, H. Tordoir, M. et al. (2003). Comparison of treatment plans for peripheral arterial disease made with multi-station contrast medium enhanced magnetic resonance angiography and duplex ultrasound scanning. *The Journal of Vascular Surgery*; **37**(6) 1255-1262.

Leng, GC. Fowler, B. and Ernst, E. (2000). Exercise for intermitted Claudication (Review). Cochrane Database Syst Revs Issue 2; Art. No.:CD000990.

Lifescan United Kingdom; http://www.lifescanuk.org/aboutlifescan/

Lindholt, JS. Vammen, S. Juul, S. et al. (2000). Optimal interval screening and surveillance of abdominal aortic aneurysms. *European Journal of Surgery*; **20**: 369-373.

Lovell, M. Harris, K. Forbes, T. et al. (2009). Peripheral arterial Disease: Lack of awareness in Canada. *Canadian Journal of Cardiology*; **25**(1):39.

Makaroun, MS. (2001). The Ancure endografting system: and update. *The Journal of Vascular Surgery*; **33**(2): 129.

Management of Peripheral arterial disease. (2000). Transatlantic inter society consensus (TASC). *The Journal of Vascular Surgery*; **31**:s1-s296.

Manning, BJ. Kristmundsson, T. Sonesson, B. and Resch, T. (2009). Abdominal aortic aneurysm diameter: A comparison of ultrasound measurements with those from standard three dimensional computed tomography reconstruction. *The Journal of Vascular Surgery*; **50**(2):263-268.

Manning, BJ. O'Neil, SM. Haider, SN. et al. (2009). Duplex Ultrasound in aneurysm surveillance following endovascular aneurysm repair: A comparison with computed tomography aortography. *The Journal of Vascular Surgery*; **49**(1):60-65.

Manning, M. Cassis, L. Huang, J. et al. (2002). Abdominal aortic aneurysms: fresh insights from a novel animal model of the disease. *Vascular Medicine*; **7**:45-54.

Marso, SP. and Hiatt, WR. (2006). Peripheral arterial disease in patients with Diabetes. *Journal of the American College of Cardiology*; **47**: 921-919.

Hussey, M. (1985). *Basic Physics and Technology of Medical Diagnostic Ultrasound*; Elsevier Publishing Company, First Edition, 1985.

McDermott, M. (2006). The magnitude of the problem of peripheral arterial disease: Epidemiology and clinical significance. *Cleveland Clinic Journal of Medicine*; **73** (4).

Meade, M. Zuhrie, R. Cook, C. et al. (2002). Bezafibrate in men with lower extremity arterial disease: randomised controlled trial. *British Medical Journal*; **325**(7373):1139.

Meier, G. LeSar, C. DeMasi, R. et al. (2003). Comparison of abdominal aortic aneurysm diameter measurements obtained with ultrasound and computed tomography: Is there a difference? *The Journal of Vascular Surgery*; **38**(3): 466-471.

Moore, WS. Barnett, HJ. Hobson, RW. (1995). Guidelines for carotid endertrectomy. A multidisciplinary consensus statement from ad hoc committee of the American heart association. *Stroke*; **26**(1): 188-201.

Moore, WS. Barnett, HJ. Beebe, HG. et al. (1995) Guidelines for carotid endarterectomy: a multidisciplinary consensus statement from the Ad Hoc Committee, American Heart Association. *Circulation.*;91:566–579

Multicentre Aneurysm Screening Group. (2002). Multicentre aneurysm screening study (MASS): cost effectiveness analysis of screening abdominal aortic aneurysms based on four year results from randomised control trial. *British Medical Journal* 2002; **325**: 1135.

Noll, R. Tonnessen, BH. Mannave, K. et al. (2007). Long term placement cost after endovascular aneurysm repair. *The Journal of Vascular Surgery*; **46**(1):9-15.

Norgren, L. Hiatt, WR. Dormandy, JA. et al. (2007). Inter society consensus for the management of peripheral arterial disease (TASC 11). *The Journal of Vascular Surgery*; **45**(1): s5-s67.

North American Symptomatic Carotid Endertrectomy Trialists' Collaborative Group. (1998). The final results of the NACSET trial. *New England Journal of Medicine*; **339**: 1415-1425.

North American Symptomatic Carotid Endertrectomy Trial Collaborators. (1991). Beneficial Effect of Carotid endertrectomy in Symptomatic patients with high grade stenosis. *New England Journal of Medicine*; 325:445-453

Oates, CP. Naylor, AR. Hartshorne, T. et al. (2008). Joint Recommendations for Reporting Carotid Ultrasound Investigations in the United Kingdom. *European Journal of Endovascular Surgery*; **10**:1016.

Oppenheimer, GM. (2010) Framingham heart study: The first 20 years. *Progress in cardiovascular diseases*; **53** (2010):55-61.

Ouriel, K. Clair, DG. Greenberg, RK. et al. (2003) Endovascular repair of abdominal aortic aneurysms: Device specific outcomes. *The Journal of Vascular Surgery*; **37**(5):991-998.

Ouriel, K. (2009). The PIVOTAL study: a randomised population of endovascular repair versus surveillance in patients with smaller abdominal aortic aneurysms. *The Journal of Vascular Surgery*; **49**(1):266-269.

Paraskevas, K. Mikhailidis, D. and Veith, F. (2009) Carotid artery stenting may be losing the battle against carotid endertrectomy for the management of

symptomatic carotid artery stenosis, but the jury is still out. *Vascular*; **17**(4): 183-189.

Paraskevas, K. (2010). Carotid artery stenting versus endarterectomy for carotid stenosis. *The Lancet*; **376**(9738):327.

Parodi, JC. Palmaz, JC. and Barone, HD. (1991). Transfemoral intraluminal graft implantation for abdominal aortic aneurysms. *Annals of Vascular Surgery*; **5**(6):491-499.

Pilcher, JM. Danaher, J. and Khaw, KT. (2000). The prevalence of asymptomatic carotid artery disease in patients with peripheral arterial disease. *Clinical Radiology*; **55**(1):56-61.

Posacioglu, H. Isiamoglu, F. Apaydin, AZ. et al. (2002). Predictive value of conventional computed tomography. *Texas Heart Institute Journal*; **29**(3):172-175.

Prinssen, M. Bushens, E. and Blankensteijn, JD. (2002). Dutch randomised endovascular aneurysm management (DREAM) - trial. Background, design and methods. The *Journal of Cardiovascular Surgery* (Torino); **43** (3):379-384.

Qureshi, AI. Jarnardhan, SE. Benett, AR. et al. (2001). Who should be screened for asymptomatic carotid artery stenosis? Experience from the Nw York stroke screening program. *The Journal of Neuro Imaging*; **11**: 105-111.

Quirel, K. Greenberg, R. and Clair, D. (2002) Endovascular treatment of Aneurysms. *Current Problems in Surgery*; **39**:233-348.

Quirel, K. McDonnell, AE. Metz, AE. and Zarins, CK.(1982). Critical evaluation of stress testing in the diagnosis of peripheral arterial disease. *Surgery*; **91**:686-693.

Quriel, K. Zarins, CK. (1982). Doppler ankle pressures (and evaluation of three methods by expression). *Arch. Surgery*; **117**: 1297-1300.

Rajzer, M. Wojciechowska, W. Klocek, M. et al. (2001) Comparison of aortic pulse wave velocity measured by three techniques: Complior, SphygmoCor and Arteriograph. *Journal of Hypertension;* **26** (10):2001-2007.

Raman, K. Missig-Carroll, N. Richardson, T. et al. (2003). Colour flow duplex ultrasound scan versus computed tomographic scan in the surveillance of endovascular aneurysm repair. *The Journal of Vascular Surgery*; **38**(4): 645-651.

Rancic, Z. Rancic, D. Radak, DJ. et al. (2002). Limited screening of asymptomatic carotid disease in patients with symptomatic limb ischemia to subgroup of patients with carotid bruit is not effective. *Medicine and Biology*; **9** (3): 231-235.

Rhee, R. Eskandari, M. Zajko, A. and Makaroun, M. (2000). Long term fate of the aneurysmal sac after endoluminal exclusion of the abdominal aortic aneurysms. *The Journal of Vascular Surgery*; **32**(4): 689-696.

Roddy, SP. (2009). Endoleak after endovascular aneurysm repair: Duplex Ultrasound imaging is better than computed tomography at determining the need for intervention. *The Journal of Vascular Surgery*; **50**(5):1239.

Rothwell, PM. and Goldstein, LB. (2004). Carotid endertrectomy for asymptomatic Stenosis. *Stroke*; **35**: 2425-2427.

Rothwell, PM. (2008). Prediction and prevention of stroke in patients with symptomatic carotid stenosis: The high risk period and high risk patient. *European Journal of Endovascular Surgery*; **35**:255-263.

Rutherford, RB. (2000). *Vascular Surgery (Fifth edition),* Philadelphia: W.B.Saunders.

Sanford, RM. Brown, MJ. Fishwick, G. et al. (2006). Duplex Screening is reliable in detection of endoleak following endovascular aneurysm repair. *European Journal of Vascular and Endovascular Surgery*; **32**:537-541.

Schei, TR. Barret, S. Jones, D. and Krupski, W. (2003). Automated Abdominal Aortic Aneurysm Segmentation using MATLAB; *Biomed SCI Instrum*; **39**:53-8

Schouten, O. Bax, J. Dunkelgrum, M. et al. (2006). Statins for the prevention of preioperative cardiovascular complications in vascular surgery. *The Journal of Vascular Surgery*; **44**(2):419-424.

Siegel, CL. and Cohen, RH. (1994). CT of abdominal aortic aneurysms. *AJR AM J Roentgenal;* **163:17**-29.

Siegel, CL. Cohan, RH. Korobkin, M. et al. (1994). Abdominal aortic aneurysm morphology: CT features in patients with ruptured and non ruptured aneurysms. *AJR AM J Roentgenal;* **163**:1123-1129.

Silvennoinen, HM. Ikonen, S. Soinne, L. et al. (2007). CT angiographic analysis of the carotid artery stenosis comparison of manual assessment, semiautomatic vessel analysis, and digital subtraction angiography. *American Journal of Neuroradiology;* **28**: 97-103.

Sing, N. O'Donnell, S. and Gillespie, DL. (2010). Atherosclerotic disease of the carotid artery; http://emedicine.medscape.com/article/463147-overview

Smith, A. Karalliedde, J. De Angelis, L. et al. (2005). Aortic Pulse Wave Velocity and Albuminuria in patients with type 2 diabetes. *Clinical Nephrology*; **16**:1069-1075.

Sprouse, LR. Meier, GH. Le Sar, C. et al. (2003). Comparison of abdominal aortic aneurysm diameter measurements obtained with ultrasound and computed tomography: is there a difference? *Journal of Vascular Surgery*; **38** (3): 466-471.

Sternberg, WC. Connors, MS. Tonnessen, BH. et al. (2003). Aortic aneurysm sac shrinkage after endograft repair is device dependent. A comparison of Zenneth and AnneuRx endografts. *The Journal of Vascular Surgery***; 17**:49-53.

Sukhija, R. Aronow, W. Yalamanchili, K. et al. (2004). Prevalence and severity of coronary artery disease, lower limb peripheral arterial disease, and cerebro vascular disease in 110 men with an abdominal aortic aneurysm. *American Journal of cardiology*; **94**: 1358-1359.

Tan, WA and Powell. (2010). Abdominal Aortic Aneurysm Rupture. E-Medicine:; http://emedicine.medscape.com/article/416397-overview

The EVAR Trial Participants. (2004). Comparison of endovascular aneurysm repair with open repair in patients with abdominal aortic aneurysm (EVAR trial1), 30 day operative mortality result: randomised control trial. *The Lancet*;**364.**

The Multicentre Aneurysm Screening Study Group. (2002). The Multicentre Aneurysm Screening Study (MASS) into the effect of abdominal aortic screening on mortality in men: a randomised control trial. *Lancet*; **360**:1531.

The UK Small Aneurysm Trial Participants. (1998). Mortality results for randomised controlled trial of early elective surgery or ultrasonographic surveillance for small abdominal aortic aneurysms. *The Lancet;* **352**:1649-1655.

The United Kingdom Small Aneurysm Trial Participants. (1999). Risk Factors for aneurysm Rupture in patients kept under ultrasound Surveillance. *Annals of Surgery*; **230** (3): 289-297.

Tullio, MR. Russo, C. Jin, Z. et al. (2009) Aortic Arch Plaques and Risk of Recurrent Stroke and Death. *Circulation Journal of the American Hearst Association;* **119**: 2376-2382.

U.S. Preventative Task Force. (2005). Screening for Abdominal Aortic Aneurysms: Recommendation Statement. *Ann Intern Med*; **142**:198-202.

Veith, F. Baum, R. Ohki, T. et al. (2002). Nature and significance of endoleaks and endotension: summary of opinions expressed at an international conference. *Journal of Vascular Surgery*; **35** (5):1029-1035.

Veith, F. Lipsitz, E. Ohki, T. et al. (2004). Variability of maximal aortic aneurysm diameter measurements on CT scan: significance and methods to minimise. *Journal of Vascular Surgery;* **39** (4): 811-815.

Villacorta, H. Bortolotto, L. Arteaga, E. and Mady, C. (2006). Aortic distendibility measured by pulse wave velocity is not modified in patients with Chagas disease. *Journal of Negative Results in Medicine*; **5**:9.

Virgillo, C. Tran, J. Lewis, R. et al. (2006). Factors affecting long term mortality after abdominal aortic aneurysms. *Archives of Surgery*; **141** (9), 905-910.

Visser, JJ. Williams, M. Kievit, J. and Boscg, JL. (2006). (4-A Study Group). Prediction of a 30 day mortality after endovascular repair or open repair in patients with ruptured abdominal aortic aneurysms. *The Journal of Vascular Surgery*; 49(5):1093-1099.

Vogt, MT. McKenna, M. Wolfson, SK. Kuller, LH. (1993). The relationship between ankle brachial index, other atherosclerotic disease, diabetes, smoking and mortality in older men and woman. *Atherosclerosis*; **101**:191-202.

Wain, RA. Lyon, RT. Veith, FJ. et al. (1998). Accuracy of duplex ultrasound in evaluating carotid artery anatomy before endertrectomy. *The Journal of Vascular Surgery*; **27**(2):235-244.

Wanhainen, A. Bergqvist, D. and Bjorck, M. (2002). Measuring the abdominal aorta with Ultrasonagraphy and computed tomography. *European Journal of Endovascular Surgery*; **24:158**-167.

Wanhainen, A. (2008). How to define an abdominal aortic aneurysm- influence on epidemiology and clinical practice. *Scandinavian Journal of Surgery*; **97**:105-109.

Weerd, MD. Greving, J. Hedblad, BO. et al. (2010). Prevalence of asymptomatic carotid artery stenosis in the general population. *Stroke*; **41**:1294.

White, GH. Yu, W. and May, J. (1996). Endoleak: a proposed new terminology to describe incomplete aneurysm exclusion by an endoluminal graft. *Journal of Endovascular surgery*; **3**:124-125.

Wolf, PA. Kannel, WB. Sorlie, P. et al. (1981). Asymptomatic carotid bruit and risk of stroke – Framingham study. *JAMA*; **245:1442**-1445.

Wolf, Y. Hill, B. Rubin, G. et al. (2000) Rate of change of abdominal aortic aneurysm diameter after endovascular repair. *The Journal of Vascular Surgery*; **32**(1):108-115.

World Health organisation; www.who.int

Yesil, S. Akinci, B. Yener, S. et al. (2009). Predictors of amputation in diabetics with foot ulcer: single centre experience in a large Turkish cohort. *Hormones;* **8**(4):286-295.

Zhang, X. and Greenleaf, J. (2005). Non-invasive generation and measurement of propagating waves in arterial walls. *Acoustical Society of America*; **119** (2): 1238-1243.

Zweibel, W. and Pellerito, J. (2005). *Introduction to vascular sonography (Fifth edition),* New York: Elsevier Saunders.

Zweibel, W. (1982). *High resolution B-mode and Duplex Carotid Sonography. Introduction to vascular sonography*, New York: Gune & Stratton.

Figure References (Last Accessed October 2011)

2.0:

http://herkules.oulu.fi/isbn951426973X/html/equation2222.png

2.1:

http://img.tfd.com/dorland/aorta.jpg

2.2:

http://www.wckleinelp.com/review_bio-112/vessels/images/a_abdominal_aorta.jpg

2.3:

http://www.wckleinelp.com/review_bio-112/vessels/pages/a_iupper_leg.htm

2.4:

http://www.wckleinelp.com/review_bio-112/vessels/pages/a_lowerleg.htm

2.5:

http://129.49.170.167/Volumes/ACSCD+January+2009/ACSCD/figures/ch0617-f13.htm

2.6:

http://www.wckleinelp.com/review_bio-112/vessels/pages/a_head_neck.htm

2.7:

http://radiopaedia.org/images/7576

2.8:

http://www.mayfieldclinic.com/PE-IntracranialStenosis.htm

2.9:

http://raiopaedia.org/uploads/radio/0001/4104/External_carotid_artery.jpg

2.10:

http://upload.wikimedia.org/wikipedia/commons/f/ff/Vertebral_artery.png

2.11:

http://emedicine.medscape.com/article/1877617-overview

3.0:

http://medinfo.ufl.edu/pa/chuck/fall/handouts/atheroma.png

3.3:

http://www.wsiat.on.ca/english/mlo/diabetic.htm

3.5:

http://www.nhlbi.nih.gov/health/dci/Diseases/stents/stents_placed.html

3.6:

http://texasheart.org/HIC/Topics/Proced/angioplasty.cfm

3.8:

http://www.dr-paraskevas.com/img/4-bypass-graft.png

3.11:

http://www.daviddarling.info/images/aneurysms.jpg

3.12:

http://www.vascularweb.org/graphics/northpoint_graphics_jpg/SurgicalAAA_01_

Base_275.jpg

3.14:

http://www.nhlbi.nih.gov/health/dci/images/aneurysm_endovascular.jpg

3.15:

http://studentweb.med.harvard.edu/MWS8/html/Reviews/Surgery/A

3.17:

http://bibamed.agcl.com/cx_2003/Raithel.pdf

3.18:

http://bibamed.agcl.com/cx_2003/Raithel.pdf

3.19:

http://bibamed.agcl.com/cx_2003/Raithel.pd

3.20:

http://bibamed.agcl.com/cx_2003/Raithel.pdf

3.21:

http://bibamed.agcl.com/cx_2003/Raithel.pdf

4.0

http://www.glogster.com/glog.php?glog_id=1265720&scale=54&isprofile=true

4.1

http://www.glogster.com/glog.php?glog_id=1265720&scale=54&isprofile=true

4.2

http://www.usra.ca/basic_p

4.3

http://www.instant-analysis.com/Principles/refraction.htm

4.4

http://www.mike-willis.com/Tutorial/PF10.htm

4.5

http://www.cis.rit.edu/research/ultrasound/ultrasoundintro/ultraintro.html

4.6

http://www.ukessays.com/essays/physics/images/physimage1.jpg

4.7

http://www.sprawls.org/ppmi2/USPRO/25USPROD08.png

4.8

http://radiographics.rsna.org/content/29/4/1179/F8.small.gif

4.9

http://radiographics.rsna.org/content/29/4/1179/F1.small.gif

4.10:

http://www.esabcutting.com/cutting/en/process/images/laser-focal_1.gif

4.13

http://www.alnmag.com/article/ultrasound-technology-small-animal-imaging?page=0,1

4.18

http://controls.engin.umich.edu/wiki/index.php/FlowSensors

4.19

http://faculty.ksu.edu.sa/mussaad/Lectures/vascular%20investigation%20-%20revised.ppt

4.28

http://books.google.ie/books?id=32XyGeuwWyAC&pg=PA107&dq=changes+in+flow+and+velocity+with+a+degree+of+stenosis&lr=&cd=5#v=onepage&q=changes%20in%20flow%20and%20velocity%20with%20a%20degree%20of%20stenosis&f=false

4.29

http://www.ceb.cam.ac.uk/pages/hydrodynamic-voltammetry.html

4.30

http://books.google.ie/books?id=32XyGeuwWyAC&pg=PA106&dq=carotid+bifurcation+flow+divider+diagram&hl=en&ei=eZcHTOjvIKig4QaDhcWmAQ&sa=X

&oi=book_result&ct=book-preview-

link&resnum=1&ved=0CDAQuwUwAA#v=onepage&q=carotid%20bifurcation%

20flow%20divider%20diagram&f=false

4.31

http://books.google.ie/books?id=gzOIX

gFgAUC&pg=PA128&dq=velocity+profile+in+a+curved+blood+vessel&hl=en&

ei=09Y1TLPLGoi6jAe0oPDZAw&sa=X&oi=book_result&ct=book-preview-

link&resnum=1&ved=0CDAQuwUwAA#v=onepage&q=velocity%20profile%20i

n%20a%20curved%20blood%20vessel&f=false

4.32

http://books.google.ie/books?id=32XyGeuwWyAC&pg=PA107&dq=changes+in

+flow+and+velocity+with+a+degree+of+stenosis&lr=&cd=5#v=onepage&q=cha

nges%20in%20flow%20and%20velocity%20with%20a%20degree%20of%20sten

osis&f=false

4.33

http://www.cvphysiology.com/Blood%20Pressure/BP019%20vascular%20pressur

es.gif

4.34:
http://books.google.ie/books?id=32XyGeuwWyAC&pg=PA107&dq=changes+in
+flow+and+velocity+with+a+degree+of+stenosis&lr=&cd=5#v=onepage&q=cha
nges%20in%20flow%20and%20velocity%20with%20a%20degree%20of%20sten
osis&f=false

5.24

http://2.bp.blogspot.com/_-p7DcK-
ba74/SPP8RnNa7UI/AAAAAAAAAbI/sBc26tVj0GI/s400/aaa.gif

5.30

http://74.220.216.190/shinchen/twn/pdf/pulsetracepwv.pdf